Volume 47 *August 1961* *Number 8*

Proceedings of the
National Academy of Sciences
of the United States of America

The Proceedings of the National Academy of Sciences

OFFICERS OF THE ACADEMY

DETLEV W. BRONK
President

J. A. STRATTON
Vice President

H. P. ROBERTSON
Foreign Secretary

HUGH L. DRYDEN
Home Secretary

L. V. BERKNER
Treasurer

EDITORIAL BOARD OF THE PROCEEDINGS

SAUNDERS MAC LANE
Chairman

HUGH L. DRYDEN, *Home Secretary*
L. V. BERKNER, *Treasurer*
H. P. ROBERTSON, *Foreign Secretary*
EDWIN B. WILSON, *Managing Editor*

HARRISON BROWN
S. CHANDRASEKHAR
ERNST CLOOS
THOMAS FRANCIS, JR.
C. H. GRAHAM
G. EVELYN HUTCHINSON
WILLARD F. LIBBY
H. W. MAGOUN
J. R. PIERCE

Subscription price is $17.50 for one year, $33.50 for two years, and $48.00 for three years. The price of a single issue beginning with volume 47 (1961), is $2.25; through volume 46 (1960), $1.50. Make all remittances payable to the National Academy of Sciences in U.S. currency or its equivalent.

Editorial correspondence should be addressed to the PROCEEDINGS OF THE NATIONAL ACADEMY OF SCIENCES, 2101 Constitution Avenue, Washington 25, D. C.

Business correspondence should be addressed to the Printing and Publishing Office, National Academy of Sciences, 2101 Constitution Ave., Washington 25, D. C.

Subscribers are requested to notify the Printing and Publishing Office of the Academy and their local postmaster immediately of change of address. Notices to the Academy should provide both the old and the new address.

Microfilms of complete volumes of this journal are available to regular subscribers only and may be obtained at the end of the volume year from University Microfilms, 313 N. First Street, Ann Arbor, Michigan.

Second-class postage paid at Easton, Pennsylvania. This publication is authorized to be mailed at the special rates of postage prescribed by Section 132.122.

PRINTED IN THE U. S. A.

THE PROCEEDINGS OF THE NATIONAL ACADEMY OF SCIENCES
is published monthly by
THE NATIONAL ACADEMY OF SCIENCES

Proceedings of the
NATIONAL ACADEMY OF SCIENCES

Volume 47 · Number 8 · August 15, 1961

SYMPOSIUM ON ENERGY-LINKED BIOLOGICAL REACTIONS

BY INVITATION OF THE COMMITTEE ON ARRANGEMENTS FOR THE AUTUMN MEETING

Presented before the Academy, November 15, 1960

DAVID R. GODDARD, *Chairman*

CONTENTS*

LOCAL AND π-π INTERACTIONS IN CHARGE TRANSFER.....
.....*Albert Szent-Györgyi, Irvin Isenberg, and Jane McLaughlin* 1089
Commentary.....*J. S. Griffith* 1093
HYDROGEN ION EFFECTS IN HIGH-ENERGY PHOSPHATE REACTIONS.....
.....*Robert J. Rutman and Philip George* 1094
THE REQUIREMENT OF ENERGY FOR RESPIRATION IN MITOCHONDRIA
(A Commentary).....*E. C. Slater and W. C. Hülsmann* 1109

* Other papers presented during the Symposium were: "Hole-Electron Pair Separation in Illuminated Chromatophores," by W. Arnold, Oak Ridge National Laboratory; "Nuclear Magnetic Resonance Spectra of ATP and its Metal Complexes," by Mildred Cohn, University of Pennsylvania; and "Interactions of Electron and Energy Transfer Reactions in Mitochondria," by Britton Chance, University of Pennsylvania. None of these has been received for publication in the PROCEEDINGS.

LOCAL AND π-π INTERACTIONS IN CHARGE TRANSFER

BY ALBERT SZENT-GYÖRGYI, IRVIN ISENBERG, AND JANE MCLAUGHLIN

INSTITUTE FOR MUSCLE RESEARCH AT THE MARINE BIOLOGICAL LABORATORY, WOODS HOLE, MASSACHUSETTS

In photosynthetic chromatophores, or chloroplasts, as well as in phosphorylating mitochondria, single electrons are transferred in a series of reactions from substance to substance. It seems possible that a similar transfer of electrons plays a wider role in the various activities of the cells or the maintenance of their living state. It is still an open question how such a transfer of electrons takes place. Our attention has been occupied, in this context, in an increasing degree by "charge transfer." Any oxidation involves a transfer of electrons from one substance to another, and we have to distinguish between "charge transfer" and "oxido-reduction." By the

latter, we usually mean the interaction of two closed-shell molecules, the final result of the reaction being two closed-shell molecules, the one of which becomes richer, the other poorer by *two* electrons. In "charge transfer," *one* (or part of one) electron is transferred from the one molecule, the donor "D," to the acceptor "A" whereas the transferred electron goes, as a rule, from the highest filled orbital of "D" to the lowest empty orbital of "A." In a somewhat simplified fashion, the reaction can schematically be denoted as

$$D + A \rightleftharpoons D^+A^-, \tag{1}$$

in which reaction a whole electron, or part of it, may be transferred, the transfer either being spontaneous or needing the energy of an absorbed photon for its transfer. D^+A^- may undergo different changes. Under favorable conditions and collaborative interaction of the solvent, the complex may dissociate, whereby two free radicals are formed:

$$D^+A^- \rightleftharpoons D^{\cdot+} + A.^- \tag{2}$$

This reaction will declare itself by a signal given in electron spin resonance (ESR) spectroscopy. Both D^+ and A^- may undergo secondary changes.

As a rule, the charge-transfer forces are insufficient to hold the two molecules together and have to be supported by the more conventional forces of complex formation to establish the necessary close proximity. Charge transfer can take place only if the two interacting orbitals overlap, which demands a very close proximity.

The current literature gives the impression that, on the whole, charge-transfer reactions can be divided into two groups. In the one, two molecules with more or less extensive π systems (as those of aromatic hydrocarbons) interact, the π pool of D giving an electron to that of A. The classical example of this interaction is the formation of quinhydrone from hydroquinone (D) and quinone (A).

In the other group of reactions, a single atom, with its lone pair of electrons, may serve as donor, called by Mulliken[1] "onium donor," while single atoms may act with their vacant orbitals also as local acceptors.

The charge-transfer reaction will depend, to a great extent, on the general tendency of the D molecules to part with one of their electrons. This tendency is expressed in their ionization potential, or their "P"* value, as calculated by the Pullmans, which expresses the energy of the highest filled orbital and is a linear function of the ionization potential. Similarly, the electron affinity of A will also be of importance and will be reflected by the P value of the lowest empty orbital of the acceptor.

We observed earlier[2] that there occurred between indoles (serotonin) and FMN (Flavinemononucleotides) a strong charge transfer—stronger than what might have been expected if one judged only by the P values of the reactants. Inquiring into this discrepancy, we replaced FMN with a series of different π acceptors,[3] like sym.-trinitrobenzene, and found that in these cases indoles reacted according to their P value. However, when iodine, I_2, was used as A, again an unexpectedly strong reaction was obtained, which declared itself in the formation of a black charge-transfer complex which gave a high and narrow ESR signal. The calculations of the Pullmans showed[4] that the C atoms of indole in positions 2 and 3 have a high

electron density and, hence, a formal negative charge. It seemed possible that the strong charge transfer was due to an interaction of the I_2 molecule with one or both of these C atoms. No such strong charge transfer could be expected from isolated C atoms, and it had to be supposed that the electron actually came from the π electron pool of the whole molecule, while the actual transfer took place at C2 or 3 or both, these atoms being conjugated to the rest of the molecule.

Various possibilities seemed to suggest themselves for the testing of this assumption. First, one had to expect that if the assumption was correct, then carbazole should give no such reaction with I_2. Carbazole, with its more extended conjugated system, can be expected on the basis of P value alone to be a better donor than indole. However, in this molecule, the C's, at positions 2 and 3, have lost their formal negative charge. The experiment showed that, according to expectations, carbazole gave no strong charge transfer with I_2.

As has been shown by the Pullmans,[5] aromatic carcinogenic hydrocarbons, such as 9–10 dimethylbenzanthracene, also have a pair of highly charged C atoms in their K-region. So, if our assumptions were correct, these hydrocarbons should also give a strong charge transfer with I_2, while closely related hydrocarbons, which have similar P values but no K-region, should give no such reactions. The experiment fully bore out this expectation. Subsequent experiments showed that all the investigated carcinogens gave such a reaction with I_2, while the noncarcinogenic homologues did not do so.[6] This suggests that carcinogenicity may actually be connected with the ability of the molecule to give off one electron in a "local" interaction. In carcinogens, this local interaction is greatly favored by the low P values.

These experiments suggest that at the side of the π-π and local interaction, a third group of charge-transfer complexes exists, in which the transfer takes place from a π pool in a "local" interaction at a specific point of the molecule. The same also holds, *mutatis mutandis*, for acceptors in which a pair of electron-deficient C atoms with a formal positive charge will favor a local electron transfer. So both acceptors and donors may react in a "local" electron transfer, and conditions for electron transfer may be favored by a proximity of the mediating C atoms. We can thus distinguish between a "π-π interaction" in the original Dewar[7] sense (in which a π pool interacts as such with another π pool, the two molecules forming a planar complex) and a "local" transfer, in which the one π pool donates an electron to the other in a local interaction, taking place at specific points of the two molecules. Naturally, there may be gradations from one type to another, and the difference can be expected to be more quantitative than qualitative. The experiments performed on this line are exemplified by the instances summed up in the slide (Fig. 1). The donors in this figure are given in the horizontal top row, the acceptors in the vertical left side column. The reactive C atoms are encircled.

The first of the acceptors, I_2, as mentioned, gave a strong interaction with indoles, none with carbazole, and again a strong one with dimethylbenzanthracene.

The second acceptor, maleic anhydride, may be expected to have two electron-deficient C atoms located between two electron-negative groups containing atoms of higher electron-negativity. Accordingly, maleic anhydride, with its two C atoms with their formal positive charge, could be expected to be a "local" acceptor. The experiment showed its reactions to be similar to those of iodine.

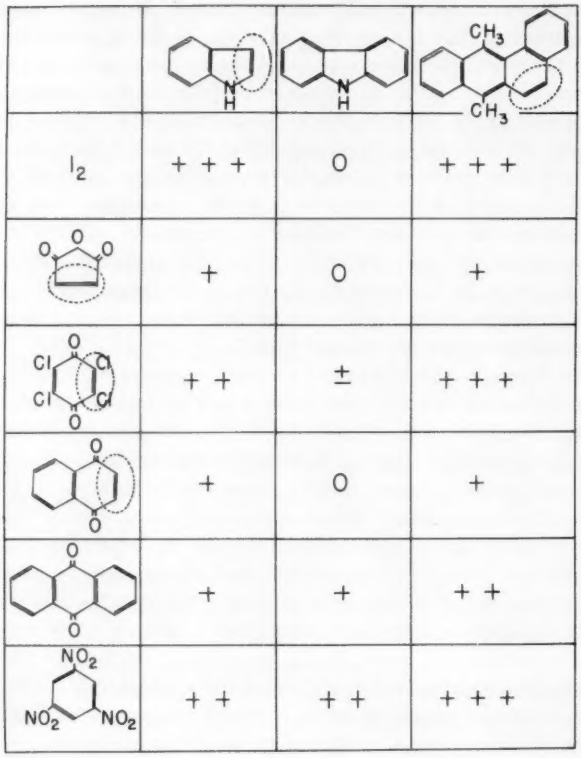

FIG. 1.

Quinones can be expected to be able to act as well in a π-π interaction as they do locally, having vicinal electron-deficient C atoms. p-Quinone actually showed a mixed behavior, but chloranil, with its more positive pairs of C atoms, shows a trend for a local interaction. This trend is even stronger in bromanil, which, as shown by Fujimori, forms with indole a charge-transfer complex which has two absorption maxima, the one corresponding, probably, to the π-π, the other to the local interaction.

In naphthoquinone, the situation seems even clearer. Contrary to naphthoquinone, anthraquinone does not distinguish between indole and carbazole. It therefore acts as π-π acceptor, having no such difference between the charge of its C atoms as naphthoquinone has. The last of the donor acceptors, sym.-trinitrobenzene, acts as a typical π acceptor (the charges being more evenly distributed between its C atoms) and does not distinguish between indole and carbazole.

The electron transfer between two C atoms seems thus not to be decided solely by the ionization potential but to depend also on the presence of electron-deficient or highly charged C atoms or atom pairs. In structures in which molecules have a fixed steric orientation, charge transfer can be expected to depend on how closely the two molecules, A and D, touch one another with their reactive points. If

these relations are unfavorable, no charge transfer may take place even if the P values may be favorable. The pyrroles, for instance, in haematoporphyrin, can be expected to react with their two peripheral C atoms as local donors, while quinones, such as Vitamin K, may act with their two electron-deficient atoms as their local acceptors. It is also believable that molecules in a crystal may be held in an orientation by the lattice which disfavors charge transfer; this may explain the increased conductivity observed on melting in certain substances. It is also believable that an extraneous molecule blocking the active point of a physiological electron transmitter could disrupt a chain of electron transfer.

The local electron transfer touches at three points upon our general outlook. It contributes to the breakdown of the strictly molecular concept of biological structures, it underlines the importance of the whole electronic profile of molecules, and it brings into the realm of electron transfer substances, such as vitamin E, which appear to be strong electron donors but are not known to take part in oxidoreductions, having no stable state which corresponds to the loss of a pair of electrons.

* The Pullmans denoted this value by "K." This connotation leads to confusion with the so-called "K" region of carcinogenic hydrocarbons. For this reason, we proposed, earlier, to supplant the letter "K" by "P."

[1] Mulliken, R. S., *J. Phys. Chem.*, **56**, 801 (1952).

[2] Isenberg, I., A. Szent-Györgyi, and S. L. Baird, Jr., these PROCEEDINGS, **46**, 1307 (1960).

[3] Szent-Györgyi, A., and I. Isenberg, these PROCEEDINGS, **46**, 1334 (1960).

[4] Pullman, B., and A. Pullman, *Les Théories Électroniques de la Chimie Organique* (Paris: Masson, 1952).

[5] Pullman, A., and B. Pullman, *Cancérisation par des Substances Chimiques et Structure Moléculaire* (Paris: Masson, 1955).

[6] Szent-Györgyi, A., I. Isenberg, and S. L. Baird, Jr., these PROCEEDINGS, **46**, 1444 (1960).

[7] Dewar, M. J. S., *The Electronic Theory of Organic Chemistry* (Oxford: The Clarendon Press, 1952).

COMMENTARY ON PAPER BY SZENT-GYÖRGYI ET AL.

BY J. S. GRIFFITH

It is my wish to draw particular attention to the g value of 2.001 observed for the black precipitates and having an intensity high enough (10^{18}–10^{19} spins per gram) to require explanation yet very low compared with the limiting possibility of one (or two) per dimer.

First, let us realize that electron spin resonance from a dimer of a conjugated molecule with iodine is rather improbable. Such a dimer is most likely to have a singlet ground state. If, however, it were appreciably in a triplet state, this should be split in the absence of the magnetic field into its three components with separations larger than the magnetic field energy ($\sim$1 cm^{-1}) used in the resonance measurements. Spin-orbit coupling belonging to the iodine nuclei is one cause of this splitting, and hence resonance would be expected not to occur or at least to show a complicated signal. Finally, there is the possibility that there are two

effectively noninteracting unpaired electrons in the dimer. Again the magnetic field energy in the resonance experiment is our yardstick here and is too small to allow this to be likely.

This makes us look elsewhere for explanation of the ESR signal and I would like to suggest for consideration the possibility that the majority of the molecules of donor D and acceptor I_2 form a polymeric aggregate of which a particularly simple version would be

$$- - - D\ I_2\ D\ I_2\ D - - -.$$

Then this aggregate might accept or reject electrons from D (or I_2), thus creating isolated single molecules (or aggregated groups) having just one unpaired electron. A narrow g value near two from, for example, an isolated D^+ would not then be surprising; however, it suggests that one should look rather carefully for hyperfine structure to try to determine the precise nature of such a radical.

The suggested interpretation has the merits that it is consistent with

(1) The relatively low number of spins detected.

(2) The narrow g near the free-spin value.

(3) The black color of the precipitate, which is natural for such a polymeric highly-conjugated and "resonant" system.

(4) The fact that the donor-acceptor ratio is not quite unity.

(5) The view that the local interaction developed by the π system of the aromatic molecule is rather akin to a simple coordination by a particular carbon atom of the molecule, as set forth by another discussant (Dr. Closs). Facts (3) and, especially, (4) are far from compelling arguments, and I would not wish in any case that the interpretation given here be regarded as more than a natural suggestion in the light of the data given.

Finally, I would like to thank Dr. Szent-Györgyi for making available to me before the meeting preprints both of his lecture and of two other writings on this subject. I have quoted experimental data from all three of these.

---

*HYDROGEN ION EFFECTS IN HIGH-ENERGY PHOSPHATE REACTIONS**

BY ROBERT J. RUTMAN AND PHILIP GEORGE

JOHN HARRISON LABORATORY OF CHEMISTRY, UNIVERSITY OF PENNSYLVANIA

The *in vivo* reactions of the high-energy phosphate compounds, so important in biosynthesis, all occur in an aqueous environment. Usually this intracellular environment exerts a buffering action, with a pH near neutrality; and in most cases the individual reactions are best studied *in vitro* if the solutions are artificially buffered in this region, since this is often a necessary condition for the optimal action of specific enzymes.

The designation as a "high-energy" compound has a precise meaning only when it is used to distinguish the labile phosphates from the stable phosphates by their more favorable free energies of hydrolysis.[1, 2] To understand how intramolecular and intermolecular properties contribute to the favorable free-energy changes,

the same approach can be adopted as that employed for aqueous solution reactions in general.[3-5] These reactions are complicated in the sense that they can be resolved into a cycle comprising several successive simpler processes; and their outcome accordingly can be attributed to the interplay between the thermodynamic quantities that characterize each step.

The starting point is the gas phase reaction between uncharged species because it is the simplest; the enthalpy change is solely determined by bond energies[6] in reactants and products. But at biological temperatures the majority of the compounds concerned are solid or liquid; so, as a consequence, heats of evaporation and fusion enter into the computation of the enthalpy change. Furthermore, for the reaction in water, heats of solution of reactants and products come in as additional terms; and, finally, if the pH of the aqueous solution is such that groups in the reactants and products ionize, heats of ionization also have to be included. Although heats of ionization are small quantities, similar in magnitude to heats of fusion and solution, i.e., a few kcal/mole, they are themselves the result of extensive compensation between other heat terms which include a bond energy, and an electron affinity, the ionization potential of the hydrogen atom and heats of solvation of ionic species, which are all comparable in magnitude to bond energies, i.e., large quantities ranging from 50 to 315 kcal/mole.[3] In terms of this cycle of simple processes, many factors are thus reflected in the enthalpy change for an aqueous solution reaction; and the entropy change can likewise be considered in terms of the same fundamental steps.

However, for the majority of aqueous-solution reactions, including those of the phosphates, all these data are not yet available, and an assessment of the importance of each of the various factors cannot be made.[7] Nevertheless, if physicochemical bond energies are to be taken into account, a cycle of this kind incorporating the gas phase reaction is obligatory, and the one outlined above has proved to be the most useful in separating out and treating effects due to intramolecular forces and to intermolecular interactions. But although values are not at hand for the individual terms, their summations give the standard thermodynamic quantities, ΔH and ΔS, for the over-all reaction. In the case of the phosphate compounds, these are the quantities that determine whether the standard free energy change is favorable for the hydrolysis reaction, which is the important feature underlying the conservation and utilization of the free energy made available by oxidation processes. It thus becomes necessary to trace the connection between these standard quantities and the free energy change as it is customarily evaluated and used as the basis for the practical distinction between compounds of "high" and "low" energy.

An examination of the stoichiometry of the phosphate reactions at biological pH reveals that in some reactions the hydrogen ion is a product, while in others it is a reactant. Reference to Le Chatelier's principle leads to the conclusion that the low constant hydrogen ion concentration of the physiological environment serves as a favorable factor in the former reactions, and as an unfavorable factor in the latter. In a previous publication we showed how one of two general equations, relating the observed standard free energy change to more fundamental standard quantities, contains a term expressing the contribution of the hydrogen ion concentration as a driving or hindering force.[7]

The purpose of the present paper is to examine in more detail the influence of hydrogen ion in the hydrolysis of typical high- and low-energy phosphate compounds. Then we shall extend the discussion to cover transfer reactions, such as acyl group, amino acid, and sulfate activation, and the synthesis of RNA and DPN.[8-10]

The Standard Free Energy Change Expressed as an "Isotherm Equation" and as a "Chemical Potential Equation."—The purpose of the two equations will be illustrated with reference to the orthophosphate split of adenosine triphosphate (ATP); namely, its hydrolysis yielding adenosine diphosphate (ADP) and orthophosphate,

$$\text{ATP} + \text{H}_2\text{O} \longleftrightarrow \text{ADP} + \text{orthophosphate}. \tag{1}$$

The free energy of hydrolysis which characterizes ATP as a high-energy compound will be denoted by ΔF_{obs}, and although it has been determined by numerical computation from free-energy changes for a series of metabolic reactions, it is related to an "observed" equilibrium constant by the expression $\Delta F_{\text{obs}} = -RT \ln K_{\text{obs}}$. K_{obs} is the equilibrium constant for reaction (1) defined by the simple expression

$$K_{\text{obs}} = \frac{[\text{ADP}]_e \times [\text{orthophosphate}]_e}{[\text{ATP}]_e}, \tag{2}$$

where $[\text{ATP}]_e$, $[\text{ADP}]_e$, and $[\text{orthophosphate}]_e$ denote total concentrations of the species at equilibrium. The ionization of groups on reactant and products occurring in different pH regions leads, however, to hydrogen ion participating in the hydrolysis over most of the pH range from 0 to 14. Hence the complete stoichiometry can be represented by reaction (1) with the inclusion of the term ϕH^+, i.e.,

$$\text{ATP} + \text{H}_2\text{O} \longleftrightarrow \text{ADP} + \text{orthophosphate} + \phi H^+, \tag{3}$$

where the number ϕ assumes positive values in pH regions where H^+ is a product, and negative values in the regions where it is a reactant. The relationship between the equilibrium constant K', for reaction (3), and K_{obs} is given by the equation

$$K' = K_{\text{obs}} \times [H^+] \tag{4}$$

from which it follows, putting $\Delta F' = -RT \ln K'$, that

$$\Delta F_{\text{obs}} = \Delta F' + \phi RT \ln [H^+]. \tag{5}$$

This is the first of the two general equations relating ΔF_{obs} to fundamental standard thermodynamic quantities.

The second equation can be derived by setting up the expression for the equilibrium constant, K_0, for the hydrolysis involving the species present at an experimental hydrogen ion concentration of 1 molal. Since all species are in equilibrium at all pH values, this particular equilibrium will still be maintained even at pH values greater than 3 where the concentrations of the unionized species of reactants and products become progressively and vanishingly smaller. The relationship between K_0 and K_{obs} is given by the equation,

$$K_0 = K_{obs} \times f([H^+]), \tag{6}$$

where $f([H^+])$ denotes a complicated function expressing the fractions of reactant and product present in their unionized forms. Putting $\Delta F^0 = -RT \ln K_0$, the second general equation follows,

$$\Delta F_{obs} = \Delta F^0 + RT \ln f([H^+]). \tag{7}$$

The term $RT \ln f([H^+])$ can be regarded as a "free-energy increment" because it is the measure of the amount by which ΔF_{obs} changes from its value at $H = 1$ molal, i.e., ΔF^0, as a consequence of the reaction being carried out in a pH region where one or more groups have undergone appreciable ionization.

For brevity $[H^+]$ will simply be denoted by H from now on, and the two general equations thus become

$$\Delta F_{obs} = \Delta F' + \phi RT \ln H \tag{8}$$

and

$$\Delta F_{obs} = \Delta F^0 + RT \ln f(H). \tag{9}$$

The complete expressions for ϕ and $f(H)$ in the case of the orthophosphate split of ATP can be shown to be

$$\phi = \left\{\frac{K_1H^2 + 2K_1K_2H + 3K_1K_2K_3}{H^3 + K_1H^2 + K_1K_2H + K_1K_2K_3}\right\}_{ADP} + \left\{\frac{K_1H^2 + 2K_1K_2H + 3K_1K_2K_3}{H^3 + K_1H^2 + K_1K_2H + K_1K_2K_3}\right\}_{orthophosphate} - \left\{\frac{K_1H^3 + 2K_1K_2H^2 + 3K_1K_2K_3H + 4K_1K_2K_3K_4}{H^4 + K_1H^3 + K_1K_2H^2 + K_1K_2K_3H + K_1K_2K_3K_4}\right\}_{ATP} \tag{10}$$

and

$$f(H) = \left\{\frac{H^3}{H^3 + K_1H^2 + K_1K_2H + K_1K_2K_3}\right\}_{ADP} \times \left\{\frac{H^3}{H^3 + K_1H^2 + K_1K_2H + K_1K_2K_3}\right\}_{orthophosphate} \div \left\{\frac{H^4}{H^4 + K_1H^3 + K_1K_2H^2 + K_1K_2K_3H + K_1K_2K_3K_4}\right\}_{ATP}, \tag{11}$$

where K_1, K_2, etc., are the ionization constants of ADP, orthophosphate, and ATP specified by the respective subscripts outside the large brackets.

Both free-energy equations can be derived in a more sophisticated manner. Equation (9) incorporating Equation (11) can be regarded as a special application of the Van't Hoff Isotherm. Equation (8) follows directly by expressing ΔF_{obs} as the difference between the chemical potentials (partial molal-free energies) of products and reactants. Hence for convenience we shall refer to them as the "isotherm equation" and the "chemical potential equation" respectively.

The two equations have been most widely applied to inorganic and organic reactions, especially to oxidation-reduction processes, although usually not in any general form but with ϕ and $f(H)$ evaluated specifically for each individual case. Since ϕ and $f(H)$ are often very cumbersome functions, see for example equations (10) and (11), the simple form in which the general equations have now been expressed greatly facilitates discussion. Interest in the thermodynamics of the phosphate reactions has almost exclusively centered around the application of the isotherm equation over a limited range of pH about neutrality: although recently, as in our previous article,[7] the application was extended to cover the wider range from pH 0 to 14.[11] In contrast, the significance of the chemical potential equation has not been well recognized, and it has been put to little use.

Although superficially similar in form, the two equations serve very different purposes. The isotherm equation gives only the variation of ΔF_{obs} with pH; but the chemical potential equation, by its very nature, expresses also the composition of ΔF_{obs} in terms of the hydrogen ion concentration driving force, $\phi RT \ln H$, and $\Delta F'$, the net driving force arising from the other species present at each particular pH. The dissociation constants for all the ionization equilibria enter into both equations via ϕ and $f(H)$, but the underlying physical significance is different, and can be described in the following way. The isotherm equation expresses the progressive influence of ionization *on* the reaction as the pH is changed from 0 to, finally, pH 14. Unionized species (or whatever species are present at $H = 1$ molal) are taken as the starting point, and ionization is regarded as exerting its influence through incremental free energy changes. On the other hand the chemical potential equation expresses the participation of ionization *in* the reaction—thus emphasizing that $\Delta F'$ refers to the actual species physically present at each individual pH.

There is a clear distinction to be made between ΔF_{obs} and $\Delta F'$. Both are standard free-energy changes relating to the species of reactants and products actually present, but in the case of ΔF_{obs} the reference state for the hydrogen ion is the particular pH itself, so, from one pH to another, the "reference state" varies. On the other hand in the case of $\Delta F'$ the reference state remains constant, namely $H = 1$ molal. On both counts $\Delta F'$ is the more fundamental standard free-energy change, and it can be subdivided into standard enthalpy and standard entropy changes in the usual way

$$\Delta F' = \Delta H' - T\Delta S'. \tag{12}$$

This consideration of standard states is an important one since it can be argued that the values of $\phi RT \ln H$ and $\Delta S'$ are interrelated and dependent on the standard chosen for the hydrogen ion concentration. The standard state of 1 molal with the properties of an infinitely dilute solution, like that for the other participating species, is clearly the most rational choice. It will be recalled that this standard is implicit in the evaluation of ionization constants; and, on this basis, values of $\Delta S'$ for the phosphate reactions can straightway be assessed in the light of the well-established trend in the partial molal entropies of ionic species, whereby the values become progressively and substantially more negative as the charge on the ion increases. These points will be taken up in more detail in a later publication

dealing with theoretical aspects, where the inter-convertibility of the two free-energy equations will also be demonstrated.

Application of the Equations to the Orthophosphate Split of ATP.—For reactions such as the orthophosphate split of ATP, where there are several ionizing groups on both products and reactant, the pH variations of ΔF_{obs}, ϕRT ln H and $\Delta F'$ are quite intricate (see Fig. 1). This behavior is due to opposing effects resulting

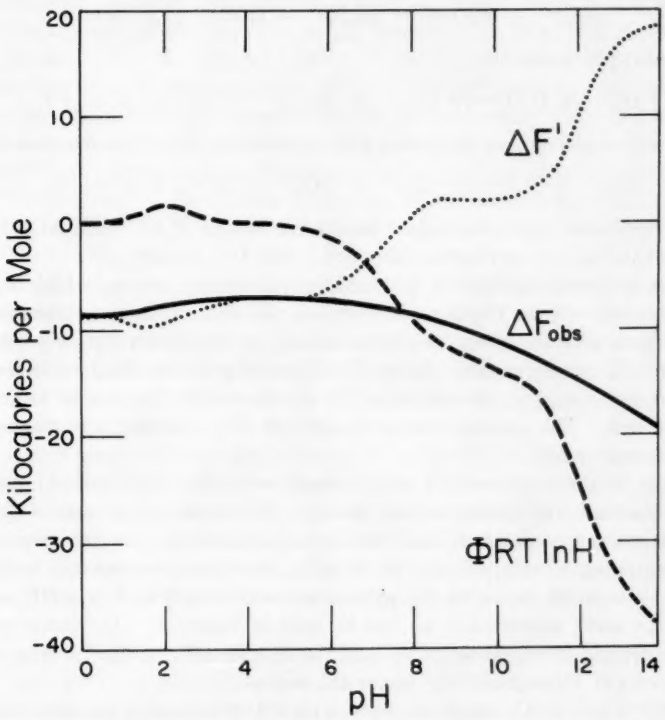

FIG. 1.—The pH variation of ΔF_{obs}, $\phi RT \ln H$ and $\Delta F'$ for the hydrolysis of ATP, ATP + $H_2O \rightleftharpoons$ ADP + orthophosphate.

from product and reactant ionizations compensating to a greater or lesser extent according to the detailed equations for ϕ and $f(H)$, i.e., Equations (10) and (11).

It can be seen that in the pH region from 0 to 7 extensive compensation occurs between all four ionizations of the phosphate groups in ATP, on the one hand, and the three phosphate ionizations of ADP together with the first ionization of orthophosphoric acid on the other. The initial effect between pH 1 and 3 is due to the first three ionizations of ATP, which, because they are ionizations on the reactant, lead to less favorable values of ΔF_{obs}, less favorable values of ϕRT ln H, but more favorable values of $\Delta F'$. However, as pH is increased, this effect is soon counteracted by the first two ionizations of ADP and the first ionization of orthophosphoric acid. Beyond pH 7 the second and third ionizations of orthophosphoric

acid, for which there are no further ionizations on the reactant that can compensate, finally dominate the reaction.

In the pH regions where it happens that both reactant and products are almost exclusively present as single species, $\Delta F'$ is constant, and the quantity, $(\Delta F' - \Delta F^0)$, is equal to the difference between the standard free-energy changes for those ionizations on the products and the reactant which are complete. In Figure 1 two such regions are well defined: between pH 4 and 5 the hydrolysis is simply,

$$\mathrm{atpH^{3-}} + \mathrm{H_2O} \longleftrightarrow \mathrm{adpH^{2-}} + \mathrm{H_2PO_4^{1-}}, \text{ i.e., } \phi = 0 \qquad (13)$$

and between pH 9 and 10,

$$\mathrm{atp^{4-}} + \mathrm{H_2O} \longleftrightarrow \mathrm{adp^{3-}} + \mathrm{HPO_4^{2-}} + \mathrm{H^+}, \text{ i.e., } \phi = +1. \qquad (14)$$

Another such region is just reached in alkaline solution where the reaction becomes,

$$\mathrm{atp^{4-}} + \mathrm{H_2O} \longleftrightarrow \mathrm{adp^{3-}} + \mathrm{PO_4^{3-}} + 2\mathrm{H^+}, \text{ i.e., } \phi = +2. \qquad (15)$$

In these equations, $\mathrm{atp^{4-}}$ and $\mathrm{adp^{3-}}$ denote the anions of ATP and ADP in which the phosphate moiety carries the charges 4− and 3−, respectively.

Another important feature of the chemical potential equation, which is brought out particularly well in Figure 1, is that in a pH region where a single ionization predominates, $\phi RT \ln H$ makes a substantially greater contribution to ΔF_{obs} the higher the pK: viz., a greater change is associated with the third ionization of the orthophosphoric acid in the pH range 11–13 than with the second ionization in the range 6–8. The greater change in $\phi RT \ln H$ is likewise accompanied by a greater change in $\Delta F'$.

However, in the biological pH region about neutrality, mixtures of ionic species of both reactant and products are present. The final ionizations of ATP and ADP are not quite complete, and the second ionization of orthophosphoric acid is just beginning to take effect. While ΔF_{obs} becomes progressively more favorable only to a small extent as the pH is increased from 6 to 8, ϕ, $\phi RT \ln H$, and $\Delta F'$ change quite appreciably, as can be seen in Figure 1. The make-up of the chemical driving force, in terms of $\phi RT \ln H$ and $\Delta F'$, is thus a very sensitive function of pH throughout the biological region.

At pH 7.5 and 25°C, which we have adopted as reference experimental conditions for ΔF_{obs}, the value for the ATP reaction is −8.3 kcal/mole,[7, 12] and the individual values of $\Delta F'$, $\phi RT \ln H$ and $RT \ln f(H)$ from Figure 1 are:

$$\Delta F_{obs} = \Delta F' + \phi RT \ln H$$

$$-8.3 = -1.3 - 7.0$$

$$\Delta F_{obs} = \Delta F^0 + RT \ln f(H)$$

$$-8.3 = -8.9 + 0.6.$$

From the experimentally determined value of $\Delta H'$, −4.8 kcal/mole,[7] $T\Delta S'$ is calculated:

$$\Delta F' = \Delta H' - T\Delta S'$$

$$-1.3 = -4.8 + 3.5.$$

Adopting likely values for the unknown heats of ionization for ATP and ADP, which in any case cancel to a large extent, ΔH^0 is found to be about -5.2 kcal/mole, so an estimate of $T\Delta S^0$ can be obtained:

$$\Delta F^0 = \Delta H^0 - T\Delta S^0$$

$$-8.9 = -5.2 - 3.7.$$

Certain features of these data call for comment. First, there is the very substantial contribution of $\phi RT \ln H$ to ΔF_{obs}, namely -7.0 in a total of -8.3 kcal/mole. On the basis of the 1 molal solution as the standard state for hydrogen ion, the factor very largely responsible for the "high-energy" nature of the reaction at pH 7.5 is thus the driving force associated with the production of H^+ in the buffered environment. Secondly, the participation of ionic species in the reaction, apart from the effect of hydrogen ion, is distinctly unfavorable, the quantity $(\Delta F' - \Delta F^0)$ being $+7.6$ kcal/mole. This is very largely due to the adverse trend in the entropy change, i.e. $-(T\Delta S' - T\Delta S^0) = +7.2$ kcal/mole, so that $(\Delta S' - \Delta S^0) = -24$ e.u.

At first sight it might appear that since ΔF_{obs} and ΔF^0 are very nearly equal, the influence of ionization through the interplay of $\phi RT \ln H$, $\Delta F'$, and $RT \ln f(H)$ terms is merely one of restoring an inherent and specific "high-energy" feature associated with the orthophosphate split. However, this is true only as far as the *magnitude* of the observed free energy of hydrolysis is concerned: the *make-up* of ΔF^0, which is simply ΔF_{obs} at the experimental hydrogen ion concentration of 1 molal, is profoundly different from that of ΔF_{obs} at pH 7.5; just as throughout the biological pH range itself there is a change in the make-up of ΔF_{obs} of comparable magnitude. It is an interesting feature that the compensation between the effects due to the ionization of the phosphate groups of ATP, ADP, and orthophosphoric acid is able to maintain ΔF_{obs} within fairly narrow limits over a wide pH range, even though there are these drastic changes in the nature of the chemical driving force.

Application of the Equations to Other Phosphate Hydrolyses.—If the reactant and product have different pK values from those of ATP and ADP, it is only to be expected that in some cases ΔF^0 will no longer approximate to ΔF_{obs} at the experimental reference pH of 7.5, and, furthermore, ΔF_{obs} will be made up of $\phi RT \ln H$ and $\Delta F'$ terms in an altogether different fashion. This conclusion is amply illustrated by the data for 14 other hydrolyses presented in Table 1. In two cases, reactions (a) and (g), ΔF_{obs} differs from ΔF^0 by as much as 9 kcal/mole; and the contribution of $\phi RT \ln H$ ranges from the highly favorable value of -20.1 kcal/mole for (a), (c), (d), and (g) to unfavorable values of more than $+2$ kcal/mole for (f), (j), (n) and (p).

The reactions have been listed in order of decreasingly favorable values of ΔF_{obs}, and it is immediately apparent that on the basis of either $\Delta F'$ or ΔF^0 the ranking is changed, and, in fact, with $\Delta F'$ as the standard, the position of the "high-energy" compounds ATP and ADP is reversed with respect to the "low-energy" mono-ester phosphates, AMP, and glycerol-2-phosphate. The reversal is due to the $\phi RT \ln H$ contribution assuming an unfavorable value of $+3.2$ kcal/mole, as for example in the case of AMP hydrolysis, compared to the substantially

TABLE 1

STANDARD FREE-ENERGY DATA FOR HYDROLYSIS, pH 7.5, 25°C (kcal/mole)

Reaction	ΔF_{obs}	ϕ	$\phi RT \ln H$	$\Delta F'$	$RT \ln f(H)$	ΔF^0	$(\Delta F - \Delta F^0)$	Reference
a. APS + H_2O = AMP + Sulf	−16.7	+1.97	−20.1	+3.4	−9.6	−7.1	+10.5	13
b. RNA·AA + H_2O = RNA + AA	−14.7	+1.0	−10.2	−4.5	−7.4	−7.3	+2.8	14, 15, 16
c. AMP·Ac + H_2O = AMP + Ac	−14.5	+1.97	−20.1	+5.6	−5.8	−8.7	+14.3	17, 18
d. DPN + H_2O = NMN + AMP	−14.4	+1.96	−20.1	+5.7	−2.0	−12.4	+18.1	19
e. ATP + H_2O = AMP + Pyro	−14.0	+0.96	−9.8	−4.2	−1.9	−12.1	+7.9	7
f. PEP + H_2O = Pyr + Ortho	−13.7	−0.28	+2.9	−16.6	−1.1	−14.8	−1.8	7
g. AMP·AA + H_2O = AMP + AA	−13.2	+1.97	−20.1	+6.9	−9.3	−3.9	+10.8	14, 15, 16
h. Acetyl · P + H_2O = Ac + Ortho[1]	−11.3	+0.64	−6.6	−4.7	+0.9	−12.2	+7.5	20
j. Cr·P + H_2O = Cr + Ortho	−10.6	−0.34	+3.5	−14.1	+5.1	−15.7	+1.6	7
k. ATP + H_2O = ADP + Ortho	−8.3	+0.68	−7.0	−1.3	+0.6	−8.9	+7.6	7, 12
l. ADP + H_2O = AMP + Ortho	−7.8	+0.67	−6.9	−0.9	−0.8	−7.0	+6.1	7
m. RNA·AMP + H_2O = RNA + AMP[2]	−7.3	+0.97	−9.9	+2.6	−2.1	−5.2	+7.8	21
n. AMP + H_2O = Ad + Ortho	−3.0	−0.31	+3.2	−6.2	+2.9	−5.9	−0.3	7
p. Glyc·2·P + H_2O = Glyc + Ortho	−2.4	−0.22	+2.2	−4.6	+1.7	−4.1	−0.5	7
q. Pyro + H_2O = 2 Ortho	−2.1	+0.41	−4.2	+2.1	+1.7	−3.8	+5.9	7

[1] This new value has been calculated from the data for the reaction: ATP + Acetate = Acetyl-P + ADP (Ref. 13), and reaction k of the Table, with corrections to pH 7.5 and replaces the older value of −13.9 kcal/mole.[7]
[2] Analysis of reaction (m) indicates that the primary ionizations (pK ~ 1.0) of both reactant and product RNA have a negligible effect on the ΔF_{obs} for the reaction at pH 7.5.

favorable value of −7.0 kcal/mole for the ATP reaction—the difference, namely 10.2 kcal/mole, exceeding that between the values of ΔF_{obs}, i.e., about 7.6 kcal/mole. The change in the $\phi RT \ln H$ contribution arises simply through the different values and different distribution of pK's in reactant and product.

$$\begin{array}{lcccc} & \text{ATP} & + H_2O \rightleftarrows & \text{ADP} + \text{orthophosphate} & (16) \\ \text{phosphate pK's:} & 1,1,2,6.5 & & 1,2,6.3 \quad 2.1,7.2,12 & \end{array}$$

$$\begin{array}{lcccc} & \text{AMP} & + H_2O \rightleftarrows & \text{Adenosine} + \text{orthophosphate.} & (17) \\ \text{phosphate pK's:} & 1,6.1 & & \text{None} \quad 2.1,7.2,12 & \end{array}$$

At pH 7.5, where the compensation between the strong ionizations on reactant and products in both reactions is complete, the secondary ionizations of the terminal phosphate groups in ATP and ADP also compensate, and the ATP hydrolysis is dominated by the favorable pK 7.2 ionization of the product orthophosphoric acid. On the other hand the AMP hydrolysis is dominated by the unfavorable pK 6.1 ionization of the reactant, the effect of which is not yet counteracted by the favorable pK 7.2 ionization of the orthophosphoric acid. As a consequence, hydrogen ion participates as a product in the ATP reaction but as a reactant in the AMP reaction, the values of ϕ being +0.68 and −0.31, respectively. Over the whole pH range the variations of ΔF_{obs}, $\phi RT \ln H$, and $\Delta F'$ for the AMP hydrolysis follow an entirely different course, as can be seen by comparing Figures 1 and 2.

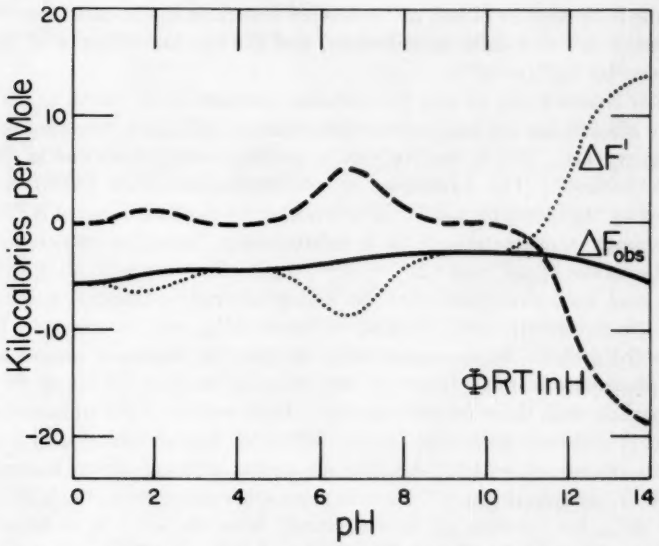

FIG. 2.—The pH variation of ΔF_{obs}, $\phi RT \ln H$, and $\Delta F'$ for the hydrolysis of AMP, AMP + $H_2O \rightleftharpoons$ Adenosine + orthophosphate

However, in the majority of the reactions in Table 1 hydrogen ion participates as a product, because there are uncompensated product ionizations with pK < 8.5 as in the ATP hydrolysis. For these reactions, namely (a) to (e), (g), (h), (k) to (m), and (q), the favorable values of ΔF_{obs} are either mainly or completely a consequence of the favorable ϕRT ln H term. The differences ($\Delta F'$ − ΔF^0) are positive, and are likewise attributable to the predominance of adverse partial molal entropies of the product species. But although most of the "high-energy" compounds come into this category, an especially favorable contribution from the ϕRT ln H term at biological pH is not a prerequisite for this class of compound. For the hydrolysis of phosphoenol pyruvate and creatine phosphate, reactions (f) and (j), its contribution is unfavorable, and for acetyl phosphate, reaction (h), it amounts to approximately half that of ΔF_{obs}.

The chemical equations (16) and (17) illustrate a point of wide significance. The extent to which compensation occurs between the ionization of groups in reactant and products is determined by the sets of pK values, and these, in turn, depend on the interrelated structural types to which the reactant and products belong. This is the reason for the absence of any simple correlation between the kind of bond broken in the reactant and the thermodynamic quantities in Table 1. For example, comparing reactions (c) and (h), both involve the rupture of a mixed anhydride bond between acetate and phosphate; but the reactants differ in structural type. Acetyl adenylate is also a phosphate ester, so that while in reaction (h) the products are acetate and free orthophosphoric acid, in reaction (c) the products are acetate and a mono-ester phosphate. The approximately equal values of ΔF_{obs} might be taken to indicate the "equivalence" of the mixed anhydride bonds. However, reaction (c) is favored only because of the favorable ϕRT ln H

term, while both $\phi RT \ln H$ and $\Delta F'$ terms are favorable in the case of reaction (h). The values of ΔF^0 also differ considerably, and likewise the influence of ionization, as expressed by $(\Delta F' - \Delta F^0)$.

A similar contrast can be seen in a detailed comparison of reactions (a) and (e), which are alike in having highly favorable values of ΔF_{obs} and involving the split of an acid anhydride. But in the first case it is a hetero-anhydride and in the second a homo-anhydride. The hydrolysis of adenylphosphosulfate (APS) is entirely dominated by the favorable $\phi RT \ln H$ term, whereas the hydrolysis of ATP yielding pyrophosphate is characterized by a substantially favorable contribution from $\Delta F'$. The values of ΔF^0 and $(\Delta F' - \Delta F^0)$ again show corresponding differences.

It has long been recognized that the highly favored hydrolyses of the acid anhydrides are not exceptional. Similar values of ΔF_{obs} are, for example, found for reactions (b) and (f) which respectively involve the fission of amino acid-ester and enolphosphate bonds. However, the data for reaction (b) afford an interesting comparison with those for reaction (g). Both reactants are amino acid derivatives, but of different structural types. RNA-AA has an amino acid-3′(2′)-ester linkage to ribose, while AMP-AA has an amino acid-anhydride linkage to the nucleotide-5′-phosphate group. As with some other anhydrides, the high favorable value of ΔF_{obs} for reaction (g) arises entirely from the $\phi RT \ln H$ term: $\Delta F'$ is unfavorable, ΔF^0 has a low favorable value, and $(\Delta F' - \Delta F^0)$ is very unfavorable. On the other hand $\Delta F'$ and ΔF^0 for reaction (b) are quite favorable, and $(\Delta F' - \Delta F^0)$ is much less unfavorable.

These several examples demonstrate very clearly how the chemical nature of the products, as well as the reactants, determine the thermodynamic data for the hydrolyses. The reactions have to be considered in their entirety.

Application of the Free-Energy Equations to Group Transfer Reactions.—Since the primary mechanism for the conservation of free energy in biological systems is the coupling of oxidation to the phosphorylation of ADP, it follows that in the utilization of this free energy to drive what would otherwise be thermodynamically unfavorable reactions a structural unit of ATP must be transferred to an acceptor molecule. The newly formed molecule may be either an intermediary in a biosynthetic pathway or its final product. In any event, the reaction(s) by which it is formed can be viewed as the composite of two or more hydrolysis reactions. In this manner the data in Table 1 provide a basis for analyzing the driving force in the more complex metabolic reactions listed in Tables 2 and 3.

Many of the transfer reactions in Table 2 involve either the split of orthophosphate or pyrophosphate from ATP, so the data for the two pathways of ATP hydrolysis take on a particular significance. Reactions (k) and (l) of Table 1, in which orthophosphate is split from ATP and ADP, are virtually identical with ΔF_{obs} values of -8.3 and -7.8 kcal/mole, respectively. According to present estimates, ΔF_{obs} for the hydrolysis of inorganic pyrophosphate (reaction 9) is about -2.1 kcal/mole.[7] From these values, ΔF_{obs} for the hydrolysis of ATP yielding pyrophosphate, reaction (e), is obtained.

$$\begin{aligned} \Delta F_{obs}\,(e) &= \Delta F_{obs}\,(k) + \Delta F_{obs}\,(l) - \Delta F_{obs}\,(q) \\ &= -8.3 \qquad -7.8 \qquad -(-2.1) = -14.0 \text{ kcal/mole} \end{aligned}$$

The split of pyrophosphate from ATP would thus contribute to the over-all driving

TABLE 2

STANDARD FREE-ENERGY DATA FOR TRANSFER REACTIONS, pH 7.5, 25°C (kcal/mole)

Reaction	Component hydrolysis reactions[1]	ΔF_{obs}	ϕ	$\phi RT \ln H$	$\Delta F'$	$RT \ln f(H)$	ΔF^0	$(\Delta F - \Delta F^0)$
a. DNA + ATP = DNA·AMP + Pyro	e and m[2]	−6.7	−0.01	−0.1	−6.8	+0.2	−6.9	+0.1
b. Pyr + ATP + PEP + ADP	k and f	+5.4	+0.96	−9.9	+15.3	+1.7	+5.9	+9.4
c. APS + ATP = PAPS + ADP	k and n[3]	−5.3	+0.99	−10.2	+4.9	−2.3	−3.0	+7.9
d. Ac + ATP = Acetyl · P + ADP	k and h	+3.0	+0.04	−0.4	+3.4	−0.3	+3.3	+0.1
e. Sulf + ATP = APS + Pyro	e and a	+2.7	−1.01	+10.3	−7.6	+7.7	−5.0	−2.6
f. Cr + ATP = Cr·P + ADP	k and j	+2.3	+1.04	−10.6	+12.9	−4.5	+6.8	−6.1
g. AMP·AA + RNA = RNA·AA + AMP	g and b	+1.5	+0.97	−9.9	+11.4	−1.9	+3.4	+8.0
h. AA + ATP = AMP·AA + Pyro	e and g	−0.8	−1.0	+10.3	−11.1	+7.3	−8.1	−3.0
j. AMP + ATP = 2 ADP	k and l	−0.5	+0.07	−0.1	−0.4	+1.4	−1.9	+1.5
k. RNA + ADP = RNA·AMP + Ortho	l and m	−0.5	−0.30	+3.1	−3.6	+1.3	−1.8	−1.8
l. Ac + ATP = AMP·Ac + Pyro	e and c	+0.5	−1.01	+10.3	−9.8	+3.9	−3.4	−6.4
m. NMN + ATP = DPN + Pyro	e and d	+0.4	−1.00	+10.2	−9.9	+0.1	+0.3	−10.2

[1] Reactions listed in Table 1.
[2] On the assumption that the data of reaction m, Table 1, for RNA·AMP are applicable to the hydrolysis of DNA·AMP.
[3] On the assumption that the data for reaction n of Table 1 for the hydrolysis of a mono-ester-phosphate are applicable to the hydrolysis of the 3′-phosphate of PAPS (see footnotes g and h, Table 11, reference 7).

TABLE 3

STANDARD FREE-ENERGY DATA FOR TWO STEP REACTIONS, pH 7.5, 25°C (kcal/mole)

Reaction	Component hydrolysis reactions	ΔF_{obs}	ϕ	$\phi RT \ln H$	$\Delta F'$	$RT \ln f(H)$	ΔF^0	$(\Delta F - \Delta F^0)$
a. NMN + 2 ATP = NTP + ADP + Pyro	d, e, k, n[1]	−4.9	+0.01	+0.1	−5.0	−2.2	−2.7	−2.3
b. Sulf + 2 ATP = PAPS + ADP + Pyro	a, e, k, n[1]	−2.6	−0.02	+0.1	−2.7	+5.4	−8.0	+5.3
c. RNA + AA + ATP = RNA·AA + AMP + Pyro	b, e, g	+0.7	−0.04	+0.4	+0.3	+5.5	−4.8	+5.1

[1] On the assumption that the data for the formation of a mono-ester-phosphate apply to the 3′-phosphorylation of DPN (see footnote 2 of Table 1).

force in a transfer reaction nearly twice the free energy of the orthophosphate split; and, since AMP and also pyrophosphate on this reckoning are "low-energy" compounds, the pyrophosphate split would entail the expense of nearly all the utilizable free energy.

With one exception the reactions in Table 2 involve the transfer of nucleotide or phosphate moieties from ATP or ADP to another metabolite; and the more complicated reactions listed in Table 3 result from combinations of these transfer reactions. Both sets of data show the same general features as the hydrolyses in Table 1. But because of the compensatory nature of the pairs of component reactions, which are noted in the second columns of Tables 2 and 3, the variation among the values of ΔF_{obs} is somewhat more limited. In many cases the value is near zero, so that appreciable amounts of both products and reactants would

be present at equilibrium. These are the reactions which are readily reversible in practice.

With respect to the component hydrolyses the transfer reactions can be regarded as a higher level of chemical organization, since one reaction serves to "drive" the other. From this standpoint it is interesting to note that there are very varied patterns of interaction between the thermodynamic quantities $\phi RT \ln H$, $\Delta F'$, $RT \ln f(H)$, and ΔF^0 for the component reactions, even though taken together, according to the two free-energy equations, the over-all effect tends to be one of compensation leading to low values of ΔF_{obs} as pointed out above.

The various patterns of interaction will be illustrated chiefly with reference to the $\phi RT \ln H$ term, to bring out once again the important role of the hydrogen ion concentration as a driving force. In reactions (a), (d), and (j) of Table 2, $\phi RT \ln H$ is nearly zero and so from the point of view of the over-all reaction the hydrogen ion driving force is negligible. Nevertheless it plays a hidden role in that almost equal and opposite $\phi RT \ln H$ terms of a sizeable magnitude are involved in the component reactions, namely, -10, -7, and -7 kcal/mole, respectively. In these cases a balanced hydrogen ion cycle thus occurs. In addition, there is almost complete cancellation between the $RT \ln f(H)$ terms, and hence ΔF_{obs}, $\Delta F'$, and ΔF^0, respectively, for these particular transfer reactions are very similar in magnitude: furthermore the influence of ionization, as expressed by $(\Delta F' - \Delta F^0)$, is remarkably small.

On the other hand in reactions (e), (g), (h), (l), and (m) an unbalanced hydrogen ion cycle occurs; about two hydrogen ions are involved in one hydrolysis and about one hydrogen ion in the other, resulting in the participation of one hydrogen ion in the over-all transfer. Yet in the majority of cases, unlike the individual hydrolyses in Table 1, hydrogen ion is a reactant, and the $\phi RT \ln H$ term is therefore unfavorable. The influence of ionization shows the expected trends. When H^+ is a reactant, i.e., reactions (e), (h), (l), and (m), $(\Delta F' - \Delta F^0)$ is favorable; whereas when H^+ is a product, i.e., reaction (g), $(\Delta F' - \Delta F^0)$ is unfavorable. As in the hydrolysis reactions entropy effects probably predominate.

In contrast to these two groups of transfer reactions in which almost complete cancellation or extensive compensation occurs between the $\phi RT \ln H$ terms for the component hydrolyses, reactions (b), (c), and (f) exhibit an altogether different feature, namely, the augmentation of $\phi RT \ln H$ terms. In all three cases this augmentation results in the participation of about one hydrogen ion as a product, so the $\phi RT \ln H$ term is large in magnitude, about -10 kcal/mole. The resemblance, however, goes no further: inherent differences in the values of ΔF^0 and $RT \ln f(H)$ for the individual hydrolyses lead to no regularity in the over-all values of $(\Delta F' - \Delta F^0)$.

At the next higher level of chemical organization, represented by the more complex metabolic reactions in Table 3 where one transfer reaction is utilized to "drive" another, the pattern of interaction between the various thermodynamic quantities is inevitably even more complicated. The net effect, however, is often quite simple. For example, in the synthesis of PAPS and RNA-AA, reactions (b) and (c), the values of ΔF^0 are substantially negative, favoring equilibrium positions far to the right. But the free-energy increments $RT \ln f(H)$ are comparable in magnitude and of opposite sign to ΔF^0, so the resulting values of ΔF_{obs}

are much nearer zero, favoring the type of equilibrium that leads to ready reversibility in practice.

Balanced and unbalanced hydrogen ion cycles are again involved in these more complex reactions. For example reaction (b), in which the components are the transfer reactions (e) and (c) of Table 2, demonstrates particularly well how the unfavorable effect due to the consumption of one hydrogen ion in the first step is almost exactly compensated by the driving force due to the release of a hydrogen ion in the second:

First step:

$$H^+ + \text{atp}^{4-} + SO_4^{2-} \longleftrightarrow \text{aps}^{2-} + HP_2O_7^{3-}$$
$$\Delta F_{obs} = +2.7,\ \Delta F' = -7.6,\ \phi RT \ln H = +10.3 \text{ kcal/mole}$$

Second step:

$$\text{aps}^{2-} + \text{atp}^{4-} \longleftrightarrow \text{paps}^{4-} + \text{adp}^{3-} + H^+$$
$$\Delta F_{obs} = -5.3,\ \Delta F' = +4.9,\ \phi RT \ln H = -10.2 \text{ kcal/mole}$$

Over-all reaction:

$$2\text{atp}^{4-} + SO_4^{2-} \longleftrightarrow \text{paps}^{4-} + HP_2O_7^{3-} + \text{adp}^{3-}$$
$$\Delta F_{obs} = -2.6,\ \Delta F' = -2.7,\ \phi RT \ln H = +0.1 \text{ kcal/mole}$$

Although data for the over-all reactions may thus be somewhat nondescript, the interplay between the driving forces of the component reactions may nevertheless involve substantially greater quantities.

Conclusions.—The very important role of hydrogen ion in phosphate hydrolyses, group transfers and more complicated biosynthetic processes is first apparent when the need arises to specify exactly their complete stoichiometry. If the one molal standard reference state is adopted for the hydrogen ion, in keeping with other aqueous solution reactions, the standard free-energy change as it is customarily evaluated can then be expressed in the form of either an "isotherm equation" or a "chemical potential" equation. The second is of more direct physical significance, because it affords a quantitative measure of the chemical driving force arising from the prevailing hydrogen ion concentration on the one hand, and from the rest of the species actually present at the pH concerned on the other. A significant feature of these reactions, which only appears when the second equation is taken into account, is that in certain cases the observed standard free-energy change is maintained within fairly narrow limits over a wide range of pH, even though drastic alterations occur in its make-up as the result of groups ionizing in reactants and products.

In practice metal ions, especially Mg^{2+}, also play a very important role. From the point of view of kinetics, they are essential components of the enzyme systems. From the point of view of thermodynamics, their participation amounts to the introduction of ancillary equilibria, whose influence is similar in principle to that of the ionization equilibria. Anions of the reactants and products are common to both reactions: the hydrogen ion combining in the one case, and the metal ion in the other. Diagrams could be constructed, resembling Figures 1 and 2, showing how, at constant pH, ΔF_{obs} varies with the metal ion concentration; and, with

a three-dimensional diagram, the simultaneous variation of ΔF_{obs} with both pH and metal ion concentration could be demonstrated.

Just as extensive compensation can occur between the effects due to ionization of reactants and products, so, in certain cases, extensive compensation can be envisaged between the effects due to metal ion complex formation, likewise resulting in relatively little change in the magnitude of ΔF_{obs}. The influence of Mg^{2+} on the orthophosphate split of ATP comes into this category, ΔF_{obs} changing by less than 2 kcal/mole.[12] However, even though the magnitude of ΔF_{obs} may be little affected, profound changes in $\phi RT \ln H$, $\Delta H'$, and $\Delta S'$ are to be expected when metal ion complexes are involved, just as these terms were found to change drastically when ionization occurred. An important factor contributing to any such change would undoubtedly be the favorable entropy of formation for this kind of metal ion complex, which is attributable to the effect of charge cancellation on solvated water molecules.

A more complete appreciation of these terms, which ultimately comprise the chemical driving force and so govern the conservation and utilization of free energy in metabolic processes, clearly depends on the experimental determination of all the missing thermodynamic data, not only for the reactions themselves, in the presence and in the absence of metal ions, but also for the associated ionization equilibria.

* This study forms part of a research program supported by grants from the National Science Foundation, G-7657, and the American Cancer Society Institutional Grant Im-38-B. The following abbreviations are used in the text and tables: ATP, adenosine triphosphate; ADP, adenosine diphosphate; AMP, adenosine monophosphate; Ad, adenosine; APS, adenosine phosphosulfate; PAPS, 3′-phospho-adenosinephosphosulfate; RNA, ribonucleic acid; AA, amino acid; RNA-AA, 3′-amino acid ester of RNA; Ac, acyl; AMP-Ac, Acyl adenylate; DPN, diphosphopyridine nucleotide; NMN, nicotinamide mononucleotide; Pyro, pyrophosphate; Ortho, orthophosphate; PEP, phosphoenolpyruvate; Pyr, pyruvate; Acetyl·P, acetyl phosphate; Cr·P, creatine phosphate; Cr, creatine; Glyc·2·P, glycerol-2-phosphate.

[1] Meyerhof, O., *J. Gen. Physiol.*, **8,** 531 (1927).

[2] Lipmann, F., *Advances in Enzymol.*, **1,** 99 (1941).

[3] Bell, R. P., *The Proton in Chemistry* (London: Methuen, 1959), pp. 90–92.

[4] Evans, M. G., and J. de Heer, *Quart. Revs. (London)*, **4,** 94 (1950).

[5] George, P., and D. S. McClure, *Progr. in Organic Chem.*, **1,** 381 (1959).

[6] Cotrell, T. L., *The Strengths of Chemical Bonds* (London: Butterworths, 1954) 1st ed.

[7] George, P., and R. J. Rutman, *Progr. in Biophys. and Biophys. Chem.*, **10,** 1 (1960).

[8] George, P., and R. J. Rutman, *Abstracts, Fourth Meeting of the Biophysical Society* (Philadelphia, 1960), p. 32.

[9] Rutman, R. J., and P. George, *Abstracts, Third Delaware Valley Regional Meeting, Am. Chem. Soc.* (Philadelphia, 1960), p. 27.

[10] George, P., and R. J. Rutman, *Federation Proc.*, **19,** 10 (1960).

[11] Carpenter, F. H., *J. Am. Chem. Soc.*, **82,** 1111 (1960).

[12] More recent work (Benzinger, Kitzinger, Hems, and Burton, *Biochem. J.*, **71,** 400 (1959)) suggests a value of −9.1 kcal/mole at pH 7.5, 25°C and I = 0.2: however, the older value of −8.3 kcal/mole for similar conditions (see reference 7) has been retained since the difference is small, and experimental data which would enable extrapolation to I = 0, giving the true thermodynamic value, are not yet available).

[13] Lipmann, F., *Science*, **128,** 575 (1958).

[14] Novelli, G. D., these PROCEEDINGS, **44,** 86 (1958).

[15] Berg, P., and E. J. Ofengand, these PROCEEDINGS, **44,** 78 (1958).

[16] Bergmann, F. H., P. Berg, J. Preiss, E. J. Ofengand, and M. Dieckmann, *Federation Proc.*, **18**, 191 (1959).
[17] Berg, P., *J. Am. Chem. Soc.*, **77**, 3163 (1955).
[18] Jencks, W. P., and F. Lipmann, *J. Biol. Chem.*, **225**, 207 (1951).
[19] Kornberg, A., *J. Biol. Chem.*, **182**, 779 (1950).
[20] Rose, I. A., M. Grunberg-Manago, P. J. Ortiz, and S. Ochoa, *J. Biol. Chem.*, **211**, 737 (1954).
[21] Grunberg-Manago, M., P. J. Ortiz, and S. Ochoa, *Science*, **122**, 907 (1955).

THE REQUIREMENT OF ENERGY FOR RESPIRATION IN MITOCHONDRIA (A COMMENTARY)

BY E. C. SLATER AND W. C. HÜLSMANN

LABORATORY OF PHYSIOLOGICAL CHEMISTRY, UNIVERSITY OF AMSTERDAM

It is well known that the passage of hydrogen atoms or electrons from substrate to oxygen, a reaction catalyzed by the mitochondria, is coupled with the production of energy in the form of ATP.* Chance and Hollunger[1] and Klingenberg, Slenczka, and Ritt[2] have recently demonstrated the reduction of pyridine nucleotide by succinate or glycerol phosphate and have interpreted this in terms of the utilization of energy to drive the electrons in the reverse direction, i.e. back towards substrate. Azzone and Ernster[3, 4] believe that oxidation of succinate by mitochondria requires the intervention of high-energy phosphate, necessary for the reaction of reduced succinic dehydrogenase with the respiratory chain.

We should like to discuss another sort of interaction between electron- and energy-transfer reactions in mitochondria, which can often be of considerable importance in experiments with isolated mitochondria—and perhaps also *in vivo*. Judging by the effects of dinitrophenol, it appears that energy is necessary for the removal of one of the products of the oxidation of Krebs-cycle substrates—oxaloacetate—which is a powerful inhibitor of two of the four oxidation steps of the cycle, namely at succinate and malate.

Dinitrophenol, in concentrations greater than about 30 μM, causes a progressive inhibition of the oxidation of succinate by rat-liver mitochondria.[5] In the presence of 2 mM Amytal, no inhibition was found even with 100 μM dinitrophenol.

A similar inhibition by dinitrophenol of the oxidation of succinate by rat-heart sarcosomes can be seen in Table 1 by comparing lines 1 and 5 of experiment 1. Amytal stimulates the oxidation of succinate (line 3—cf. also ref. 6) and prevents the inhibition by dinitrophenol (compare lines 3 and 7).

These results can be most simply explained on the assumption that the rate of oxidation of succinate is controlled by the steady-state concentration of oxaloacetate within the mitochondria[6, 7] and that this concentration is increased by dinitrophenol. Since it is known[8] that Amytal completely prevents the oxidation of malate and, therefore, the formation of oxaloacetate, the stimulation by Amytal of the oxidation of succinate and the lack of effect of dinitrophenol in the presence of Amytal are easily understandable on this basis. We shall now discuss the experimental evidence that dinitrophenol causes an increased steady-state concentration of oxaloacetate.

It has proved difficult reproducibly to demonstrate this accumulation by direct analysis. The amounts of oxaloacetate in a deproteinized reaction mixture after oxidation of succinate are very small (less than 0.01 μmole/mg mitochondrial protein). However, since the oxaloacetate would be formed within the mitochondria, perhaps in the vicinity of the succinic dehydrogenase, its effective concentration

TABLE 1

EFFECT OF ACETATE, DINITROPHENOL, OR AMYTAL ON OXIDATION OF SUCCINATE AND GLUTAMATE BY RAT-HEART SARCOSOMES

The reaction mixture contained (in 1 ml) 15 m*M* KCl, 2 m*M* ethylenediaminetetraacetate, 20 m*M* glucose, 30 m*M* phosphate buffer (pH 7.5), 25 m*M* Tris-HCl or Tris-acetate buffer (pH 7.5), 0.1 m*M* ATP, 5 m*M* $MgCl_2$, 50 m*M* sucrose, hexokinase, 0.8 mg sarcosomal protein and 20 m*M* succinate or 10 m*M* L-glutamate.
Reaction time, 20 min.
Temperature, 25°.

Experiment	Substrate	Acetate	Dinitrophenol (μ*M*)	Amytal (m*M*)	Δ O (μ atoms)
1	Succinate	*	—	—	2.0
	Succinate	†	—	—	3.1
	Succinate	*	—	1.4	3.6
	Succinate	†	—	1.4	3.7
	Succinate	*	50	—	1.0
	Succinate	†	50	—	1.0
	Succinate	*	50	1.4	3.3
	Succinate	†	50	1.4	3.1
2	Glutamate	*	—	—	2.1
	Glutamate	†	—	—	1.3

* Indicates that Tris-HCl buffer was used.
† Indicate that Tris-acetate buffer was used.

as an inhibitor could be several orders of magnitude greater. We have obtained the following indirect evidence that dinitrophenol causes the accumulation of oxaloacetate.

1. The addition of glutamate to rat-heart sarcosomes oxidizing succinate in the presence of arsenite (which completely prevents the oxidation of glutamate by these mitochondria) had very similar effects to Amytal, viz. a 2-fold increase of the oxygen uptake in the absence of dinitrophenol, a 3.2-fold increase in the presence of dinitrophenol. Glutamate almost completely prevented the inhibition of succinate oxidation by dinitrophenol. It is known that glutamate can remove oxaloacetate by transamination to aspartate

2. Succinate (70 m*M*) was allowed to be oxidized by rat-heart sarcosomes for 26 min, in one flask with 0.1 m*M* dinitrophenol, in the other without dinitrophenol. Glutamate (20 m*M*) and arsenite (0.5 m*M*) were then added, and the oxidation was allowed to proceed for a further 10 min, after which the reaction was stopped and aspartate determined on the deproteinized extract, by means of aspartate decarboxylase. 0.5 μmole was found with dinitrophenol, 0.15 μmole without. Thus, 3.5 times as much oxaloacetate became available from the oxidation of succinate for reaction with the transaminase in the presence as in the absence of dinitrophenol.

3. Table 1 shows that added acetate stimulates the oxidation of succinate by rat-heart sarcosomes but that this stimulation is not found in the presence of Amytal or of dinitrophenol. Experiment 2 shows that glutamate oxidation is inhibited by acetate Thus, in the absence of Amytal or dinitrophenol, acetate removes an inhibitor of succinate oxidation and a stimulator of glutamate oxidation. Oxaloacetate is the only substance known to the authors which both in-

hibits succinic dehydrogenase[9, 10] and is necessary for glutamate oxidation by rat-heart sarcosomes.[11, 12] The absence of an effect of acetate in the presence of Amytal also strongly suggests that, in the absence of Amytal, it exerts its effect on oxaloacetate, since the latter is not formed in the presence of Amytal. The effect of dinitrophenol is readily understandable, since, unless activated by ATP or other high-energy compounds, acetate is biochemically inert. It is probable that acetate is operative in the form of its coenzyme A compound.

Several possible mechanisms whereby acetyl-CoA could bring about the removal of oxaloacetate come to mind (cf. refs. 13 and 14).

$$\text{Acetyl-CoA} + \text{Oxaloacetate} \rightarrow \text{Citrate} + \text{CoA} \qquad (1)$$

$$\begin{aligned} &\text{Acetyl-CoA} + \text{Oxaloacetate} \rightarrow \text{Malonyl-CoA} + \text{Pyruvate} \\ &\text{Malonyl-CoA} \rightarrow \text{Acetyl-CoA} + CO_2 \\ \text{Sum:}\ &\text{Oxaloacetate} \xrightarrow{\text{(Acetyl-CoA)}} \text{Pyruvate} + CO_2 \end{aligned} \qquad (2)$$

$$\begin{aligned} &\text{Acetyl-CoA} + \text{Oxaloacetate} \rightarrow \text{Malonyl-CoA} + \text{Pyruvate} \\ &\text{Pyruvate} + \text{CoA} + O \rightarrow \text{Acetyl-CoA} + CO_2 \\ &\text{Malonyl-CoA} \rightarrow \text{Acetyl-CoA} + CO_2 \\ \text{Sum:}\ &\text{Oxaloacetate} + \text{CoA} + O \rightarrow \text{Acetyl-CoA} + 2\,CO_2 \end{aligned} \qquad (3)$$

In mechanisms (2) and (3), acetyl-CoA would play a catalytic role.

Some of the malonyl-CoA formed as intermediate in these mechanisms could be used for fat synthesis.[15] In fact, one of us[16] has recently demonstrated the incorporation of labeled acetate into the long-chain fatty acids of heart sarcosomes, coupled with the oxidation of succinate, malate, α-ketoglutarate, citrate, or isocitrate in the presence of ATP, coenzyme A, and TPNH. The incorporation with succinate was inhibited 66 per cent by Amytal. There was little incorporation in the absence of added substrate or with glutamate as substrate. These results strongly suggest that oxaloacetate formed by the oxidation of Krebs-cycle intermediates can, in the presence of acetate and a source of energy, be used for fat synthesis. The absence of fatty acid synthesis in the presence of glutamate, which is as rapidly oxidized as succinate, is particularly suggestive since, as already mentioned above, this is the substrate which removes oxaloacetate by transamination.[11, 12]

The amounts of acetate incorporated into the fatty acids are relatively small (about 3 mμmoles/mg protein/h), and it is doubtful if fat synthesis is quantitatively important in the effect of acetate in removing oxaloacetate. However, mechanisms (2) and (3), which also involve malonyl-CoA as an intermediate, might very well be important.

The question needs now to be discussed: what is the mechanism whereby dinitrophenol could cause an increased concentration of oxaloacetate within the mitochondria, in the absence of added acetate? Since the most characteristic property of dinitrophenol is its ability to uncouple oxidative phosphorylation, and the concentrations which inhibit succinate oxidation are about the same as those which uncouple, it is reasonable to assume that the increased accumulation of oxaloacetate is due to the effect of dinitrophenol on the concentration of ATP or other high-energy intermediates within the mitochondria. It should be em-

phasized, in this connection, that the experiments in Table 1 were carried out in the presence of excess hexokinase. If we are to explain the results on the basis of ATP formed by oxidative phosphorylation, it must be in terms of intramitochondrial ATP which can react either directly or indirectly with oxaloacetate before it reacts with hexokinase outside the mitochondria.

It appears unlikely that ATP promotes the removal of oxaloacetate by the reaction

$$\text{ATP} + \text{oxaloacetate} \xrightleftharpoons{(\text{GDP})} \text{CO}_2 + \text{phospho-enol-pyruvate} + \text{ADP}$$

since the enzyme catalyzing this reaction, phospho-enol-pyruvate carboxykinase,[17] has only a very low activity in rat heart.[18]

It is possible that endogenous fatty acids present in the mitochondrial preparation[2] give rise, in the presence of ATP, to acetyl-CoA which then promotes the removal of oxaloacetate by one or more of the three mechanisms considered above.

In conclusion, these experiments and those of Chance[1] and Klingenberg[2] suggest that the ATP formed by oxidative phosphorylation may have various effects on the electron transfer:

1. By promoting the removal of an inhibitory product, it can stimulate the flow of electrons along the respiratory chain in their normal direction towards oxygen.
2. It can drive the respiratory chain backwards.[1, 2]
3. Under the autocatalytic influence of endogenous fatty acids, ATP can be used to resynthesize long-chain fatty acids, a reduction requiring TPNH, which could be made, for example, via the DPNH formed by the Chance mechanism.

This work was supported in part by Research Grant No. 6569 from the U.S. Public Health Service.

*Abbreviations: ATP, adenosine triphosphate; ADP, adenosine diphosphate; CoA, coenzyme A; DPNH, reduced diphosphopyridine nucleotide; TPNH, reduced triphosphopyridine nucleotide; Tris, tris(hydroxymethyl)aminomethane.

[1] Chance, B., and G. Hollunger, *Fed. Proc.*, **16,** 163 (1957); *Nature*, **185,** 666 (1960).
[2] Klingenberg, M., W. Slenczka, and E. Ritt, *Biochem. Z.*, **332,** 47 (1959).
[3] Azzone, G. F., and L. Ernster, *Nature*, **187,** 65 (1960).
[4] Azzone, G. F., L. Ernster, and M. E. Klingenberg, *Nature*, **188,** 552 (1960).
[5] Borst, P., and E. C. Slater, *Biochim. et Biophys. Acta*, in press.
[6] Greengard, P., K. Minnaert, E. C. Slater, and I. Betel, *Biochem. J.*, **73,** 637 (1959).
[7] Tyler, D. B., *Fed. Proc.*, **16,** 130 (1957).
[8] Jalling, O., O. Lindberg, and L. Ernster, *Acta Chem. Scand.*, **9,** 198 (1955).
[9] Das, N. B., *Biochem. J.*, **31,** 1124 (1937).
[10] Keilin, D., and E. F. Hartree, *Proc. Roy. Soc.* (*London*), **B 129,** 277 (1940).
[11] Krebs, H. A., and D. Bellamy, *Biochem. J.*, **75,** 523 (1960).
[12] Borst, P., and E. C. Slater, *Biochim. et Biophys. Acta*, **41,** 170 (1960).
[13] Swick, R. W., and H. G. Wood, these PROCEEDINGS, **46,** 28 (1960).
[14] Utter, M. F., and D. B. Keech, *J. Biol. Chem.*, **235,** PC 17 (1960).
[15] Wakil, S. J., and J. Ganguly, *J. Am. Chem. Soc.*, **81,** 2597 (1959).
[16] Hülsmann, W. C., *Biochim. et Biophys. Acta*, **45,** 623 (1960).
[17] Utter, M. F., and K. Kurahashi, *J. Biol. Chem.*, **207,** 787, 803, 821 (1954).
[18] Utter, M. F., *Ann. N. Y. Acad. Sci.*, **72,** 451 (1959).

THE MOLECULAR WEIGHTS OF T2 BACTERIOPHAGE DNA AND ITS FIRST AND SECOND BREAKAGE PRODUCTS

By I. Rubenstein, C. A. Thomas, Jr., and A. D. Hershey

BIOPHYSICS DEPARTMENT, JOHNS HOPKINS UNIVERSITY, AND DEPARTMENT OF GENETICS, CARNEGIE INSTITUTION OF WASHINGTON

Communicated by A. D. Hershey, May 29, 1961

Recent evidence indicates that DNA molecules of uniform size and high molecular weight can be extracted from phage T2.[1, 2] Controlled degradation by stirring yields fragments tentatively identified as halves and quarters of the original molecules.[3] In previous work, these materials were partially characterized by physical methods, but their absolute molecular weights remained unknown.

Our purpose in the work reported here was threefold: to determine the size and number of DNA molecules per phage particle, to check these measurements against the putative half and quarter molecules (and vice versa), and to calibrate sedimentation coefficients for DNA in terms of molecular weight in a high molecular weight range previously unmeasurable. These objectives are pertinent to the organization of the phage "chromosome," which by genetic criteria is a single structure.[4]

We show below that, contrary to earlier indications,[2, 3] the particle of phage T2 contains indeed a single molecule of DNA of molecular weight at least 130 million. Some of our results are supported by those presented in the companion paper by Davison, Freifelder, Hede, and Levinthal.[5]

Our conclusions are reached by employing a method of molecular autoradiography.[6] When phage particles or DNA molecules labeled with P^{32} are embedded in a radiation-sensitive ("nuclear") emulsion, the emitted β-particles produce tracks which, emanating from a point source, give rise to characteristic figures recognizable as "stars." If it is assumed that every β-particle forms a track, counts of the average number of tracks per star measure the number of P^{32} atoms per particle and, depending on the specific radioactivity, the total phosphorus content per particle. Less accurately, the number of labeled particles can be measured from the ratio of stars to added polystyrene latex spheres.

Materials and Methods.—Escherichia coli strain H was grown for 2 hours with aeration at 36°C in 7 ml of a synthetic culture medium,[7] to which was added 0.2 mg/ml of bacteriological peptone and the required amount of radiophosphate (Squibb and Sons, 1,000 c/g). The total phosphorus content of the medium (about 3 μg/ml) was measured colorimetrically and the P^{32} content was determined by comparison with a standard P^{32} solution (calibrated by the National Bureau of Standards). After the bacterial mass had increased 10-fold and the number approached 10^8/ml, the culture was infected with three particles of phage T2H per bacterium. One hour later the culture was lysed by shaking with a few drops of $CHCl_3$ and digested serially for 10 minutes each with small quantities of deoxyribonuclease, ribonuclease, and pancreatin. After this treatment 10^{11}/ml of carrier phage, heavily irradiated with a germicidal lamp, were added and the lysate was filtered through a layer of analytical grade Celite on filter paper in a small Gooch crucible. A sample of the filtrate was diluted 10^6-fold in buffered peptone solution[8] for daily titration of surviving phage particles.

Five ml of the filtrate was mixed with 1.8×10^{13} purified unlabeled phage particles. An aliquot of this mixture was purified by centrifugation for assay of P^{32} and DNA contents, and for the star-size measurements of whole phage particles. The remainder of the mixture (2×10^{12} phage per ml) was shaken twice with phenol and five times with ether to yield 8 ml of DNA solution (about 0.4 mg/ml.)[9] The carrier phage provide a high concentration of DNA which serves to protect both the labeled and unlabeled molecules from breakage during extraction. Also, the

large excess of unlabeled molecules prevents the aggregation of labeled molecules which would distort the autoradiographic results.

Aliquots of the DNA solution were stirred under conditions ("5,000 rpm") expected to produce mainly half molecules, or ("9,000 rpm") to produce mainly quarter molecules.[3] Stirred and unstirred samples were then passed through separate fractionating columns[9] and the resulting fractions were analyzed spectrophotometrically for DNA content and by radioassay for P^{32} content. Fractions were selected for embedding in the nuclear emulsion.

It should be noted that the procedure described avoids purification of radioactive phage particles before extraction of the DNA and relies on the column to effect final purification. This procedure prevents possible radiation damage to phage particles packed in the centrifuge, shortens the time required to get the DNA into the emulsion, and undoubtedly removes some broken or radiation-damaged DNA from the preparations.[9] We observed that the labeled DNA does in fact fragment at an appreciable daily rate, dependent on specific radioactivity, even when stored at effectively infinite dilution. In the experiments reported here, DNA was embedded in the emulsion within 24 hours or less after the time of synthesis. Less than four atoms of P^{32} per molecule of DNA decayed in the interim.

A few modifications of the autoradiographic procedures[6] were introduced mainly to minimize inadvertent mechanical breakage of the DNA. Samples were diluted with carrier DNA solutions (40 to 400 μg/ml) and volumes were measured in wide-mouth pipettes operated by screw-delivery. Solutions were mixed mechanically in tubes rotated at 10 rpm while inclined at 30° to the horizon. Five ml of melted emulsion and 1 ml of DNA (total 400 μg containing 10,000 to 50,000 labeled particles and an equal number of styrene latex spheres) were rotated for 5 minutes while submerged in water at 45°C. In a control test DNA of very high specific radioactivity was mixed with emulsion, and two drops of the mixture (the maximum amount compatible with satisfactory chromatography) were passed through the column. This test revealed that not more than 8% mechanical breakage was caused by the mixing.

Samples of the emulsion mixtures were poured into glass rings attached with paraffin to coated glass slides[6] to form a disk two to three mm thick before drying. After drying, the plates were stored for not more than two weeks and replicate samples were developed at appropriate intervals. They were viewed with an oil immersion objective at a total magnification of 575 ×. The specimens were counted by two observers (I. R. and C. A. T.) and the results were compared, usually with good agreement. Histograms shown in this paper include the results of both observers.

The number of styrene latex spheres[6] added to the emulsion was determined by counting an aqueous suspension in a calibrated Petroff-Hauser bacterial counting chamber. The ratio of spheres to stars counted in the emulsion measured the number of radioactive particles per ml and, together with the P^{32} assay, the number per phage equivalent of radioactive DNA.

Sedimentation constants were measured in an aluminum cell at 35,600 rpm, 10 μg DNA/ml, in 0.72 *M* NaCl, pH 6.7, at 22°C. and are reported without correction.[3]

DNA concentrations were measured spectrophotometrically in terms of the specific extinction (carefully measured for T2 DNA both before and after chromatographic purification) of 0.208 $cm^2/\mu g$ P or 0.0181 $cm^2/\mu g$ DNA. The latter figure, and all molecular weights cited in this paper, refer to the sodium nucleate with an average residue weight of 357 daltons, 8.7% P.

We also measured the specific extinction of phage particles: 0.311 $cm^2/\mu g$ P at 260 mμ. Since 98% or more of the phosphorus in phage particles is in DNA,[2] the absorbancy includes a contribution of 0.208/0.311 = 67% from the DNA and a contribution of 33% mainly due to light scattering. The absorbancy of phage particles was therefore corrected for scattering by subtracting 33% of the observed optical density.

Results.—Our principal results are derived from three independent experiments of the type just described. Their general plan is depicted schematically in Figure 1A.

Characterization of labeled DNA molecules: Our objective in this work is to characterize *unlabeled* DNA molecules. On the other hand, the autoradiographic information is obtained from *labeled* molecules. Therefore, it is important to demonstrate that the two classes of molecules are identical in the properties we seek to measure.

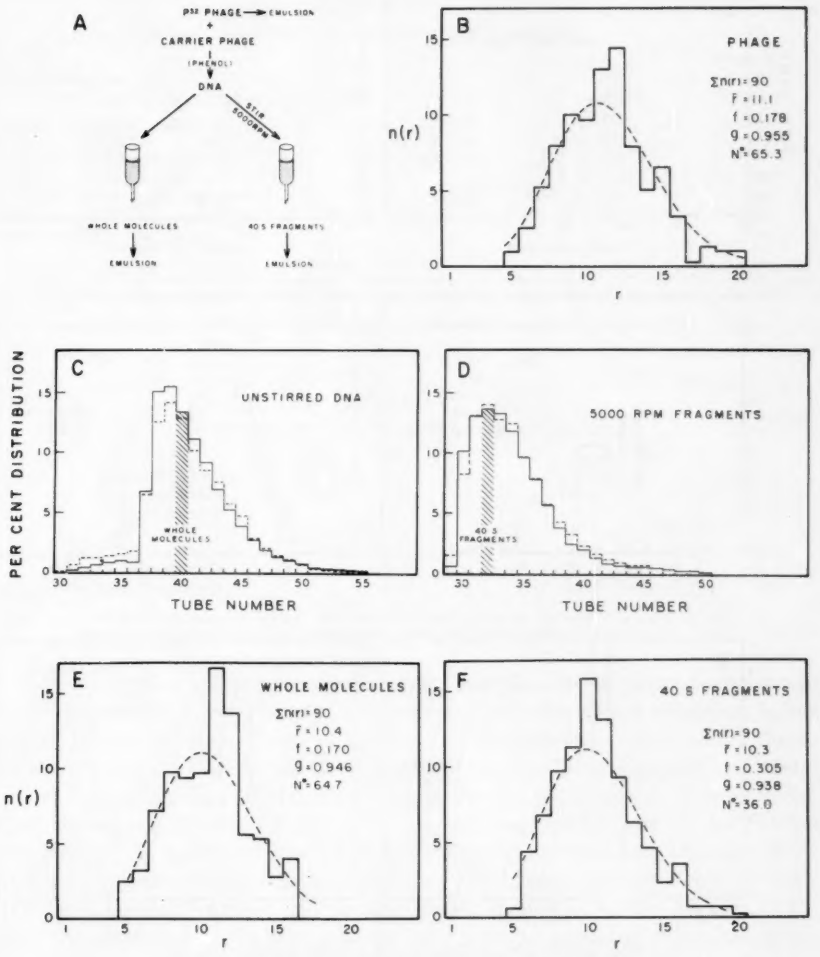

FIG. 1.—Results of Experiment 2.

A, experimental plan. *B*, *E*, and *F*, frequency distributions of star sizes. *C* and *D*, DNA chromatograms. Solid line, optical density; broken line, P^{32}. The shaded fractions were selected for autoradiography.

In Figures 1 and 2 the chromatograms of the mixed DNA preparations are shown. In all cases the elution of the P^{32} and optical density overlaps quite well. This indicates that, of the molecules which pass through the column, the two classes have similar chromatographic properties and similar sensitivity to breakage by stirring.

There is little preferential retention of labeled molecules by the column. This is evidenced by the constancy of the specific activity determinations listed in Table 1. Here one can see that the specific activity of the mixed phage stock or of the extracted DNA is essentially the same as that of the DNA fractions collected from the column.

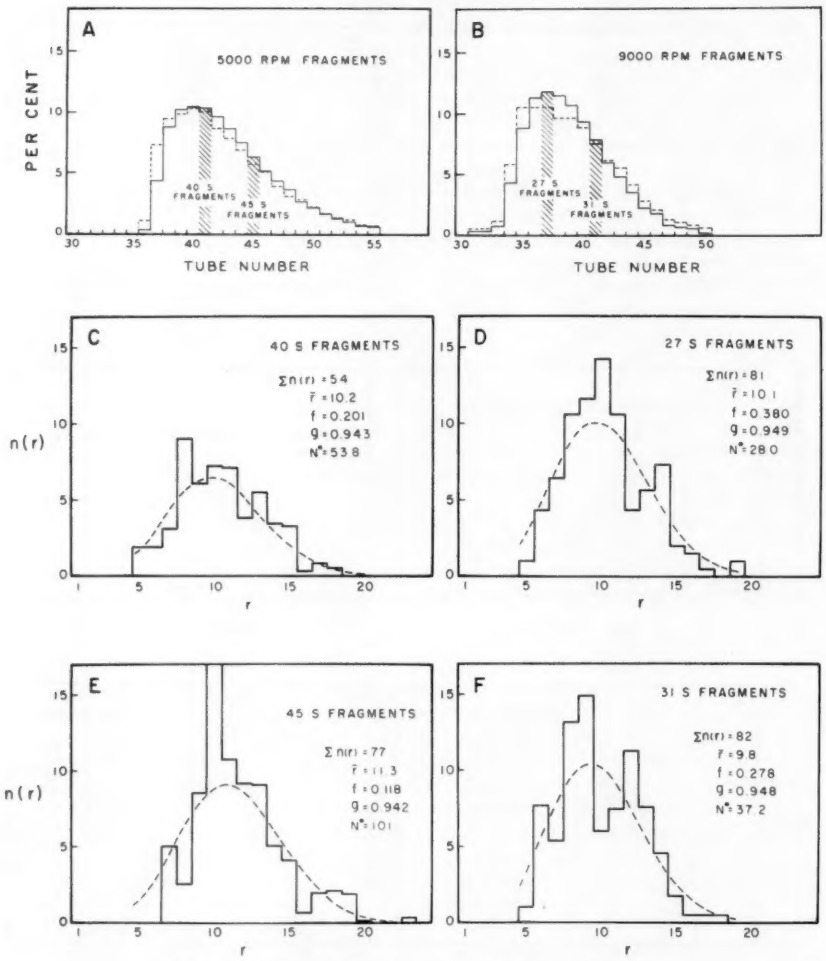

FIG. 2.—Results of Experiment 3. See legend, Fig. 1.

To summarize, labeled and unlabeled DNA respond similarly to stirring and column chromatography.

The first two entries in Table 1 show determinations of the specific radioactivity of the growth medium, the first by direct measurement, the second by employing an empirical relation between the rate of phage inactivation by "suicide" and the specific activity of the growth medium.[10, 11] The two determinations agree. The suicide experiments gave linear plots indicating that more than 90% of the viable phage had been uniformly labeled at the specific activities quoted.

Table 2 lists the sedimentation velocity measurements that were made on pertinent fractions from the column. Because of the similar response of the labeled and unlabeled DNA to stirring and column chromatography it is assumed that their sedimentation constants were also the same.

TABLE 1

SPECIFIC RADIOACTIVITY MEASUREMENTS

	Expt. 1	Expt. 2	Expt. 3
Growth medium (c/g P)	71	49	109
Same, from suicide rate of phage*	70	54	106
Labeled + carrier phage†	13,000	3,800	1,000
Extracted DNA‡	9,200	3,800	950
Unbroken DNA from column	13,000	3,800	...
5000 rpm, 45 S fragments	...	...	740
5000 rpm, 40 S fragments	13,000	3,700	790
9000 rpm, 31 S fragments	...	...	830
9000 rpm, 27 S fragments	...	...	750

* Equation (2) of Hershey *et al.*,[10] $\alpha N = 43{,}000$.
† Cpm/μg DNA, corrected for 33% scattering contribution to the absorbancy at 260 mμ. The specific radioactivities of DNA are not simply related to those of the growth medium because of the arbitrary admixture of carrier phage.
‡ Cpm/μg DNA. Sample purified before radioassay by Schmidt-Thannhauser fractionation.[7]

TABLE 2

SEDIMENTATION COEFFICIENTS OF DNA FRACTIONS

	Expt. No.	s (Svedbergs)
Whole molecules	1	61.4 (..., 64.0)*
45 S fragments	3	45.3 (43.9, 47.2)
40 S fragments	1	40.7 (38.7, 41.6)
"	2	40.0 (36.8, 43.3)
"	3	40.0 (38.4, 41.9)
31 S fragments	3	31.3 (29.5, 31.7)
27 S fragments	3	27.4 (23.8, 27.7)

* Figures in parentheses are sedimentation coefficients of fractions eluting from the columns imediately before and after, respectively, the fractions used for star counts. They serve as checks.

Autoradiography: The β-ray stars arising from the labeled phage particles and the DNA molecules were counted and grouped into size classes according to the number of rays per star. Some of the resulting frequency distributions are shown in Figures 1 and 2. The dotted curve in each of the histograms represents a Poisson distribution having the same mean and size as the star population. As one can see, all of the star populations follow a distribution reasonably close to the Poisson distribution. In each star histogram the following numbers are quoted: $\Sigma n(r)$, the number of stars counted in this collection; $\bar{r}$, the mean number of rays per star; f, the fraction of P^{32} atoms that decayed in the emulsion; g, the fraction of P^{32} atoms that remained at the time of embedding (used to correct all N^* values to the time of phage growth); and N^*, the calculated number of P^{32} atoms per star-forming unit found by dividing $\bar{r}$ by fg.

The autoradiographic results are summarized in Table 3. In the first column for each of the three experiments is seen N^*, the calculated number of P^{32} atoms per star-forming unit, and in brackets the total number of stars counted. In some cases these data were collected from plates that had been exposed for different lengths of time. The values of N^* were in good agreement indicating that the efficiency of β-ray detection was the same for plates stored for different lengths of time.[6, 12]

The number of P^{32} atoms per phage, N_0^*, was determined in each experiment. Hence, the ratio N^*/N_0^* in Table 3 indicates the fractional P^{32} content of the DNA molecules as compared to the P^{32} content of the phage particle. This ratio is approximately one for the whole DNA molecule, a fact which indicates that there is only one molecule per phage particle. This ratio is about one-half for the 45 S and

TABLE 3

RELATIVE MOLECULAR WEIGHTS

	Experiment 1			Experiment 2			Experiment 3		
	N^*	N^*/N_0^*	$(s/s_0)^{1.88}$	N^*	N^*/N_0^*	$(s/s_0)^{1.88}$	N^*	N^*/N_0^*	$(s/s_0)^{1.88}$
Phage	92.4 (31)	1.00	...	65.3 (90)	1.00	...	130.1 (91)	1.00	...
Whole molecules	83.4 (178)	0.90	1.00	64.7 (90)	0.99	1.00	...	...	1.00
45 S fragments	...	...	...	...	...	...	94.9 (128)	0.73†	0.54
40 S fragments	39.3 (19)	0.43	0.42	33.1 (196)	0.51	0.43	53.8 (54)	0.41	0.43
31 S fragments	...	...	...	...	...	...	37.2 (82)	0.29	0.27
27 S fragments	...	...	...	...	...	...	28.0 (81)	0.22	0.21

N^* = number of P^{32} atoms per star-forming unit measured autoradiographically, with number of stars counted in parentheses.
N^*/N_0^* = fractional phosphorus content.
$(s/s_0)^{1.88}$ = fractional molecular weight from sedimentation coefficients in Table 2 according to Burgi and Hershey.[3]
† This measurement is presumably in error.

40 S fragments, which represent "half molecules," and about one-quarter for the 31 S and 27 S fragments, which represent "quarter molecules."

Finally, the fractional molecular weight, $(s/s_0)^{1.88}$, calculated from the sedimentation coefficient is listed in the third column. In this expression s_0 is the nominal average (63) of many measurements on unbroken DNA (values range from 60 to 65). The exponent 1.88 is taken from the work of Burgi and Hershey,[3] whose estimates are 1/0.55 for the upper portion and 1/0.51 for the lower portion of the range of s here considered. One may see that the fractional phosphorus content determined by autoradiography corresponds with the fractional molecular weight computed from the sedimentation coefficient.

An independent measure of the number and size of the fragments can be obtained by employing polystyrene latex spheres to measure the number of stars per phage-equivalent of radioactivity. For experiments 1 and 2, respectively, this ratio was 1.52 and 1.15 for intact phage, and 1.14 and 1.36 for unbroken DNA molecules. In experiment 3, the number of stars per phage equivalent of counts ranged from 1.35 for the 45 S fragments to 5.68 for the 27 S fragments. Although these data are qualitatively clear, they lack the precision that was expected. After a consideration of many sources of error, we concluded that we were undercounting the number of polystyrene indicator particles.

Absolute molecular weights: Our conclusion that the T2 phage particle contains a single molecule of DNA reduces the problem of molecular weight measurement to that of determining the amount of DNA per phage particle. From the autoradiographic data of Table 3, five such estimates can be made. The appropriate relation is

$$M = 1.05 \times 10^8 \frac{N^*}{A_0} \qquad (1)$$

where A_0 is the specific radioactivity in c/g, the DNA is assumed to contain 8.7%

P, and all β-emissions are assumed to produce countable tracks in the emulsion. The estimates of N^* (from the counts of phage particles and unbroken DNA molecules) listed in Table 3 together with the specific activities given in Table 1 yield five measures of M ranging from 123 to 140 $\times$ 10^6, with a mean of 133 $\times$ 10^6. The measurements of N^* are evidently repeatable (as is also shown by the measurements of broken DNA) and are subject to a purely statistical error of only a few percent. The measurements do contain a known bias, since it is not certain that all of the emissions produce countable tracks in the emulsion. On this basis 133 million is a minimum estimate.

A maximum molecular weight is obtained by direct measurements of DNA per infective phage particle. A careful analysis of three phage preparations yielded an optical cross section at 260 mμ of 7.3, 7.5, and 7.6 $\times$ 10^{-12} cm^2/plaque-forming particle and 2.3, 2.3, and 2.5 $\times$ 10^{-11} μg P per plaque-forming particle, respectively. These yield an average sodium polynucleotide molecular weight of 162 $\times$ 10^6, which is a maximum since it is unlikely that every phage particle forms a plaque.

We conclude that the sodium polynucleotide molecular weight of T2 DNA lies between 130 $\times$ 10^6 and 160 $\times$ 10^6. The lower limit is consistent with a recent estimate of the weight of the whole phage particle based on sedimentation-diffusion measurement.[13] The phage particle weight was found to be 215 $\times$ 10^6 daltons, which correspond to a DNA molecular weight of 130 million if the phosphorus content of the dry phage is 5.2%.[14]

If the molecular weight is taken to be 130 $\times$ 10^6, the relationship between sedimentation coefficient and molecular weight is that shown in Figure 3. The best straight line corresponds to the equation

$$s = 0.00244\ M^{0.543} \qquad (2)$$

The coefficient of this equation has a standard error of less than 10%, while the error in the exponent is less than 1%. This relation disagrees with a commonly employed extrapolation from the low molecular weight region.[15] The exponent 0.543 agrees with that arrived at by stepwise degradation by stirring.[3]

Systematic errors: The errors in the autoradiographic technique have been discussed previously[6] and only a few comments will be made here.

First, we recall that the possibility that our results are biased by molecular aggregation is ruled out by the method of measurement, in which a small minority of radioactive molecules is examined in the presence of a large excess of carrier DNA.

It is possible that there is some difficulty in the enumeration and classification of the stars shown in the histograms in Figures 1 and 2. Stars with only a few (five to six) rays can be classified accurately, but they are not always seen. Stars with 18 to 25 rays are easy to find, but there is probably some tendency to undercount the number of rays. Thus there is a tendency to overestimate the mean number when it is small, and to underestimate it when large. When the mean lies between 9 and 13 rays per star, there may be a tendency to see a narrower size distribution than actually exists.

To counteract this tendency, plates that had been exposed for various periods were examined. After long exposures, it proved feasible to count rays per star for small stars and at the same time score the total number of stars. The observed

frequency of small stars was in reasonable agreement with the Poisson distribution based on counts made at earlier times.

In the extreme case, the tendencies discussed above could be expected to generate a spurious Poisson distribution when the distribution was in fact very broad. Three experiments with phage T4 performed shortly before those reported above are pertinent in this connection. In the T4 experiments, radioactive and carrier phage particles were mixed and purified by differential centrifugation, and DNA was extracted from them either by osmotic shock or by the phenol method. In each case, the DNA preparations yielded many stars equivalent in size to those produced by phage particles, but also yielded smaller stars. Figure 4 illustrates the broad,

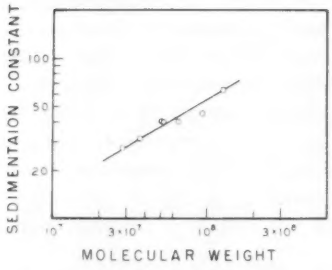

FIG. 3.—The relation between autoradiographically determined molecular weight and sedimentation coefficient for T2 DNA and its breakage products. The straight line is given by equation (2).

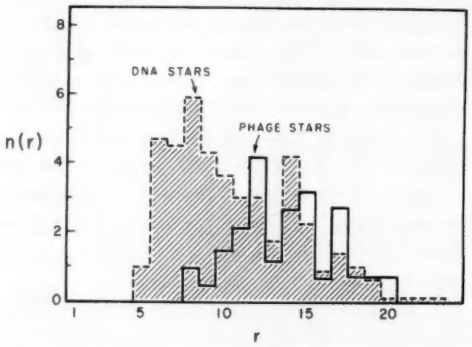

FIG. 4.—Frequency distribution of star sizes for T4 phage and DNA. The DNA was apparently partly broken during preparation.

often bimodal, distributions observed. These results certainly do not mean that the DNA of T4 differs from that of T2. Both have the same sedimentation coefficient and are broken at the same critical speed of stirring. The two phages show the same DNA content per infective particle, and are closely related by all biological criteria. For reasons that have not been determined, the T4 DNA preparations must have been partly broken before embedding. Since each break produces two fragments, very little breakage is sufficient to distort the histograms.

For present purposes, the results of these unsuccessful experiments are valuable in showing that one can detect by autoradiography heterogeneous DNA populations when they exist.

Another source of error anticipated in these experiments failed to materialize. Since DNA solutions are highly viscous, the molecules must be greatly extended in solution. In the extreme cases, such molecules might fail to produce countable stars or might produce spuriously small ones. In point of fact, some two or three per cent of the countable stars appeared to have diffuse centers as much as 10 to 20 microns across. The remainder of the DNA stars, like all of those produced by phage particles, emanated from a single point. Evidently most of the molecules are crumpled in the emulsion so as to lie within volumes not greatly exceeding one micron in diameter. This is shown most convincingly by the similarity of the star-size distributions of T2 phage particles and whole DNA molecules in the present work (Figs. 1*B* and *E*).

To summarize, after considerable experience we have not found any significant source of error in the autoradiographic method that might tend to bias the results or alter the conclusions presented in this paper.

The stability of the DNA molecule: We refer to the DNA structures isolated from phage T2 as "molecules" because of their physical and functional uniformity. The possibility remains that nonphosphodiester linkages exist uniting the polynucleotide chains. It is appropriate to summarize some results which indicate that the molecule is a stable structure.

Passing DNA through the column does not alter its sedimentation coefficient or the band width seen in a CsCl density gradient. Banding in CsCl does not alter the chromatographic behavior. Heating whole molecules to 70°C for 10 minutes in 0.1 *M* NaCl, 0.032 *M* PO_4, pH 7 does not alter the chromatographic behavior of T2 DNA nor diminish its intrinsic viscosity. The star population from T4 DNA (similar to that in Fig. 4) is not altered by heating under the conditions stated above. The intrinsic viscosity of T4 DNA is not altered by prolonged exposure to protease.[2] Study of the kinetics of breakage[3] indicate that the molecules are not characterized by a few weak bonds. The presumed separation of polynucleotide chains from the helical structure is accompanied by only a two-fold decrease in apparent molecular weight.[16] Thus, if unknown linkages exist, they must be at least as stable as the polynucleotide bonds.

Discussion.—Our first conclusion, that the particle of T2 contains a single molecule of DNA, seems quite unambiguous and has been reached independently by Davison *et al.*[5] Previous autoradiographic studies[6, 12] leading to a different conclusion were undoubtedly influenced by the then unknown susceptibility of the molecules to mechanical breakage,[17] though certain details of the early results remain a mystery.

The finding that there exists a single DNA molecule in T2 bacteriophage is consistent with the fact that the known genes in T2 form a single linkage group[4] and with the idea that the "chromosome" is a molecular structure. Phage T2 belongs to a class of phages having the largest known particle size. One of the smallest, phage ϕX-174, also contains a single DNA molecule, in this case single-stranded, with a molecular weight of only 1.7×10^6 (see ref. 18). One may anticipate that other phages will be found to contain a single molecule of nucleic acid. If so, it follows that different viruses will provide a continuous series of unique DNAs covering a wide range of molecular weights.

Our second conclusion, that molecules of T2 DNA break successively into halves and quarters at critical rates of shear, suggests that the molecules are linear. Recent evidence that the genetic map of phage T4 is circular[19] might suggest that the DNA molecule is ring-shaped. Ring-shaped molecules would be expected to break under shear into fragments of $^1/_3$ to $^1/_5$ the original length of the molecule.[3] Since T2 and T4 DNAs are very similar, it is unlikely that either molecule has a circular shape, at least after phenol extraction.

Our third conclusion, that the molecular weight of T2 DNA lies between 130×10^6 and 160×10^6, likewise seems unambiguous. For the molecular weight to be lower than these limits, it would be necessary for the observers to count β-disintegrations that did not occur, which is unlikely, if not impossible. Moreover, the molecular weight measured autoradiographically is supported by estimates based

on the mass and composition of the phage particles.[13]

The physical-chemical methods of molecular weight determination of DNA do not provide much assistance here; indeed it was one of the objectives of this work to relate molecular weight and sedimentation coefficient. In short, the molecular weights calculated from sedimentation and intrinsic viscosity are about a factor of two too low to agree with the autoradiography. Molecular weights calculated from band widths in CsCl are also too low.[2]

Summary.—The bacteriophage T2 contains a single molecule of DNA which accounts for virtually all of the phosphorus of the virus particle.

The first and second breakage products produced by controlled stirring are, on the average, one-half and one-quarter of the total molecular weight.

The sodium salt of T2 DNA has a molecular weight of at least 130×10^6 and less than 160×10^6.

An empirical relation between molecular weight and sedimentation coefficient over a five-fold range downward from 130×10^6 is proposed.

This work was aided by grants from the Atomic Energy Commission (AT(30-1)-2119) and from the National Institutes of Health (E-3233 and C-2158).

It is a pleasure to acknowledge the contribution of Mr. T. C. Pinkerton, who performed several equilibrium sedimentations pertinent to this work.

[1] Hershey, A. D., and E. Burgi, *J. Molec. Biol.*, **2,** 143–152 (1960).

[2] Thomas, C. A., Jr., and K. I. Berns, *J. Molec. Biol.*, in press.

[3] Burgi, E., and A. D. Hershey, *J. Molec. Biol.*, in press.

[4] Streisinger, G., and V. Bruce, *Genetics*, **45,** 1289–1296 (1960).

[5] Davison, P. F., D. Freifelder, R. Hede, and C. Levinthal, these PROCEEDINGS, **47,** 1123–1129 (1961).

[6] Levinthal, C., and C. A. Thomas, Jr., *Biochim. et Biophys. Acta*, **23,** 453–465 (1957).

[7] Hershey, A. D., and N. E. Melechen, *Virology*, **3,** 207–236 (1957).

[8] Matheson, A. T., and C. A. Thomas, Jr., *Virology*, **11,** 289–291 (1960).

[9] Mandell, J. D., and A. D. Hershey, *Anal. Biochem.*, **1,** 66–77 (1960).

[10] Hershey, A. D., M. D. Kamen, J. W. Kennedy, and H. Gest, *J. Gen. Physiol.*, **34,** 305–319 (1951).

[11] Stent, G. S., and C. R. Fuerst, *J. Gen. Physiol.*, **38,** 441–458 (1955).

[12] Thomas, C. A., Jr., *J. Gen. Physiol.*, **42,** 503–523 (1959).

[13] Cummings, D. J., and L. M. Kozloff, *Biochim. et Biophys. Acta*, **44,** 445–458 (1960).

[14] Herriott, R. M., and J. L. Barlow, *J. Gen. Physiol.*, **36,** 17–28 (1952).

[15] Doty, P., J. Marmur, J. Eigner, and C. Schildkraut, these PROCEEDINGS, **46,** 461–476 (1960).

[16] Berns, K. I., and C. A. Thomas, Jr., *J. Molec. Biol.*, in press.

[17] Davison, P. F., these PROCEEDINGS, **45,** 1560–1568 (1959).

[18] Sinsheimer, R. L., *J. Molec. Biol.*, **1,** 43–53 (1959).

[19] Streisinger, G., R. S. Edgar, and G. Harrar, personal communication.

*THE STRUCTURAL UNITY OF THE DNA OF T2 BACTERIOPHAGE**

By P. F. Davison, D. Freifelder,† R. Hede, and C. Levinthal

DEPARTMENT OF BIOLOGY, MASSACHUSETTS INSTITUTE OF TECHNOLOGY

Communicated by Francis O. Schmitt, June 15, 1961

The molecular weight of the DNA extracted from the phages T2 and T4 has been the subject of several investigations in recent years. Autoradiographic studies (Levinthal[1] and Levinthal and Thomas[2]) of P^{32}-labeled DNA showed that the material after embedding in photographic emulsions consisted on the average of one large piece of DNA per phage particle plus smaller material. The large piece had a molecular weight of about 45 million and in these experiments comprised about 40 per cent of the total DNA of the cells. The smaller pieces were later shown by the same method (Thomas[3]) to have a molecular weight of about 12 million.

On the other hand, the molecular weight as measured by equilibrium sedimentation in cesium chloride (Meselson, Stahl, and Vinograd[4]) showed no evidence for any large piece of DNA, but rather a homogeneous distribution of pieces of size about 14 million. Sedimentation velocity, viscosity, and light-scattering measurements (Fleischman[5]) failed to detect any evidence of a large piece of DNA but showed that the material had a molecular weight of about 12 million and was homogeneous in size. The experimental demonstration (Davison[6]) that the DNA after its extraction from the phage is extremely susceptible to shear degradation, in addition to the theoretical analysis of the shear degradation process (Levinthal,[7] Levinthal and Davison[8]), resolved a part of the apparent difference. The mean molecular weight of a DNA preparation can be reduced by the shear forces resulting from velocity gradients in a solution and can, if the shearing is done sufficiently vigorously and in a uniform manner, result in an apparently homogeneous distribution. The fact that sufficiently large shear forces were produced in the hypodermic needle used to load the ultracentrifuge cell probably accounted for the reduced molecular weight observed in these experiments. Thus the uniformly small material observed in the centrifuge, viscosity and light-scattering experiments, could be explained as an artifact of the preparation of the material and the loading of the centrifuge cells. However, the original problem was now inverted, since no evidence of smaller pieces could be found in centrifuge runs on the undegraded material. Davison (unpublished results) showed by centrifuging sheared and unsheared DNA together that a small percentage of material of lower molecular weight could readily have been detected (assuming it had an unfolded structure). Furthermore, chromatographic analysis of T2 DNA extracted without shear degradation showed that the material was homogeneous with respect to its chromatographic behavior (Hershey and Burgi[9]). It seemed possible that the large piece originally observed in the autoradiographic studies was itself a degradation product of an even larger unit, which could be the complete DNA content of the virus. On the other hand, it was also possible that the DNA of the virus consisted of a small number, perhaps two or three, of large pieces, some of which were degraded by putting the material in the photographic emulsion.

Unfortunately the physical-chemical methods such as light-scattering or cen-

trifugation are inadequate for measuring the molecular weights of such very large pieces of DNA, since there is no satisfactory theory to describe their behavior in solution. We have repeated the autoradiographic measurements under conditions which reduce the probability of shear degradation of the material and have also altered the method of purifying the phage so as to reduce possible damage to the DNA by irradiation from the P^{32} β-particles. The sedimentation properties of the material introduced onto the photographic emulsion were tested by zone sedimentation, using a D_2O-H_2O gradient to stabilize the boundaries. In addition, the same material was run on a chromatographic column prepared after the method of Mandell and Hershey.[10] As will be seen below, the results indicate that the phage DNA, extracted either by osmotic shock or by the phenol method, appears to consist of one DNA molecule per phage.

Materials and Methods.—(*a*) *Growth and purification of the phage:* *Escherichia coli* strain B was grown in a Tris-glucose synthetic medium, containing 4 μg of phosphorus as inorganic phosphate per ml, with sufficient P^{32} to bring the specific activity to approximately 45 microcuries per microgram phosphorus. Bacteria were allowed to multiply by a factor of 8 to a density of 2×10^8 cells per ml, prior to infection with phage T2r+ at a multiplicity of about one phage per bacterium. After 2 hrs the cells were lysed by chloroform and the lysate was filtered through Celite filter aid (Johns-Manville Products). Five milliliters of lysate was diluted fourfold with 0.01 *M* phosphate buffer (pH 7.4) and put onto a DEAE cellulose column (Peterson and Sober[11]), 1 cm in diameter and 2 cm high. The column was washed with 20 ml 0.01 *M* phosphate and then successively by the same buffer containing 0.1 *M* NaCl and 0.2 NaCl. Under these conditions, all of the viable phage remained attached to the column. The phage was eluted from the column with the same buffer containing 0.3 *M* NaCl and the bulk of the active phage was collected in about 2 ml of eluate. Labeled phage as prepared by this method was demonstrated to be free from P^{32} contaminants by the fact that over 95% of the radioactivity absorbed in 3 minutes to several volumes 5×10^8 per ml sensitive bacteria and less than 3% absorbed to T2 resistant cells. In addition, when zone sedimentation was performed with the intact phage, using the methods described in Levinthal and Davison,[8] essentially all of the radioactivity appeared in a peak sedimenting with the virus (Fig. 1).

The specific activity of the phage was measured from the death rate due to the decay of incorporated P^{32}, assuming 10 disintegrations produced one lethal hit (Stent and Fuerst[12]). This measurement indicated that each phage contained approximately 60 P^{32} atoms.

(*b*) *Extraction of DNA:* The DNA was liberated from the virus either by osmotic shock, in which 0.5 ml of phage in 4 *M* NaCl solution was rapidly diluted with 9.5 ml of distilled water, or by shaking a suspension of the phage, with added nonlabeled carrier phage, with water-saturated phenol (Mandell and Hershey[10]). The high concentration of DNA contributed by the carrier phage prevented shear degradation during phenol treatment.

(*c*) *Chromatography of the DNA:* The properties of DNA obtained by the phenol method were checked using a chromatographic column, according to the methods of Mandell and Hershey.[10]

(*d*) *Zone sedimentation:* The zone sedimentation of the DNA and the phage was carried out as described by Levinthal and Davison.[8]

(*e*) *Autoradiography:* In order to reduce the possible shear effect when mixing the DNA solution with the photographic emulsion, the liquid emulsion mixture previously used was avoided in these experiments. The DNA solutions were diluted with precautions to avoid shear degradation, and microdrops of a phage or DNA suspension were placed on an Ilford G-5 prepared photographic plate of thickness 100 microns, using an Agla microsyringe which could deliver accurately volumes of 1, 2, or 3 microliters. The drops were allowed to dry on the photographic plate and this was then covered by a layer of liquid G-5 emulsion, resulting in the material being embedded in a sandwich between two layers of emulsion. The photographic slides were then dried, stored, and developed after various lengths of time, according to the methods discussed by Levinthal and Thomas.[2] In all cases the intact phage, osmotically shocked phage, DNA extracted by the phenol method, and various fractions isolated from the main peak eluted from the Mandell-Hershey column were placed on the same photographic plate. In this way any variation in latent image

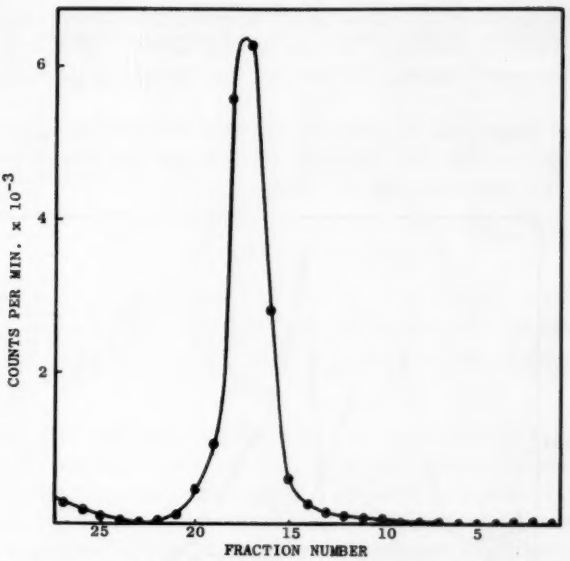

FIG. 1.—Distribution of P^{32}-labeled phage in centrifuge tube after zone centrifugation 30 minutes at 12,000 rpm in Spinco model L. Direction of sedimentation: left to right.

fading or in the development process would affect equally the intact phage and the various DNA suspensions. The plates were all counted by four observers, who for the most part were not aware of either the exposure time or the nature of the sample they were counting.

Results.—(a) *Chromatography:* When the DNA extracted from labeled phage mixed with excess unlabeled phage was chromatographed, the radioactivity was found to follow exactly the distribution in the eluate of the material absorbing at 260 mμ (Fig. 2).

(b) *Zone centrifugation:* When the P^{32}-DNA released by shocking the freshly prepared heavily labeled phage was centrifuged, the distribution of radioactivity

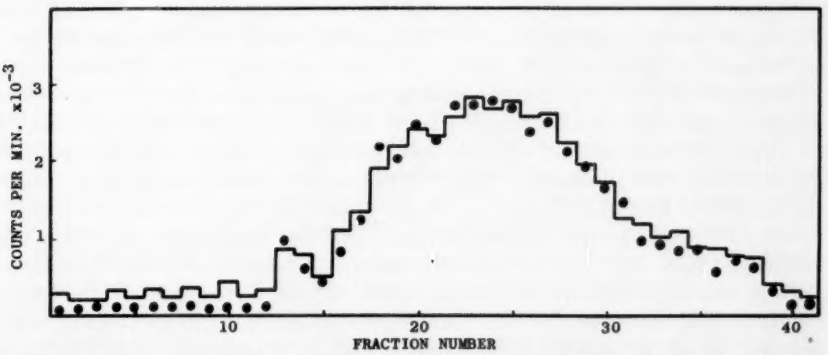

FIG. 2.—Optical density at 260 mμ (solid line) and radioactivity (indicated by dots) in fractions of a mixture of labeled and carrier phage DNA prepared by phenol method and eluted from Celite-methylated albumen column.

was essentially the same as that of lightly labeled DNA (about one P^{32} per phage particle). This result indicates that the heavily labeled DNA shows no obvious evidence of damage or degradation resulting from growth in the highly radioactive medium.

When more phage was shocked 14 days after preparation and the DNA was centrifuged, the change of distribution of DNA expected from the chain scission by P^{32} decay was observed (Fig. 3).

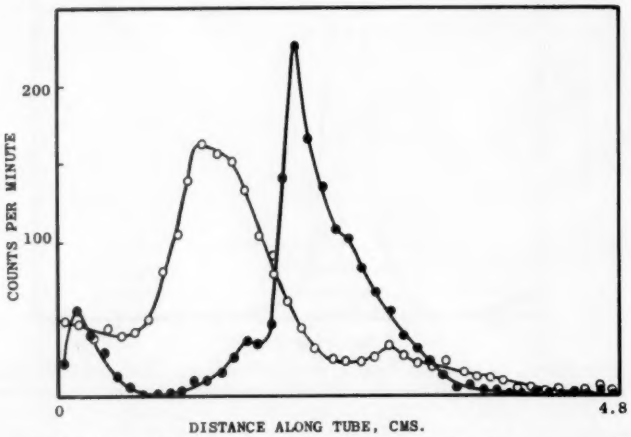

FIG. 3.—Distribution of P^{32}-labeled DNA in centrifuge tube after zone centrifugation 1 hour at 35,000 rpm on Spinco model L: (*a*) solid dots indicate DNA released from phage and centrifuged within 6 hours of P^{32} incorporation: (*b*) hollow circles refer to DNA released 17 days later from same phage as in (*a*).

(c) *Autoradiography results:* When the emulsion is examined in a microscope, stars can be seen resulting from several P^{32} tracks emanating from a point in the emulsion. The number of rays in such stars gives a measure of the amount of P^{32} at the point of origin and the number of stars per drop gives a measure of the number of pieces of P^{32}-containing material per volume of solution which was put on the emulsion.

(i) *Star number:* The intact phage and the osmotically shocked material were put on the photographic plate at a concentration which was the same for both and designed to give about 40 viable phage units per drop. For the count of the total number of star-forming units per drop the exposure was allowed to proceed to the point where the mean star size was 20 to 30. These stars were too large for the count of the number of rays per star, but they eliminated any ambiguity in the detection of the star-forming units. The number of star-forming units (that is, the number of large pieces of DNA) in the osmotically shocked material was approximately equal to the number of phage particles from which the DNA was extracted (Table 1). For the material which had been eluted from the column the star number could only be compared with the total radioactivity. The results indicated that there was the same number of star-forming units per unit of radioactivity put on the slide for the material which had been deproteinized by phenol and eluted from the column as there was for the intact phage, again indicating that for this material there was one large piece of DNA per phage particle.

TABLE 1

COUNTS OF AUTORADIOGRAPHS OF P^{32}-LABELED PHAGE AND DNA

Sample	A	B	C	D	E	F
(a) f = 0.24 No. of stars counted	44				14	
Mean rays per star	10.0				10.1	
(b) f = 0.34 No. of stars counted	61	70	75	29	71	31
Mean rays per star	13.3	12.2	13.9	12.6	12.7	13.0
(c) f = 0.78 No. of stars per drop*	39	43	29	162	204	96
Each count refers to a single drop	40	51	41	153	189	108
	44	49	37			106
(d) Radioactive counts per unit vol. of material plated	4.5	5.9	3.4	23.9	30.0	11.6
(e) Ratio (c)/(d)	9.2	8.1	10.6	6.6	6.6	8.9

Samples: A, intact phage.
B, phage shocked with added carrier.
C, phage shocked without cold carrier.
D, E, F, samples from the leading, middle, and trailing fractions of the DNA eluted from the chromatographic column.
f indicates the fraction of the P^{32} disintegrations completed at the time of development of the plates.
* In the course of counting the stars per drop, a rough count of the rays per star was also made. No evidence of a bimodal size distribution of stars was found.

(ii) *Star size:* The number of rays per star in these emulsions is considerably more difficult to determine with precision than the number of stars per drop. Use of the sandwich procedure consisting of a prepared slide plus a layer of solidified liquid emulsion results in a somewhat higher background than a complete layer of liquid emulsion. When the exposure was allowed to proceed to the point where the star size was approximately 10 to 15 per star, the counts of the same star made by various observers agreed to within one or two rays. This variation was due to occasional uncertainties as to whether a given track was produced by one or two β-particles, and there were also a few cases of uncertainty due to straight tracks passing near the center of the stars. These difficulties were approximately the same for all the preparations examined and contributed an inherent uncertainty in the counting of approximately 10 per cent. To within this uncertainty the figures of Table 1 indicate that the stars produced by the DNA after the osmotic shock or the DNA deproteinized by phenol extraction and separated on the column, all had approximately the same size as the stars produced by the intact phage. Thus we can conclude that the material which is in solution after either of these methods of preparation had about the same P^{32} content, and therefore the same DNA content as the phage themselves.

Discussion.—The autoradiographic experiments indicate that all the DNA in the T2 bacteriophage is contained in one physical entity. Rubenstein, Thomas, and Hershey[13] in an accompanying paper present evidence leading to the same conclusion. Quantitative considerations of the susceptibility of the DNA-containing structure to hydrodynamic shear (Levinthal and Davison[8]) make it highly likely that this structure is a single long filament. Freese[14] and Kellenberger[15] have proposed that chromosomes are built up from DNA molecules joined end-to-end by hypothetical "linkers." If any such linkers were present in the T2 DNA they would be expected to be points of weakness since they would form a single chain bridge between the twin helices of the DNA molecules. Hershey and Burgi[9] found no evidence for any preferential breaking point in the T2 DNA molecules under shearing, nor is there presently any other good evidence for the presence of linkers.[16] It may therefore be reasonably assumed that the DNA is present as one uninterrupted, double helix. From previous analyses (see Ruben-

stein *et al.*[13] and Cummings and Kozloff[17]) the molecular weight is probably between 90×10^6 and 150×10^6. The DNA from phage grown in media with phosphorus of very high specific activity as well as phosphorus of very low specific activity was similar chromatographically to DNA from phage grown in unlabeled media, and no difference in the zone sedimentation behavior of any of the preparations was found, except after sufficient time had elapsed to cause double chain scission by the P^{32} decay. This suggests that in the former autoradiographic experiments[1, 2] the large pieces found, which were only about 40 per cent of the total DNA content of the phage, were probably produced by degradation of the whole molecule either through shear in placing the material in the liquid emulsion or by the radiation damage suffered by the phage when they were pelleted in the centrifuge for purification. In view of the suggested mechanism for the production of small pieces by shear degradation one would have expected that a significant fraction of the small pieces would be of a size of approximately 20 per cent of the intact phage molecule. Such pieces were not found (Levinthal and Thomas[2]) and in fact the small pieces were identified as having a molecular weight of about 12 million (Thomas[3]). This discrepancy may have resulted from an error in the counting of the stars or it may have resulted from some special characteristic of the shear degradation in the nonhomogeneous, highly viscous, liquid photographic emulsion in which the phage was suspended or to a combination of the shear degradation and radiation damage. In any case, we can conclude that the large piece previously observed was a partial breakdown product of the intact molecule while the smaller pieces observed by Meselson, Stahl, and Vinograd[4] and by Fleischman[5] were material more completely degraded under more extreme conditions of shearing.

The experimental results on the transfer of P^{32} label to intact phage after labeled phage particles had infected single cells do not appear to be affected by these findings as to the nature of the phage chromosome, nor is the interpretation that a significant fraction of the label is transferred in a large semiconservative fragment. On the other hand, the interpretations of the mechanism of recombination[1] which were based on the assumption that the 40 per cent piece was the intact chromosome are clearly in error, and the experiments do not represent any evidence against the idea that when recombination occurs it is accompanied by physical breakage of the chromosome (Meselson and Weigle[18]).

Summary.—*E. coli* heavily labeled with P^{32} was infected with T2 bacteriophage, and the progeny phage released on the lysis of the cells were purified by chromatography. The zone centrifugation and chromatographic behavior of the P^{32}-DNA obtained from this phage preparation did not differ from that of unlabeled T2 DNA, demonstrating that growth in radioactive solutions did not detectably modify the DNA. Comparison of the autoradiographs obtained from the phage or the DNA released from the phage showed that all the DNA in each particle was present in one structural entity which might be identified as a DNA molecule.

Part of this work was performed in the laboratory of Professor Francis O. Schmitt for whose helpful cooperation the authors are grateful. They are also indebted to Mr. D. Baltimore, who assisted in counting some of the autoradiographs, and Mrs. P. Kahn, who developed the chromatographic method of purifying the phage.

* This research was aided by Grants E-1469 and E-2028 from the National Institute of Allergy and Infectious Diseases.

† Supported by Post-doctoral fellowship No. GF-7617-C2 from the Division of General Medical Sciences of the U.S. Public Health Service.

[1] Levinthal, C., these PROCEEDINGS, **42,** 394 (1956).
[2] Levinthal, C., and C. A. Thomas, *Biochim. et Biophys. Acta*, **23,** 453 (1957).
[3] Thomas, C. A., *J. Gen. Physiol.*, **42,** 503 (1959).
[4] Meselson, M., F. W. Stahl, and J. Vinograd, these PROCEEDINGS, **43,** 581 (1957).
[5] Fleischman, J. B., *J. Molec. Biol.*, **2,** 226 (1960).
[6] Davison, P. F., these PROCEEDINGS, **45,** 1560 (1959).
[7] Levinthal, C., in *Conference on Genetics*, (Princeton: Josiah Macy, Jr., Foundation, 1960), p. 41.
[8] Levinthal, C., and P. F. Davison (in preparation).
[9] Hershey, A. D., and E. Burgi, *J. Molec. Biol.*, **2,** 143 (1960).
[10] Mandell, J. D., and A. D. Hershey, *Analytical Biochem.*, **1,** 66 (1960).
[11] Peterson, E. A., and H. A. Sober, *J. Am. Chem. Soc.*, **78,** 751 (1956).
[12] Stent, G. S., and C. R. Fuerst, *Advances in Biol. and Med. Phys.*, **7,** 2 (1960).
[13] Rubenstein, I., C. A. Thomas, and A. D. Hershey, these PROCEEDINGS, **47,** 1113 (1961).
[14] Freese, E., *Cold Spring Harbor Symposia Quant. Biol.*, **23,** 13 (1958).
[15] Kellenberger, E., in *Microbial Genetics* (Cambridge University Press, 1960), p. 39.
[16] For economy of hypothesis we exclude from consideration the model of double linker strands bridging DNA segments. DNA itself admirably fulfills the requirements of such linkers (such linkers would have to replicate, for instance) and it seems unnecessary to postulate an added complication without experimental justification.
[17] Cummings, D. J., and L. M. Kozloff, *Biochim. et Biophys. Acta*, **44,** 445 (1960).
[18] Meselson, M., and J. Weigle, these PROCEEDINGS, **47,** 857 (1961).

STEREOSPECIFICITY AND FIREFLY BIOLUMINESCENCE, A COMPARISON OF NATURAL AND SYNTHETIC LUCIFERINS

BY H. H. SELIGER,* W. D. MCELROY,* E. H. WHITE,† AND G. F. FIELD†

JOHNS HOPKINS UNIVERSITY

Communicated by H. M. Kalckar, June 2, 1961

Synthetic firefly luciferin and dehydroluciferin (oxyluciferin) have been prepared for the first time and the structures are given in Figure 1. The complete chemical analysis and method of synthesis will be given in a separate paper by E. White *et al.*[1] In the last step of the chemical synthesis of luciferin, 2-cyano-6-hydroxybenzthiazole is reacted with cysteine. When D-cysteine is used, a luciferin (D-LH_2) is obtained which is activated by ATP, forming the adenylate derivative and releasing pyrophosphate. The enzyme complex formed then reacts with oxygen and bioluminescence is observed. When L-cysteine is used in the final step of synthesis, the resulting luciferin, L-LH_2, also reacts with ATP to form the adenylate derivative and to release pyrophosphate. The unusual feature of this L-enantiomorph, however, is that it is subsequently oxidized by molecular oxygen in a manner indistinguishable from D-luciferin or natural luciferin but *without light emission.* It is the purpose of this paper to present the physical and biochemical evidence establishing the identity of the synthetic with the natural products and to describe the remarkable stereospecificity in the bioluminescent reaction.

Enzyme Reactions.—The following reactions are catalyzed by firefly luciferase:

$$LH_2 + ATP + E \rightleftarrows E{\cdot}LH_2\text{-}AMP + PP \qquad (1)$$

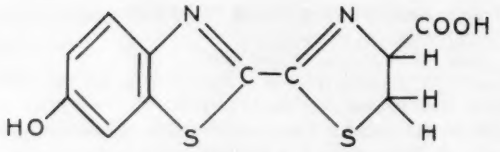

FIREFLY LUCIFERIN

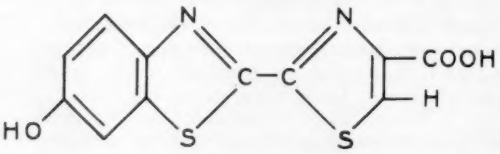

FIREFLY OXYLUCIFERIN
(DEHYDRO-LUCIFERIN)

FIG. 1.—Structures of firefly luciferin and dehydroluciferin.

$$E{\cdot}LH_2{\text{-}}AMP + O_2 \rightarrow E{\cdot}L{\text{-}}AMP + \text{Light} \quad (2)$$

$$L + ATP + E \rightleftarrows E{\cdot}L{\text{-}}AMP + PP \quad (3)$$

$$E{\cdot}L{\text{-}}AMP + CoA \rightleftarrows L{\cdot}CoA + E + AMP \quad (4)$$

In the initial activation step the carboxyl group of luciferin (LH_2) reacts with adenosine triphosphate (ATP) to form a luciferyl-adenylic acid-enzyme complex and inorganic pyrophosphate (PP). The progress of these reactions can be followed by observing light emission, pyrophosphate release, or fluorescence intensity changes.[2,3] For example, consider reactions 3 and 4. If a small amount of luciferase (E) is added to natural dehydroluciferin (L) with excess adenosine triphosphate (ATP) and magnesium ion (Mg^{++}) reaction 3 can be followed by observing the decrease in intensity of the 544 mμ fluorescence of free L. The binding of L onto the enzyme in the activation step with ATP produces essentially a nonfluorescent species (dehydroluciferyl-adenylic acid-enzyme complex). The addition of excess coenzyme A as shown by reaction 4 will release enzyme and eventually by virtue of 3 and 4 all of the L present will be converted to L·CoA. Since L·CoA is also a nonfluorescent molecule, we add excess cysteine which results in the following nonenzymatic reaction:

$$L{\cdot}CoA + \text{cysteine} \rightarrow L{\cdot}\text{cysteine} + CoA. \quad (5)$$

L·cysteine is a fluorescent molecule and the progress of reaction 5 can be followed as a fluorescence increase with time. This three-stage fluorescence assay technique has now been demonstrated for synthetic dehydroluciferin.

Synthetic D-luciferin reacts with ATP, luciferase, Mg^{++}, and O_2 to give bioluminescence. The bioluminescence emission spectrum of the *in vitro* natural luciferin-luciferase reaction at neutral pH has a peak emission which, for various samples, varies between 562 mμ and 565 mμ. Using the same purified enzyme preparation the shapes and the peak positions of the bioluminescence emission

spectra were identical for both natural luciferin and synthetic D-luciferin. At acid pH the bioluminescence emission spectrum of synthetic D-luciferin exhibited the same red-shift as reported previously for natural luciferin;[4] there is a disappearance of the 565 mμ yellow-green band and the appearance of the new 616 mμ red band.

An equal amount of synthetic L-luciferin under identical conditions gives essentially no light emission. Synthetic L-luciferin, while not effective for the light-emitting reaction, is a potent competitive inhibitor of luminescence for both natural luciferin and synthetic D-luciferin. The inhibition data would suggest that in reaction 1 the luciferase makes no distinction between the L- and D- forms of luciferin. To test this hypothesis equal amounts of synthetic D- and L-luciferin were reacted separately, and the amount of pyrophosphate released was determined as a function of time. The initial rate of pyrophosphate release is the same for both the D- and the L-luciferin. In addition, chromatographic and fluorometric analyses of the reaction products indicate that dehydroluciferin is formed from both D- and L-luciferin. Thus, chemically there does not appear to be any difference between D- and L-luciferin; the only difference being that bioluminescence attends the enzymatic oxidation of D-luciferin while the enzymatic oxidation of L-luciferin is a dark reaction.

We have been able to convert both synthetic L- and D-luciferin to dehydroluciferin with equal facility in alkaline solution by heating or by oxidation at room temperature with ferricyanide ion. The chromatographic separation both on paper and on celite columns of the initial synthetic D- and L-luciferins and of the dark-oxidized (dehydroluciferin) products showed the same R.F.'s and bands as the natural products.

As expected from the structure it has been possible to convert synthetic L-luciferin into D-luciferin by an alkali-catalyzed isomerization. If L-luciferin is heated to approximately 80°C in 1*N* sodium hydroxide in the absence of oxygen one obtains significant amounts of D-luciferin as judged by its ability to produce bioluminescence. Similarly a solution of synthetic D-luciferin treated as above will produce less light even though there is no apparent loss of luciferin as measured by absorbance.

Absorption and Fluorescence Spectroscopy and Optical Rotation.—The normalized absorbance spectra of natural luciferin and dehydroluciferin are shown in Figure 2. At neutral pH or below, natural luciferin has an absorption peak at 327 mμ and at alkaline pH the absorption peak shifts to 381 mμ. The corresponding peaks for natural dehydroluciferin are 348 and 393 mμ, respectively. These shifts, with a pK of 8.25 correspond to the ionization of the OH group of the molecule. The effect of the ionic forms of the molecules is evident in Figure 3 which shows the large increases in the fluorescence quantum yields of both natural luciferin and dehydroluciferin at alkaline pH; the pK of the fluorescence yield shifts is identical with that of the absorption peak shifts. Both the acid-base shifts in absorbance and the acid-base shifts in fluorescence yields have been observed for both synthetic D- and L-luciferin and for synthetic dehydroluciferin.

The fluorescence emission spectra of natural luciferin and dehydroluciferin have peaks at 535 mμ and 544 mμ, respectively. These peak positions remain independent of pH changes even though the ionization resonance lowers the absorption peak energies by 12.5 and 9.3 kcal/mole, respectively. Insofar as absorbance and

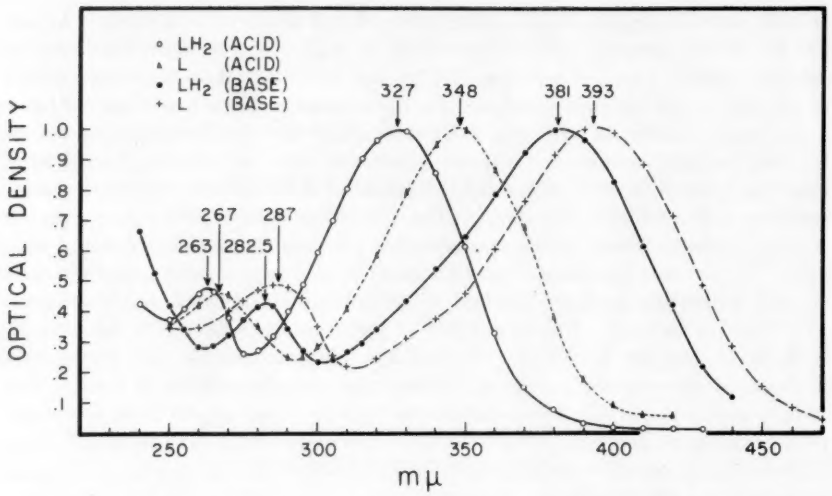

FIG. 2.—Normalized absorbance spectra of luciferin and oxyluciferin. The points of crossing of the acid and base curves are isobestic points.

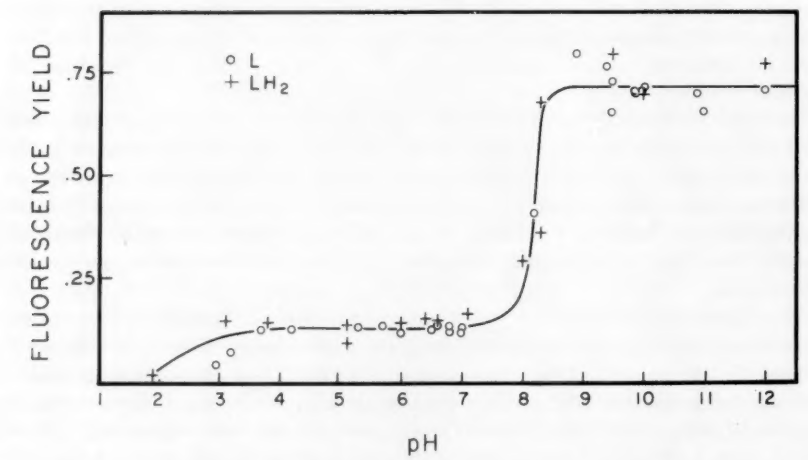

FIG. 3.—Fluorescence yields of luciferin and dehydroluciferin as functions of pH. The measurements were complicated by the absorption shifts shown in Figure 2. The quality of the emission, however, was unchanged by pH. Measurements were made relative to fluorescein in alkaline solution.

fluorescence are concerned, synthetic D-luciferin, synthetic L-luciferin, and natural luciferin are identical, as are synthetic and natural dehydroluciferin.

The synthetic D- and L-luciferins are enantiomorphs with specific rotations for the sodium D doublet in dimethyl formamide solvent of minus and plus approximately 30 degrees, respectively. The maximum rotation observed depends somewhat upon the method of synthesis since racemization can take place. Natural

luciferin is not readily available in the concentrations normally required for optical rotation measurements and therefore measurements have not been too accurate. The natural luciferin that we have measured is levo-rotatory indicating that natural product is predominantly the D-isomer.

Discussion.—It is surprising that natural firefly luciferin is D-luciferin in view of the preponderance of L-amino acids over D-amino acids in biological systems. Unfortunately, we have no evidence concerning the biosynthesis of firefly luciferin.

The quantum yield (number of light quanta emitted per luciferin molecule oxidized) of purified natural firefly luciferin was found to be 0.88 ± 0.25.[5] Since the assay of the initial amount of luciferin present was based on absorbance spectrophotometry and since any L-luciferin present would not have contributed to the light emission, this value is a lower limit, depending upon the isomeric purity of the luciferin samples used.

The stereospecificity for the bioluminescence reaction is a biological example of a general mechanism of chemiluminescence proposed earlier.[6] That is, in an exothermic chemical reaction such as oxidation by molecular oxygen, luminescence is specifically the fluorescence of the product molecule which upon formation is in a highly excited vibrational state. If the product molecule is not a fluorescent species or if it is bound in such a way as to be quenched, chemiluminescence will not be observed. Here, apparently, in the case of firefly luciferin the L-isomer complex of luciferin, after undergoing oxidation, is either nonfluorescent or very strongly quenched.

Unfortunately, we do not know the exact oxidative mechanism which leads to light emission. We are certain of products indicated in reaction 2 but there are transients which have not as yet been identified. The continuous spectrophotometric assay of the luciferin oxidation in excess enzyme (reactions 1 and 2) indicates that as the reaction proceeds the 327 mμ absorption peak of luciferin decreases and is replaced by a new absorption peak at 383 mμ. The new absorption band is presumably due to the "E·LAMP" complex indicated in reaction 2. However, a comparable set of absorbance curves for the enzyme reaction with dehydroluciferin show relatively little decrease in the 348 mμ absorption peak of dehydroluciferin and no new absorption peaks corresponding to "E·LAMP" of reaction 2. Thus, at least in our *in vitro* enzyme reactions the enzyme-intermediate complex formed is different from E·LAMP formed directly as in reaction 3. It may be significant that the enzyme complex formed in reaction 2, at neutral pH, behaves in absorption as though the product were closely related to luciferin in basic solution. The crossover point between the disappearance of the original 327 mμ peak and the appearance of the new 383 mμ peak is just the 348 mμ isobestic point for luciferin as shown in Figure 2.

While we cannot yet identify the enzyme complex responsible for the new 383 mμ absorption peak we have been able to verify that both synthetic D- and L-luciferin in the enzymatic reaction give this same 383 mμ absorption peak with a crossover point at 348 mμ. Synthetic dehydroluciferin gives the same results as natural dehydroluciferin.

The luminescence stereospecificity which we have observed seems to be a most unusual type of enzyme stereospecificity, inasmuch as the D- and L-luciferins appear to combine with the enzyme with the same affinity. Both forms have the same

Briggs-Haldane constants and dehydroluciferin is formed from both to the same degree. We are forced to conclude, therefore, that the intermediate formed in the oxidation of L-luciferin is either a different nonfluorescent species or is the same molecule as that resulting from D-luciferin oxidation but vibrationally quenched with very high efficiency. This difference might be ascribed to the mode of binding of the intermediate to the enzyme.

It is of interest to compare this observed luminous stereospecificity with the fluorescence of the α- and β- forms of reduced diphosphopyridine nucleotide (DPNH). It has been found that the 260 mμ adenine absorption results in fluorescence emission at 460 mμ of β-DPNH. However, the α-glycoside linkage of the nicotinamide riboside grouping alters the molecular configuration so that, although the adenine moiety absorbs as strongly at 260 mμ in α-DPNH, there is no resulting 460 mμ fluorescence.[7] Perhaps on the enzyme the D- and L-forms of LH_2-AMP give rise upon oxidation to a fluorescent and nonfluorescent intermediate species respectively. Alternatively, it is known that different enzymes catalyze the formation of the A and B stereoisomers of DPNH.[8] It may be that the D- or L-luciferyl adenylate can react with molecular oxygen in different ways, the former resulting in a highly resonant complex and the latter participating in a dark oxidation similar to that observed by heating in alkali in the presence of oxygen.

It would, therefore, be of considerable interest to look for possible differences in absorption or fluorescence of intermediates which might be formed in other enzyme reactions where optically active substrates are available. Quite possibly there may be bioluminescence observed upon substitution of stereoisomers into normal oxidase reactions.

This work has been supported in part by the Atomic Energy Commission, the National Institutes of Health and the National Science Foundation. The authors would like to thank Joan Friedland and Eleonore Kayser for their technical assistance.

* McCollum-Pratt Institute and Department of Biology, Johns Hopkins University, Baltimore, Md.

† Department of Chemistry, Johns Hopkins University, Baltimore, Md.

[1] White, E. H., F. McCapra, G. F. Field, and W. D. McElroy, *J. Am. Chem. Soc.*, **83,** 2402 (1961).

[2] Airth, R. L., W. C. Rhodes, and W. D. McElroy, *Biochem. et Biophys. Acta.*, **27,** 519 (1958).

[3] Rhodes, W. C., and W. D. McElroy, *J. Biol. Chem.*, **233,** 1528 (1958).

[4] Seliger, H. H., and W. D. McElroy, *Radiation Research Suppl.*, **2,** 528 (1960).

[5] Seliger, H. H., and W. D. McElroy, *Arch. Biochem. and Biophys.*, **88,** 136 (1960).

[6] Seliger, H. H., in *Light and Life*, ed. W. D. McElroy and B. Glass (Baltimore: Johns Hopkins Press, 1961), p. 239.

[7] Shifrin, S., and N. O. Kaplan, *Nature*, **183,** 1529 (1959).

[8] Fisher, H. F., E. E. Conn, B. Vennesland, and F. H. Westheimer, *J. Biol. Chem.*, **202,** 687 (1953); San Pietro, A., N. O. Kaplan, and S. P. Colowick, *J. Biol. Chem.*, **212,** 941 (1955).

*THE OCCURRENCE OF NATURAL DNA-RNA COMPLEXES IN E. COLI INFECTED WITH T2**

By S. Spiegelman, Benjamin D. Hall, and R. Storck†

DEPARTMENTS OF MICROBIOLOGY AND CHEMISTRY, UNIVERSITY OF ILLINOIS

Communicated by T. M. Sonneborn, May 31, 1961

In a previous publication, Hall and Spiegelman[1] showed that RNA-DNA complexes were formed when mixtures of single-stranded T2-DNA and purified[2] "T2-specific RNA" were subjected to slow cooling.[3, 4] It would appear from this that the Volkin and Astrachan[5] observation of a similarity in base composition between T2-RNA and DNA is a reflection of a more profound homology. The fact that hybrid formation was found to be unique to the homologous pair led to the conclusion that the nucleotide sequences of T2-RNA and DNA are complementary in the sense of the hydrogen bonding scheme proposed by Watson and Crick.[6]

An obvious implication of these findings is that the normal process of transferring information from DNA to the protein synthesizing machine involves a mechanism whereby single-stranded DNA serves as a template for the polymerization of a complementary ribopolynucleotide. If continued formation of complementary RNA is a necessary concomitant, it should be possible to find RNA-DNA hybrids in any cell actively engaged in protein synthesis.

The T2-*E. coli* complex was selected as the most suitable system in the initial search for native hybrid. This choice was dictated by the fact that RNA synthesis in a T2-infected cell is virtually confined to the class which is complementary to the viral DNA. The experimental devices employed were in essence similar to those used in the previous[1] investigation on artificially formed complexes. These involved the use of double labeling (H^3 and P^{32}) and equilibrium centrifugation in CsCl gradients[7] employing swinging bucket rotors. T2-DNA was labeled with P^{32} by growth of the virus in a medium containing this isotope. T2-specific RNA was marked with H^3 by introducing H^3-uridine in the early periods of infection. In this experimental setup, the presence of DNA-RNA hybrids would be signalled by the appearance of coincident peaks of the two isotopes. Further, these peaks should occupy a position in the CsCl gradient differing from those which characterize the densities of RNA and double-stranded DNA.

It is the primary purpose of the present paper to present the results of such experiments. The data demonstrate that native hybrids involving DNA and RNA strands do indeed exist.

Materials and Methods.—1. *Growth of cells and conditions of infection:* Cells of *E. coli* B were grown in a synthetic medium (medium C of Roberts *et al.*[8]). As a routine, cells were grown overnight in a glucose limiting medium. They were then harvested, washed, and resuspended in a fresh glucose medium at an $O.D._{660}$ of 0.270. Incubation was resumed and continued until logarithmic growth was established and an $O.D._{660}$ of between 0.285 and 0.300 attained. The cell suspensions were then centrifuged and concentrated tenfold in cold medium lacking glucose. A chilled concentrated bacteriophage suspension was then added in an amount to yield a multiplicity of between 10–30. The mixture was then held at 4°C for 30 minutes to allow for adsorption and then diluted tenfold into fresh glucose-synthetic medium prewarmed to 30°C. Aeration was immediately instituted and this moment was taken as the zero time of the experiment. In all experiments reported, cell survivors were less than 0.02%.

2. *H^3-uridine pulses of infected cells:* In the usual experiment, approximately 300 ml of in-

fected cells were pulsed at once. Tritiated uridine (1,600 μc–530 μc per μM) at final concentrations ranging from 0.3 μg–1.0 μg per ml was introduced at the appropriate time and the pulse continued for 3 minutes with vigorous aeration. At the end of this period, the entire suspension was poured on 120 grams of frozen Tris (0.01 M) + NaCl (0.005 M) to stop further incorporation. The cells were harvested by centrifugation, resuspended in 8 ml of the Tris-NaCl buffer, distributed in separate tubes, and frozen to await centrifugal analysis.

3. *Preparation of nucleic acid:* The following procedure was finally adopted for preparing material suitable for the detection of hybrid material in CsCl density gradients. A typical protocol is given. 2.0 ml of frozen cells (equivalent to 80 ml of the original pulsed suspension of infected cells) are thawed, 0.5 ml of 30% sodium dodecyl sulfate added, and the mixture shaken at room temperature for 10 minutes. 0.5 ml of $NaClO_4$ are then added and the shaking continued for 5 minutes. This is followed by the addition of 3 ml of chloroform and 0.3 ml of isoamyl alcohol. The mixture is then shaken for 15 minutes following which it is centrifuged in the Servall swinging bucket rotor (HS) for 20 minutes at 6,000. The top aqueous layer is removed and saved. To the residue are added 2.0 ml of Tris-saline and 0.5 ml of 5 M $NaClO_4$. The resulting mixture is then shaken for 10 minutes, centrifuged and the aqueous layer removed as previously described. The two aqueous layers are combined and again subjected to the deproteinization procedure by adding 6 ml of $CHCl_3$ and 1.2 ml of isoamyl alcohol. The mixture is then shaken, centrifuged again in the swinging bucket rotor (6K15′) and the aqueous layer removed. Two volumes of cold abso'ute EtOH are then added and the mixture held at 0°C for 10 minutes following which the nucleic acid precipitate is collected by centrifugation at 7,000 rpm for 10 minutes. The resuspended pellet is redissolved in Tris (0.001 M) and saline (0.005 M). After solution is complete, the buffer concentration is brought up to standard strength (0.15 M NaCl, 0.015 M Tris).

4. *Preparation of P^{32}-labeled T2:* Cells growing logarithmically in glucose-synthetic, low-phosphate medium (0.002 M PO_4 and 0.02 M Tris; pH 7.4) were infected with T2 (multiplicity of infection, 0.02) when an $O.D^{660}$ of 0.150 was attained. Simultaneously, 10 mc of P^{32} were added per liter. The resulting suspension was incubated overnight with shaking at 37°C. After removal of cell debris from the lysate, the virus particles were purified by three cycles of low (3.5K30) and high (12K45) centrifugations. The preparation had 5×10^{-7} cpm/particle at the outset.

5. *Separation of nucleic acid components by density-gradient centrifugation:* The method of fractionation by CsCl density centrifugation is very similar to that described previously.[1] A layering technique was, however, introduced to cut the centrifugation time required to obtain adequate separation of free RNA from hybrid material. To 0.5 ml of the nucleic acid preparations described in paragraph 3 were added 0.8 gm of solid CsCl. The resulting solution was introduced as a bottom layer in a centrifuge tube containing a CsCl solution of density 1.770. This was accomplished by allowing the sample to run through a "dispo-pipette" to the bottom of the tube. Prior to its removal, the top of the pipette was plugged with a small stopper to eject the last bit of sample and prevent contamination of the upper portion of the tube when the pipette was withdrawn. The tubes were then placed in the SW-39 rotor of the Spinco model L and centrifuged at 33,000 rpm for 60 hours at 25°C. At the end of each run, fractions corresponding to various density levels in the tube were obtained by piercing the bottom of the tube and collecting drops, *ca.* 30 for each fraction. These were diluted to a volume of 1.2 cc for measurement of ultraviolet absorption and radioisotope concentration.

6. *Counting of H^3-RNA and P^{32}-DNA:* Counting of the two isotopes was carried out as described previously[1] using trichloracetic acid washing on millipore membranes and the Packard Tri-Carb Scintillation Counter which permits counting of P^{32} and H^3 in the same sample.

Results.—A variety of procedures was surveyed for obtaining material suitable for the reliable detection of DNA-RNA hybrids by CsCl density equilibrium centrifugations. These included methods (e.g. freezing and thawing in the presence of lysozyme[9, 10]) of cell rupture and fractionation which conserve the DNA and permit its isolation as a relatively intact fraction. However, none of these was reproducibly successful. Ultimately, attempts at preliminary fractionation of cell components were abandoned. Attention was focused on the use of detergents which lysed cells and simultaneously inactivated the enzyme activity of the lysate. It

was empirically established that removal of most of the protein was a necessary step prior to introducing the material into the CsCl. In the absence of this preliminary purification, much of the nucleic acid, including hybridized material, was trapped in the protein layer found floating at the top of the gradient.

The procedure described in *Methods* (section 3) was found to yield highly reproducible results. It consists essentially of the first few deproteinization stages employed for preparing[11] DNA from bacterial cells. Two modifications were made. None of the steps designed to remove RNA is included, and at the alcohol precipitation stage, centrifugation, rather than winding around a glass rod, is used to collect the nucleic acid. Such DNA preparations are, of course, heavily contaminated with RNA (50% and more) but served well the purposes of the present experiment.

The conditions used in the current investigation (synthetic medium, 30°C) were such as to yield a latent period of 35–40 minutes and an onset of DNA synthesis sometime after 15 minutes. It is known[12, 13] that some uridine ends up in the DNA once its formation begins in the T2-*coli* B complex. To avoid the complications which this would introduce in identifying radioactive peaks, experiments designed to detect hybrid formation were confined to the period (2–5 minutes) when no DNA synthesis can be detected.

In experiments which employ P^{32}-labeled T2-DNA and tritiated uridine as the RNA label, existence of hybrid would be detected as a tritium peak in the DNA region, somewhat heavier than the P^{32} peak corresponding to the T2-DNA. The P^{32}-peak should exhibit signs of bi-modality as evidence of a distribution of the T2-DNA between hybrid and unhybridized T2-DNA.

Several independent experiments were performed with essentially similar results. Figures 1 and 2 describe the results of two typical profiles obtained by subjecting nucleic acid preparations from different pulses to equilibrium gradient centrifugation. The general conditions of infection, pulsing, preparation of nucleic acid and separation in the CsCl gradients are all as described under *Methods*. Detailed differences are found in the legends. Three peaks are readily discernible. The lightest one corresponds to the input P^{32}-labeled DNA of T2. The optical density peak identifies the position of double-stranded *E. coli* DNA put in as a marker. The tritium peak locates the hybrid. It will be noted that in each instance one observes the existence of a shoulder on the heavy side of the P^{32} profile corresponding in position to the tritium peak region. The relative positions of the peaks and the bi-modality of the P^{32} distribution are all consistent with what would be predicted from the existence of a DNA-RNA hybrid.

If we assume that a small amount of T2-DNA can be synthesized even in this early period of infection, another interpretation of the optical density and radioactive profiles can be entertained. This would presume the appearance of new T2-DNA, all in the form of single-stranded material, along with the conversion of a portion of the input P^{32}-labeled DNA to single strands. To test for this possibility, the alkali lability of the H^3 and P^{32} in relevant fractions of a number of experiments was examined. The same results were obtained in all cases and are exemplified by the data summarized in Table 1. Here, the two fractions (7 and 26) indicated by arrows in Figure 2 were subjected to alkali digestion and the resultant effect on the acid precipitability of H^3 and P^{32} examined. Fraction 7 was included as a free RNA control. It is evident from the data in Table 1 that all of the H^3

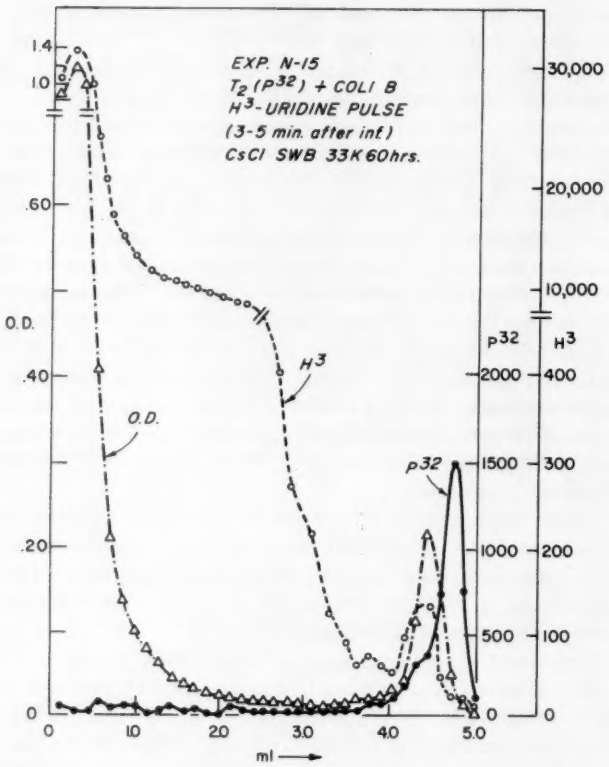

FIG. 1.—Adsorption of phage was carried out at a multiplicity of 45. P^{32}-labeled phage diluted 2-fold with unlabeled virus. Pulsing was done between 3–5 minutes after 0 time with H^3-uridine having a specific activity of 1,600 $\mu c/\mu M$ at a level of 0.3 μg/ml. All other details are as described under *Methods*. Note that the radioactivity scale is expanded in the hybrid region.

TABLE 1

EFFECT OF ALKALI DIGESTION ON ACID PRECIPITABILITY

Fraction No.	Isotope	Acid Precipitable Counts/ml	
		Control	After alkali treatment
	H^3	230	5
26	P^{32}	735	720
	H^3	1950	10
7	P^{32}	...	...

0.4 ml aliquots of Fractions 7 and 26, indicated by arrows in Fig. 2, were made 0.3 *N* with respect to NaOH and incubated for 24 hours at 30°C. Equivalent aliquots were held as controls under the same conditions. Following the incubation, the alkali was neutralized, carrier herring sperm DNA added, and the contents precipitated with TCA; washing and counting was then carried out as described under *Methods*.

and none of the P^{32} counts are alkali labile. These data appear to eliminate the possibility that the displaced tritium peak can be ascribed to newly synthesized single-stranded DNA. It is also evident that the displaced P^{32} cannot be ascribed to a conversion of the input viral DNA to an RNA polynucleotide. We may, there-

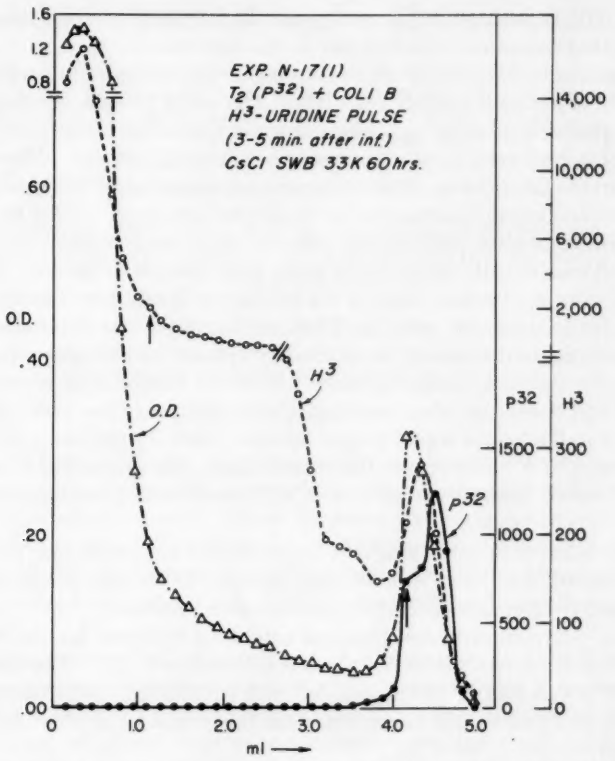

FIG. 2.—Adsorption of phage was carried out at a multiplicity of 15 of undiluted P^{32}-labeled virus. Pulsing was done between 3–5 minutes after 0 time with H^3-uridine having a specific activity of 530 $\mu c/\mu M$ at a level of 1 μg/ml. All other details are as described under *Methods*. Note that the radioactivity scale is expanded in the hybrid region.

fore, conclude that a hybrid region exists containing newly synthesized T2-specific RNA complexed with some of the input P^{32}-labeled DNA.

Discussion.—The existence of native DNA-RNA hybrids in T2-infected *E. coli* is consistent with the assumption that DNA serves as a template for the synthesis of complementary informational RNA. This view would require the existence of a DNA-dependent enzymatic mechanism for synthesizing polyribonucleotide. Evidence suggesting the presence of such a pathway emerged from a study[14] of cell-free preparations derived from *E. coli* which possessed considerable capacity to synthesize polyribonucleotide. The observed synthetic activity exhibited a requirement for riboside tri-phosphates and Mn, and was sensitive to DNAase. More recently a number of laboratories[15–17, 20] have independently achieved considerable purification of an RNA polymerase capable of synthesizing polyribonucleotide from ribose triphosphate in the presence of DNA. Furthermore, the base ratio of the polyribonucleotide synthesized bears a striking homology to that of the DNA used as a primer.[18, 19] It would appear from the preliminary reports available that considerable information will soon be available on the enzymological

aspects of DNA-mediated RNA synthesis. It will be of obvious interest to see whether hybrid formation is the first step in this process.

The experiments described in the present paper were designed primarily to detect the presence of native RNA-DNA hybrids. The use of isotopic labeling combined with CsCl gradients in swinging buckets provides a sensitive method for the certain detection of hybrid even when it is present in minute quantities. However, these methods are too laborious to permit the rapid accumulation of the kind of detailed quantitative and kinetic information we would like to possess. Other more efficient and less time-consuming methods for both the detection and estimation of hybrid material will undoubtedly be developed as we learn more of its nature. It may perhaps be of value for further efforts if we summarize briefly here the experience we have thus far accumulated with the T2-*E. coli* complex. As determined by their relative position, the densities of the natural hybrids are very similar to those formed artificially by the slow cooling process. In seven experiments involving pulses between 3 and 5 minutes after infection, the proportion of the newly synthesized RNA found in the hybrid region ranged between 1 and 0.1 per cent. As measured by the amount of P^{32} shifted into the hybrid region, the proportion of input DNA hybridized varied from 15–30 per cent in all cases where approximations could be made.

Our experience with other stages of infection are not as extensive. However, it may be noted that hybrids involving the input DNA were observed in pulses covering both 9–12 minutes and 19–22 minutes after infection.

Summary.—Experiments are described exhibiting evidence for the existence of natural DNA-RNA hybrids in *E. coli* cells infected with T2. The use of double labeling (P^{32}-DNA and H^3-RNA) coupled with equilibrium centrifugation in CsCl gradients in swinging bucket rotors permitted the isolation and identification of the hybrid regions.

The authors would like to thank Mr. Saul Yankofsky for his skillful assistance in the performance of the experiments described here. In addition, the many helpful discussions with their colleagues, Professors K. C. Atwood and N. Sueoka, are gratefully acknowledged.

* This investigation was aided by grants in aid from the U.S. Public Health Service, National Science Foundation, and the Office of Naval Research.

† Present address: Bacteriology Department, University of Texas, Austin, Texas.

[1] Hall, B. D., and S. Spiegelman, these PROCEEDINGS, **47,** 137 (1961).

[2] Nomura, M., B. D. Hall, and S. Spiegelman, *J. Molec. Biol.*, **2,** 306 (1960).

[3] Marmur, J., and D. Lane, these PROCEEDINGS, **46,** 453 (1960).

[4] Doty, P., J. Marmur, J. Eigner, and C. Schildkraut, *op. cit.*, **46,** 461 (1960).

[5] Volkin, E., and L. Astrachan, *Virology*, **2,** 149 (1956).

[6] Watson, J. D., and F. H. C. Crick, *Nature*, **171,** 964 (1953).

[7] Meselson, M., F. Stahl, and J. Vinograd, these PROCEEDINGS, **43,** 581 (1957).

[8] Roberts, R. B., P. H. Abelson, D. B. Cowie, E. T. Bolton, and R. J. Britten, *Studies of Biosynthesis in E. coli* (Washington: Carnegie Institution of Washington, 1957), p. 5.

[9] Kohn, A., *J. Bacteriol.*, **79,** 697 (1960).

[10] Hall, B. D., R. Storck, and S. Spiegelman, *J. Biophys.* (in press).

[11] Marmur, J., *J. Molec. Biol.* (in press).

[12] Cohen, S. S., H. D. Barner, and J. Lichtenstein, *J. Biol. Chem.* (in press).

[13] Ben-Porat, T., "RNA Metabolism in Phage Infected Protoplasts," Doctoral Thesis, University of Illinois (1959).

[14] Spiegelman, S., *Recent Progr. Microbiol.*, **7,** 82 (1959).

[15] Weiss, S. B., these PROCEEDINGS, **46,** 1020 (1960).

[16] Hurwitz, J., A. Bresler, and R. Dinger, *Biochem. Biophys. Research Commun.*, **3**, 15 (1960).
[17] Stevens, A., *op. cit.*, **3**, 92 (1960).
[18] Furth, J. J., J. Hurwitz, and M. Goldmann, *op. cit.*, **4**, 362 (1961).
[19] Weiss, S. B., and T. Nakamoto, these PROCEEDINGS, **47**, 694 (1961).
[20] Ochoa, S., D. P. Burma, H. Kröger, and J. D. Weill, *op. cit.*, **47**, 670 (1961).

CORRELATION BETWEEN BASE COMPOSITION OF DEOXYRIBONUCLEIC ACID AND AMINO ACID COMPOSITION OF PROTEIN

BY NOBORU SUEOKA

DEPARTMENT OF MICROBIOLOGY, UNIVERSITY OF ILLINOIS

Communicated by A. D. Hershey, June 1, 1961

It has been known that the base composition of deoxyribonucleic acid (DNA) is quite variable from organism to organism. A good example of this variability is provided by bacterial species. Here, the mean guanine-cytosine content ranges from 26 to 74 per cent.[1, 2] Moreover, the heterogeneity of base composition of DNA molecules from each species is relatively small.[3–6] These observations would appear to provide a fruitful basis for comparative biological investigations in molecular terms.

In the current views of DNA-protein coding, it is assumed that the base sequence of DNA has a direct correspondence with amino acid sequence in protein. However, whether the implied correlations between DNA base composition and amino acid composition of protein exist or not depends upon the mechanism of coding, its universality, and the magnitudes of the participating fractions of DNA and protein in the coding relation. If the majority of proteins do have coding relations with DNA, and if, in particular, the code is universal and four-symboled, we may expect some correlations between DNA and protein in their composition.

From these points of view, a search for possible correlations between DNA base composition and amino acid composition of protein has been initiated. In the present paper, the results of the first stage of our work which is concerned with total protein (microsomal plus soluble) of bacterial cells will be presented. Amino acid compositions of bulk protein preparations isolated from 11 bacterial species whose DNA base composition varies from 35 to 72 per cent in guanine-cytosine content have been examined. The results indicate that correlations between component compositions of DNA and protein do indeed exist.

Materials and Methods.—Most bacterial species used in the present investigation have been obtained from the American Type Culture Collection. One liter of an enriched nutrient broth medium[7] was inoculated and incubated at 37°C for about 15 hr with constant shaking. The minimal medium used was *M* 26 basal minimal medium.[8] This medium was supplemented with glutamic acid (0.5 gm per liter) for *Bacillus subtilis* and *Serratia marcescens*. Cells were concentrated by centrifugation at 4,000 *g* for 15 min at 5°C, washed once with tris magnesium buffer (10^{-2} *M* Tris (hydroxymethyl) aminomethane plus 10^{-3} *M* Mg, pH 7.3), and suspended in the same buffer to make the final volume 20 ml. In order to disrupt the cells, the cell suspension was put through a French press twice under a pressure of 12,000 lb/inch^2, keeping the system as cold as possible. The resulting suspension was centrifuged at 6,000 *g* for 15 min at 5°C, and the

TABLE 1 AMINO ACID COM-

Strains§	*Bacillus cereus* ATCC 6464		*Bacillus megatherium* KM	*Bacillus subtilis* NCTC 3610			*Salmonella typhimurium*	*Escherichia coli* B			
DNA GC* Content (%)	35		38	42			50	50			
Medium†	EBM Prep 2	EBM Prep 2	EBM Prep 2	EBM Prep 2	EBM Prep 2	MM Prep 2	EBM Prep 2	EBM Prep 1	EBM Prep 2	EBM Prep 2	MM Prep 2
					Stable						
Lys	6.8	10.4	10.1	11.6	9.4	10.0	9.5	8.9	8.9	8.9	8.5
His	2.8	2.9	2.7	2.8	4.1	3.0	2.7	2.8	2.8	2.9	2.9
Arg	6.1	5.9	5.1	6.3	5.4	5.8	5.9	7.4	7.6	7.7	7.0
AspX	14.5	12.7	14.6	13.4	14.8	14.2	17.2	14.2	14.4	14.2	14.4
GluX	17.2	17.4	18.3	15.7	16.8	16.4	14.7	15.6	15.0	15.3	15.6
Pro	5.2	4.9	5.6	7.1	5.6	6.0	5.0	5.8	5.7	5.8	5.8
Ala	13.6	14.6	13.0	11.9	12.4	12.6	15.0	14.5	14.7	14.3	14.7
Val	10.7	10.7	10.7	10.7	10.4	10.6	9.1	10.0	10.0	10.2	10.0
Leu	12.8	11.6	11.7	11.8	11.5	11.9	11.1	12.1	11.9	12.0	12.4
Tyr	4.8	3.8	3.6	3.7	4.0	4.0	5.0	3.8	4.0	3.9	3.9
Phe	5.6	5.0	4.5	4.9	5.5	5.4	4.8	4.9	4.9	4.8	4.8
Total	99.9	99.9	99.9	100.0	99.9	99.9	100.0	100.0	100.0	100.0	100.0
					Unstable						
Gly	13.1	13.7	11.7	11.6	11.7	12.9	10.6	12.8	12.4	11.9	12.0
Thr	7.8	7.9	7.8	6.2	7.7	8.2	7.6	7.7	7.6	7.8	7.8
Ser	5.8	6.1	6.3	4.5	7.2	7.1	6.1	6.4	6.3	6.2	6.5
Ileu	10.7	8.4	8.2	8.9	8.1	7.0	6.2	7.5	7.4	7.5	7.5
Met	1.4	4.0	3.4	1.1	3.9	3.7	4.4	4.1	3.9	3.9	4.3
Cys	0.2	0.5	0.7	0.2	0.3	—	0.4	0.5	0.6	0.7	0.9
Total	39.0	40.6	38.1	32.5	38.9	38.9	35.3	39.0	38.2	38.0	39.0
Unknown‡ (%)	0.28	0.62	0.35	0.26	0.38	0.51	0.45	0.47	0.40	0.39	0.31
					Contamination**						
DNA (%)		1.4		1.5		1.4		4.5	1.3	3.9	1.7
RNA (%)		23.3		21.0		12.4		18.6	7.1	11.7	2.4

* GC contents of DNA adopted in this table were taken from reference 1.
† EBM: Enriched broth medium (ref. 7). MM: Minimal medium (ref. 8).
‡ Expressed as a percentage in area of the ninhydrin positive, unknown material over that of the total area.

supernatant (a crude extract) was saved. "Preparation 1" was obtained by heating the crude extract at 100°C for 10 min and then by dialyzing against three liters of distilled water for 24 hr at 4°C with constant stirring. The external water was changed once. A further purification of the crude extract for "preparation 2" was achieved by adding urea to a final concentration of 4.5 *M*, and by stirring the solution at room temperature for 30 min. Ammonium sulfate (0.6 gm per ml) was added to the mixture, and the solution was centrifuged at 12,000 *g* for 20 min at 5°C. The precipitate was washed with 20 ml of 90% ethanol twice, suspended in 10 ml of distilled water, and dialyzed against 3 liters of distilled water for 24 hr at 4°C with constant stirring. The external water was changed once. The resulting preparation is called "preparation 2."

The amounts of protein of preparations 1 and 2 were determined by the Biuret method. The contents of DNA and RNA were determined by indole[9] and orcinol[10] methods, respectively. These are expressed as weight per cent of protein (Tables 1 and 2). On the average, 2.8 per cent of DNA and 16 per cent of RNA were found in the preparations listed in Table 1. For amino acid analyses, the procedure of reference 11 was followed. An aliquot of preparation 2 containing 5 mg of protein was taken in a test tube, and water was added to make the volume 2 ml. Two milliliters of concentrated HCl (12 *N*) was added to it, and the tube was sealed under vacuum after the sample was frozen. The sealed tube was kept in an air-drying oven at 110 ± 1°C for 22 hr. The hydrolyzate was dried and redissolved in 5 ml of a 0.2 *N* sodium citrate buffer, pH 2.2.[11] Minute amounts of carbon appeared after hydrolysis. This was removed by filtration. The amino acid composition was analyzed by a SPINCO Automatic Amino Acid Analyzer.

In all but three of the samples analyzed, unknown ninhydrin positive peaks were quite rare, and they occupied less than 1 per cent of the total peak area. The exceptions were *Serratia mar-*

POSITION OF TOTAL PROTEINS

Aerobacter aerogenes 57 EBM Prep 2	*Serratia marcescens* ATCC 264 58 EBM Prep 2	*Serratia marcescens* ATCC 264 58 MM Prep 2	*Sarcina lutea* ATCC 381 64 EBM Prep 2	*Sarcina lutea* ATCC 381 64 EBM Prep 2	*Pseudomonas aeruginosa* ATCC 10197 65 EBM Prep 2	*Pseudomonas aeruginosa* ATCC 10197 65 MM Prep 2	*Alcaligenes faecalis* ATCC 8750 67 EBM Prep 2	*Micrococcus lysodeikticus* ATCC 4698 72 EBM Prep 2	*Micrococcus lysodeikticus* ATCC 4698 72 EBM Prep 2	*Tetrahymena pyriformis* 1A 25 1% broth medium Prep 2
					Stable					
7.7	7.6	8.2	6.6	7.7	7.2	8.2	9.5	6.5	5.5	11.9
2.5	2.6	2.5	2.8	3.3	3.0	2.7	3.3	2.4	2.1	2.8
6.8	6.3	7.1	9.3	10.4	8.4	8.4	10.2	8.2	6.5	6.1
14.8	16.7	14.5	12.4	11.5	13.2	12.7	12.3	12.1	12.4	16.5
15.6	13.0	15.5	15.8	14.9	15.8	15.6	12.9	16.5	17.6	17.6
5.9	5.0	5.7	6.4	6.3	6.3	6.4	6.5	6.4	6.2	5.1
15.7	15.4	15.5	17.9	17.6	15.5	16.2	14.9	19.8	21.6	10.3
10.2	9.8	10.1	11.0	10.6	10.0	10.0	10.4	11.1	11.8	8.0
12.5	12.5	12.2	10.9	11.4	12.4	12.5	11.8	11.7	11.2	11.7
3.7	5.1	4.0	3.0	2.5	3.5	2.9	3.4	1.7	2.1	4.3
4.5	6.0	4.7	3.9	3.7	4.9	4.4	4.6	3.4	3.0	6.0
99.9	100.0	100.0	100.0	99.9	100.0	99.9	99.9	100.0	100.0	100.0
					Unstable					
12.9	11.9	13.1	14.3	13.9	12.7	12.9	12.7	14.9	15.2	11.0
7.6	6.9	7.4	8.4	6.9	9.2	6.8	6.8	7.7	8.1	7.7
6.7	7.4	6.9	4.5	4.7	6.4	6.3	6.3	4.9	5.8	8.1
7.1	6.1	6.6	4.5	5.6	6.5	6.5	7.0	5.6	5.0	8.8
2.4	4.2	6.0	1.0	1.1	3.2	3.3	4.0	0.1	2.1	1.6
0.5	0.6	0.7	—	—	0.8	0.4	—	—	—	—
37.2	37.1	40.7	32.7	32.2	38.8	36.2	36.8	33.2	36.2	37.2
0.69	1.13	1.11	0.78	0.77	0.48	0.39	0.34	0.87	1.02	0.50
					Contamination**					
4.7		2.6			3.2	2.9				6.4
31.5		18.8			28.2	19.3				21.1

§ ATCC: American Type Culture Collection. KM: A nonsporulating strain. NCTC: National Collection of Type Cultures, London, England. *T. pyriformis* 1A-10602b was given by Dr. D. L. Nanney.
** Expressed as a weight per cent of protein. All available samples were examined and presented here.

cescens grown on either enriched broth medium (1.1%) or minimal medium (1.1%) and one culture of *Micrococcus lysodeikticus* grown on enriched broth medium (1.0%).

Results.—The relative molar content of each amino acid was expressed in the following manner: molar amounts of amino acids, lysine, histidine, arginine, aspartic acid and asparagine, glutamic acid and glutamine, proline, alanine, valine, leucine, tyrosine, and phenylalanine, which are known to be stable and to be well recoverable in the analysis,[12] were summed. Other amino acids including glycine, threonine, serine, isoleucine, methionine, and cysteine are classified as "unstable amino acids." Glycine was not included in the "stable" class, because some glycine is produced by the decomposition of contaminating nucleic acids.[13] It is evident from the data of Tables 1 and 2 that no correlations exist between the extent of contamination with nucleic acid and the observed amino acid composition of the different protein preparations. Subsequently, the amount of each amino acid, both "stable" and "unstable," was expressed by its proportion to the sum of the stable amino acids.[14] The values expressed in this way are presented in Table 1 and Figure 1. The base compositions of DNA of bacteria used are taken from reference 1 and expressed as molar guanine-cytosine content in percentage. The above way of calculation has several advantages which may be listed as follows. (*a*) It obviates the error in estimating the relative amounts of the stable amino acids stem-

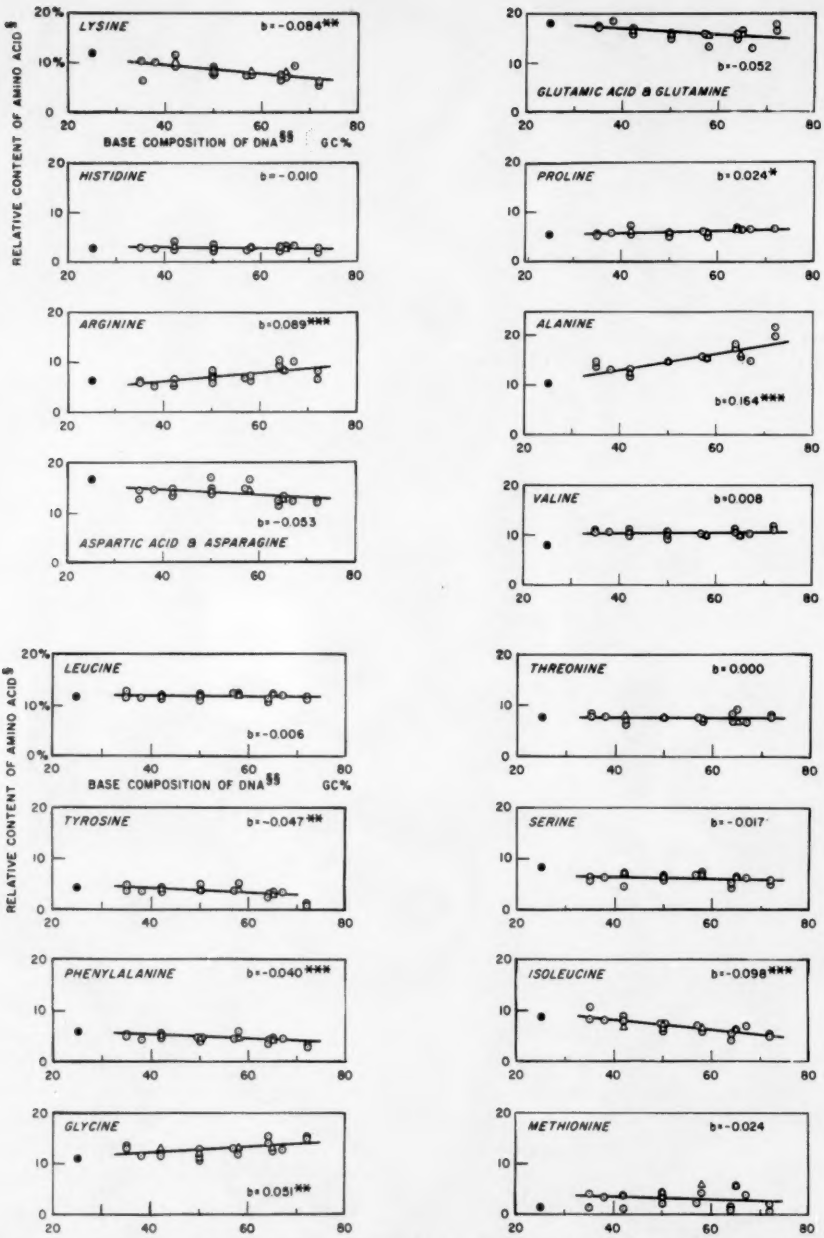

FIG. 1.—Relation between DNA base composition and amino acid composition of protein in bacteria. The relative molar content of each amino acid is expressed as a percentage of the amino acid content over the sum of stable amino acids: lysine, histidine, arginine, aspartic acid plus asparagine, glutamic acid plus glutamine, proline, alanine, valine, leucine, tyrosine, and phenylalanine. The base composition of DNA is expressed as a molar content (%) of guanine plus cytosine (GC). The GC contents of bacterial species adopted in this work are the data of reference 1. Regression coefficient (b). *Tetrahymena* data are not included in the calculation. Levels of significance of b's (or slope) are shown by asterisks.

* Significant ($0.02 < p < 0.05$).
** Highly significant ($0.001 < p < 0.02$).
*** Extremely significant ($p < 0.001$).
⊙ Enriched broth medium.
△ Minimal medium.
● *Tetrahymena pyriformis* (1A-10602 b) in 1 per cent broth medium.

ming from poor recoveries of unstable amino acids. (*b*) Relative contents of all amino acids are not changed after the calculation. (*c*) The sum of the "stable" amino acids is used as the denominator, and these have both positive and negative regression coefficients. Moreover, "stable" amino acids, the sum of which is used as

TABLE 2

AMINO ACID COMPOSITION OF TOTAL PROTEIN OF *E. coli* IN VARIOUS CONDITIONS

Medium Temperature (°C) Growth phase Preparation	EBM 37 Stationary Prep 1	EBM 37 Stationary Prep 2	EBM 37 Stationary Prep 2	EBM 37 Logarithmic Prep 2	EBM 30 Stationary Prep 2	MM 37 Stationary Prep 2	Data of Roberts *et al.* (1957)
				Stable			
Lys	8.9	8.9	8.9	9.3	8.8	8.5	10.0
His	2.8	2.8	2.9	2.6	2.8	2.9	1.3
Arg	7.4	7.6	7.7	8.2	7.3	7.0	7.7
AspX	14.2	14.4	14.2	13.5	14.3	14.4	14.2
GluX	15.6	15.0	15 3	15.8	15.2	15.6	15.1
Pro	5.8	5.7	5.8	5.4	5.7	5.8	6.6
Ala	14.5	14.7	14.3	14.9	14.8	14.7	18.2
Val	10.0	10.0	10.2	11.0	10.3	10.0	7.9
Leu	12.1	11.9	12.0	11.2	11.9	12.4	11.3
Tyr	3.8	4.0	3.9	3.4	4.1	3.9	3.0
Phe	4.9	4.9	4.8	4.6	4.8	4.8	4.7
Total	100.0	100.0	100.0	99.9	99.9	100.0	100.0
				Unstable			
Gly	12.8	12.4	11.9	15.9	12.6	12.0	11.5
Thr	7.7	7.6	7.8	7.6	7.5	7.8	6.7
Ser	6.4	6.3	6.2	7.5	6.3	6.5	8.7
Ileu	7.5	7.4	7.5	7.6	7.5	7.5	6.6
Met	4.1	3.9	3.9	3.2	3.8	4.3	4.8
Cys	0.5	0.6	0.7	0.4	0.6	0.9	2.5
Total	39.0	38.2	38.0	42.2	38.3	39.0	40.8
Unknown* (%)	0.47	0.40	0.39	0.44	0.36	0.31	
				Contamination†			
DNA (%)	4.5	1.3	3.9	0.8	2.1	1.7	
RNA (%)	18.6	7.1	11.7	45.5	9.9	2.4	

* Expressed as a percentage in area of the ninhydrin-positive unknown material over that of the total area.
† Expressed as a weight percentage of protein.

a common denominator, include a majority (13) of the twenty amino acids. As a consequence, the calculation will hardly affect the regression coefficients for the unstable amino acids.

Although there is no special reason to choose linear relations between the GC content of DNA and the amino acid content of protein, a straight line was simulated by least square methods. A summary of the statistical analysis is given in Table 3. Several amino acids show significant regression coefficients, both positive and negative.

The relative amino acid content is quite reproducible, which is indicated by the results on duplicate cultures of most species. The effect of environmental differences on the relative amino acid content of the total protein was examined by changing the composition of medium and the culture temperature and by comparing logarithmic and stationary phases of growth (Tables 1 and 2). No significant differences were observed. The present data on the amino acid composition of *E. coli* protein agree fairly well with those obtained by Roberts *et al.*[15] (Table 2). Selective enrichment of particular amino acids during the protein isolation procedure seems to be unlikely from the data on preparations 1 and 2 in *E. coli*. The relative amounts of amino acids in both fractions are very similar.

TABLE 3

ANALYSIS OF TABLE 1

Amino acid	Average content ($\bar{y}$)	Regression coefficient (b)	Confidence limits of b (5% level)	Probability	Extrapolation of GC content to 0%	Extrapolation of GC content to 100%
			Stable			
Lys	8.46	−0.084	±0.046	0.01–0.001	12.96	4.56
His	2.48	−0.010	±0.015	0.10–0.20	3.38	2.38
Arg	7.23	+0.089	±0.043	<0.001	2.46	11.36
AspX	13.85	−0.053	±0.054	0.10–0.05	16.69	11.39
GluX	15.77	−0.052	±0.050	0.05–0.10	18.14	12.98
Pro	5.89	+0.024	±0.020	0.02	4.60	7.00
Ala	15.30	+0.164	±0.055	<0.001	6.51	22.91
Val	10.39	+0.008	±0.023	0.30–0.50	9.96	10.76
Leu	11.90	−0.006	±0.020	0.50–0.70	12.22	11.62
Tyr	3.63	−0.047	±0.035	0.01–0.02	6.15	1.45
Phe	4.68	−0.040	±0.022	<0.001	6.82	2.82
			Unstable			
Gly	12.80	+0.051	±0.039	0.01–0.02	10.07	15.17
Thr	7.61	+0.0001	±0.027	>0.90	7.60	7.62
Ser	6.11	−0.017	±0.033	0.30–0.50	7.12	5.32
Met	3.07	−0.024	±0.062	0.30–0.50	4.36	1.96
Ileu	7.06	−0.098	±0.032	<0.001	12.31	2.51

Least-square method was used to calculate a and b for a linear relation $y = a + b(x - \bar{x})$. Here y is a relative molar content of an amino acid, and $\bar{y}$, its average, while x and $\bar{x}$ are GC content of DNA and its average. It is noted that a is equal to $\bar{y}$, the average of y. The way of regression analysis used here is described in reference 21. In calculating regression coefficents all but Tetrahymena data were included.

Discussion.—Several interesting features emerge from this investigation. In the first place, no unknown amino acids are found which are correlated to the base compositions of DNA. Secondly, the amino acid composition of the total protein is remarkably invariant to environmental changes as shown in Table 2 for *E. coli* data. For example, minimal versus enriched medium, stages of growth, and culture temperature do not affect the results appreciably. The amino acid composition of the total protein of any species is obviously an average composition of many kinds of protein. The constancy of the over-all composition suggests that no proteins possessing an amino acid composition widely disparate from the average are produced in large proportions under the conditions examined. In this respect it will be remembered that the compositional heterogeneity of DNA of a bacterial species is rather small compared with that of higher organisms.[6] It is possible that the extent of compositional heterogeneity in DNA may reflect that of amino acid composition in protein. Thirdly, individual amino acids appear in distinguishably different molar proportions. For example, histidine, tyrosine, phenylalanine, and methionine are found at distinctly lower levels when compared with other amino acids. This information seems to be extremely important when we realize that the relative content of each amino acid could reflect the frequency of a certain sequence of nucleotides in DNA. Finally, and most significant of all, the present results indicate that there exist several significant correlations between DNA base composition and amino acid composition of protein. According to the nature of correlations, we can classify amino acids into three groups. Among 18 amino acids tested, alanine, arginine, glycine, and proline are positively correlated with the guanine-cytosine (GC) content of DNA. Isoleucine, lysine, aspartic acid plus asparagine, glutamic acid plus glutamine, tyrosine, and phenylalanine are negatively correlated. Histidine, valine, leucine, threonine, serine, and possibly methionine are extremely uniform with no detectable evidence of correlation.

The correlation disclosed here may not, however, represent the true picture for coded protein, since some noncoded proteins may exist. Consequently, the correlations reported here may represent underestimations of the true values. When more data on amino acid composition of different cellular components become available, we will be in a better position to evaluate this evidence in relation to the coding problem. For this reason, any detailed deductions of a coding model from the present data are not attempted in this paper. Nevertheless, some qualitative discussions will be attempted with the hope that they may stimulate further investigations along this line.

(1) The present data seem to support universality of the code among bacteria. The presence of different codes among the bacteria would clearly preclude finding any correlation. Relevant to this issue are the preliminary data on amino acid content of total protein of *Tetrahymena pyriformis* included in Table 1. *T. pyriformis* strain 1A has 25 per cent GC content with a small heterogeneity.[16] The amino acid content of its protein fits remarkably well with the extrapolated lines of the data obtained with the bacteria (see Table 1). This may suggest that the underlying coding is also common to protozoa. (2) The argument that the wide variation of DNA base composition is due to the presence of large amounts of "nonsense" DNA[4, 17] seems to be rather unlikely because of the presence of correlations. This is particularly true of the correlations observed with arginine, tyrosine, and isoleucine, where the extrapolation to 0 or 100 per cent GC content makes the amino acid content almost zero. (3) The "6 keto-6 amino two-symbol code"[4, 18] is not supported by the present data, for in such a system we would expect no correlations. (4) If the coding ratio is universal and relatively small (e. g., 3, 4, 5, 6, etc.), it seems logical to have even numbers, namely 4 or 6, rather than odd numbers to explain the existance of amino acids which show neither positive nor negative correlations. To illustrate this point, let us take triplet and quadruplet nonoverlapping four-symbol codes.[19, 20] Since our analysis is based on the GC content of DNA, two base pairs, A-T and T-A, are indistinguishable, and they are expressed as α-pairs. Similarly G-C and C-G pairs are denoted as γ-pairs. Following this terminology, we can classify the possible triplets into two classes, *exclusive* and *asymmetric*. The triplets of the exclusive class are those which contain only α or γ, and we may designate them by the symbols, α_3 and γ_3. Analogously, asymmetric triplets are ones which have both α and γ but in different numbers, namely $\alpha_2\gamma$ and $\alpha\gamma_2$.

Following a similar argument, we can classify the quadruplets into three classes, exclusive (α_4 and γ_4), asymmetric ($\alpha_3\gamma$ and $\alpha\gamma_3$), and *symmetric* ($\alpha_2\gamma_2$). The symmetric class consists of quadruplets with equal numbers of α's and γ's. Then the frequency of each type of triplet or quadruplet will have correlations of different signs and magnitudes with the GC content of DNA depending on the content of γ in the particular type. Accordingly, the same kinds of correlations will be expected between amino acids in protein corresponding to each triplet (or quadruplet) and the GC content of DNA (Table 4). It is noted that the symmetric class will have no correlation when a linear regression line is estimated. The expected correlations within our GC range of analysis (25 to 75 per cent) are shown in Table 4. If we force our data to this scheme, the best fit is given by assignments similar to that in Table 4.

TABLE 4

NON-OVERLAPPING TRIPLET AND QUADRUPLET CODES AND EXPECTED CORRELATIONS BETWEEN DNA BASE COMPOSITION (GC CONTENT) AND AMINO ACID CONTENTS OF PROTEINS

Triplets

Classes	Type	Expected regression to GC content of DNA
Exclusive	α_3	− −
	γ_3	+ +
Asymmetric	$\alpha_2\gamma$	−
	$\alpha\gamma_2$	+

Quadruplets

Classes	Types	Expected regression to GC content of DNA	Amino acids classified
Exclusive	α_4	− −	Lysine, isoleucine
	γ_4	+ +	Arginine, alanine
Symmetric	$\alpha_2\gamma_2$	0	Histidine, valine, leucine, threonine, serine, methionine
Asymmetric	$\alpha_3\gamma$	−	Aspartic acid + asperagine, glutamic acid + glutamine, tyrosine, phenylalanine
	$\alpha\gamma_3$	+	Glycine, proline

α: Either A-T or T-A. γ: Either G-C or C-G. A: adenine. T: thymine. G: guanine. C: cytosine. +, + +: positively correlated. −, − −: negatively correlated. 0: no correlation.

Needless to say, the validity of these issues must be subjected to further experimental tests. Nevertheless, the results are encouraging for our faith in the existence of a coding mechanism amenable to an ultimate resolution.

Summary.—Amino acid composition of the bulk protein isolated from 11 bacterial species whose DNA base compositions vary from 35 to 72 per cent in guanine-cytosine content has been examined. The following points are of interest.

1. The amino acid composition of the total protein is remarkably invariant to environmental changes.

2. Individual amino acids appear in distinguishably different molar proportions with rather uniform values.

3. There exist several significant correlations between DNA base composition and amino acid composition of protein. Among 18 amino acids tested, alanine, arginine, glycine, and proline are positively correlated with guanine-cytosine content of DNA. Isoleucine, lysine, aspartic acid plus asparagine, glutamic acid plus glutamine, tyrosine, and phenylalanine are negatively correlated. Histidine, valine, leucine, threonine, serine, and possibly methionine are extremely uniform with no detectable evidence of correlation.

The results obtained were discussed in relation to the coding problem.

I wish to thank Mrs. C. W. Luker and Mr. R. Igarashi for their help with the amino acid analysis and Mrs. M. E. McCarty for her aid in preparation of the manuscript. I am grateful to Drs. S. Spiegelman and A. D. Hershey for reading and criticizing the manuscript. This work was supported by a grant from the National Science Foundation (G-15080).

[1] Lee, K. Y., R. Wahl, and E. Barbu, *Ann. Inst. Pasteur*, **91**, 212 (1956).
[2] Belozersky, A. N., and A. S. Spirin, *Nature*, **182**, 111 (1958).
[3] Rolfe, R., and M. Meselson, these PROCEEDINGS, **45**, 1039 (1959).
[4] Sueoka, N., J. Marmur, and P. Doty, *Nature*, **183**, 1429 (1959).
[5] Sueoka, N , these PROCEEDINGS, **45**, 1480 (1959).
[6] Sueoka, N., *J. Mol. Biol.*, **3**, 31 (1961).

[7] Tissières, A., J. D. Watson, D. Schlessinger, and B. R. Hollingworth, *J. Mol. Biol.*, **1**, 221 (1959).
[8] Sistrom, W. R. See Folsome, C. E., *Genetics*, **45**, 1111 (1960).
[9] Keck, K., *Arch. Biochem. Biophys.*, **63**, 446 (1956).
[10] Dische, Z., and K. Schwarz, *Mikrochim. Acta*, **2**, 13 (1937).
[11] Spackmann, D. H., W. H. Stein, and S. Moore, *Anal. Chem.*, **30**, 1190 (1958).
[12] Tsugita, A., and H. Fraenkel-Conrat, these PROCEEDINGS, **46**, 636 (1960).
[13] Fraser, D., *J. Biol. Chem.*, **227**, 711 (1957).
[14] In order to express the molar content of each amino acid as the percentage of the total amino acids, the value listed in Tables 1 and 2 should be divided by a factor of 1.4.
[15] Roberts, R. B., D. B. Cowie, P. H. Abelson, E. T. Bolton, and R. J. Britten, *Studies of Biosynthesis in Escherichia coli*, Publ. 607 of the Carnegie Institute of Washington (1957), p. 28.
[16] Sueoka, N., and D. L. Nanney (in preparation).
[17] Crick, F. H. C., *Brookhaven Symp. Biol.*, No. 12, 35 (1959).
[18] Sinsheimer, R. L., *J. Mol. Biol.*, **1**, 218 (1959).
[19] Crick, F. H. C., J. S. Griffith, and L. E. Orgel, these PROCEEDINGS, **43**, 416 (1957).
[20] Golomb, S. W., Welch, L. R., and Delbrück, M., *Biol. Medd. Dan. Vid. Selsk.*, **23**, 9 (1958).
[21] Mather, K., *Statistical Analysis in Biology* (London: Methuen & Co., Ltd., 1951), pp. 109–128.

ON THE SPECIES SPECIFICITY OF ACCEPTOR RNA AND ATTACHMENT ENZYMES

BY SEYMOUR BENZER AND BERNARD WEISBLUM

DEPARTMENT OF BIOLOGICAL SCIENCES, PURDUE UNIVERSITY

Communicated June 26, 1961

One of the steps in protein biosynthesis appears to be the attachment of each amino acid to a specific acceptor (SRNA) molecule. According to the adaptor hypothesis, each SRNA molecule would then fit to a specific complementary base sequence on a linear RNA template, specifying the sequence of amino acids in the resultant protein.[1, 2] An adaptor molecule thus could have two specificities: one recognizing the correct amino acid and activating enzyme; the other, the proper position on the template. The correctness of the amino-acid sequence therefore would depend upon the precision and constancy of the adaptors. However, the structures of the enzymes and adaptors are presumably under the genetic control of the organism and might be subject to heritable modifications. It is therefore conceivable that one or both ends of an adaptor might change sufficiently to cause occasional errors and, in the long run, an alteration of the genetic code might evolve. This notion, prompted by genetic observations[3] which suggested that mutation of a bacterium might modify its translation of genetic information, lead to the present comparison of the specificities of the acceptor RNA and activating enzymes of different organisms.

Several differences in specificity have been reported previously. Berg *et al.*[4] demonstrated that SRNA from *Escherichia coli* contains two distinguishable acceptors for methionine. An enzyme prepared from yeast could attach methionine to one of these, while the enzyme from *E. coli* could attach to both. Webster found, in pig liver, a difference between the nuclear and cytoplasmic attachment enzymes for alanine. Rendi and Ochoa[6] noted that, for leucine, the enzymes in

yeast and in *E. coli* could attach only to their homologous SRNA. Furthermore, in the case of leucine, rat liver enzyme and SRNA were interchangeable with those from *E. coli*.

The observations presented below show that whether the enzymes and/or acceptors from two organisms are interchangeable depends upon not only the organisms in question but also the particular amino acid.

Materials and Methods.—Preparation of SRNA: SRNA from *E. coli* was prepared by the method of Ofengand *et al.*[7] (but omitting the fractionation on ECTEOLA) and dissolved in ammonium formate buffer (0.6 *M*, pH 4.7). The solution had an optical density at 260 mμ of 123 measured by dilution in 0.1 *M* NaCl at pH 9. Yeast SRNA was prepared from bakers' yeast (Anheuser Busch Co.) according to the method of Holley *et al.*[8] and dissolved in formate buffer. The solution had an optical density at 260 mμ of 139 measured by dilution in 0.1 *M* NaCl at pH 9.

Preparation of enzyme extracts: Extracts containing amino acyl-RNA synthetase activity were obtained by the method of Bergmann *et al.*[9] Suspensions of the cells or tissue (*E. coli*, yeast, or rabbit liver) in Tris buffer, 0.025 *M*, pH 8.0, were stirred with fine glass beads in a Waring blendor, and diluted after blending to a final concentration of 1 gm wet weight of cells per 8 ml buffer. The homogenates were centrifuged (20,000 *g* for 1 hr) and the supernatant solutions were dialyzed overnight against 40 volumes of buffer (0.01 *M* Tris, pH 8.0). The preparations were stored frozen at −20°C and thawed prior to use. *C^{14} amino acids* were obtained from the California Corporation for Biochemical Research. The specific activities were: L-arginine, 5.0 μc/μM; L-tyrosine, 1.2 μc/μM; DL-lysine, 0.94 μc/μM.

Assay of amino acid acceptor activity of SRNA: The procedure used was that of Berg *et al.*[4] The reaction mixture contained the following ingredients, in a total volume of 0.5 ml: 50 μ moles of sodium cacodylate buffer, pH 7.0; 0.5 μ mole of ATP; 5 μ moles of $MgCl_2$; 0 to 4 units of SRNA; 0.2 μc of C^{14}-L-arginine, or 0.2 μc of C^{14}-L-tyrosine, or 0.4 μc of C^{14}-DL-lysine; 100 μg of crystalline beef serum albumin; 2μ moles of reduced glutathione; 5μ moles of KCl; and 0.06 ml of dialyzed enzyme extract. One unit of SRNA represents 0.06 ml of the SRNA solution in formate buffer. Assuming an optical density at 260 mμ of about 24 for a solution of 1 mg/ml, this corresponds to approximately 0.3 mg of RNA. Unless otherwise stated, the reaction mixture was incubated at 30°C for 25 minutes. The mixture was then chilled in an ice bath, and 3 ml of cold salt-ethanol (0.5 *M* NaCl, 67% ethanol) added to precipitate the SRNA. SRNA of the same kind was then added as carrier, making the total amount of SRNA constant (4 units) in all tubes. After 5 minutes, the tubes were centrifuged (6,000 *g*, 5 minutes) in the cold. The pellets were resuspended in cold salt-ethanol and the centrifugation cycle repeated three times more. Finally, the samples were dissolved in 1 ml. of 1.5 *M* NH_4OH, dried on planchets, and counted with a thin window gas flow counter.

Some of the observed counts may be expected due to SRNA present in the enzyme preparation itself and some due to coprecipitation of labelled amino acid with SRNA and protein after the addition of salt-ethanol. The sum of these was measured in a control. To this tube, no SRNA was added during the incubation period, but, after chilling and addition of salt-ethanol, four units of SRNA were added. As can be seen in the figures, the number of counts in such control tubes was relatively insignificant.

Results.—A. *Comparison of E. coli and yeast for three amino acids:* (1) Arginine: Curve A in Figure 1 shows the acceptor activity for C^{14}-arginine of SRNA from *E. coli*, assayed with an enzyme extract from the same organism. The conditions were such that the SRNA was maximally labelled, as shown by kinetic experiments, for homologous combinations of SRNA and enzyme extract. Note that the amount of C^{14}-arginine attached is proportional to the amount of SRNA added. Furthermore, as shown by the solid circle, incubation for twice the length of time, with twice as much enzyme, and twice as much C^{14}-arginine does not increase the number of counts significantly. Thus, the amount of SRNA is the limiting factor, and the slope of the curve is a measure of specific acceptor activity.

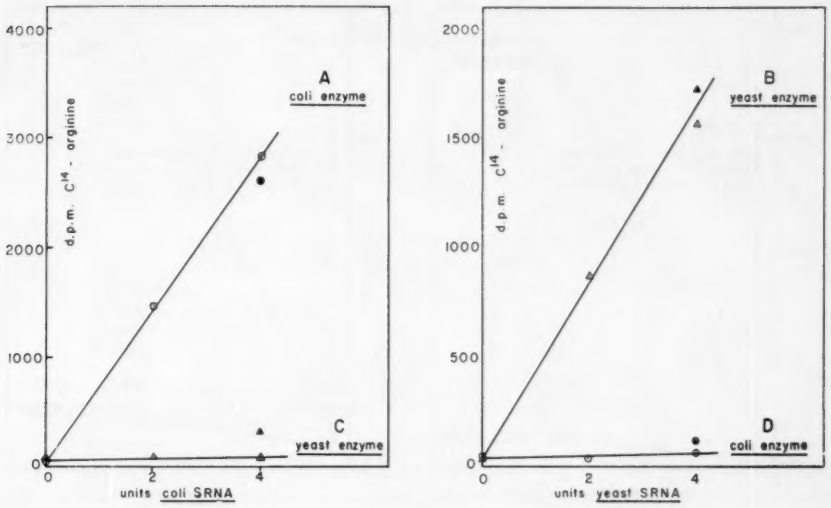

FIG. 1.—Attachment of C^{14}-arginine to *E. coli* SRNA and to yeast SRNA using enzyme preparations from either organism. The conditions are designed so that the SRNA, when treated with the homologous enzyme, becomes saturated with C^{14}-amino acid. The solid points represent samples incubated for twice the regular time, with twice the regular concentration of enzyme and twice the regular concentration of C^{14}-amino acid.

Curve B shows the activity of yeast SRNA assayed with yeast enzyme. In contrast, curves C and D for the heterologous mixtures show very little response indeed. (In the latter cases, slightly more attachment does occur in the controls with more enzyme, amino acid, and time of incubation, suggesting that the inability of the enzyme extract to catalyze attachment is not absolute.) This experiment shows that the arginine acceptors in *E. coli* and yeast are different and also that the attachment enzymes are different.

(2) Tyrosine: The same experiment for tyrosine is shown in Figure 2. Again, the strong homology requirement shows that both the acceptors and the enzymes for tyrosine are different in *E. coli* and yeast. Therefore, for at least three amino acids, arginine, tyrosine, and leucine, the enzymes and acceptors in yeast and in *E. coli* are almost completely non-interchangeable.

(3) Lysine: Turning now to the amino acid lysine, a different pattern is obtained. As shown in Figure 3, curves A and C, either the *E. coli* or the yeast enzyme extract is effective in attaching lysine to *E. coli* SRNA. However, it would be premature to conclude from this that the two enzymes are identical in their specificity. Testing the same enzyme extracts with yeast SRNA, curves B and D, shows them to be different. Furthermore, the fact that the yeast SRNA discriminates between the two enzymes, while the *E. coli* SRNA does not, shows that the SRNA's are not identical in the two organisms. The curves suggest that yeast SRNA may contain at least two different acceptors for lysine.

(4) Other amino acids: Preliminary studies with other amino acids indicate that various patterns are possible, with various degrees of interchangeability of the enzymes and/or the SRNA's. However, complete interchangeability for both

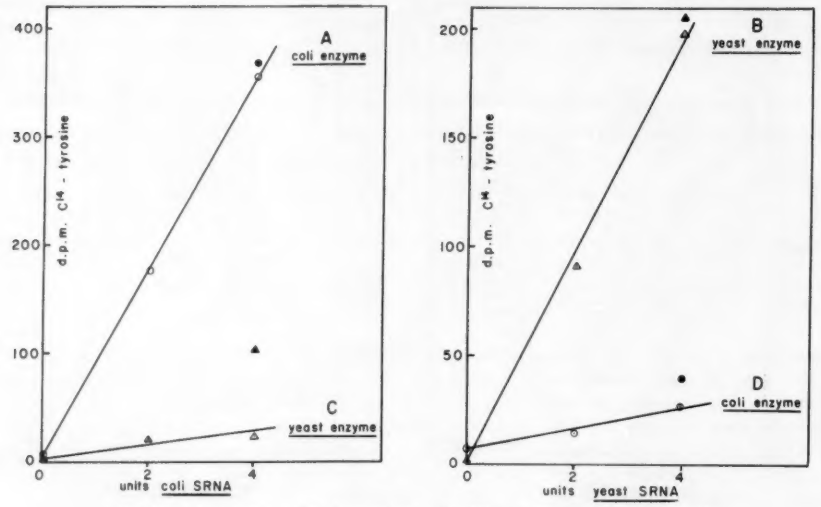

FIG. 2.—Attachment of C^{14}-tyrosine. Conditions same as for Figure 1.

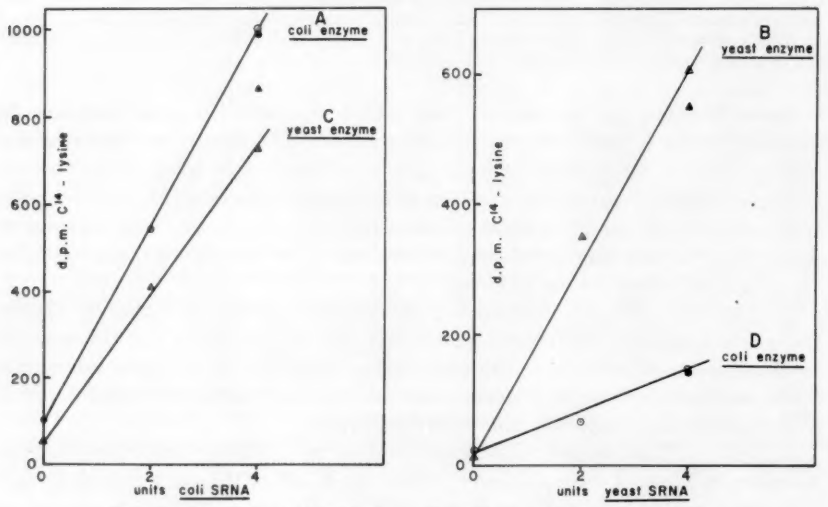

FIG. 3.—Attachment of C^{14}-lysine. Conditions same as for Figure 1.

the enzymes and the SRNA's of *E. coli* and yeast for a given amino acid is certainly not the rule.

B. *Rabbit enzyme:* The acceptor activity of SRNA from *E. coli* and yeast has also been assayed for two amino acids using an enzyme extract from rabbit liver. As shown in Table 1, rabbit liver enzyme extract attaches arginine to *E. coli* SRNA as efficiently as does the *E. coli* enzyme extract, but is ineffective with yeast SRNA. For tyrosine, however (Table 2), the situation is reversed; the rabbit enzyme specificity resembles more closely that of yeast.

TABLE 1

ATTACHMENT OF C^{14}-ARGININE

Enzyme extract	*E. coli* SRNA	Yeast SRNA
E. coli	1.00	0.02
Yeast	0.01	1.00
Rabbit	1.18	0.02

Relative arginine acceptor activities of *E. coli* SRNA and yeast SRNA when assayed with enzyme extracts from *E. coli*, yeast, or rabbit liver. The values given are the slopes of the curves, measured as in Figure 1, normalized to the value obtained for each SRNA with homologous enzyme.

TABLE 2

ATTACHMENT OF C^{14}-TYROSINE

Enzyme extract	*E. coli* SRNA	Yeast SRNA
E. coli	1.00	0.10
Yeast	0.05	1.00
Rabbit	0.01	1.12

Relative tyrosine acceptor activities of *E. coli* SRNA and yeast SRNA when assayed with enzyme extracts from *E. coli*, yeast, or rabbit liver. The values given are the slopes of the curves, measured as in Figure 1, normalized to the value obtained for each SRNA with homologous enzyme.

If a mixture of the coli and rabbit enzyme extracts is used with *coli* SRNA, the amount of arginine attached is no greater than with rabbit enzyme alone. This implies that both enzymes attach arginine to the same acceptor. The same applies to the attachment of tyrosine to yeast SRNA by a mixture of yeast and rabbit enzyme extracts.

Discussion.—The present results may bear only on one part of the SRNA molecule—that determining which amino acid is attached. It is conceivable that, for a given amino acid, the portion of its SRNA molecule that determines the specific attachment to the template is identical in all organisms. In that case the genetic code would remain universal. However, since the specificity of interaction of the SRNA molecule with the enzyme catalyzing attachment of a particular amino acid is subject to wide species variations, it is not difficult to imagine that the SRNA molecule could change sufficiently to accept a different amino acid. If this has happened in nature (and if the adaptor hypothesis is correct) the genetic code might well not be universal.

A direct demonstration of this could come from an experiment in which a given amino acid, attached to the SRNA from one organism, were to become incorporated in place of another amino acid when added to the protein synthetic machinery of a second organism. This did not occur in one such experiment performed by von Ehrenstein and Lipmann[10] where amino acids attached to *E. coli* SRNA (using *E. coli* enzymes), were efficiently incorporated into rabbit hemoglobin, and the leucine, which was labelled with C^{14}, apparently went into its normal positions in the protein. It may be desirable to extend such experiments to other amino acids with SRNA from species which show as little as possible activation with the amino-acyl-RNA synthetases from rabbit. To establish the universality of the code by this means would be difficult, whereas one instance could suffice to contradict it.

In the experiments described here, crude enzyme extracts were used. This was preferable in order to avoid the possibility of discarding any of the attachment enzymes. However, the question might be raised whether some role could be attributed to the enzyme-catalyzed repair mechanism which regenerates the required terminal sequence (CCA) at the acceptor ends of partially degraded SRNA

molecules. In this connection, it should be noted that addition of cytidine triphosphate (1 micromole) to the reaction mixtures did not increase the amount of arginine attached to either coli SRNA or yeast SRNA, with either homologous or heterologous enzyme extracts. Furthermore, since the repair enzyme (in coli) does not appear to be sufficiently specific to distinguish even between the acceptors for different amino acids,[11] it seems most unlikely to be responsible for the effects observed. In any case, specificity in the repair reaction would be an equally valid demonstration that the SRNA chains specific for a single amino acid are manifestly variable in different organisms.

While the species differences observed are quite striking, it is equally impressive that certain homologies should exist, as for a rabbit and a bacterium or for a rabbit and a yeast. This suggests that the number of possible variations in an SRNA acceptor for a given amino acid is severely restricted. The data, while still scanty, show sufficient variety to suggest that any generalization is precarious.

Summary.—The specificities of acceptor SRNA and attachment enzymes in *Escherichia coli* and yeast are compared. Striking differences are found, but the pattern depends upon the particular amino acid in question. Enzyme from rabbit liver resembles *E. coli* enzyme for one amino acid (arginine), but for another amino acid (tyrosine) it resembles yeast enzyme. The implications of these facts for the problem of the universality of the genetic code are discussed.

We are particularly grateful to Paul Berg for making several manuscripts available to us before publication. The research was supported by grants from the National Science Foundation and the National Institutes of Health.

[1] Hoagland, M. B., *Brookhaven Symposia in Biol.*, **12**, 40 (1959).

[2] Crick, F. H. C., "The Biological Replication of macromolecules," in *Symposia of the Society for Experimental Biology* (London: Cambridge Univ. Press, 1959), vol. 12, p. 138.

[3] Benzer, S., and S. P. Champe, these PROCEEDINGS, **47**, 1025 (1961).

[4] Berg, P., F. H. Bergmann, E. J. Ofengand, and M. Dieckmann, *J. Biol. Chem.*, **236**, 1726 (1961).

[5] Webster, G. C., *Biochem. Biophys. Research Commun.*, **2**, 56 (1960).

[6] Rendi, R., and S. Ochoa, *Science*, **133**, 1367 (1961).

[7] Ofengand, E. J., M. Dieckmann, and P. Berg, *J. Biol. Chem.*, **236**, 1741 (1961).

[8] Holley, R. W., J. Apgar, B. P. Doctor, J. Farrow, M. A. Marini, and S. H. Merrill, *J. Am. Chem. Soc.*, **82**, 5757 (1960).

[9] Bergmann, F. H., P. Berg, and M. Dieckmann, *J. Biol. Chem.*, **236**, 1735, (1961).

[10] von Ehrenstein, G., and F. Lipmann, these PROCEEDINGS, **47**, 941 (1961).

[11] Preiss, J., M. Dieckmann, and P. Berg, *J. Biol. Chem.*, **236**, 1748 (1961).

*ANOMALOUS ROTATORY DISPERSION OF ENZYME COMPLEXES, II. THE ASYMMETRIC BINDING OF COENZYMES AND INHIBITORS TO LIVER ALCOHOL DEHYDROGENASE**

By David D. Ulmer,† Ting-Kai Li,‡ and Bert L. Vallee

BIOPHYSICS RESEARCH LABORATORY OF THE DEPARTMENT OF MEDICINE, HARVARD MEDICAL SCHOOL, AND PETER BENT BRIGHAM HOSPITAL, BOSTON

Communicated by Eric G. Ball, June 16, 1961

The inhibition of the yeast and liver alcohol dehydrogenases[1] by chelating agents is accompanied by progressive changes in optical rotation.[2, 3] Such alterations of the optical rotatory properties of yeast alcohol dehydrogenase are due to the binding of chelating agents to the asymmetric zinc site of the enyme resulting in a characteristic Cotton effect. The rotatory power of this Cotton effect, when superimposed upon the background dispersion curve of the native protein, accounts for the rotational changes which appear during the course of enzymatic inhibition, and these changes can be differentiated from those due to alterations in protein conformation.[4] Such observations suggested that changes in optical rotatory dispersion might be a frequent concomitant of the binding of small molecules to proteins and might, thereby, be used to identify the interactions with enzymes of optically active, chromophoric substrates, coenzymes, inhibitors, and other site specific reagents.[4]

To this end we have investigated the alcohol dehydrogenase of horse liver. This zinc containing enzyme[5, 6] interacts stoichiometrically with two moles of coenzyme, DPN(H), to form the enzymatically active holoenzyme[7] and is inhibited by a number of chelating agents.[8] Zinc is not removed during chelation nor does the enzyme dissociate into subunits by electrophoresis or ultracentrifugation. 1,10-phenanthroline, OP, reversibly inhibits the enzyme by chelation of the zinc atom forming a mixed complex: LADH·Zn·OP.[9] The coenzyme binds in a specific though as yet unknown manner at or near the zinc site of the enzyme.[10] A variety of approaches indicate that zinc is a component of the "active center" of liver alcohol dehydrogenase.[11]

The present report demonstrates that the binding of reduced diphosphopyridine nucleotide to liver alcohol dehydrogenase is accompanied by the appearance of a pronounced Cotton effect at 327 mμ. The magnitude of this Cotton effect is a direct function of the molar ratio of the interactants, thereby permitting a quantitative assessment of coenzyme binding. Moreover, characteristic changes in the optical rotation of the enzyme-coenzyme complex identify its interaction with substrate and inhibitors. Similar effects are observed when the analogues of DPNH bind to liver alcohol dehydrogenase.

The considerations pertinent to the choice of metalloenzymes for the exploration of the molecular basis of enzyme action have been discussed[3] and preliminary accounts of the present studies have been reported.[12, 13]

Methods and Materials.—Crystalline alcohol dehydrogenase of horse liver was obtained from C. F. Boehringer and Soehne, Mannheim, W. Germany. Prior to use, the enzyme was dialyzed for 5 days against 0.1*M* phosphate buffer, pH 7.5 at 4° to remove low molecular weight impurities which absorb radiation at 280

mμ. The concentration of protein was determined by measurement of the optical density at 280 mμ based on an absorbancy index of 0.455 mg^{-1} cm^2.[14] The enzyme was monodisperse upon sedimentation in the analytical ultracentrifuge.

DPNH and TPNH were obtained from Sigma Chemical Co. DPN and the coenzyme analogues were obtained from Pabst Laboratories; DPN was 95% pure as estimated by cyanide complex formation.[15] Acetamide was purchased from the Coleman and Bell Co. Urea (J. T. Baker Chemical Co.) was recrystallized three times from metal-free water in the presence of amberlite MB-1(Fisher Chemical Co.); 1,10-phenanthroline (G. F. Smith Co.) was dissolved in 0.1*M* phosphate buffer and adjusted to pH 7.5 with NaOH prior to use. Sodium dihydrogen phosphate, sodium pyrophosphate, and 95% ethanol were all of reagent grade and used without further purification. Dialyses were carried out in precleaned[16] cellulose casings (Visking Company). The purification of water, chemicals, and glassware has been described.[17]

Catalytic activity was measured spectrophotometrically at 23° observing the rate of DPNH formation at 340 mμ as described previously.[4] The 3.0 ml. reaction mixture contained 5 μmoles of DPN, 50 μmoles of ethanol, 0.5 ml. of 0.1*M* pyrophosphate buffer, pH 8.8, and 10 μgm. of enzyme.

Optical rotation was measured by means of a model 200S-80Q photoelectric spectropolarimeter with an oscillating polarizer prism (O. C. Rudolph and Sons). A high-intensity, high-pressure mercury lamp (A-H6, General Electric Co.) was used as a light source. Excellent stability was obtained by circulating cooled, metal-free water through the lamp housing which was fitted with a quartz water jacket for determination of rotations at the shorter wavelengths. All measurements were performed in 5 cm semi-micro polarimeter tubes with fused quartz end plates. Temperature control was achieved by circulation of water from an external bath through the housing of the polarimeter. A stream of nitrogen gas was directed onto the polarimeter tube end plates to prevent fogging. Rotation angles were measured by the method of symmetrical angles[18] and, under the conditions employed, the values for specific rotation are precise to ±1.0°. Specific rotations measured in the presence of urea are corrected for the change in the refractive index.[19] Dispersion constants were obtained as suggested by Yang and Doty.[20]

Results.—Liver alcohol dehydrogenase in 0.1*M* phosphate buffer, pH 7.5, 12°C, exhibits a specific rotation, $[\alpha]_D$ of −8°. In the spectral range 275–700 mμ the rotatory dispersion is plain[21] although the data do not fit a one-term Drude equation. A perturbation in the dispersion curve at 275–285 mμ may well reflect the influence upon total rotation of the aromatic amino acid residues of the protein.[22]

In the presence of the reduced coenzyme, the optical rotatory dispersion of liver alcohol dehydrogenase becomes anomalous (Fig. 1). The addition of $4 \times 10^{-5}M$ DPNH[23] to a $2 \times 10^{-5}M$ solution of enzyme results in the appearance of a pronounced, single, negative Cotton effect, characterized by a trough at 355 mμ, a peak at 305 mμ, a breadth of 50 mμ, and an amplitude of 70°. The mid-point or point of inflection of the Cotton effect, λ_0, is at 327 mμ. This value corresponds to the absorption maximum for the LADH·DPNH complex, representing a shift from the absorption maximum of the free coenzyme at 340 mμ.[7]

The negative Cotton effect is superimposed upon the background rotatory dis-

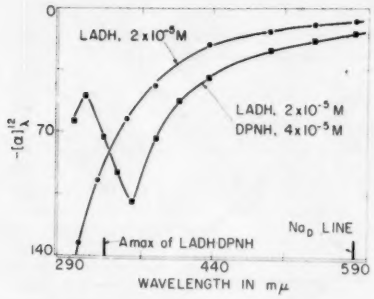

FIG. 1.—The effect of DPNH on the optical rotatory dispersion of liver alcohol dehydrogenase. Specific rotation at 12°, $-[\alpha]_\lambda^{12}$, is plotted against wavelength. In the presence of DPNH, the rotatory dispersion of the enzyme is anomalous due to a pronounced negative Cotton effect centered about the absorption maximum of the enzyme-coenzyme complex at 327 mμ. Increased levorotation at the sodium D line is a direct consequence of the Cotton effect. All measurements in 0.1 *M* phosphate, pH 7.5, 12°. The enzyme concentration is 1.66 mg per ml. Based on a molecular weight of 83,000, the molar concentration is 2×10^{-5} *M*.

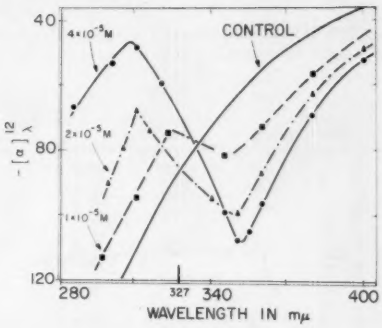

FIG. 2.—The effect of DPNH concentration on the magnitude of the Cotton effect of the LADH·DPNH complex. Specific rotation at 12°, $-[\alpha]_\lambda^{12}$, is plotted against wavelength. At a fixed enzyme concentration of 2×10^{-5} *M*, the magnitude of the Cotton effect increases with increasing DPNH concentration to become maximal at 4×10^{-5} *M* DPNH. Conditions: 1.66 mg per ml of LADH in 0.1 *M* phosphate, pH 7.5, 12° (control); 1.66 mg per ml of LADH and 1×10^{-5} *M* DPNH (■– –■), 2×10^{-5} *M* DPNH (▲·—·▲), 4×10^{-5} *M* DPNH (●——●).

persion curve of LADH and its rotatory power adds to that of the enzyme. As a consequence, the specific rotation of the enzyme is rendered more negative at longer wavelengths. This is reflected even at wavelengths as far removed from the chromophore as that of the sodium D line, where measurements reveal a shift from −8° to −15° (Fig. 1).

The magnitude of the Cotton effect is a function of the concentration of the interactants. When 2×10^{-5}*M* enzyme is titrated with increments of DPNH at pH 7.5, both the amplitude and the breadth of the Cotton effect increase in direct proportion to the DPNH concentration (Fig. 2). The effect reaches a maximum at 4×10^{-5}*M* DPNH and is not changed by further addition of the coenzyme. The small dissociation constant for the enzyme-coenzyme complex[10] assures that virtually all the added DPNH—up to twice that of the enzyme concentration—will exist in the bound form.

When the amplitude or breadth of the Cotton effect is plotted according to the method of molar proportions, a titration curve results which exhibits a sharp break at 2*M* DPNH per *M* LADH (Fig. 3). Hence, at saturation, 2 moles of DPNH interact asymmetrically with each mole of enzyme; the stoichiometry of this binding, measured by means of such a Rotatory Dispersion Titration, is in accord with previous spectrophotometric studies.[7]

It has been shown that at pH 10 only one mole of DPNH binds to this enzyme.[7] Hence the accuracy of this method can be validated by modification of the system to result in this known change in stoichiometry. Rotatory Dispersion Titration confirms the binding of 1 mole of DPNH to each mole of LADH at pH 10, and demonstrates that this one mole of DPNH is still bound asymmetrically (Fig. 3). Further, it is well known that LADH spontaneously reduces DPN in the absence

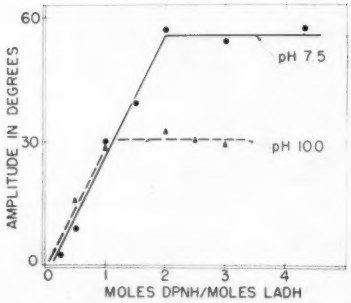

FIG. 3.—Rotatory Dispersion Titration of liver alcohol dehydrogenase with DPNH. The amplitude of the Cotton effect (vertical distance in degrees of rotation between the peak and the trough—see Fig. 2) is plotted against the moles of DPNH added per mole of LADH. At pH 7.5, two moles of coenzyme bind to each mole of enzyme. At pH 10 only one mole DPNH binds per mole LADH.

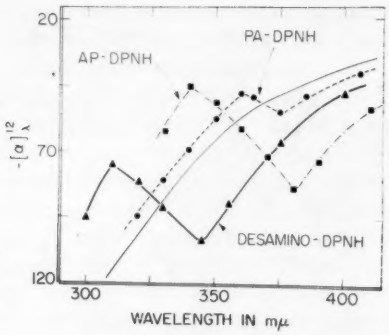

FIG. 4.—Anomalous dispersion of liver alcohol dehydrogenase in the presence of analogues of DPNH. Specific rotation at 12°, $-[\alpha]_\lambda^{12}$, is plotted against wavelength. The complex formed by each coenzyme analogue with LADH is identified by the negative Cotton effect in its absorption band. Conditions: 1.66 mg per ml of LADH in 0.1 *M* phosphate, pH 7.5, 12° (———); 1.66 mg per ml of LADH and 4×10^{-5} *M* desamino DPNH, (▲——▲), 4×10^{-5} *M* 3-acetylpyridine DPNH (■- · - · ■), and 4×10^{-5} *M* pyridine-3-aldehyde DPNH (●– –●).

of added ethanol;[24] the DPNH so produced binds to the enzyme also resulting in a characteristic Cotton effect.

The binding by the enzyme of a number of catalytically active analogues of DPNH results in a series of Cotton-effect curves characteristic for each interacting species (Fig. 4). In all instances, the Cotton effect is centered about the absorption maximum of the enyzme-analogue complex and 2 moles of each coenzyme analogue bind to the apodehydrogenase as has been reported[13] and will be documented in detail elsewhere.[25] Substitution at the 3-position of the pyridine ring of DPNH alters both the spectral location and amplitude of the Cotton effect while removal of the adenine amino group only decreases the amplitude (Table 1). Changes in specific rotation, proportional to the amplitude of the responsible Cotton effect, are observed in all instances at wavelengths far removed from the absorption bands of these analogues.

Denaturation of liver alcohol dehydrogenase not only disrupts the Cotton effect of the enzyme-coenzyme complex once it has formed, but completely destroys the capacity of the protein to interact asymmetrically with added DPNH. When the enzyme is exposed to 8*M* urea for one hour at 23°, catalytic activity is irreversibly lost. Concomitantly, as with denaturation of most globular proteins, specific rotation becomes markedly more negative at all wavelengths and the data fit a one-term Drude equation with a dispersion constant, λ_c, of 210 mμ. A Cotton effect does not appear upon addition of DPNH to the urea denatured enzyme; nor does DPNH protect the enzyme against changes in activity and optical rotation induced by urea, since urea also destroys the Cotton effect once formed. Thus

TABLE 1

COMPARISON OF ABSORPTION SPECTRA AND OPTICAL ROTATORY DISPERSION OF DPNH, THE DPNH ANALOGUES AND THEIR COMPLEXES WITH LIVER ALCOHOL DEHYDROGENASE

Coenzyme or Coenzyme Analogue	Spectrophotometry: Coenzyme A_{max} (in mμ)	Spectrophotometry: Coenzyme $\epsilon \times 10^{-3}$	Spectrophotometry: Enzyme-Coenzyme Complex A_{max} (in mμ)	Spectrophotometry: Enzyme-Coenzyme Complex $\epsilon \times 10^{-3}$	Spectropolarimetry: Enzyme-Coenzyme Cotton Effect* Inflection Point (λ_0) (in mμ)	Spectropolarimetry: Enzyme-Coenzyme Cotton Effect* Amplitude (in degrees)	Spectropolarimetry: Enzyme-Coenzyme Cotton Effect* $\Delta [\alpha]$ 436 (in degrees)†
DPNH	340	6.2	327	5.9	327	57	18
Desamino DPNH	340	6.2	331	4.7	329	30	12
3-Acetylpyridine DPNH	363	9.1	359	8.6	360	36	13
Desamino-3-acetylpyridine DPNH	363	9.1	362	8.9	365	10	8
Pyridine-3-aldehyde DPNH	358	9.3	357	8.3	360	10	4
Desamino pyridine-3-aldehyde DPNH	358	9.3	357	8.6	360	4–5	4
TPNH	340	6.2	340	6.2	...	...	0

* At the concentrations employed in these experiments, there is no discernible optical rotation of solutions of the coenzyme and coenzyme analogues in the absence of enzyme.

† $\Delta [\alpha]_{436}$ is the specific levorotation of the enzyme-coenzyme complex *minus* the specific levorotation of the enzyme at 436 mμ.

the conformation of the native protein appears to be crucial to the maintenance of asymmetry at the coenzyme binding site.

Acetaldehyde, the substrate of liver alcohol dehydrogenase, in contrast to DPNH, the coenzyme, does not exhibit chromophoric properties in an experimentally accessible wavelength range as would be required to examine the asymmetry of its binding directly. The addition of acetaldehyde to the apoenzyme does not produce changes in optical rotation; moreover, its addition to the LADH·DPNH complex destroys the demonstrated Cotton effect since the enzyme oxidizes DPNH and hence the chromophore is obliterated. However, the effects of the enzymatically inactive substrate homologue, acetamide,[26] on the optical rotatory properties of the chromophore of the LADH·DPNH complex can be discerned *indirectly*. Like acetaldehyde, acetamide does not alter the optical rotatory dispersion of the apoenzyme; it does, however, markedly increase the amplitude of the Cotton effect of the enzyme-coenzyme complex and in direct proportion to the acetamide concentration (Fig. 5). Notably, the increase in amplitude of this Cotton effect is not accompanied by a corresponding increase in breadth; this distinguishes the effect of the substrate homologue from that brought about by increments of DPNH binding. Acetamide does not affect the stoichiometry of the enzyme-coenzyme complex as can be shown by Rotatory Dispersion Titration.[13] Similar results have also been observed with another substrate homologue, isobutyramide.

In addition to the interaction of LADH with DPNH and the coenzyme and substrate homologues, the binding of inhibitors to this enzyme can also be demonstrated by means of optical rotatory dispersion as exemplified by 1,10-phenanthroline. The LADH·Zn·OP chromophore is optically active.[12, 13] Upon addition of $5 \times 10^{-5} M$ OP, the optical rotatory dispersion of $1 \times 10^{-5} M$ LADH becomes anomalous as a result of a pronounced Cotton effect at 297 mμ, the wavelength of the absorption maximum of LADH·Zn·OP[9] (Fig. 6). Over the range which can be measured with available equipment, the amplitude of this Cotton effect is proportional to the OP concentration although the absorption of the complex is too intense to allow titration of the zinc sites to saturation. A perturbation in

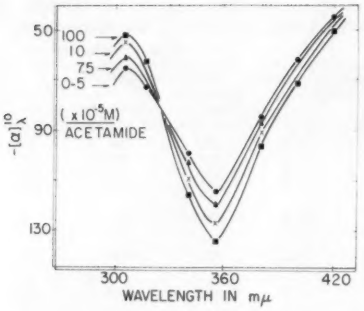

FIG. 5.—The effect of acetamide on the amplitude of the Cotton effect of the LADH·DPNH complex. Specific rotation at 10°, $-[\alpha]_{\lambda}^{10}$, is plotted against wavelength. Acetamide increases the amplitude but not the breadth of the Cotton effect to a maximum at 100×10^{-5} *M* acetamide. Conditions: 1.66 mg per ml LADH and 4×10^{-5} *M* DPNH in 0.1 *M* phosphate, pH 7.5, 10°.

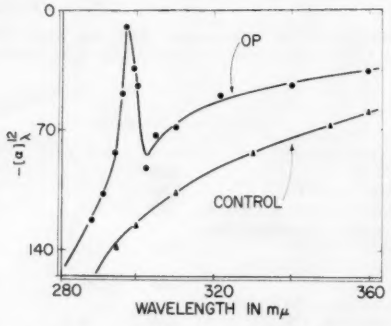

FIG. 6.—Anomalous dispersion of liver alcohol dehydrogenase in the presence of 1,10-phenanthroline (OP). Specific rotation at 12°, $-[\alpha]_{\lambda}^{12}$, is plotted against wavelength. The LADH·Zn·OP complex exhibits a positive Cotton effect centered at 297 mμ, the maximum of its principle absorption band. Conditions: 0.83 mg per ml of LADH in phosphate, pH 7.5, 12°, control, (▲——▲); 0.83 mg per ml LADH and 5×10^{-5} *M* OP (●——●).

rotatory dispersion due to a less intense absorption band at 313 mμ can also be discerned.

The inhibition of catalytic activity by OP is competitive with DPNH;[10] therefore, it would be anticipated that the Cotton effects of the enzyme-coenzyme complex and that of the LADH·Zn·OP complex should change *interdependently*, the magnitude of one increasing as that of the other decreases. This relationship is confirmed by the experiments shown in Figures 7 and 8. Excess OP diminishes the amplitude of the Cotton effect of the LADH·DPNH complex (Fig. 7), while increments of DPNH lead to corresponding decrements in the amplitude of the Cotton effect of the LADH·Zn·OP chromophore (Fig. 8). The concentrational relationships of DPNH and OP required for these competitions are in accord with those previously ascertained both by kinetic measurements and by chemical measurements at equilibrium.[3, 9–11] Thus it is apparent that the binding of OP to liver alcohol dehydrogenase can be demonstrated both *directly*, by means of a characteristic Cotton effect, and *indirectly* by virtue of an influence on the Cotton effect of the LADH·DPNH complex.

Discussion.—The active center of an enzyme is generally assumed to be localized in an area which is small compared to that of the large apoenzyme, and which is highly organized chemically and physically.[27] Delineation of this area involves the characterization both of its specific reactive groups, and of their *three-dimensional relationships* achieved through folding of the protein,[3, 28] resulting in the highly asymmetric nature of enzymes which is thought to govern their stereospecificity.

The polyaffinity theory of enzymatic specificity suggests that attachment to the asymmetric active enzyme site might generate asymmetry in substrates, coenzymes or inhibitors even when these molecules are symmetrical in space.[29] This bonding should render the absorption bands of these site specific reactants optically active.

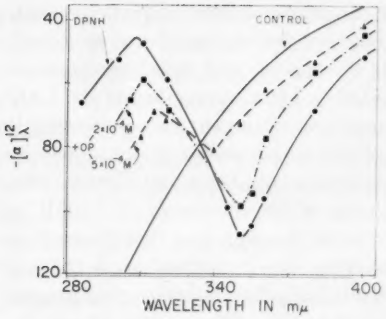

FIG. 7.—The effect of 1,10-phenanthroline (OP) on the Cotton effect of the LADH·DPNH complex. Specific rotation at 12°, $-[\alpha]_\lambda^{12}$, is plotted against wavelength. Increasing concentrations of OP decrease the magnitude of the Cotton effect of the enzyme-coenzyme complex. Conditions: 1.66 mg per ml of LADH in 0.1 *M* phosphate, pH 7.5, 12° (control); 1.66 mg per ml of LADH and 4×10^{-5} *M* DPNH (●——●); 1.66 mg per ml of LADH 4, $\times 10^{-5}$ *M* DPNH, and 2×10^{-4} *M* OP, (■- · - · -■), or 5×10^{-4} *M* OP, (▲- - -▲). At these concentrations of OP and DPNH, the high absorbancy of the solutions prohibits rotational measurements at wavelengths shorter than 305 mμ; therefore, the Cotton effect of LADH·Zn·OP, expected to appear at 297 mμ upon addition of OP, could not be examined under these circumstances.

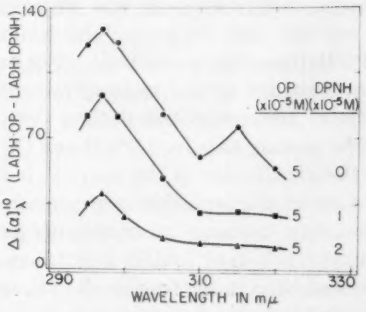

FIG. 8.—The effect of DPNH on the Cotton effect of the LADH·Zn·OP complex. The *difference rotation*, $[\alpha]^{10}$, (the specific rotation of LADH·Zn·OP *minus* the specific rotation of LADH·DPNH) is plotted against wavelength. Increasing concentrations of DPNH decrease the magnitude of the Cotton effect of LADH·Zn·OP. All measurements with 0.83 mg per ml of LADH in 0.1 *M* phosphate, pH 7.5, 10° with the indicated concentrations of 1,10-phenanthroline (OP) and DPNH.

The resultant optical rotatory properties of the *complexes* should be characteristic and distinct from those due to the interactants, i.e., protein, coenzyme, substrates, or inhibitors, alone.

In fact, a symmetrical chromophore, such as 1,10-phenanthroline, may even become optically active through interaction with *one* specific group of the enzyme, for example when the zinc atom is placed in the asymmetric environment of the active, enzymatic center of alcohol dehydrogenase.[4] The inducement of asymmetry in the electron distribution of the zinc-phenanthrolinate chromophore is accompanied by anomalous rotatory dispersion and brings to mind the symmetric carbonyl chromophore when attached to asymmetric steroids.[30] This Cotton effect can be measured directly and permits identification of the asymmetric bonds and groups which might give rise to optical activity.[30, 31] In view of these considerations the optical rotatory properties of enzyme complexes might permit a delineation of the *three-dimensional structure* of the active site as well as of its reactive groups. Toward this end we have examined, under equilibrium conditions, the complexes of LADH with DPNH, coenzyme analogues, substrate homologues, and inhibitors.

The binding of DPNH, its analogues, and OP to LADH induces optical activity in the absorption bands of the enzyme-bound chromophores resulting in characteristic Cotton effects. In the absence of enzyme and at the concentrations here em-

ployed, neither the chelating agent nor the coenzymes exhibit anomalous rotatory dispersion; nor is this phenomenon observed when the chromophores are added to proteins which do not bind them through site specific and selective interactions comparable to those which bind them to LADH. The Cotton effect of the LADH-DPNH complex is destroyed by urea denaturation of the enzyme, indicating that the integrity of the asymmetric features of the active center is dependent upon protein conformation at this site. The inflection points of the Cotton effects, λ_0, coincide with the known absorption maxima of the complexes of LADH with DPNH, its analogues, and OP. For these reasons, it seems clear that these chromophores acquire optical rotatory power by binding to asymmetric loci on the native protein; the competition of their Cotton effects indicates the topological proximity of the binding sites for DPNH and OP (Figs. 7 and 8). Since OP has been shown to chelate the zinc of the enzyme, it may be presumed that the zinc atom serves as a center of orientation, as previously suggested for yeast alcohol dehydrogenase.[4] Deuterium exchange measurements have shown that the hydrogen transfer in the catalytic action of LADH is stereospecific.[32] Such stereospecificity may have its physical basis in the fixation of the coenzyme to the asymmetric topography of the protein about the active zinc site.

Neither acetaldehyde nor the substrate homologue, acetamide, alter the optical rotatory properties of LADH, nor do they affect the Cotton effect of the LADH··Zn·OP complex, as would be predicted by the kinetic studies.[10] However, acetamide increases the amplitude without a corresponding increase in breadth of the Cotton effect of the enzyme-coenzyme complex while the absorption spectrum of the LADH·DPNH complex remains unaltered. We have not been able to find examples in the literature of similar spectropolarimetric alterations in related systems. This somewhat unusual disparity between amplitude and breadth of the Cotton effect of the DPNH chromophore may well denote an interaction of the substrate homologue with DPNH, based on mechanisms similar to those which increase fluorescence intensity under analogous circumstances.[26]

The magnitude of the Cotton effect of the LADH·DPNH complex is directly proportional to the moles of DPNH bound per mole of LADH, thus permitting determination of the stoichiometry of this binding on the basis of its asymmetry. The details of the resultant procedure, which we have termed Rotatory Dispersion Titration[13] will be described elsewhere.[25] It appears to constitute a general method for the quantitative determination of the asymmetric binding of a variety of small chromophoric molecules to proteins. In this manner we have measured the stoichiometry of interaction of LADH with the analogues of DPNH shown in Table 1, and, like DPNH, 2 moles of each bind to each mole of LADH. The λ_0 and amplitude of the Cotton effect are characteristic for each specific analogue.

The magnitude of the molar rotations in dye-polypeptide interactions has been employed as a significant parameter in the interpretation of the resultant Cotton effects.[33] Similarly, the amplitude of the Cotton effect of the LADH·DPNH and LADH·OP complexes, centered at 327 and 297 mμ, can be expressed as degrees of rotation per mole DPNH and OP, respectively. This assumes, of course, that DPNH and OP *alone* are responsible for these effects. These values would be unusually high when compared to those of most low molecular weight organic molecules in solution; however, they are not unusual for proteins and other macro-

molecules. In fact, when such molar rotations are calculated based on the assumption that it is the *complexes* of the enzyme protein with DPNH and OP which are responsible for the Cotton effects, the values are of the same order of magnitude as those for the apoenzyme alone. It is clearly difficult to decide at this juncture what the proper basis of reference for the calculation of molar rotations of asymmetric, mixed complexes should be, since the fraction of the protein molecule which contributes to the inducement of the Cotton effect is of unknown dimensions and magnitude.

Since only *one* mole each of DPNH and OP respectively have been shown to bind to or near each zinc atom of the enzyme in this system at pH 7.5[9] (Fig. 3), formation of chromophoric clusters induced by a sterically determined "seeding center" of the enzyme[33] can be eliminated as a possible cause of the Cotton effects observed in the LADH system.

The Cotton effects attributable to site specific chromophoric groups such as DPNH are superimposed upon, and therefore alter, the background rotation of LADH. While the change in specific rotation of the protein is maximal nearest the Cotton effect, it is also discernible at wavelengths far removed from the ultraviolet absorption bands of the chromophores. Thus in the presence of DPNH the $[\alpha]_D$ for liver alcohol dehydrogenase changes from $-8°$ to $-15°$ and similar increases in specific levorotation of the enzyme in the visible spectrum result from formation of its complexes with the coenzyme analogues (Table 1). In contrast, complexation with OP causes the enzyme to exhibit a more positive rotation in the visible spectrum. Obviously, such changes in optical rotation due to site specific chromophores could be erroneously attributed to other causes unless the underlying Cotton effect were identified.

The present study illustrates that the optical rotatory properties of enzyme-complexes differ in kind from those of solitary proteins. The chromophores of proteins have remained relatively inaccessible to spectropolarimetry due to their location in the ultraviolet spectrum, and few Cotton effects have been detected in these macromolecules. In spite of technical difficulties a vast amount of valuable understanding has been gained through studies relating the optical rotation of proteins to their conformation, since changes in optical rotatory dispersion correlate well with the results obtained by other physical-chemical methods when polypeptides and proteins are exposed to variations in solvents, pH, temperature, salt concentration and to oxidizing, reducing, and denaturing agents.[19, 34–37] The considerations pertinent to these alterations in optical rotation are distinct from those described in the present investigation.

The demonstration of Cotton effects in enzyme complexes requires the measurement of optical rotatory dispersion throughout the absorption bands of the bound chromophores. Hence, it is important in such determinations to work with light sources of high intensity, solutions of low absorbancy, cells of short path length, and sensitive detector elements. LADH is particularly suitable in this regard, since the dissociation constants of its complexes with DPNH, the coenzyme analogues, and OP are small, permitting measurements at low molar concentrations of these interactants. Since the dissociation constants for complexes with DPN or TPNH, and for complexes of the yeast enzyme with the pyridine nucleotides are much larger, solutions of much greater concentration are required for signifi-

cant binding to occur. The resulting increase in absorbancy precludes examination of these complexes in the critical, spectral regions with present equipment.

Summary.—The binding of reduced diphosphopyridine nucleotide and its analogues to liver alcohol dehydrogenase is accompanied by the appearance of pronounced Cotton effects at the wavelengths of maximal absorption of the enzyme-coenzyme (analogue) complexes. The magnitudes of these effects are functions of the molar ratios of the interactants; this phenomenon is the basis of a new method to measure the stoichiometry of binding of small chromophoric molecules to proteins: *Rotatory Dispersion Titration.* A chelating inhibitor, 1,10-phenanthroline, also induces a Cotton effect by forming a mixed complex with the active zinc site of the enzyme: LADH·Zn·OP. The competition of this agent with DPNH can be shown spectropolarimetrically.

The anomalous rotatory dispersion of these enzyme-coenzyme and enzyme-inhibitor complexes demonstrates the asymmetric nature of interactions at the active enzymatic site. Such studies provide an approach both to the three-dimensional structure of the active center and to investigation of the mechanisms of enzymatic stereospecificity.

* This work was supported by a grant-in-aid from the National Institutes of Health, No. H-3117 (C1), and the Nutrition Foundation.

† Post-doctoral Fellow of the National Institute of Arthritis and Metabolic Diseases, National Institutes of Health, U. S. Public Health Service.

‡ Fellow of the Helen Hay Whitney Foundation.

[1] The abbreviations used are: LADH, alcohol dehydrogenase of horse liver; DPN, diphosphopyridine nucleotide; DPNH, reduced diphosphopyridine nucleotide; AP-DPNH, 3-acetylpyridine DPNH; PA-DPNH, pyridine-3-aldehyde DPNH; OP, 1,10-phenanthroline.

[2] Ulmer, D. D., and B. L. Vallee, *Federation Proc.*, **19,** 27 (1960).

[3] Vallee, B. L., in *The Enzymes*, ed. P. D. Boyer, H. Lardy, and K. Myrbäck (New York: Academic Press, 1960), vol. 3, 2nd ed., p. 225.

[4] Ulmer, D. D., and B. L. Vallee, *J. Biol. Chem.*, **236,** 730 (1961).

[5] Theorell, H., A. P. Nygaard, and R. Bonnichsen, *Acta Chem. Scand.*, **9,** 1148 (1955).

[6] Vallee, B. L., and F. L. Hoch, *Federation Proc.*, **15,** 619 (1956).

[7] Theorell, H., and R. Bonnichsen, *Acta Chem. Scand.*, **5,** 1105 (1951).

[8] Vallee, B. L., and F. L. Hoch, *J. Biol. Chem.*, **225,** 185 (1957).

[9] Vallee, B. L., and T. L. Coombs, *J. Biol. Chem.*, **234,** 2615 (1959).

[10] Vallee, B. L., R. J. P. Williams, and F. L. Hoch, *J. Biol. Chem.*, **234,** 2621 (1959).

[11] Vallee, B. L., in *Fourth International Congress of Biochemistry, Proteins*, ed. H. Neurath and H. Tuppy (New York: Pergamon Press, 1960), vol. 8, p. 138.

[12] Ulmer, D. D., T. K. Li, and B. L. Vallee, *Federation Proc.*, **20,** 222 (1961).

[13] Li, T. K., D. D. Ulmer, and B. L. Vallee, *Abstracts of the 139th Meeting of the American Chemical Society*, St. Louis, Missouri, 1961, p. 22C.

[14] Bonnichsen, R. K., *Acta Chem. Scand.*, **4,** 715 (1950).

[15] Colowick, S. P., N. O. Kaplan, and M. M. Ciotti, *J. Biol. Chem.*, **191,** 447 (1951).

[16] Hughes, T. R., and I. M. Klotz, in *Methods of Biochemical Analysis*, ed. D. Glick (New York: Interscience Publishers, 1956), vol. 3, p. 265.

[17] Vallee, B. L., and F. L. Hoch, these PROCEEDINGS, **41,** 327 (1955).

[18] Rudolph, H., *J. Opt. Soc. Am.*, **45,** 50 (1955).

[19] Harrington, W. F., and J. A. Schellman, *Compt. rend. trav. lab. Carlsberg. Sér. chim.*, **30,** No. 12 (1957).

[20] Yang, J. T., and P. Doty, *J. Am. Chem. Soc.*, **79,** 761 (1957).

[21] The terminology is in accord with Djerassi.[20]

[22] Schellman, J. A., and C. G. Schellman, *Arch. Biochem. Biophys.*, **65,** 58 (1956).

[23] β-DPNH is itself optically active. In the spectral ranges employed and at the concen-

trations used in these studies, however, the optical rotation of the coenzyme in phosphate buffer, employed as a polarimeter blank, is barely detectable.

[24] Kaplan, N. O., and M. M. Ciotti, *J. Biol. Chem.*, **211,** 431 (1954).

[25] Li, T. K., D. D. Ulmer, and B. L. Vallee (in preparation).

[26] Winer, A. D., and H. Theorell, *Acta Chem. Scand.*, **13,** 1038 (1959).

[27] Linderstrom-Lang, K. U., and J. A. Schellman, in *The Enzymes*, ed. P. D. Boyer, H. Lardy, and K. Myrbäck (New York: Academic Press, 1960), vol. 1, 2nd ed., p. 443.

[28] Fraenkel-Conrat, H., in *The Enzymes*, ed. P. D. Boyer, H.Lardy, and K. Myrbäck (New York: Academic Press, 1960), vol. 1, 2nd ed., p. 589.

[29] Ogston, A. G., *Nature*, **162,** 963 (1948).

[30] Djerassi, C., ed., *Optical Rotary Dispersion* (New York: McGraw-Hill, 1960).

[31] Lowry, T. M., *Optical Rotary Power* (London: Longmans, Green and Co., Ltd., 1935).

[32] Levy, H. R., and R. Vennesland, *J. Biol. Chem.*, **228,** 85 (1957).

[33] Stryer, L., and E. R. Blout, *J. Am. Chem. Soc.*, **83,** 1411 (1961).

[34] Blout, E. R., in *Optical Rotatory Dispersion*, ed. C. Djerassi (New York: McGraw-Hill, 1960), p. 238.

[35] Doty, P., in *Fourth International Congress of Biochemistry*, ed. H. Neurath and H. Tuppy (New York: Pergamon Press, 1960), vol. 8, *Proteins*, p. 8.

[36] Schellman, J. A., *Compt. rend. trav. lab. Carlsberg, Sér. Chim.*, **30,** 363 (1958).

[37] Schellman, C. G., and J. A. Schellman, *Compt. rend. trav. lab. Carlsberg, Ser. Chim.*, **30,** 463 (1958).

---

*INDUCTION OF PLANT TUMORS BY ULTRAVIOLETR ADIATION**

BY CARL R. PARTANEN AND JANE NELSON

THE CHILDREN'S CANCER RESEARCH FOUNDATION AND THE DEPARTMENT OF PATHOLOGY, THE CHILDREN'S HOSPITAL MEDICAL CENTER, BOSTON†

Communicated by Ralph H. Wetmore, May 31, 1961

It has been previously shown that spontaneous tumors occur at a very low frequency in the gametophytic generation of the fern, *Pteridium aquilinum* (the Bracken fern)[1] and that the frequency of occurrence of such tumors can be increased greatly by the application of ionizing radiations to the dormant spores prior to their germination.[2, 3] These tumors have been characterized as to some of their morphological,[1] cytological,[4, 5] and physiological[6, 7] peculiarities. The present report extends the studies on this tumor system to include now another causal agent, namely ultraviolet irradiation.

Materials and Methods.—For the irradiation, dormant spores were spread into essentially a monolayer on a 33 cm coarse filter paper. The irradiation was administered by placing the paper bearing the spores 50 cm below an ultraviolet germicidal tube (Westinghouse G36T6L Slimline Sterilamp). The ultraviolet energy incident at the level of the spores was approximately 40 ergs/sec/mm^2, with approximately 95% of the energy in the range of 2537 Å.[8] After irradiation the spores were sown quantitatively in the manner previously described[7] and were grown aseptically *in vitro* on our basal medium[6] for the dose-relationship study, and upon modifications of this medium for the physiological comparison of these tumors with those studied earlier.

Results and Discussion.—It was observed that after dormant spores of *P. aquilinum* were given a suitable exposure to ultraviolet radiation, upon subsequent germi-

nation they would develop numbers of disorganized tumorous growths. These tumors were identical in general appearance to those spontaneously occurring and earlier described,[1, 4, 5] and to those induced by ionizing radiations.[2, 3] Morphologically, the tumors that arise in response to ultraviolet radiations are also like the earlier ones, ranging between the two recognizable extremes of expression from the completely parenchymatous to that in which the basic structure is essentially filamentous. In each type, however, the general appearance is that of a nodular mass of tissue which increases in size and which retains this growth habit in separate culture through repeated subcultures. Cytological examination showed that in newly isolated tumors all nuclear divisions were apparent haploids whereas after a longer period in culture such tumors showed some tendency toward polyploidy through endomitosis, as did the earlier studied spontaneous and X-ray induced tumors.

After the initial observation of the induction of tumors with ultraviolet radiation and the approximation of the effective dose range, the dose-response relationship was determined. Identical lots of spores were irradiated under the conditions described for periods of 0, 2, 4, 6, 8, and 10 minutes, sown quantitatively on agar slants of the basal medium with 24 replicates of each dose level. After a culture period of 6 weeks all tumors detectable under 7× magnification were counted. The results are shown in Figure 1, with the frequency of tumors per million spores at each dose-

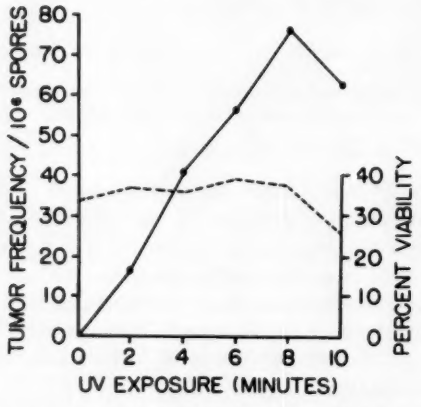

FIG. 1.—Dosage-response relationship of ultraviolet radiations applied to dormant spores of *Pteridium aquilinum*. The frequency of tumors per million spores after 6 weeks in culture (solid line) and the per cent viability (dashed line) are plotted against the ultraviolet dose in m utes.

level of radiation. The response in tumor frequency is essentially linear up to 8 minutes' exposure, after which it declines abruptly. Spore viabilities were also determined for each lot by making absolute counts from diluted inocula[3] and are plotted in Figure 1 as per cent viability (dashed line). Viability is not significantly affected by doses up to 8 minutes, but at 10 minutes it also declines abruptly. Therefore, the decrease in tumor frequency at 10 minutes' exposure is quite clearly a reflection of the decrease in general viability. Until altered viability becomes a factor, the tumor response is very probably a truly linear one, as is also the case

with X-rays in the lower dose range.[3] Thus, since this is a haploid organism, this type of response seems consistent with our earlier hypothesis that the primary event causal to subsequent tumorization is a mutation, or a group of similar mutations which produce the same morphogenetic effect.

That these mutations may be biochemically definable has been suggested by the observation that the occurrence of potential tumors in X-rayed spores can be suppressed or inhibited by the addition of certain amino acids. Thus, the irradiated potentially tumorous spore seems to behave as a biochemical "deficient," i. e., in the absence of a certain amino acid the tumorous type of development occurs, but if the "deficiency" is met by the addition of the amino acid, then the development is not tumorous. By this reasoning, therefore, a tumor in this system may be a mutant, one of whose manifestations is detectable as a biochemical "deficiency," but of the type which, if not fulfilled, is not lethal but instead leads to an altered developmental pattern which we recognize as a tumor.

One of the best tested and reproducible agents in the suppression of X-ray-induced tumors in this system is methionine. The addition of a 1 mM concentration of L-methionine to the basal medium will reduce the frequency of tumors to 15% of that observed on the control (basal medium) with no significant effect on total viability. To test the ultraviolet-induced tumors for a similar response, a quantity of spores was exposed to ultraviolet light under our standard conditions for 8 minutes. These were sown on two media, basal and basal + 1 mM L-methionine. The methonine was found to be equally effective in suppressing the ultraviolet-induced tumors, the frequency being 13% of that on the controls. Other amino acids or antagonists that have characteristic effects on X-rayed spores are L-lysine, canavanine sulfate, L-hydroxyproline, and DL-allylglycine. All of these, when tested on ultraviolet-irradiated spores, produced their characteristic effects by suppressing tumor frequency to varying degrees. Thus, on the basis of their morphological, cytological, and physiological characteristics, the tumors that arise after ultraviolet exposure appear to be identical to those induced by X-rays.

Ultraviolet-induced phenomena are often reversible by the simultaneous or subsequent administration of visible light (3000–5000 Å), i. e. "photorecovery" or "photoreactivation."[9] Consequently, this system was tested for such an effect by first irradiating similar lots of spores simultaneously for a 10-minute dose of ultraviolet. Immediately thereafter, while one lot was stored in the dark, the other was placed under an H100A lamp at a distance of one foot with a window-glass filter interposed, for exposures up to one hour. Subsequently, both lots were sown in the usual manner on the basal medium. The first week of germination and growth occurred in a dark cabinet. The remaining five weeks of the culture period were in the customary low-level of illumination.[7] Under these conditions no photorecovery effect was noted either in restored viability or in reduced tumor frequency.

The phenomenon of fern gametophyte tumorization is not peculiar to Pteridium, both spontaneous[4, 5] and X-ray-induced[10] tumors having been observed in *Osmunda cinnamomea*. However, with ultraviolet doses up to one hour on spores of Osmunda, no tumor response occurred nor was viability noticeably affected. Thus ultraviolet light does not seem to be a tumorigenic agent in Osmunda. However, there are possible problems of penetrability, the spores of Pteridium being brown and having a mean diameter of approximately 30 μ whereas those of *O. cinnamomea* are green

and have a mean diameter of about 60 μ. Perhaps the ultraviolet is unable to reach the effective site in Osmunda either as a consequence of its greater size or because of possible absorption by pigments or other interfering substances.

However, the phenomenon of ultraviolet-induced tumorization is quite distinctive in Pteridium. Since the ultraviolet output was primarily at 2537 Å, near the peak of absorption of nucleic acids, it is tempting to suggest that in this system the primary lesion causal to subsequent tumorization occurs in the nucleic acids as a mutation. Although the somatic mutation hypothesis appears not to fit the data for ultraviolet-induced cancers in animals,[11] it seems a fairly attractive hypothesis in the present case. But this is a much simpler system than most in which comparable phenomena have been studied. Conceivably more than one factor or condition is necessary for a cell to give rise to a tumor. Two conditions that would seem basic would be the capacity for cell division and the failure of morphogenetic influences, both spatial and temporal, upon this division. These could well be separate factors, not necessarily related in origin. However, the capacity for, and initiation of a division would be a necessary condition for the revelation of the other factor, which expresses itself only in the *manner* of division. If the foregoing be true, then the fern gametophyte system is a particularly suitable one for analyzing specifically the nature of the morphogenetic factors involved in tumorization since the other condition is already satisfied; the tumorigenic agent is administered only to single cells which predictably are going to divide, quite unlike the situation in most experimental tumorigenesis in multicellular organisms. Furthermore, if a mutation underlies the one final factor necessary for the phenomenon of tumorization, the haploidy of these cells would be an added advantage. It would seem that we may possibly be analyzing simply one component of a multiple, at least dual, component phenomenon, unencumbered by the dependence upon the occurrence of a second independent event.

Summary.—Tumors can be induced in gametophytes of *Pteridium aquilinum* by exposing the dormant spores to ultraviolet radiations prior to germination. The tumor frequency increases linearly with dosage up to the level at which general viability of the spores is significantly affected. These ultraviolet-induced tumors are in every way comparable to spontaneously occurring ones and to those induced by ionizing radiations.

The authors wish to acknowledge the technical assistance of James Corscadden and to thank James Stauffer for having made the spore collections.

* Supported in part by a grant (no. CY-3335) from the National Institutes of Health, U. S. Public Health Service.

† Present address: Department of Biological Sciences, University of Pittsburgh, Pittsburgh 13, Pennsylvania.

[1] Steeves, T. A., I. M. Sussex, and C. R. Partanen, *Am. J. Botany*, **42**, 232 (1955).

[2] Partanen, C. R., and T. A. Steeves, these PROCEEDINGS, **42**, 906 (1956).

[3] Partanen, C. R., *Science*, **128**, 1006 (1958).

[4] Partanen, C. R., I. M. Sussex, and T. A. Steeves, *Am. J. Botany*, **42**, 245 (1955).

[5] Partanen, C. R., *Cancer Res.*, **16**, 300 (1956).

[6] Partanen, C. R., *Science*, **131**, 926 (1960).

[7] Partanen, C. R., these PROCEEDINGS, **46**, 1206 (1960).

[8] Based on manufacturer's data in technical bulletin, *Westinghouse Sterilamp Germicidal Ultraviolet Tubes and Their Application*.

[9] Jagger, J., *Bacteriol. Rev.*, **22**, 99 (1958).

[10] Partanen, C. R. (unpublished data). In *Osmunda cinnamomea* spontaneous tumors are very rare. If spores are X-rayed 5,000 to 10,000 r, there occur numerous tumors upon subsequent development *in vitro*.

[11] Blum, H. F., *Carcinogenesis by Ultraviolet Light*, Princeton University Press, 1959).

ON THERMODYNAMIC COUPLING OF CHEMICAL REACTIONS

BY G. J. HOOYMAN*,†

DEPARTMENT OF CHEMISTRY, UNIVERSITY OF WISCONSIN, MADISON

Communicated by J. W. Williams, June 5, 1961

In a recent paper[1] Koenig *et al.* have investigated the division of a set of r chemical reactions into "coupled" and "coupling" reactions as defined by De Donder, Prigogine, and Defay (cf. ref. 1 for specific references). Reactions are called "coupled" if they give rise to a negative production of entropy (i.e., proceed in a direction opposite to that suggested by their own affinity), the reactions with positive entropy production then being called "coupling" reactions. The above authors verify that without further specification the number of coupled reactions in a given set is arbitrary, in the sense that this number can be given any value from 0 to $r - 1$ by appropriate linear transformations of the chemical reactions. Hence they conclude that the concept of thermodynamic coupling without reference to reaction mechanism should be rejected.

It is the object of the present paper to show how a given set of chemical reactions can always be written as the production or consumption of a suitably chosen set of reacting components. The division into reactions with positive or with negative entropy production is then uniquely determined.[2]

In order to avoid any confusion we will not use the terms "coupled" and "coupling" reactions. In thermodynamics of irreversible processes it is generally assumed that each reaction rate is a function of *all* the affinities. This assumption implies that in general *any* two chemical reactions are coupled. It is only the sum of the entropy productions of the various reactions that is a positive definite quantity outside equilibrium and in the absence of other scalar irreversible phenomena. In this sense, chemical reactions in isotropic media are not coupled to vectorial phenomena such as diffusion and heat conduction. In view of this state of affairs we will avoid the terms coupled and coupling and, for lack of generally accepted terms, call a chemical reaction *positive* or *negative* according to the sign of its entropy production in a given system at a given time.

We consider a closed system of n components $Q_1, Q_2, \ldots, Q_n$ with mole numbers n_k among which r independent chemical reactions are possible ($2 \leq r < n$). We denote these reactions by the equations

$$\sum_{i=1}^{n} \nu_{ji} Q_i = 0 \qquad (j = 1, \ldots, r) \tag{1}$$

where the ν_{ji} are proportional to the ordinary stoichiometrical coefficients. Conservation of mass in a chemical reaction is then expressed by

$$\sum_{i=1}^{n} \nu_{ji} M_i = 0 \qquad (j = 1, \ldots, r) \tag{2}$$

if M_i is the molecular weight of i.

If $d_j n_i/dt$ is the time rate of change of n_i due to the chemical reaction j the reaction rates v_j can be defined by

$$\frac{d_j n_i}{dt} = \nu_{ji} v_j \qquad (i = 1, \ldots, n; \; j = 1, \ldots, r) \tag{3}$$

from which

$$\frac{dn_i}{dt} = \sum_{j=1}^{r} \frac{d_j n_i}{dt} = \sum_{j=1}^{r} \nu_{ji} v_j \tag{4}$$

The entropy production σ (per unit time) due to these reactions is[3]

$$\sigma = -\frac{1}{T} \sum_{i=1}^{n} \frac{dn_i}{dt} \mu_i = -\frac{1}{T} \sum_{i=1}^{n} \sum_{j=1}^{r} \nu_{ji} v_j \mu_i = \frac{1}{T} \sum_{j=1}^{r} A_j v_j \tag{5}$$

where μ_i is the chemical potential (partial molar Gibbs function) of component i and A_j is the chemical affinity of reaction j

$$A_j = -\sum_{i=1}^{n} \nu_{ji} \mu_i \tag{6}$$

We know σ to be a positive quantity although one or more of the separate terms $A_j v_j$ may be negative. Upon linear transformation of the chemical reactions the affinities and the coefficients ν_{ji} are transformed by the same transformation matrix. The corresponding transformation of the reaction rates is contragredient to this transformation.[4] Such transformations may in general change the numbers p and $r - p$, respectively, of negative and positive reactions and thus transform a scheme with $p > 0$ into a scheme with $p = 0$ or vice versa. This has been explicitly shown by Koenig *et al.*[1] who conclude from the indefiniteness of p that the concept of thermodynamic coupling of chemical reactions seems to be useless.

In the following we want to show how a precise meaning can be given to the number p of negative reactions. To clarify the underlying idea we refer to the example quoted by Koenig *et al.* of the synthesis of urea in the presence of the oxydation of glucose. It is important to note that in their first set of two reactions urea occurs *only* in the first and glucose occurs *only* in the second reaction. With this restriction the two reactions are unique and the statement that "the synthesis of urea is a negative reaction in the presence of the oxydation reaction" is unambiguous.

How can we generalize such a statement to a general set of r reactions among n components? Consider the rectangular matrix of coefficients ν_{ji}

$$\begin{pmatrix} \nu_{11} & \nu_{12} \ldots\ldots \nu_{1n} \\ \cdot & \cdot & \cdot \\ \cdot & \cdot & \cdot \\ \cdot & \cdot & \cdot \\ \cdot & \cdot & \cdot \\ \nu_{r1} & \nu_{r2} \ldots\ldots \nu_{rn} \end{pmatrix} \tag{7}$$

in which each row corresponds to one reaction and each column to one component. (Components that do not take part in at least one reaction are excluded.) Since the reactions are linearly independent the $r \times n$ matrix, equation (7), has the rank r which means that at least one nonsingular $r \times r$ square submatrix can be formed from equation (7). Furthermore, one can easily show that any column C_i occurs in at least one nonsingular $r \times r$ submatrix (cf. Appendix 1).

We first fix our attention to one particular component, e.g., Q_i, and we choose a nonsingular submatrix containing C_i (the choice may not be unique; we will come back to this later). By this choice we single out a set of r columns in the matrix (7) and along with it a certain set of components. Without any loss of generality we may take this set to be given by $Q_1, Q_2, \ldots, Q_r$. This can always be achieved by a simple rearrangement of columns. Since this particular submatrix is nonsingular we can in a unique way reduce it to a unit matrix by a linear transformation of rows (cf. Appendix 2). The matrix of transformed coefficients ν'_{ji} then takes the form

$$\begin{pmatrix} 1 & 0 & \ldots & 0 & \nu'_{1,r+1} & \ldots & \nu'_{1n} \\ 0 & 1 & \ldots & 0 & \cdot & & \cdot \\ \cdot & \cdot & & \cdot & \cdot & & \cdot \\ \cdot & \cdot & & \cdot & \cdot & & \cdot \\ 0 & 0 & \ldots & 1 & \nu'_{r,r+1} & \ldots & \nu'_{rn} \end{pmatrix} \tag{8}$$

In this new scheme each chemical reaction can be said to describe completely the production or consumption of one member of the set $Q_1, \ldots, Q_r$. Using this scheme the reaction rates are

$$v'_j = \frac{dn_j}{dt} \tag{9}$$

and the affinities are

$$A'_j = -\mu_j - \sum_{i=r+1}^{n} \nu'_{ji}\mu_i \tag{10}$$

From (8) we see that reaction 1 and hence the sign of $A'_1v'_1$ is uniquely determined by the requirements that component Q_1 occurs only in reaction 1 and that this reaction does not involve components $Q_2, \ldots, Q_r$. Furthermore, the value of $A'_1v'_1$ is not affected by linear transformations of reactions 2, 3, ..., r. If $A'_1v'_1 < 0$ we may call the production (or consumption) of Q_1 a "negative reaction with respect to the chemistry involving $Q_2, \ldots, Q_r$."

Likewise, the first p reactions ($p < r$) in the transformed scheme may be negative (after proper rearrangement of rows and columns in equation (8)). We then may call the production or consumption of $Q_1, \ldots, Q_p$ negative with respect to the chemistry involving $Q_{p+1}, \ldots, Q_r$. It is then understood that each component $Q_1, \ldots, Q_p$ occurs only in one of the first p reactions which do not involve the components $Q_{p+1}, \ldots, Q_r$.

As was already stated above the set of components $Q_1, \ldots, Q_r$ may not be uniquely determined even if we require it to include a given component Q_i. This does not invalidate the reasoning given above but can only give rise to different schemes. In practical cases a particular set of r components may present itself more naturally than other possible choices. But once a permissible set of components (i.e., with a

corresponding nonsingular matrix in equation (7)) is chosen out of a finite number of choices, statements about positive or negative reactions can be given a definite meaning which may be of interest in the description of living systems.

APPENDIX

1. Column C_1 in matrix (7) contains at least one nonzero element for which we can always take ν_{11}. Subtracting suitable multiples of the first row from the other rows the matrix transforms into

$$\begin{bmatrix} \nu_{11} & \nu_{12} & \cdots & \nu_{1n} \\ 0 & x & \cdots & x \\ 0 & . & & . \\ . & . & & . \\ . & . & & . \\ 0 & x & \cdots & x \end{bmatrix} \tag{11}$$

with rank r. Let M be the rectangular matrix resulting from equation (11) by crossing out the first row and column. Suppose that every $r \times r$ submatrix of equation (11) containing C_1 would be singular. Then every $(r-1) \times (r-1)$ submatrix of M would of necessity be singular. But then also every $r \times r$ submatrix of (11) would be singular whether it included C_1 or not. This contradicts the fact that the matrix (11) has the rank r. Hence there must be at least one nonsingular $r \times r$ submatrix of (11) containing C_1.

2. The transformation of (7) into (8) involves the set of equations

$$\sum_{k=1}^{r} \alpha_{jk}\nu_{ki} = \delta_{ji} \quad (j, i = 1, \ldots, r) \tag{12}$$

where δ_{ji} is the Kronecker symbol.

For each j, equation (12) gives a set of r linear equations in the coefficients α_{jk}. This set has a unique solution since the determinant $|\nu_{ki}|$ was supposed to be nonzero.

Summary.—Recently some doubt has been cast upon the physical meaning of thermodynamic coupling in a set of chemical reactions. In the present paper a general procedure is described to distinguish between reactions with positive and with negative production of entropy in terms of a specified set of reacting components.

It is a great pleasure to thank J. W. Williams for his hospitality during the author's stay at the University of Wisconsin and the Netherlands Organization for the Advancement of Pure Research for a travel grant (NATO Science Fellowship). Stimulating discussions with J. W. Williams, L. J. Gosting, and their co-workers are gratefully acknowledged. The author wishes to thank F. O. Koenig for reading the manuscript, expressing his agreement with this analysis, and, through P. Van Rysselberghe, calling his attention to an earlier contribution of De Donder.

* On leave of absence from the Physics Laboratory, The University, Utrecht, The Netherlands.

† This investigation was supported by Public Health Service Research Grant A-3030(C6).

[1] Koenig, F. O., Fr. H. Horne, and D. M. Mohilner, *J. Am. Chem. Soc.*, **83**, 1029 (1961).

[2] A similar idea is implicit in a paper by De Donder [*Bull. acad. roy. Belg.*, Cl.Sc. (5), **23**, 770 (1937)] in which the concept of "intrinsic reactions" is introduced but not completely defined.

[3] de Groot, S. R., *Thermodynamics of Irreversible Processes* (New York: Interscience Publishers, and Amsterdam: North Holland Publishing Company, 1951); I. Prigogine, *Thermodynamics of*

Irreversible Processes (Springfield, Ill.: Charles C. Thomas Co., 1956); J. Meixner and H. G. Reik, "Thermodynamik der irreversiblen Prozesse" in *Encyclopedia of Physics* (Berlin: Springer-Verlag, 1959), vol. III/2.

[4] Hooyman, G. J., S. R. de Groot, and P. Mazur, *Physica*, **21**, 360 (1955).

THEORETICAL STRUCTURE OF PLASMA EQUATIONS AND APPLICATION TO A SIMPLE PROBLEM

BY JOSEPH SLEPIAN

1115 LANCASTER STREET, PITTSBURGH 18, PENNSYLVANIA

Communicated June 5, 1961

The Transport Equations Used by (R & R).—This paper is a criticism of a paper by Rosenbluth and Rostoker.[1] That paper will be denoted henceforth by (R & R), and we shall use the notation of that paper. Numerous other papers and books accept the conclusions of (R & R) and are therefore also the subjects of my criticism.

(R & R) write for the "collision-free" transport equations of a plasma

$$\frac{\partial f_i}{\partial t} + \boldsymbol{v}\cdot\nabla f_i + \frac{\boldsymbol{F}_i}{m_i}\cdot\nabla_v f_i = 0 \qquad \text{(R \& R 4)}$$

with $i = 1$ for electrons and $i = 2$ for ions. They thereby neglect the terms $(\partial f_i/\partial t)_{\text{coll}}$ normally on the right-hand side of these equations, apparently justifying themselves by the fact that the plasma is "sufficiently dilute." But the dilute condition of the plasma in no way suffices to make $(\partial f_i/\partial t)_{\text{coll}}$ negligible in their effect on the motion of the plasma.

When the single transport equation is written for a gas of uncharged particles, then the reduction of "collisions" by "sufficient dilution" will justify the elimination of the $(\partial f_i/\partial t)_{\text{coll}}$ from the equation. But when the gas is made up of two types of particles, oppositely charged, the relative motion of the one type to that of the other type can give rise to forces per particle which do not vanish with the density of the gas. The motion of one type of particles relative to the other gives rise to microscopic high frequency electromagnetic fields which will react upon the other particles with a force per particle which will not approach zero as the density of the particles approaches zero, so long as the plasma as such has a physical meaning.

The Corrected Transport Equations.—Let us write the corrected equations (R & R 4) as

$$\frac{\partial f_1}{\partial t} + \boldsymbol{v}\cdot\nabla f_1 - \frac{e}{m_1}\left(\boldsymbol{E} + \frac{1}{c}\boldsymbol{v}\times\boldsymbol{B}\right)\cdot\nabla_v f_1 = \left(\frac{\partial f_1}{\partial t}\right)_{\text{coll}} = \frac{1}{m_1}\frac{c}{n}\boldsymbol{P}_{21}$$

(R & R 4 corrected)

$$\frac{\partial f_2}{\partial t} + \boldsymbol{v}\cdot\nabla f_2 + \frac{e}{m_2}\left(\boldsymbol{E} + \frac{1}{c}\boldsymbol{v}\times\boldsymbol{B}\right)\cdot\nabla_v f_2 = \left(\frac{\partial f_2}{\partial t}\right)_{\text{coll}} = \frac{1}{m_2}\frac{c}{n}\boldsymbol{P}_{12}$$

where $n_1 = \int f_1 d^3v$, $n_2 = \int f_2 d^3v$ and where $n_2 - n_1$ is completely negligible com-

pared to $n_1 \cong n_2 \cong n$. $\boldsymbol{P}_{21} + \boldsymbol{P}_{12} = 0$ is the condition for dilute plasma and not $\boldsymbol{P}_{21} = \boldsymbol{P}_{12} = 0$.

Suppose that m_1 is completely negligible compared to m_2. Let $\boldsymbol{v}_2$ be the mean velocity of the ions, $\boldsymbol{v}_2 = \frac{1}{n}\int \boldsymbol{v} f_2 d^3v$. Let $\boldsymbol{v}_1$ be the mean velocity of the electrons, $v_1 = \frac{1}{n}\int v f_1 d^3v$. Let $\boldsymbol{j} = ne(v_2 - v_1)$. Let $p = p_1 + p_2$. Let

$$p_1 = n\int m_1(\boldsymbol{v}_1 - \boldsymbol{v})(\boldsymbol{v}_1 - \boldsymbol{v})d^3v$$

and

$$p_2 = n\int m_2(\boldsymbol{v}_2 - \boldsymbol{v})(\boldsymbol{v}_2 - \boldsymbol{v})d^3v.$$

Let ρ be the density, $\rho = nm_2$. Let Φ be the gravitational potential. Then the following equations are the equivalent of the two transport equations (R & R 4 corrected).

$$\rho \frac{d\boldsymbol{v}_2}{dt} = \rho\left(\frac{\partial \boldsymbol{v}_2}{\partial t} + \boldsymbol{v}_2 \cdot \nabla \boldsymbol{v}_2\right) = \boldsymbol{j} \times \boldsymbol{B} - \nabla \cdot p_1 - \nabla \cdot p_2 - \rho \nabla \Phi \tag{1}$$

$$\frac{m_1 c^2}{ne^2}\frac{\partial \boldsymbol{j}}{\partial t} = \boldsymbol{E} + \boldsymbol{v}_2 \times \boldsymbol{B} + \frac{c}{en}\nabla \cdot p_1 - \frac{c}{en}\boldsymbol{j} \times \boldsymbol{B} - \frac{c}{en}\boldsymbol{P}_{12} \tag{2}$$

The terms arising from $(\partial f_1/\partial t)_{\text{coll}}$ and $(\partial f_2/\partial t)_{\text{coll}}$ in (R & R 4 corrected) appear only in equation (2) as $-(c/en)\boldsymbol{P}_{12}$. It is proportional to $\boldsymbol{j}$ but the factor of proportionality is very different from η, the local resistivity of the plasma. That is nearly zero by the low density of the plasma.

Application of (1) *and* (2) *to a Simple Problem.*—Apply (1) and (2) to the circular distribution of a high-temperature plasma within a circular long straight insulating tube whose walls are kept cold enough to condense all ions which reach them. Let an external longitudinal magnetomotive force be applied at the wall of the tube, so that $\boldsymbol{B}_z = \boldsymbol{B}_0$ there.

We will take Φ equal to zero, and we will assume $m_1c^2/ne^2\ \partial \boldsymbol{j}/\partial t$ to be negligible compared to the other terms of equation (2). Then writing the r and θ components of (1) and (2) we get

$$\rho\left(\frac{\partial \boldsymbol{v}_2}{\partial t} + \boldsymbol{v}_2 \cdot \nabla \boldsymbol{v}_2\right)_r = j_\theta B_z - (\nabla \cdot p_1)_r - (\nabla \cdot p_2)_r \tag{3}$$

$$\rho\left(\frac{\partial \boldsymbol{v}_2}{\partial t} + \boldsymbol{v}_2 \cdot \nabla \boldsymbol{v}_2\right)_\theta = 0 - 0 - 0 \tag{4}$$

$$0 = E_r + v_{2\theta}B_z + \frac{c}{en}(\nabla \cdot p_1)_r - \frac{c}{en}j_\theta B_z - 0 \tag{5}$$

$$0 = 0 - v_{2r}B_z - 0 - 0 - \frac{c}{en}P_{12\theta} \tag{6}$$

Equation (6) tells us that $(c/en)P_{12\theta} = -v_{2r}B_z$ is proportional to B_z and is large compared to any effect due to direct "collisions" of electrons with positive ions which we keep small by a low-enough density of the plasma.

Equation (4) tells us that the convective rate of change of the moment of momen-

tum is zero. If at any time $v_{2\theta} \equiv 0$ then at all times later $v_{2\theta} \equiv 0$. Let us assume then that $v_{2\theta} \equiv 0$ at all times.

Eliminate $j_\theta B_z$ from the two equations (3) and (5). We then get

$$\rho \left(\frac{\partial \boldsymbol{v}_2}{\partial t} + \boldsymbol{v}_2 \cdot \nabla \boldsymbol{v}_2 \right)_r = \frac{en}{c} E_r - (\nabla \cdot p_1)_r \tag{7}$$

Study of this equation shows that E_r which must only make $v_{2r} = v_{1r}$ and $(\nabla \cdot p_2)_r$ which from its definition can only depend on the r distribution of $\boldsymbol{v}_{2r}$, n, and the local temperature will be independent of the magnitude of the magnetic field impressed at the wall of the tube. A change in $\boldsymbol{B}_0$ will cause a change in $(\nabla \cdot p_1)$ which will just be balanced by the change in $j_\theta B_z$. The containment time of the plasma will be independent of $\boldsymbol{B}_0$ and will be the same as for $\boldsymbol{B}_0 \equiv 0$.

Conclusion and Applications.—The two "collision-free" transport equations of a plasma do not have mutual interaction terms equal to zero although the plasma may be dilute enough to make actual "collisions" a rare possibility. These interaction terms make it impossible to contain a high-temperature plasma in a simply connected container kept at a low temperature.

These results are more nearly consistent with the findings of Lehnert.[3]

They also are entirely consistent with the numerous results obtained with the Ionic Centrifuge[4] with the end plates at negative voltage and the cylinder floating.

[1] Rosenbluth, M. N., and N. Rostoker, *Phys. Fluids*, **2**, 23 (1959).

[2] Spitzer, L., *Physics of Fully Ionized Gases* (New York: Interscience Publishers, Inc., 1956), pp. 20–21.

[3] Lehnert, B., *Nuovo Cimento Supplemento*, vol. 13, ser. 10, pp. 59–107.

[4] Slepian, J., these PROCEEDINGS, **47**, 313 (1961).

---

*GENETIC CONTROL OF THYMUS LYMPHOID DIFFERENTIATION**

BY ROBERT AUERBACH†

DEPARTMENT OF ZOOLOGY, UNIVERSITY OF WISCONSIN

Communicated by M. R. Irwin, June 1, 1961

As our knowledge of the functional and pathological aspects of lymphoid systems in their central role in immunity and leukemia increases, the lack of understanding of the primary differentiative mechanism leading to the formation of such systems becomes limiting. Thus we find that theories of antibody formation as well as of leukemia etiology hinge ultimately on hypothetical differentiative mechanisms which are neither established from lymphoid systems nor generally valid for any differentiating system as yet analyzed in multicellular organisms.

We have recently reported that the embryonic mouse thymus, isolated as an epithelial rudiment prior to lymphoid differentiation, can develop into a lymphoid system upon isolation in tissue culture[1] as well as after transplantation to the anterior chamber of adult mouse eyes.[2] The present paper concerns itself entirely with grafts grown for seven days in the anterior eye chamber, and takes into consideration the genetic constitution of donor and host tissues. The experiments

demonstrate that in contrast to other embryonic systems the developmental direction of the thymus can be profoundly and rapidly influenced, typical lymphoid differentiation depending on donor-host compatibility.

The unique nature of the results is interpreted as manifestation of a release from tissue-level control mechanisms normally associated with differentiation in multicellular organisms. The operational feasibility of both directive and selective influences in lymphoid differentiation is discussed. Finally, a hypothesis is developed which states that the thymus represents the primary rudiment of the mammalian immunological system.

Materials and Methods.—Mice of strains C_3H, Bagg albino C, and AKR/Lw were used. Embryonic age was determined by observation of vaginal plugs. Thymus rudiments were obtained from 12-day embryos of C_3H, C, and F_1 (C ♀ × C_3H ♂) matings, and from 13-day (12-day equivalent) embryos of AKR matings, lung rudiments from the same embryos serving as source of control material when required. With a few exceptions in transplants to AKR mice, recipients were adult male mice of 2–5 months' age. Normally, each mouse received only one graft, but in experiments in which lung and thymus morphogenesis were compared, both eyes were utilized, one receiving lung, the other receiving thymus. Grafts were made into nembutal-anaesthetized animals in standard fashion,[3] recovered after seven days, fixed in Bouin's, sectioned at 5–7 μ, and stained with hematoxylin and eosin.

Results.—As previously reported, when an F_1 (C × C_3H) thymus rudiment is transplanted into F_1 (C × C_3H) host eye, the rudiment develops rapidly into a lymphoid structure, and within one week becomes histologically similar to the thymus of a newborn animal.[2, 4] Preliminary studies on the sequence of events show that after two days the graft is well established and growing, that after four days it is clearly shifting in a lymphoid direction, and that in the next three days rapid growth and lymphopoiesis occur. The timing parallels the differentiation of thymus *in situ*, where lymphocytes appear in 15- to 16-day embryos, and reach *ca.* 12 million in the newborn (19-day) mouse.[5] While there is considerable variation in the size attained by implants, the histological differentiation seen seven days after transplantation is characteristic and consistent. The graft is almost exclusively lymphoid, with a few scattered epithelial foci and dispersed stromal material.

The initial rationale in the transplantation experiments to be reported (Table 1 and Figs. 1–4) was that in view of the known role of the thymus in AKR-strain leukemia[6] an effect of AKR environment on the differentiation of thymus rudiments from nonleukemic strains might be expected. F_1 (C × C_3H) rudiments were transplanted into AKR mouse eyes, grafts into F_1 (C × C_3H) mice serving as controls; grafts were recovered after one week. Control grafts behaved in a typical manner. Grafts implanted into AKR eyes had become established and well vascularized and had grown considerably, although somewhat less than control grafts. The histological appearance of the grafts was, however, strikingly different from the control grafts. In place of the expected lymphoid differentiation, these grafts had grown into a large, somewhat disorganized mass of epithelial and fibrous material interspersed with vesicles and some debris. The total amount of lymphoid material varied from little to none, and where found, it seemed restricted to the areas furthest removed from the host-donor tissue interfaces; furthermore, such lymphoid areas

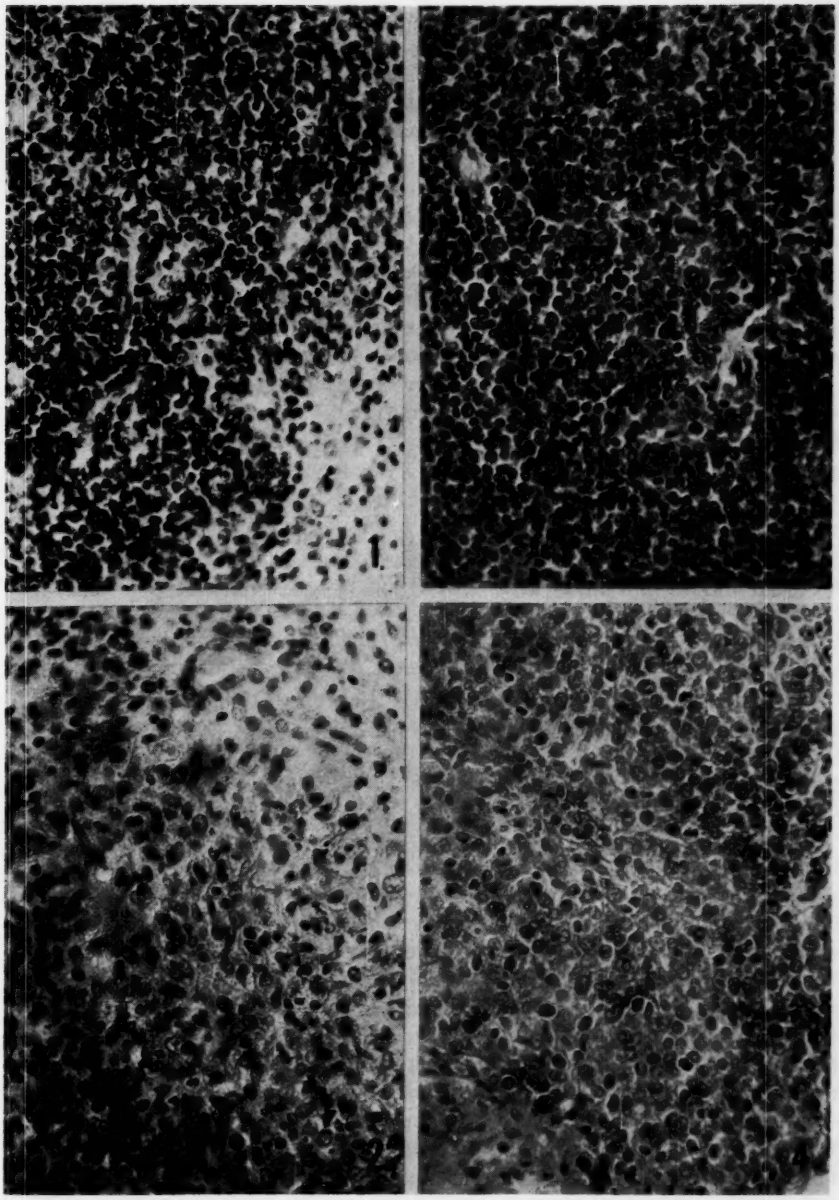

12-DAY EMBRYONIC THYMUS RUDIMENTS GROWN FOR 7 DAYS IN THE ANTERIOR EYE CHAMBER OF ADULT MALE MICE.

FIG. 1.—C_3H thymus rudiment in F_1 ($C \times C_3H$) host eye.
FIG. 2.—F_1 ($C \times C_3H$) thymus rudiment in AKR host eye.
FIG. 3.—AKR thymus rudiment in F_1 ($AKR \times C_3H$) host eye.
FIG. 4.—C_3H thymus rudiment in C host eye.

appeared to be undergoing regression or alteration.

The experiments were repeated, using lung rudiments as control tissue. F_1 ($C \times C_3H$) lung tissue growing in AKR mice was indistinguishable from similar tissue growing in F_1 ($C \times C_3H$) mice. On the other hand, F_1 ($C \times C_3H$) thymus growing in AKR mice again showed the predominantly nonlymphoid direction of differentiation.

Reciprocal experiments were now performed, in which AKR thymus rudiments were transplanted into AKR and F_1 ($C \times C_3H$) hosts, lung tissue again serving as control. The results were comparable. AKR lung tissue grew well in both types of hosts, and no distinction was seen between the two groups. On the other hand, while AKR thymus rudiments developed into typical lymphoid grafts when transplanted into isologous AKR hosts, they developed into characteristic non-lymphoid type grafts when grown in F_1 ($C \times C_3H$) hosts.

At this point it was felt that the transplantation effect might well be independent of the leukemic properties of the AKR strain, so that a large number of graft combinations were made using C_3H, C, AKR, F_1 ($C \times C_3H$) and F_1 ($C_3H \times AKR$) mice. The results, summarized in Table I, were consistent. In all situations in-

TABLE 1

LYMPHOID DIFFERENTIATION AS A FUNCTION OF DONOR-HOST COMPATIBILITY

	Predominant Differentiation			
	Lymphoid		Non-lymphoid	
Donor Strain	Host strain	Number	Host strain	Number
C_3H	C_3H	5/5	C	10/12
	F_1 ($C \times C_3H$)	11/11		
C	C	4/4	C_3H	10/10
	F_1 ($C \times C_3H$)	5/5		
F_1($C \times C_3H$)	F_1 ($C \times C_3H$)	100+/100+ [a]	C	4/4
			C_3H	6/7
			AKR	37/41 [b]
AKR	AKR	8/8 [c]	F_1 ($C \times C_3H$)	6/8
	F_1 ($C_3H \times AKR$)	9/9		

[a] Standard control used in numerous experiments in addition to the ones reported in this paper.[3, 4]
[b] Includes 14 severely leukemic mice.
[c] Includes four severely leukemic mice.

volving the implantation of inbred-line thymus into its own strain (three types) or into an F_1 hybrid of that strain (three types) typical lymphoid differentiation ensued. No readily recognizable differences in growth or histological differentiation between implants into the strain of origin and implants into F_1 hybrids were observed. In all situations involving the implantation of thymus from one inbred line into a different inbred line (three types) lymphoid differentiation generally failed to ensue. In transplants of an F_1 hybrid into either of the parental strains nonlymphoid differentiation was predominant.

Finally, two preliminary experiments may be reported. In the first, F_1 ($C \times C_3H$) tissue was grafted into AKR mice, F_1 ($C \times C_3H$) mice serving as control hosts; grafts were recovered after two, four, and seven days. Differences between the two groups were apparent after four days in 3 out of 4 cases. In a second experiment, F_1 ($C \times C_3H$) tissue was grafted into 2-week-old C_3H mice (in four cases). In this instance the grafts grew well, became lymphoid, and were indistinguishable from control grafts.

Discussion.—The anterior chamber of the eye has been considered refractory to

early immunological phenomena as evidenced by the ready maintenance and growth for two or more weeks of highly heterologous combinations such as human or mouse tissues in rat eye or chick tissues in mouse eye.[3, 4, 7] Yet in the present experiments the results parallel those that would be expected on the basis of transplantation compatability, lymphoid differentiation being restricted to a compatible host-donor relationship. On the other hand, the rapidity of the effect would be unusual even for adult tissues grown in immunologically active transplantation sites. Furthermore, the response is limited to the lymphoid elements; for growth and vacularization of the implant is not prevented, and there is no general graft rejection.

Whether the process involved in the results is actually immunological, i.e., a specific host response to donor tissue which is lymphocyte inhibiting in effect, is open to conjecture. Experimentally, the same results would be expected if specific lymphocyte-promoting substances, subject to genetic control, were required for lymphoid differentiation. Tissue culture experiments aimed at distinguishing between these possibilities are in progress.

In view of the contrast between the results obtained with thymus transplants and those obtained with other systems it becomes essential to examine critically the properties and functions of the developing thymus lymphoid system. One striking feature of thymus differentiation is the loss of tissue cohesion concomitant with the appearance of lymphoid cells. Whereas reticular, stromal, and epithelial cells are firmly bound to the thymus tissue architecture, the lymphoid series of cells is essentially nonadhesive. Since cellular adhesion is normally an adjunct of embryonic systems, and since intercellular materials are becoming increasingly implicated as controlling elements in differentiative events,[8–10] the change in adhesion accompanying lymphoid differentiation may represent a key factor in our results. Loss of adhesiveness may signify that the normal developmental-control mechanisms are bypassed or play a relatively minor role, and that different control mechanisms can under these conditions become operative or manifest. This rationale suggests that certain other systems such as germ-cell differentiation, would behave in a similar fashion; transplantation experiments to test this point are contemplated.

Although the functions of specific cells in the lymphoid series are not clear, it seems likely that the lymphoid system plays a leading role in immune phenomena. Recent theories of antibody-forming mechanisms[11] have tended to emphasize selection or directed differentiation of certain cells in response to antigen (or antibody). In this connection the present results and preceding discussion seem significant. The transplantation results indicate that the thymus lymphoid differentiating system is subject to genetically-determined external controls. In addition to the directive (or permissive) nature of the host environment, selective models can be designed, e.g., a situation in which cells from two strains are mixed prior to transplantation; the significance of such models remains to be determined. The rationale that the present results are related to loss of tissue cohesion is attractive in this connection, for it permits the application of principles developed for unicellular organisms for this system in distinction to other multicellular differentiating systems.

The experiments focus attention on the lack of information concerning thymus function. Since the thymus represents the dominant lymphoid rudiment of the early embryo and since it differentiates during the period of development when the

embryo is most sensitive to external modifications of the immunological system,[12] it seems appropriate to suggest that the thymus represents the major rudiment of the mammalian immunological system.[13] Implicit in this suggestion is the assumption that lymphoid cells which arise in the thymus subsequently become disseminated in a selective fashion. That thymic lymphoid cells originate *in situ* from nonlymphoid cells has been recently demonstrated by transplantation and tissue culture studies;[4] the presence of a lymphocyte circulation has been shown;[14] and the selective nature of thymus cell localizations in other lymphoid regions has been established.[15] The precision of selective settling of thymic lymphoid cells is seen in the regional intra-splenic distribution of thymic cells introduced into lethally irradiated animals;[16] and this conforms well with the demonstrated depression of spleen germinal center activity following thymectomy.[17]

A summary of the points of discussion leads to the presentation of a unified view of thymus function, lymphocyte differentiation, and the development of immune systems. Initially the thymus is subject to typical inductive tissue interactions, but during development the loss of tissue adhesion leads to the establishment of a new set of controlling and directing elements. Cells selected and/or directed toward lymphoid differentiation then develop into thymic lymphoid cells which migrate from the thymus into specific areas of the developing spleen. Here, in their new environment they directly or indirectly become foci for production of antibody-forming cells.

The hypothesis, though speculative, is attractive in being readily amenable to testing. One would predict that embryonic thymectomy would lead to a reduction of the antibody-forming capacity; this experiment can be performed in lower vertebrates. One would expect that heterotypic combinations of embryonic spleen and thymus would lead to complex differentiation not attainable by these rudiments individually. And finally, one would hope that such heterotypic combinations involving the differentiation simultaneously of spleen and thymus in tissue culture would lead to the formation of a system competent to perform immunological reactions *in vitro*.

Summary.—Thymus rudiments from 12-day-old mouse embryos of C, C_3H, and C♀ × C_3H♂ matings and from 13-day (12-day equivalent) embryos of AKR matings were grown for 7 days in the anterior eye chamber of adult male C, C_3H, AKR, F_1 (C × C_3H) and F_1 (C_3H × AKR) mice.

In all situations involving the implantation of inbred-line thymus in its own strain or in an F_1 hybrid of that strain, as well as of F_1 hybrid thymus in a similar F_1 hybrid host, typical lymphoid differentiation occurred. In all combinations in which the thymus from one strain was implanted into an unrelated strain or in which thymus from an F_1 hybrid was implanted into either parental strain or into an unrelated strain, lymphoid differentiation was reduced. Instead, grafts developed into disorganized, large masses of fibrous and epithelial material.

It is suggested that the explanation may lie in the loss of tissue adhesion concomitant with lymphoid differentiation, that this constitutes a release from tissue-level control mechanisms normally associated with differentiation, and that this permits different control mechanisms to become operative or manifested.

A hypothesis is developed which states that the thymus may represent the major primordium of the mammalian immunological system.

* Supported by research funds from the National Institutes of Health (C-3985) and funds administered by the Research Committee of the University of Wisconsin.

† With the technical assistance of William D. Ball and E. Mattie Morin.

[1] Ball, W. D., and Auerbach, R., *Exptl. Cell Research*, **20**, 245 (1960).

[2] Auerbach, R., *Dev. Biol.*, **2**, 271 (1960).

[3] Greene, H. S. N., *Cancer Res.*, **3**, 809 (1943).

[4] Auerbach, R., *Dev. Biol.*, **3**, 336 (1961).

[5] Ball, W. D., and Auerbach, R., (unpublished observations).

[6] McEndy, D. P., Boon, M. C., and Furth, J., *Cancer Res.*, **4**, 377 (1944).

[7] Browning, H. C., *Cancer*, **2**, 646 (1949).

[8] Grobstein, C., *Exptl. Cell Research*, **13**, 575 (1957).

[9] Auerbach, R., "The organization and reorganization of embryonic cells," in *Self-Organizing Systems* (New York: Pergamon Press, 1960).

[10] Moscona, A., "Patterns and mechanisms of tissue reconstruction from dissociated cells," in *Developing Cell Systems and Their Control*, ed. D. Rudnick (New York: Ronald Press Co., 1960).

[11] E.g., *Mechanisms of Antibody Formation* (Prague: Publishing House of the Czechoslovakiau Academy of Science, 1960); "Symposium on Antibodies," *J. Cellular Comp. Physiol.*, **50**, suppl. 1 (1957); "Cellular Aspects of Immunity," in *Ciba Foundation Symposium on Cell Metabolism* (Boston: Little, Brown and Co., 1960).

[12] Billingham, R. E., and Brent, L., *Proc. Roy. Soc.* (*London*), **B242**, 439 (1959).

[13] Cf. Ruth, R. F., *Federation Proc.*, **19**, 579 (1960).

[14] Yoffey, J. M., Everett, N. B., and Reinhardt, W. O., "Cellular migration streams in the hemopoietic system," in *The Kinetics of Cellular Proliferation*, ed. F. Stohlman, Jr. (New York: Grune and Stratton, 1959).

[15] Fichtelius, K. E., *Acta Anat.* (Suppl.) **19**, 1 (1953).

[16] Congdon, C. C., Makinodan, T., Gengozian, N., Shekarchi, I. C., and Urso, I. S., *J. Natl. Cancer Inst.*, **21**, 193 (1958).

[17] Metcalf, D., *Brit. J. Haematol.*, **6**, 324 (1960).

---

*ACTION OF RADIATION ON MAMMALIAN CELLS, IV. REVERSIBLE MITOTIC LAG IN THE S3 HELA CELL PRODUCED BY LOW DOSES OF X-RAYS**

BY MASA-ATSU YAMADA† AND THEODORE T. PUCK

DEPARTMENT OF BIOPHYSICS, FLORENCE R. SABIN LABORATORIES, UNIVERSITY OF COLORADO MEDICAL CENTER, DENVER

Communicated June 16, 1961

In previous studies reproductive death, reversible mitotic lag, and visible chromosomal damage were described in mammalian cells irradiated *in vitro*.[1, 2] Presumptive evidence was presented that chromosomal damage is the underlying lesion responsible for cell killing by radiation. Several laboratories have recently reported life-cycle analyses of cells exposed *in vitro* to high doses of radiation, where the bulk of the cell population has suffered irreversible loss of the capacity to reproduce indefinitely.[3] These studies have yielded divergent results about the stage in the life cycle which is most characteristically damaged by such lethal radiation experience. The randomness of chemical bond breakage produced by ionization makes possible a wide variety of molecular changes when a cell is irradiated. At low doses, however, one may expect a relatively simplified picture of radiation injury, since presumably only the most vulnerable cell functions wil]

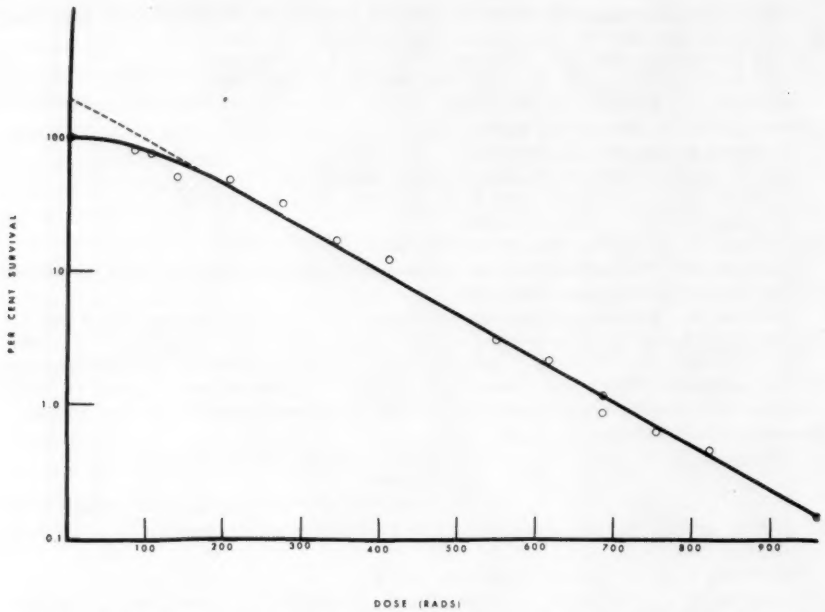

FIG. 1.—Survival curve for *S*3 cells irradiated with 230 KV X-rays.[10] The dose in roentgens, which is known within a few per cent, has been multiplied by a factor of 1.35 which is known only approximately (1.20–1.50) and which converts the dose for glass-attached cells to rads.[8,9]

reflect appreciable damage. Therefore, studies were initiated to examine the effects elicited with the lowest possible doses.[4]

A number of studies, both *in vivo* and *in vitro*, have shown that relatively low doses of irradiation produce prophase mitotic inhibition.[5] These results are often difficult to interpret quantitatively because of the unknown degree to which reversible and irreversible processes have contributed to the observed effects. The *S*3 HeLa cell is particularly suitable for studies of reversible mitotic lag with little complication by cell killing because the pronounced shoulder in its survival curve (Fig. 1) makes possible irradiation with doses as large as 135 rads without killing more than one-third of the cell population, while less than 11 per cent of the cells lose the capacity to form colonies at doses below 68 rads. The present experiments utilize methods of life cycle analysis through labeling of deoxyribonucleic acid (DNA) by H^3-thymidine[3,6] to examine aspects of the reproductive delay induced by irradiation of S3 HeLa cells with doses of 34 to 135 rads of 230 KV X-rays.

Methods and Materials.—S3 HeLa cells were plated on glass cover slips in standard growth medium,[7] incubated at 37°C for 24–48 hours, and then irradiated with 230 KV X-rays at a dose rate of 150–250 rads per minute in accordance with procedures described elsewhere.[1] All doses were measured in roentgens by a standardized ionization chamber, and converted to rads by multiplication by 1.35 to correct for back-scattering from the glass surface.[8,9] In all but a few experiments, the cells were maintained continuously at 37°C throughout irradiation, to eliminate complication due to temperature fluctuations. The inocula of 10^5 cells which were

employed yielded cultures well randomized with respect to division, as evidenced by lack of periodicity in the mitotic index.

After irradiation, H^3-labeled thymidine was added in a concentration of 0.01 to 0.05 μc/ml and cell incubation at 37°C was continued for various time intervals, at the end of which the cells were fixed in Carnoy's solution. H^3-thymidine which had not been incorporated in macromolecular DNA was washed out, a photographic emulsion was applied, and the preparations were stored in the dark for several days. The autoradiographs were developed and the cells stained either with orcein or by the Feulgen reaction as described elsewhere,[10] and the resulting preparations were studied microscopically. The frequency of mitoses, of H^3-labeled nuclei, and of H^3-labeled mitotic figures in several thousands of cells was scored for different radiation exposures and after different incubation periods subsequent to irradiation. Analysis of the duration of the various phases of the cell life cycle was carried out by the standard methods.[3c, 6]

The mitotic frequency in unirradiated cultures in which 66,000 cells were scored averaged 2.7 ± 0.4%. This relatively large dispersion is due to the tendency of the mitotic index to be influenced by a variety of factors such as the batch of medium used, the age of the culture before trypsinization, etc. Hence, the practice was adopted of expressing mitotic frequency in irradiated cultures in terms of its ratio to that found in an unirradiated culture otherwise treated in exactly the same way throughout the experiment. This procedure tended somewhat to compensate for unavoidable small fluctuations in metabolic state of the culture. In some experiments the metaphase frequency rather than the total mitotic frequency was counted because it was felt that the more highly condensed chromosomes of this state permitted more accurate counting than the more diffuse condition characteristic of prophase, particularly when H^3-labeling also produced dark spots over the nucleus. The relative frequency of the different phases of mitosis in normal cultures is shown in Table 1. These figures may differ somewhat from

TABLE 1

RESULTS OF SCORING A STANDARD POPULATION OF 7000 UNIRRADIATED CELLS FOR MITOTIC FIGURES

(Sets of 1,000 cells were scored after 7 different incubation intervals ranging from 48 to 72 hours)

	Frequency in unirradiated cell population	Relative proportion of the mitotic interval
Prophase	0.0043	0.146
Metaphase	0.0144	0.490
Anaphase	0.0060	0.204
Telophase	0.0047	0.160
Total mitotic frequency	0.0294	1.00

those obtained in other laboratories because of some arbitrariness in decision about the point at which the various phases begin and end.

Experimental Results.—The life cycle of the normal HeLa cell under our conditions of growth is shown in Figure 2. The results agree within the limits of experimental uncertainty with those reported in other laboratories,[3c] although differences in conditions can affect both the absolute and relative duration of the different periods.

A. *Effect of irradiation on frequency of mitoses:* In Figure 3 are presented the averaged results from six different experiments in which the metaphase frequency

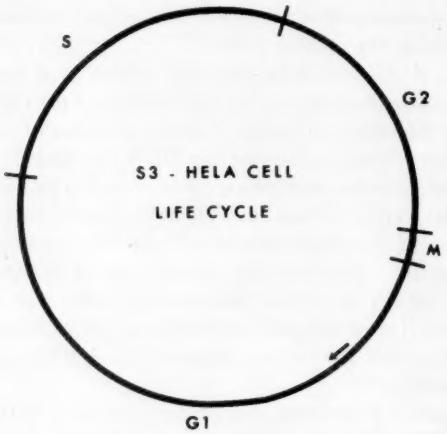

FIG. 2.—The following values were found for the different periods of the life cycle of the *S*3 HeLa cell: *M* (mitosis), 0.6 ± 0.1 hours; *G*1 (postmitotic period), 8.2 ± 1 hours; *S* (DNA synthesis), 6.2 ± 1 hours; *G*2 (pre-mitotic period), 4.6 ± 2 hours; and *T* (total generation time), 19.6 ± 1 hours.

Separate values for *T*, determined from a standard growth curve, and for *M* from time-lapse cinephotomicrography, confirmed those obtained by the other methods described.

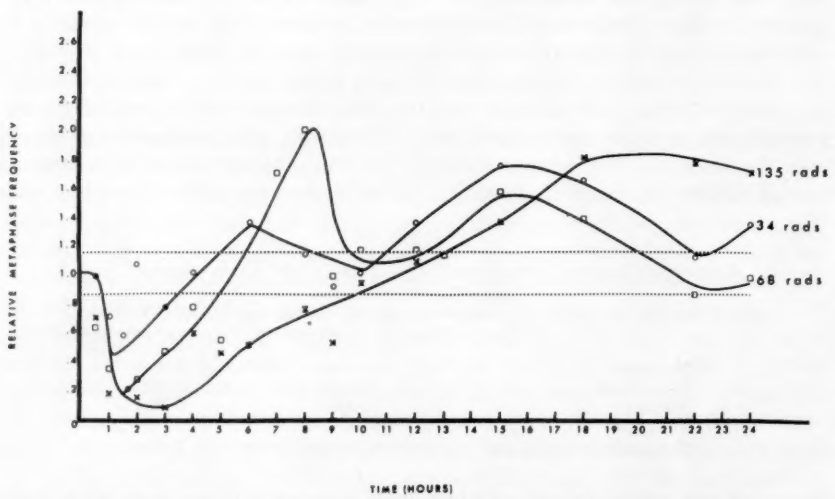

FIG. 3.—Relative metaphase frequencies as compared to unirradiated controls, of *S*3 cultures irradiated with 34, 68, and 135 rads, respectively. The standard deviation of the control is indicated by the dotted lines. While the general shape of the curves is reproducible, the number of maxima and their location differs somewhat in various experiments, so that an averaged curve like that shown here displays somewhat more scatter than would a single curve.

was measured at various times after irradiation. The general shape of the curves agrees with those carried out in other systems.[5] While a certain amount of scatter in the points appears inevitable because of inherent variability even of unirradiated cultures, and the rapid changes in mitotic frequencies in irradiated cells, the general

features of the curves are clear: (a) Within 30 minutes after irradiation the frequency of metaphases begins to fall. The rate of fall is reasonably similar in all doses studied. (b) After reaching a minimum, the mitotic frequency rises again at a rate which is slower, the greater the dose. Thus, at 34 rads, the normal frequency is attained within 2 hours; at 68 rads it takes approximately $5^1/_2$ hours; and with 135 rads, about 11 hours are required to regain the value of the control. (c) The mitotic frequency then overshoots, attaining values considerably higher than the unirradiated culture. (d) Secondary peaks often occur, and the total areas above the normal mitotic index tend to exceed those below this line, particularly at the higher doses.

The reduction in metaphase figures shown in Figure 3 could be due to a specific disturbance at metaphase causing the condensed chromosomes to unwind and so lose their definition, or to failure of cells to arrive in a metaphase because of a block in a previous portion of the life cycle. In the former case, cells should still continue to arrive into prophase at the normal rate. An experiment was carried out in which the separate frequencies of the mitotic phases were carefully scored at various periods following irradiation with 68 r. The results demonstrated that the prophase frequency exhibits a rise and fall, in parallel with that of metaphase. It can be concluded that the block caused by irradiation operates to prevent arrival of cells in prophase, or regression of cells in early prophase, or both. Since the mitotic frequency has fallen within 1 hour after irradiation, the block must lie within 1 hour of the onset of mitosis, in the *G2* period.

These data suggest provisional interpretation as follows:

(a) The fact that a temporary suppression of mitosis occurs in about 90 per cent of the cells irradiated with 68 rads, and in at least half of the cells irradiated with 34 rads, indicates that D^0, the dose affecting 37 per cent of the cells, is in the neighborhood of 40 rads, as compared to 135 rads for cell killing. Thus, the sensitivity of the reaction involved in lag is greater than, though of similar order of magnitude to, that responsible for cell killing. This is in contrast to functions like active transport of neutral red by these cells which are unaffected by doses of several thousand rads.[11]

(b) Since the time of the initial fall in mitotic index seems reasonably constant despite considerable variation in dose, it appears likely that some critical process occurring at this point is particularly radiation sensitive so that the rate of fall reflects failure of cells to enter mitosis.

(c) Some aspect of the repair process is mirrored by the period of subnormal mitotic index, which is strongly dose dependent.

(d) The prolonged overshoot in mitotic index usually was more pronounced at higher doses and suggests that additional complications may be involved. In addition to release of the block, prolongation of the mitotic state might occur, particularly at the highest dose where a significant fraction of the cells may enter abnormal or even lethal mitotic configurations. Time-lapse photomicrography has revealed a relatively higher incidence of mitotic bridge formation in cells irradiated with 300 rads. Study of lower doses is in progress.

(e) Since, after exposure to 135 rads, approximately 10 to 11 hours are required before the depressed metaphase index regains a value as high as the preirradiation one, it can be concluded that the cells affected by irradiation were

not confined to a single small region of the life cycle, but rather included those at least as far back as 9 hours before mitosis. Therefore, even cells in the S period have been affected by the irradiation.

B. *Measurement of the fraction of nuclei labeled with H^3-thymidine:* H^3-labeled thymidine was added immediately after X-irradiation and the culture incubated continuously until fixation. Under these circumstances, a plot of the per cent-labeled-nuclei versus the incubation time ascends in approximately linear fashion and ultimately levels off as the point is approached at which almost 100 per cent of the cells are labeled. The intercept of this curve with the y-axis yields the value of S/T, the fraction of the life cycle during which H^3-thymidine incorporation occurs.[6]

In Figure 4 is presented the per cent of labeled nuclei in cells incubated contin-

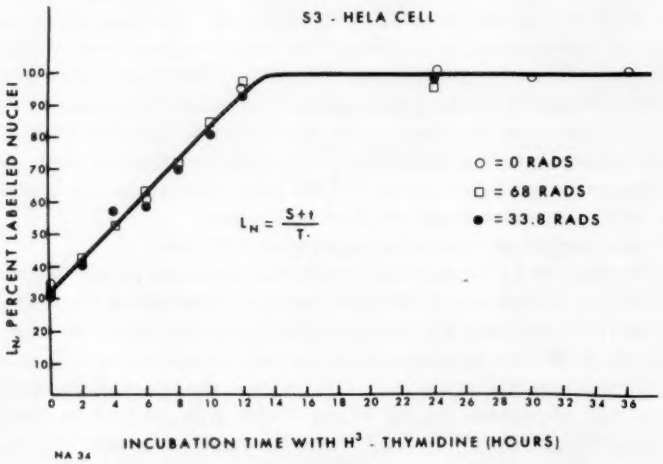

FIG. 4.—Variation of the percent labeled nuclei with time, for *S*3 HeLa cells irradiated with 0, 34, and 68 rads, respectively, and incubated continuously thereafter with H^3-thymidine. The duration of *S*, the DNA synthetic period, is obtained from the equation shown which is exact only at zero time.[6b] Hence values of *S* were determined from the intercept of the curve with the *y*-axis. All curves yielded identical values for *S* and were superposable. The curve for 135 rads was also superposable except for a slight, questionable fall in the per cent of labelled nuclei after 10 hours' incubation.

uously with H^3-labeled thymidine for varying periods after irradiation with 0, 34, and 68 rads, respectively. All curves are superposable, and so is that for 135 rads, except for a marginally significant drop in the latter after about 8 hours of incubation, which may be due to the larger delay in re-entering S^{3d} which occurs at the higher dose. Figure 4 shows that *S*, the time of DNA synthesis, is unchanged by these doses of irradiation. Therefore, no cessation of DNA synthesis has occurred during the 10 hours following irradiation. Any changes of this kind must be less than 10 to 20 per cent, a fact which contrasts sharply with the drop in mitotic index of more than 90 per cent found in the same experiment. Similarly, one can exclude any significant block in *G*1, the post-mitotic period, for

in that case the linear part of the curve of Figure 5 would have had to bend over toward the horizontal, as the supply of new cells to *S* was cut off.

Measurement was made of the distribution pattern of the number of grains found in the labeled nuclei in the irradiated and unirradiated cultures. No sig-

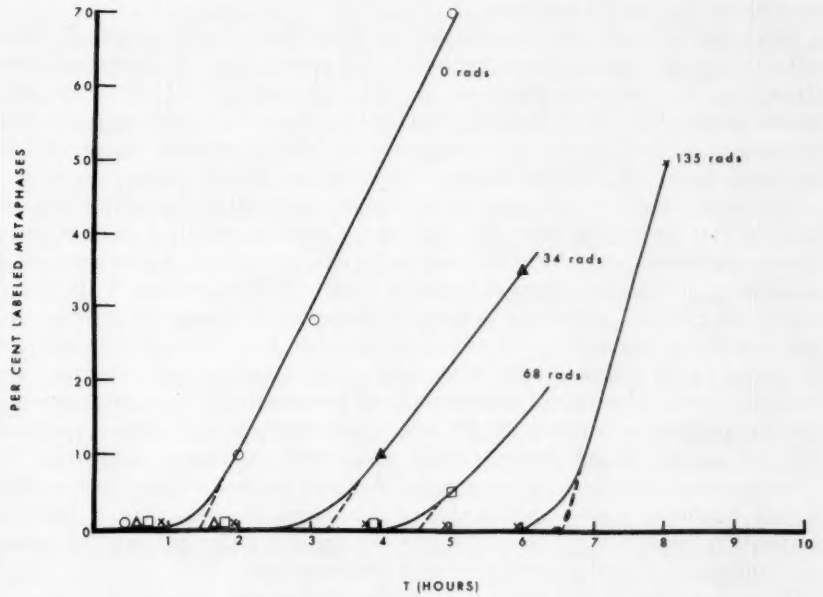

FIG. 5.—Direct demonstration of the localization of a block in the *G*2 period, as a result of irradiation of *S*3-HeLa cells. The time of appearance of an H^3-labeled mitotic figure is an index of the time taken for a cell to traverse the G_2 interval. Metaphase figures are somewhat easier to score quantitatively in these experiments, though prophases show a similar dose dependence. The fact that the labeled prophases exhibit the same time dependence also indicates that the block occurs before intiation of prophase. Irradiation occurred at zero time and the cells were incubated continuously thereafter in H^3-thymidine.

nificant difference was found at any of these doses. Thus the mean and standard deviation of the nuclear grain counts[6] (for cells with more than the background number of 4 grains) in a culture irradiated with 68 rads, and incubated continuously thereafter in H^3-thymidine was 51 ± 4, 102 ± 11, and 93 ± 8 at $^1/_2$, 2, and 5 hours, respectively. The corresponding counts for unirradiated cells were 59 ± 5, 96 ± 7, and 93 ± 9. Therefore, the total amount of DNA synthesis as well as the time of synthesis are not appreciably affected by irradiation with doses up to 135 rads.

C. *Determination of the percent labeled mitoses:* Counting the fraction of mitotic figures in which H^3-thymidine has been incorporated into the chromosomes affords a direct measure of any block produced in the *G*2 period, since each such cell has traversed the entire *G*2 interval during the period of study. (By limiting measurements to the first several hours, complication by labeled cells coming through a second mitosis as well as the burst of mitosis that follows the initial fall, is avoided.)

The counts obtained on the irradiated and nonirradiated populations are presented in Figure 5, which confirms directly the presence of the block in the vicinity of mitosis, and places its position just before the initiation of prophase. Figure 5 also shows that the delay in *G2* produced by irradiation increases directly with the dose, in a roughly linear fashion, although more precise measurements are needed to establish the exact dependence.

Discussion.—These data indicate that sublethal X-irradiation of the *S*3 HeLa cell produces a temporary block late in *G2* (and possibly extending into early prophase) but no observable effects on the DNA synthetic period, *S*, or the postmitotic period, *G*1. More detailed consideration of this block and its repair, and comparison of these results with previous work both *in vivo* and *in vitro* will be presented elsewhere. Certain general considerations require comment here.

The thesis that reversible mitotic lag represents an action basically similar in kind to that underlying irreversible killing by ionizing radiation has been previously considered, and, at least in some cases, rejected because of apparent lack of parallelisms of these two effects of radiation in other kinds of systems.[12] However, one of the principal arguments in favor of chromosomal damage as the basic action underlying mammalian cell killing by radiation was the small dose required for killing which implied a rather large value for the apparent target volume. The size of the total chromosomal complement was consistent with these requirements, and the parallelism between the D^0 values and chromosomal volume in cells of different species (though similar ploidy) was offered as evidence supporting the chromosomes as the site of the lethal action.[13] Since the dose required for reversible mitotic inhibition is even smaller than that required for cell killing, it becomes particularly important to determine whether lag and killing proceed by similar mechanisms, and whether these involve the chromosomes.

The present data neither prove nor exclude chromosomal damage as the mechanism underlying reversible lag. The complexity of the events which follow irradiation of these cells makes necessary further analysis of these phenomena before a definitive test can be devised. However, the data so far available offer a reasonable suggestion that the underlying defect is chromosomal:

(a) Localization of the block late in the *G2* period offers a possible mechanism for the critical action.[4, 14] This is the period in which chromosomal condensation begins. Chemically mediated mechanical forces presumably act to cause the chromosomes to form coils of high order. The production of chromosomal aberrations weakening, or completely breaking, the structure might well interfere with normal progression of the condensation process. (Defective chromatid coiling following X-irradiation in a variety of cells has been described by several investigators.[5b]) The block in the *G2* period might then represent the time taken for the chromosome damage to be repaired before normal condensation can be resumed. The period during which the mitotic index is subnormal would be a measure of the repair time for chromosome damage in those cells where repair was not yet complete by the time the critical point in *G2* had been reached.

An alternative chromosomal scheme to account for the present experimental data is that chromosome breaks occur but are restituted much more rapidly than the period represented by the subnormal region of the mitotic index of Figure 2. Such breaks, if sufficiently numerous, might in many cases be resealed abnormally,

by the joining of fragments from different chromosomal sites. Such events would produce chromosomal configurations which would permit only the first part of the condensation to occur, but would block its completion by production of topologies incompatible with completion of the normal spiralization pattern. If this mechanism contributes in a material way to the effects here described, the observed block may reflect a process in which the chromosomal strands which have developed blocked configurations are rebroken by the chemical forces engendered by the condensation process. It is conceivable that breakage and sealing cycles would continue until each chromosome had achieved a configuration able to complete the coiling process. Still other mechanisms are possible.

(b) Either of the mechanisms proposed in the preceding paragraph would lead to the expectation that chromosome breaks would be observable after sublethal doses which produce only mitotic lag. However, the number of such breaks and their variation with time after irradiation would be different for each of these mechanisms. Meaningful interpretation of visible chromosome breaks is also complicated by the possibility that small chromosomal damage, insufficient to break a chromosome arm, might be converted to complete breaks by the mechanical forces engendered during the condensation period, and by the fact that visible chromosome breaks represent only that fraction of the total which have not become restituted before mitosis.

For these and other reasons,[3] it has not yet seemed advisable to attempt more than semiquantitative analysis of chromosome breakage following cell irradiation since very different results might be obtained depending on which of a variety of models is selected as the basis of numerical computation. However, qualitatively we have demonstrated that sublethal doses of X-irradiation produce extensive chromosomal breakage in the *S*3 HeLa cells. Thus, in preliminary experiments, analysis of 300 mitoses of *S*3 cells revealed no chromosome breaks in unirradiated cells, and an average of 0.26 breaks per cell and 0.8 breaks per cell for cultures receiving 13.5 and 33.8 rads, respectively. Detailed analysis of these frequencies at different times after irradiation with various doses is now in progress.

With increase in dose into the cell-lethal range, the number of basic acts of chromosome damage within each cell would increase. Hence, the number of frank breaks visible at mitosis will also increase, as will the frequency of abnormal chromosome rejoinings. Bizarre configurations would be produced which may make impossible completion of the condensation process. Such cells may never even reach mitosis. Other cells may reach mitosis but be unable to complete it because of the formation of anaphase bridges or other mechanical impediments. Finally, some cells may complete mitosis but the daughter cells produced may contain chromosomal structural abnormalities or genetic defects which may prevent continuous reproduction through mechanical interference or biochemical imbalance. This unitary picture, attributing to a common cause reversible lag, irreversible reproductive death, and those chromosomal aberrations which are visible at mitoses, would provide an explanation for the fact that all three of these phenomena occur extensively at doses below 250 rads, in contrast to physiological effects, like inhibition of active transport or loss of the ability to synthesize virus particles, which are unaffected by doses of several thousand roentgens.

This discussion should dispose of an objection recently raised to the theory at-

tributing cell killing to chromosomal injury. It has been proposed that, since DNA synthesis may, at least in some cases, continue with little or no impairment after a lethal irradiation, the damage can hardly have been localized in the chromosomes.[15] However, the synthesis of DNA is only one of the functions carried on by the chromosomes, and their mechanical role may well be the one most vulnerable to gross radiation damage.

Test of these hypotheses requires comparison of the present data on the effects of sublethal radiation doses with those in the supralethal range. However, the studies previously reported dealing with effects of high doses of radiation on the life cycle of mammalian cells *in vitro* have revealed divergent results[3]: some have observed an inhibition of DNA synthesis through a block in *G*1 or *S*; some have reported no effect on DNA synthesis; and at least one case of an increase in the number of cells brought into DNA synthesis has been found.

The lack of uniformity in these results may be due to the greater complexity of events attending the use of large doses of irradiation and to the fact that different experiments employed different cell types and conditions of growth. However, the study of Whitmore *et al.*[3d] is particularly noteworthy in this connection. These investigators irradiated mouse L cells (whose mean lethal dose, D_0, is 240 rads) with 2,000 and 5,000 rads, and found no significant effect on either the *G*1 or *S* periods but a large block in *G*2 period, which was a direct function of the amount of radiation administered. The experimental results obtained by us with sublethal doses applied to the *S*3 HeLa cell correspond in remarkably close fashion to the supralethal effects of the Whitmore group and, therefore, suggest that reversible lag and killing may indeed have a common basis. However, since different cells were used in these two studies, and since other investigators applying high doses to the HeLa cell reported a different pattern of events,[3c] firm conclusions must await completion of further studies. We have found that the radiation response of different cells differs greatly, even for low doses. Thus, preliminary studies with normal diploid human cells have shown that, in contrast to the *S*3 cell, low doses of irradiation, like those used in the present study, produced a block in *G*1 as well as a block in *G*2. Studies are continuing on the effects of cell type and total dose in eliciting these different patterns of metabolic block.

Summary.—The life cycle of hyperploid *S*3 HeLa cells, irradiated with sublethal doses of X-rays, has been studied. A reversible mitotic lag is readily demonstrable at doses of 34 to 135 rads, produced by a block localized in the *G*2, pre-mitotic period. Visible chromosomal aberrations are produced in a majority of the cell population at these doses. It is proposed that this reversible mitotic lag, like irreversible reproductive death, is due to chromosomal damage, and that the reversible lag may reflect interference with chromosomal condensation just prior to and perhaps in the early parts of mitosis.

* Contribution No. 175 from the Department of Biophysics, Florence R. Sabin Laboratories, University of Colorado Medical Center, Denver. This work was supported by grants from The National Foundation, and The Damon Runyon Memorial Fund.

† Fellow of Rockefeller Foundation.

[1] (*a*) Puck, T. T., and P. I. Marcus, *J. Exptl. Med.*, **103**, 653 (1956); (*b*) Puck, T. T., D. Morkovin, P. I. Marcus, and S. J. Cieciura, *J. Exptl. Med.*, **106**, 485 (1957).

[2] Puck, T. T., these PROCEEDINGS, **44**, 772 (1958).

[3] (*a*) Lajtha, L. G., R. Oliver, R. Berry, and W. D. Noyes, *Nature*, **182**, 1788 (1958); (*b*)

Lajtha, L. G., R. Oliver, T. Kumatori, and F. Ellis, *Radiation Research*, **8**, 1 (1958); (c) Painter, R. B., and J. S. Robertson, *Radiation Research*, **11**, 206 (1959); (*d*) Whitmore, G. F., C. P. Stanners, J. E. Till, and S. Gulyass, *Biochim. et Biophys. Acta*, **47**, 66 (1961); (*e*) Other pertinent studies are listed by Painter, R. B., V. W. R. McAlpine, and M. Germanis, *Radiation Research*, **14**, 653 (1961).

[4] (*a*) Puck, T. T., and M. Yamada, *Federation Proc.*, **20**, 150 (1961); (*b*) Puck, T. T., *Mod. Med.*, **29**, 64 (1961).

[5] (*a*) Reviewed by Lea, D. E., *Actions of Radiations on Living Cells* (New York: Macmillan Co., 1947), p. 296; (*b*) Carlson, J. G., in *Radiation Biology*, ed. A. Hollaender (New York: McGraw-Hill, 1954), vol. 1, part 2, p. 763.

[6] (*a*) Painter, R. B., and R. M. Drew, *Lab. Invest.*, **8**, 278 (1959); (*b*) Stanners, C. P., and J. E. Till, *Biochim. et Biophys. Acta*, **37**, 406 (1960).

[7] Puck, T. T., P. I. Marcus, and S. J. Cieciura, *J. Exptl. Med.*, **103**, 273 (1956); Ham, R. G., and T. T. Puck, *Methods in Enzymology*, **60** (in press).

[8] Morkovin, D., and A. Feldman, *Brit. J. Radiol.*, **32**, 282 (1959).

[9] Puck, T. T., *Animal Cell Information Service Newsletter*, **2**, 11 (1960).

[10] Tjio, J. H., and T. T. Puck, *J. Exptl. Med.*, **108**, 259 (1958).

[11] Puck, T. T., *Scientific American*, **202**, 142 (1960).

[12] Lea, D. E., *op. cit.*

[13] Puck, T. T., *Revs. Modern Physics*, **31**, 433 (1959).

[14] Puck, T. T., in *Methodology in Human Genetics*, ed. W. J. Burdette, (in press).

[15] Alper, T., *Annual Rev. of Nuclear Science*, **10**, 523 (1960).

RENORMALIZATION TECHNIQUES AND MEAN SQUARE AVERAGING, I. DETERMINISTIC EQUATIONS

BY RICHARD BELLMAN AND JOHN M. RICHARDSON

THE RAND CORPORATION, SANTA MONICA, CALIFORNIA, AND HUGHES RESEARCH LABORATORIES, MALIBU, CALIFORNIA

Communicated by S. Lefschetz, June 21, 1961

1. *Introduction.*—Since the fundamental equations of mathematical physics are in the main nonlinear, a major effort must be devoted to the determination of simple analytic approximations to the solutions of these equations and to the construction of effective computational logarithms. In this paper, we wish to outline a general technique for obtaining analytic approximations to the solutions of nonlinear vector equations of the form

$$\frac{dx}{dt} = Ax + \epsilon g(x), \tag{1.1}$$

where x is an n-dimensional vector, $g(x)$ is a nonlinear vector function of x, A is an $n \times n$ matrix or a more general linear operator, and ϵ is a small quantity. This last condition is not essential, since there are systematic ways for transforming methods applicable to small ϵ to methods applicable to large ϵ; cf. Shohat,[1] Bellman.[2]

In subsequent longer papers, we shall present further details, treatment of higher approximations, discussion of periodic and random forcing terms, and applications to different areas of mathematical physics. Here, we wish merely to outline the method and to indicate the application of the method to the de-

termination of the periodic solutions of the Van der Pol equation and the equation of the nonlinear spring.

2. *Linear Averaging.*—Let us now consider the equation of (1.1) in which we assume that all of the quantities that appear are real. Our aim is to approximate to $g(x)$ by means of a linear expression in x,

$$g(x) \sim Bx + b, \tag{2.1}$$

where the matrix B and the vector b are to be chosen so as to minimize the mean square difference between the two sides. We shall measure the mean square deviation by means of a norm of the following type

$$\sigma^2 = \langle (g(x) - Bx - b, g(x) - Bx - b) \rangle, \tag{2.2}$$

where (x, y) denotes the usual inner product of two vectors and $\langle \ldots \rangle$ denotes an *expected value*, given by time or space averaging, in a sense which will be made more precise below.

It follows immediately that this mean deviation is minimized by the following values for B and b:

$$\begin{aligned} B &= \langle \Delta g \otimes \Delta x \rangle \langle \Delta x \otimes \Delta x \rangle^{-1}, \\ b &= \langle g(x) \rangle - B\langle x \rangle, \end{aligned} \tag{2.3}$$

where Δy denotes the difference between a quantity y and its expected value, $\Delta y = y - \langle y \rangle$. Thus, $\Delta g = g - \langle g \rangle$, $\Delta x = x - \langle x \rangle$. The expression $x \otimes y$ denotes the Kronecker product of two vectors, i.e., the matrix

$$x \otimes y = (x_i y_j), \quad i, j = 1, 2, \ldots, n, \tag{2.4}$$

cf. reference 3.

If we set

$$Bx + b = Pg(x), \tag{2.5}$$

where P is a projection operator defined by

$$Pg = \langle g \rangle + \langle \Delta g \otimes \Delta x \rangle \langle \Delta x \otimes \Delta x \rangle^{-1} \Delta x, \tag{2.6}$$

then $P^2 = P$ and

$$\sigma^2_{\min} = \langle (g(x), (1 - Pg(x))) \rangle. \tag{2.7}$$

3. *Calculation of Expected Values.*—In connection with the determination of periodic and almost-periodic solutions, one of the most useful expectations is the time average

$$\langle g(x) \rangle = \lim_{T \to \infty} \frac{1}{T} \int_0^T g(x(t)) dt. \tag{3.1}$$

Clearly, the calculation of the expectation, and thus the optimal linear approximation, requires a knowledge of the actual solution. To obtain approximating linear equations, we use in the calculation of B and b above the solution of the linear equation obtained from (1.1) by setting $\epsilon = 0$. The determination of higher approximations to $g(x)$ is not a trivial matter and will be discussed in subsequent communications.

Another type of expected value is obtained by ensemble averaging. For an arbitrary function of $x(t)$, this type of averaging is defined by the expression

$$\langle g(x(t)) \rangle = \int g(x) dG(x, t), \tag{3.2}$$

where $G(x, t)$ is the distribution of x at the time t and the integration spans the accessible x-space. It is necessary to emphasize the point that, apart from certain cases where the ensemble possesses ergodic properties, the ensemble average will be a function of time.

4. *Examples.*—As simple examples of the foregoing techniques, let us consider the Van der Pol equation

$$u'' + \lambda(u^2 - 1)u' + u = 0, \quad \lambda > 0. \tag{4.1}$$

Approximating the term $(u^2 - 1)u'$ by a linear expression $c_1 u + c_2 u'$ and using a time average, we find that the optimal choices of c_1 and c_2 are given by

$$\left.\begin{aligned} c_1 &= \lim_{T \to \infty} \int_0^T (u^2 - 1)u'^2 dt \Big/ \int_0^T u^2 dt = 0, \\ c_2 &= \lim_{T \to \infty} \int_0^T (u^2 - 1)u'^2 dt \Big/ \int_0^T u'^2 dt. \end{aligned}\right\} \tag{4.2}$$

For the function u, we use the zeroth approximation, $u = a \cos t$. Hence the approximate equation to (4.1) is given by

$$u'' + c_2 u' + u = 0,$$

$$\text{where} \qquad c_2 = \lim_{T \to \infty} \int_0^T (a^2 \cos^2 t - 1) \sin^2 t \, dt \Big/ \int_0^T \sin^2 t \, dt. \tag{4.3}$$

Hence, for small λ, the amplitude a of the periodic solution is determined to the first approximation by the well-known condition

$$\int_0^{2\pi} (a^2 \cos^2 t - 1) \sin^2 t \, dt = 0. \tag{4.4}$$

Similarly, for the nonlinear spring,

$$u'' + u + \epsilon g(u) = 0, \tag{4.5}$$

we write $g(u) = c_1 u + c_2 u'$, where

$$\left.\begin{aligned} c_1 &= \lim_{T \to \infty} \int_0^T g(u) u dt \Big/ \int_0^T u'^2 dt, \\ c_2 &= \lim_{T \to \infty} \int_0^T g(u) u' dt \Big/ \int_0^T u'^2 dt = 0, \end{aligned}\right\} \tag{4.6}$$

and we assume that $g(u)$ has a vanishing average.

This yields the well-known relation between amplitude and frequency of the periodic solution when we use the zero-order approximation $u = a \cos t$ to calculate c_1; cf. Krylov and Bogoliuboff.[4]

5. *Higher Approximations.*—There are several directions along which one

may proceed to achieve higher approximations. One possibility is to use series expansion (if it converges) in ϵ' in the modified equation

$$\frac{dx}{dt} = Ax + \epsilon Pg(x) + \epsilon'(1 - P)g(x)$$

and afterwards set $\epsilon' = \epsilon$. Another approach is to enlarge the dimensionality of the dependent vector variable by adding components containing approximately chosen nonlinear functions of x and reapply the same renormalization techniques. This approach will be treated in future communications.

[1] Shohat, J., "On Van der Pol's and related nonlinear differential equations," *J. Appl. Physics*, **15**, 568–574 (1944).

[2] Bellman, R., "On perturbation methods involving expansions in terms of a parameter," *Q. Appl. Math.*, **13**, 195–200 (1955).

[3] Bellman, R., *Introduction to Matrix Analysis* (New York: McGraw-Hill Book Co., Inc., 1960).

[4] Krylov, N., and N. Bogoliuboff, *Introduction to Nonlinear Mechanics* (Princeton University Press, 1947), Annals of Mathematics, vol 11.

ON GROUP REPRESENTATIONS OVER A VALUATION RING

By Alex Heller

UNIVERSITY OF ILLINOIS

Communicated by J. L. Doob, June 2, 1961

In what follows, G, is a finite group of order g and R a valuation ring of characteristic 0 with maximal ideal (π). We suppose $g \in (\pi)^{e+1}$. "Modules" are always finitely generated left $\Lambda = RG$ modules. We denote by an asterisk the completion functor so that R^* is the completion of R and $\Lambda^* = R^*\Lambda = R^*G$. The quotient field of R is K; that of R^* is K^*.

Maranda has proved[4, 5] the following theorems.

M1. *If A, B are R-projective modules such that $A/\pi^{e+1}A \approx B/\pi^{e+1}B$, then $A \approx B$.*

M2. *If A, B are R-projective modules such that $A^* \approx B^*$ (as Λ^* modules), then $A \approx B$.*

M3. *If R is complete and A is an R-projective module such that $A/\pi^{2e+1}A$ is decomposable, then A is decomposable.*

Reiner has observed[3] that these imply the following result:

R. *If R is complete, then the Krull-Schmidt theorem holds for R-projective modules.*

We shall strengthen these results by omitting the condition of R-projectivity and, under suitable conditions, the hypothesis of completeness.

1. *Preliminary Lemmas.*—The central tool in the proof of Maranda's results is the following lemma (for proof cf. ref. 2).

Lemma 1.1. *If A is R-projective, then $\pi^e \, Ext_\Lambda^1(A, B) = 0$.*

Now for any module B we write B' for the R-torsion submodule and $B'' = B/B'$ so that the sequence

$$0 \to B' \xrightarrow{\beta'} B \xrightarrow{\beta''} B'' \to 0,$$

where β' is the inclusion and β'' the canonical projection, is exact, and B'' is R-projective. We denote by $t(B)$ the smallest integer t such that $\pi^t B' = 0$.

We introduce also the following notation. For any A, let ΩA be the kernel of the map $\lambda \otimes a \to \lambda a$ of $\Lambda \otimes A$ into A, so that $0 \to \Omega A \to \Lambda \otimes A \to A \to 0$ is exact. Now $\mathrm{Hom}_\Lambda(\Lambda \otimes A, B)$ may be identified with $\mathrm{Hom}_R(A,B)$; making this identification, we have an exact sequence.

$$0 \to \mathrm{Hom}_\Lambda(A,B) \xrightarrow{\subset} \mathrm{Hom}_R(A,B) \xrightarrow{\square} \mathrm{Hom}_\Lambda(\Omega A, B) \xrightarrow{\delta} \mathrm{Ext}_\Lambda^1(A,B).$$

Thus for $\varphi \in \mathrm{Hom}_R(A, B)$, $\square\varphi$ is the deviation of φ from being a Λ-homomorphism.

LEMMA 1.2. *If $\varphi \in Hom_R(A,B)$ and im $\square\varphi \subset \pi^{k+e+t(B)}B$, then there is a $\theta \in Hom_R(A'',B)$ such that $\varphi - \pi^k\theta\alpha'' \in Hom_\Lambda(A,B)$.*

We consider the diagram

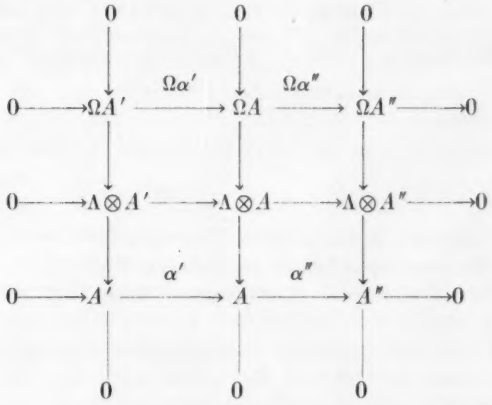

Since this commutes and has exact rows and columns, we have a diagram

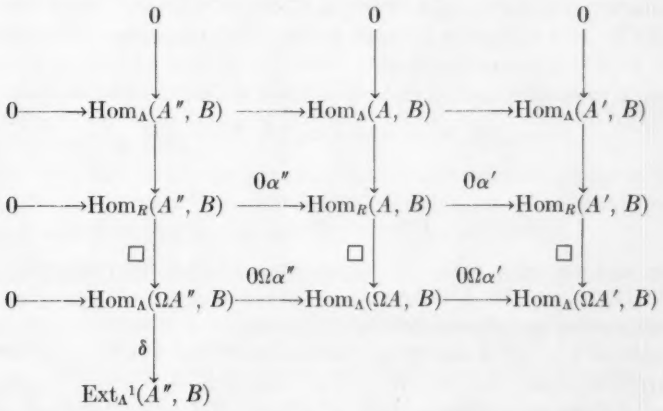

which again commutes and has exact rows and columns. Now $(\square\varphi)\Omega\alpha' = \square(\varphi\alpha')$ has its image in $B' \cap \pi^{k+e+t(B)}B = \{0\}$. Thus $\square\varphi = \psi(\Omega\alpha'')$ for $\psi \in \mathrm{Hom}_\Lambda(\Omega A'', B)$. Since im$\psi$ = im$\square\varphi$ and $\Omega A''$ is R-projective, we have $\psi = \pi^{k+e+t(B)}\sigma$ for

$\sigma \in \mathrm{Hom}_R(\Omega A'',B)$. But $\pi^{k+e+t(B)}\square\sigma = \square\psi = 0$ so that im $\square\psi \subset B'$ and $\pi^{t(B)}\square\sigma = 0$, i.e. $\pi^{t(B)}{}_\sigma \in \mathrm{Hom}_\Lambda(\Omega A'',B)$. By 1.1, $\delta\pi^{e+t(B)}\sigma = 0$, so that $\pi^{e+t(B)}\sigma = \square\theta$ for $\theta \in \mathrm{Hom}_R(A'',B)$. We now need only observe that $\square(\varphi - \pi^k\theta\alpha'') = 0$.

LEMMA 1.3. *If $\varphi \in \mathrm{Hom}_\Lambda(A/\pi^mA,B/\pi^mB)$, where $m = max(2t(A),\ t(A) + t(B) + e + k)$, then there is a $\psi \in Hom_\Lambda(A,B)$ such that the reductions $\tilde{\varphi}$, $\tilde{\psi}$ of φ and ψ to $Hom_\Lambda(A/\pi^kA,B/\pi^kB)$ are the same.*

Notice first that if $n \geqslant t(A)$ then $0 \to A' \to A/\pi^nA \to A''/\pi^nA'' \to 0$ is exact. The image of the composition $A' \to A/\pi^mA \to B/\pi^mB \to B''/\pi^mB''$ is annihilated by $\pi^{t(A)}$. Thus we have a commuting diagram

$$\begin{array}{ccccccccc} 0 & \longrightarrow & A' & \longrightarrow & A/\pi^{m-t(A)}A & \longrightarrow & A''/\pi^{m-t(A)}A'' & \longrightarrow & 0 \\ & & \downarrow{\scriptstyle \varphi'} & & \downarrow{\scriptstyle \tilde{\varphi}} & & \downarrow{\scriptstyle \tilde{\varphi}''} & & \\ 0 & \longrightarrow & B' & \longrightarrow & B/\pi^{m-t(A)}B & \longrightarrow & B''/\pi^{m-t(A)}B'' & \longrightarrow & 0 \end{array}$$

where $\tilde{\varphi}$ is the reduction of φ. Since A'' is R-projective we may lift this to a diagram

$$\begin{array}{ccccccccc} 0 & \longrightarrow & A' & \longrightarrow & A & \longrightarrow & A'' & \longrightarrow & 0 \\ & & \downarrow{\scriptstyle \varphi'} & & \downarrow{\scriptstyle \psi_0} & & \downarrow{\scriptstyle \psi_0''} & & \\ 0 & \longrightarrow & B' & \longrightarrow & B & \longrightarrow & B'' & \longrightarrow & 0 \end{array}$$

with $\psi_0 \in \mathrm{Hom}_R(A,B)$, $\psi_0'' \in \mathrm{Hom}_R(A'',B'')$. But then $\square\psi_0$ has its image in $\pi^{m-t(A)}B \subset \pi^{k+e+t(B)}B$. The conclusion follows immediately from 1.2.

LEMMA 1.4. *For any modules A, B, the image of $Hom_\Lambda(A,B) \to Hom_{\Lambda^*}(A^*,B^*)$ is dense.*

It is of course clear that the image of $\mathrm{Hom}_R(A,B) \to \mathrm{Hom}_{R^*}(A^*,B^*)$ is dense. Now suppose $\varphi \in \mathrm{Hom}_{\Lambda^*}(A^*,B^*)$ and that $\psi \in \mathrm{Hom}_R(A,B)$ is such that $\psi^* - \varphi \in \pi^{k+e+t(B)}\mathrm{Hom}_{R^*}(A^*,B^*)$. It follows that the image of $\square\psi$ is in $B \cap \pi^{k+e+t(B)}B^* = \pi^{k+e+t(B)}B$. By 1.2 there is a $\theta \in \mathrm{Hom}_R(A,\ B)$ such that $\psi - \pi^k\theta \in \mathrm{Hom}_\Lambda(A,\ B)$. But $(\psi - \pi^k\theta)^* - \varphi \in \pi^k\mathrm{Hom}_{R^*}(A^*,B^*) \cap \mathrm{Hom}_{\Lambda^*}(A^*,B^*)$.

LEMMA 1.5. *If A is R-projective, then for any B the completion map $c: Ext_\Lambda{}^1(A,B) \to Ext_{\Lambda^*}{}^1(A^*,B^*)$ is an epimorphism.*

It is also a monomorphism, a fact whose proof we omit. The diagram

$$\begin{array}{ccccc} \mathrm{Hom}_\Lambda(\Omega A,\ B) & \longrightarrow & \mathrm{Ext}_\Lambda{}^1(A,\ B) & \longrightarrow & 0 \\ \downarrow & & \downarrow{\scriptstyle C} & & \\ \mathrm{Hom}_{\Lambda^*}(\Omega A^*,\ B^*) & \longrightarrow & \mathrm{Ext}_{\Lambda^*}{}^1(A^*,\ B^*) & \longrightarrow & 0 \end{array}$$

commutes and has exact rows. It follows from 1.4 that the image of c is dense. But by 1.1, $\mathrm{Ext}_{\Lambda^*}{}^1(A^*,B^*)$ is discrete.

2. *Isomorphism and decomposability of modules.*

PROPOSITION 2.1. *If A and B are modules such that $A/\pi^mA \approx B/\pi^mB$, where $m = max(2t(A),\ 2t(B),\ t(A) + t(B) + e + 1)$, then $A \approx B$.*

For by 1.3 there are $\psi \in \mathrm{Hom}_\Lambda(A,B)$, $\psi' \in \mathrm{Hom}_\Lambda(B,A)$ such that their reductions $\bar{\psi} \in \mathrm{Hom}_\Lambda(A/\pi A,B/\pi B)$, $\bar{\psi}' \in \mathrm{Hom}_\Lambda(B/\pi B,A/\pi A)$ are inverse. By Nakayama's lemma, then, $\psi'\psi$ and $\psi\psi'$ are isomorphisms, hence also ψ and ψ'.

PROPOSITION 2.2. *If A and B are modules such that $A^* \approx B^*$, then $A \approx B$.*

This follows immediately; indeed $A^*/\pi^n A^* = A/\pi^n A$.

PROPOSITION 2.3. *If R is complete and A is a module such that $A/\pi^m A$ is decomposable, where $m = 2t(A) + e + 1$, then A is decomposable.*

Decomposability is equivalent to the existence of a nontrivial idempotent endomorphism. If $\varphi: A/\pi^m A \to A/\pi^m A$ is such an idempotent then by 1.3 there is a $\psi_0 \in \mathrm{Hom}_\Lambda(A,A)$ such that $\bar{\psi}_0 = \bar{\varphi} \in \mathrm{Hom}_\Lambda(A/\pi A, A/\pi A)$. Thus $\psi_0^2 - \psi_0$ has its image in πA. The usual process for lifting idempotents leads to an idempotent endomorphism $\psi \in \mathrm{Hom}_\Lambda(A,A)$ with $\bar{\psi} = \bar{\psi}_0$, which is accordingly nontrivial.

These imply the following theorem.

THEOREM 2.4. *If R is complete, then the Krull-Schmidt theorem holds for Λ-modules.*

We need only prove uniqueness of a decomposition $A \approx A_1 \oplus \ldots \oplus A_n$ into indecomposables. Setting $m = 2t(A) + e + 1$ (and observing that $t(A_i) \leq t(A)$) we have by 2.3 a decomposition $A/\pi^m A \approx A_1/\pi^m A_1 \oplus \ldots \oplus A_n/\pi^m A_n$ into indecomposables. Since these are modules over the Artinian ring $(R/(\pi)^m)G$, this decomposition is unique. The conclusion then follows from 2.1.

The condition that R be complete may be relaxed as follows. We shall say that K is a *splitting field for G Relative to K^** if whenever A is an irreducible KG-module then A^* is an irreducible K^*G-module. This is the case for example if K is an absolute splitting field for G.

PROPOSITION 2.5. *If K is a splitting field for G relative to K^* then $A \to A^*$ gives rise to a bijective correspondence between isomorphism classes of Λ-modules and isomorphism classes of Λ^*-modules.*

In view of 2.2 we need only prove that every Λ^*-module B is isomorphic to some A^*. If B is a torsion-free Λ^*-module then $B \subset K^*B$, and, since KG is semi-simple and K is a relative splitting field, K^*B has a KG submodule M such that $[M:K] = [K^*B:K^*]$ and $K^*B = K^*M$. Since $M \subset K^*B$ is dense and $B \subset K^*B$ is open, $A = M \cap B$ is dense in B, i.e. $A^* = B$. But A is of finite rank and contains no elements of infinite height and is hence a finitely generated Λ-module.

We observe also that an R^*-torsion Λ^*-module is already a (discrete) Λ-module.

For the general case, if B is a Λ^*-module then we have $B' \approx A'^*$, $B'' \approx A''^*$ for Λ-modules A', A''. The conclusion follows from 1.5.

Since this correspondence is clearly additive, we have, finally,

THEOREM 2.6. *If K is a splitting field for G relative to K^*, then the Krull-Schmidt theorem holds for Λ-modules.*

Remark: The fact that Λ is a group algebra entered essentially only in 1.1. The above results (with suitable terminological modifications) are equally valid for separable R-orders in algebras (cf. ref. 2).

This research was supported in part by a National Science Foundation contract. The author wishes to thank Professor I. Reiner for helpful conversations.

[1] Cartan, H., and S. Eilenberg, *Homological Algebra* (Princeton University Press, 1956).

[2] Higman, D. G., "On orders in separable algebras," *Canadian J. Math.*, **7**, 509–515 (1955).

[3] Reiner, I., "The Krull-Schmidt theorem for integral group representations," *Bull. Am. Math. Soc.* (to appear).

[4] Maranda, J. M., "On P-adic integral representations of finite groups," *Canadian J. Math.*, **5**, 344–355 (1953).

[5] Maranda, J. M., "On the equivalence of representations of finite groups by groups of automorphisms of modules over Dedekind rings," *Canadian J. Math.*, **7**, 516–526 (1955).

*SOLUTION OF THE $\bar{\partial}$-NEUMANN PROBLEM ON STRONGLY PSEUDO-CONVEX MANIFOLDS**

By J. J. Kohn

DEPARTMENT OF MATHEMATICS, BRANDEIS UNIVERSITY

Communicated by D. C. Spencer, May 15, 1961

Introduction.—The main theorem of this note solves the $\bar{\partial}$-Neumann problem on strongly pseudo-convex manifolds. Only a brief outline of the proof is given here; details will be supplied elsewhere.[1] Using the main theorem we obtain a representation of the $\bar{\partial}$-cohomology by harmonic forms, thus generalizing the theory of harmonic integrals for compact manifolds. Another application which we obtain is a new proof of the theorem of Newlander and Nirenberg[2] on the existence of local holomorphic coordinates on an integrable almost-complex manifold.

A variant of the $\bar{\partial}$-Neumann problem was first formulated by Garabedian and Spencer.[3] The $\bar{\partial}$-Neumann problem in its present form was investigated by D. C. Spencer and the author[4] by means of integral equations. Morrey[5] solved the problem in the special case of (0,1)-forms on sufficiently small tubular neighborhoods of real analytic manifolds (obtained by complexification) by establishing certain *a priori* estimates; it is this approach which we adopt in our work.

Notation and Definitions.—Let M' be a complex analytic hermitian manifold of complex dimension n and let M be an open submanifold of M' such that bM, the boundary of M, is a closed C^∞ submanifold of M' and such that $\bar{M}$, the closure of M in M', is compact. Let $\mathfrak{A}$ be the space of C^∞ complex-valued forms on M'. Following the customary convention we say that a form ϕ is of type (p,q) if, in terms of local holomorphic coordinates, ϕ may be expressed in the form

$$\phi = \sum_{\substack{i_1<\ldots<i_p \\ j_1<\ldots<j_q}} \phi_{i_1\ldots i_p j_1\ldots j_q}\, dz^{i_1}\wedge\ldots\wedge dz^{i_p}\wedge d\bar{z}^{j_1}\wedge\ldots\wedge d\bar{z}^{j_q}.$$

We abbreviate our notation and write $\phi = \phi_{IJ}dz^I d\bar{z}^J$. We denote by $\mathfrak{A}^{p,q}$ the space of forms of type (p,q). Then the exterior derivative d maps $\mathfrak{A}^{p,q}$ into $\mathfrak{A}^{p+1,q} \oplus \mathfrak{A}^{p,q+1}$, and this induces the decomposition $d = \partial + \bar{\partial}$ where $\bar{\partial}:\mathfrak{A}^{p,q} \to \mathfrak{A}^{p,q+1}$. In terms of the hermitian metric we have the operator $*:\mathfrak{A}^{p,q} \to \mathfrak{A}^{n-q,n-p}$, the inner product

$$(\phi, \psi) = \int_M \phi\wedge *\bar{\psi}$$

and the norm $\|\phi\|^2 = (\phi, \phi)$. We denote by $\mathfrak{L}^{p,q}$ the Hilbert space of complex-valued norm-finite forms of type (p,q). The formal adjoint of $\bar{\partial}$, denoted by $\mathfrak{d}$, is defined by $\mathfrak{d} = -*\partial*$ and the Laplace operator $\square:\mathfrak{A}^{p,q} \to \mathfrak{A}^{p,q}$ is defined by $\square = \bar{\partial}\mathfrak{d} + \mathfrak{d}\bar{\partial}$. Let $r:M' \to R$ be the function such that $|r(P)|$ is the geodesic distance from P to bM and $r(P) > 0$ if $P\in\bar{M}$, $r(P) < 0$ if $P\in M$. At each $P\in bM$ the space $\mathfrak{A}_P$ of forms evaluated at P decomposes into the space of normal forms, those divisible by dr, and its orthogonal complement, the tangential forms. If $\phi\in\mathfrak{A}$, $n\phi$ denotes the normal component of ϕ on bM. Let

$$\dot{\mathfrak{D}}^{p,q} = \{\phi\in\mathfrak{A}^{p,q} \mid n\phi = 0 \quad \text{and} \quad n\bar{\partial}\phi = 0 \text{ on } bM\}$$

and let $\Box'$ be the closure of $\Box$ restricted to $\mathfrak{D}^{p,q}$. We denote the domain of $\Box'$ by $\mathfrak{D}^{p,q}$ and let $\mathfrak{K}^{p,q} = \{\phi \in \mathfrak{D}^{p,q} \mid \Box'(\phi) = 0\}$.

Finally we recall that M is called *strongly pseudo-convex* if whenever f is a local C^∞ real-valued function such that, $df \neq 0$, $f(P) < 0$ if $P \in M$ and $f(P) > 0$ if $P \in \bar{M}$ then if $0 \neq (a^1, \ldots, a^n) \in \mathbf{C}^n$ and $\Sigma f_{z^i z^j} a^i = 0$ we have $\Sigma f_{z^i \bar{z}^j} a^i \bar{a}^j > 0$.

Representation of $\bar{\partial}$-Cohomology.—As a consequence of the main theorem we can define (on a strongly pseudo-convex manifold M) the operator $N: \mathfrak{L}^{p,q} \to \mathfrak{D}^{p,q}$ by $N\Box'\psi = \psi$ if $\psi \in \mathfrak{D}^{p,q}$ and $\psi \perp \mathfrak{K}^{p,q}$, and by $N\phi = 0$ if $\phi \in \mathfrak{K}^{p,q}$. The main theorem and the interior differentiability theorem for elliptic systems imply the following:

PROPOSITION. *The operator N defined above has the following properties:* (a) *N is bounded and, if $q \neq 0$, it is completely continuous.* (b) $\bar{\partial}N = N\bar{\partial}$. (c) *If $\phi \in \mathfrak{L}^{p,q}$ and is of class C^∞, then $\phi = \bar{\partial}\delta N\phi + \delta\bar{\partial}N\phi + \gamma$ where $\gamma \in \mathfrak{K}^{p,q}$ and each term is C^∞ on M.*

To study the $\bar{\partial}$-cohomology by means of forms in $\mathfrak{L}^{p,q}$ we first observe that, if M is strongly pseudo-convex, then there exists a manifold $\bar{M}$ such that $M \subset \bar{M} \subset \bar{M} \subset M'$ and such that the restriction map $H^q(\bar{M}, \Omega^p) \to H^q(M, \Omega^p)$ is surjective for $q > 0$ (see Grauert[6]). Here Ω^p is the sheaf of germs of holomorphic $(p, 0)$-forms. Our main inequality also implies that if $\phi = \bar{\partial}\alpha$ and $\phi \in \mathfrak{L}^{p,q}$ for $q \neq 0$, then there exists $\beta \in \mathfrak{L}^{p,q-1}$ such that $\phi = \bar{\partial}\beta$. By the isomorphism theorem of Dolbeault, there is a form on M in each $\bar{\partial}$-cohomology class in M $(q \neq 0)$. Hence we obtain

PROPOSITION. *If $q > 0$, then $\mathfrak{K}^{p,q} \approx H^q(M, \Omega^p)$.*

Applications to Deformations of Complex Structure.—Let M_t', $t \in (-1,1)$, be a differentiable family of complex structures on a differentiable manifold (see Kodaira and Spencer[7]). Suppose that $M_0 \subset M_0'$ is strongly pseudo-convex. Then for small t, $M_t \subset M_t'$ is strongly pseudo-convex, so the main theorem holds and the constants in the inequalities can be chosen independent of t.

PROPOSITION. *If f_0 is holomorphic on M_0' and if $\mathfrak{K}_0^{0,1} = 0$ then, for small t, there exists a function f_t which is holomorphic on M_t such that f_t and its first derivatives are continuous in t.*

The function f_t is defined by $f_t = f_0 - g_t$, where $g_t = \delta_t N_t \bar{\partial}_t f_0$. Our inequalities imply that $\lim_{t \to 0} \|g_t\| = 0$. We observe that $\Box_t g_t = \Box_t f_0$; thus the continuity in t follows from the L_p estimates given by Agmon, Douglis, and Nirenberg.[8]

It is easily shown that the above proposition holds for integrable almost-complex manifolds. If P is a point of an integrable almost-complex manifold, then for each $t \in (0, 1)$ there exists a neighborhood V_t of P such that $\cap V_t = \{P\}$ and such that there exists a diffeomorphism λ_t: $V_t \to B$, where B is the unit ball in the holomorphic tangent space. Furthermore the λ_t and V_t can be so constructed that B_t, the almost-complex structure induced by λ_t, is part of a differentiable family of integrable almost-complex structures on B which includes the complex structure B_0. Applying the above proposition to B_t and taking for f_0 the coordinate functions on B_0, we obtain holomorphic coordinates on B_t for sufficiently small t. This argument gives a new proof of the result of Newlander and Nirenberg[2] along lines similar to those originally suggested by Spencer.[9] That is, we obtain the

PROPOSITION. *If M is an integrable almost-complex manifold, then each point of M has a neighborhood on which there exist holomorphic coordinates.*

The Principal Results.—The following proposition states the "weak decomposi-

tion" and it is proved by showing that $\Box' = TT^* + T^*T$, where T denotes the closure of $\bar{\partial}$ in $\mathcal{L}^{p,q}$. The self-adjointness then follows as in the work of Gaffney.[10]

PROPOSITION. *The operator* $\Box'$: $\mathfrak{D}^{p,q} \to \mathcal{L}^{p,q}$ *is self-adjoint and* $\mathcal{L}^{p,q}$ *has the following orthogonal decomposition:* $\mathcal{L}^{p,q} = [\Box'\mathfrak{D}^{p,q}] \oplus \mathfrak{H}^{p,q}$. *Here we mean by* $[S]$ *the closure of* S.

The Kähler metric whose existence is asserted in the proposition below is constructed by taking a real-valued function f which defines the boundary globally and observing that (because of strong pseudo-convexity) the form $(\exp(Af))_{z^i\bar{z}^j}$ is positive definite for sufficiently large A.

PROPOSITION. *If* $M \subset M'$ *is strongly pseudo-convex, then there exists a Hermitian metric on* M' *which is Kähler in a neighborhood of* bM.

MAIN THEOREM. *If* $M \subset M'$ *is strongly pseudo-convex with a Hermitian metric on* M' *which is Kähler in a neighborhood of* bM, *then* $\mathcal{L}^{p,q} = \Box'\mathfrak{D}^{p,q} \oplus \mathfrak{H}^{p,q}$. *Furthermore,* $\mathfrak{H}^{p,q}$ *is finite dimensional, if* $q \neq 0$.

The proof of the theorem depends on the inequality (*) given in the following lemma. This inequality is also important for other applications.

LEMMA. *Under the hypothesis of the theorem and if* $q \neq 0$, *then there exists* $C > 0$ *such that for all* $\phi \in \mathfrak{D}^{p,q}$ *we have*

$$(*) \qquad (\Box\phi, \phi) + \|\phi\|^2 \geq C(\|\phi\|_{\frac{1}{2}}^2 + \int_{bM} |\phi|^2 * dr + \|\phi\|^2),$$

where $\|\phi\|_{\frac{1}{2}}^2$ *is defined by means of a fixed covering* $\{U_\alpha\}$ *by holomorphic coordinate neighborhoods,*

$$\|\phi\|_{\frac{1}{2}}^2 = \sum_{\alpha,I,J,k} \int_{M \cap U_\alpha} |\phi_{IJ,\bar{\alpha}}^{\quad k}|^2 * (1).$$

Outline of the Proof: To establish (*) we cover $\bar{M}$ with finitely many coordinate neighborhoods each of diameter less then ρ, where ρ is a fixed small number. Now, by use of a partition of unity, it suffices to prove (*) for forms $\phi \in \dot{\mathfrak{D}}^{p,q}$ whose supports lie in a single coordinate neighborhood U_α. If U_α does not intersect bM then the inequality is obtained by standard techniques of elliptic equations (see, for example, Nirenberg[11]). If U_α intersects bM, we choose a holomorphic coordinate system on U_α whose origin is on bM and such that at the origin $g_{ij}(0) = 0$ and $(dg_{ij})_0 = 0$, where g_{ij} are the components of the metric tensor (such a coordinate system exists because of the Kähler property). We also choose the coordinates so that $r_{z^i\bar{z}^j}(0)$ is diagonal. Let $D(\phi)^2 = (\Box\phi, \phi) + \|\phi\|^2$ and

$$E(\phi)^2 = \|\phi\|_{\frac{1}{2}}^2 + \int_{bM} |\phi|^2 * dr + \|\phi\|^2.$$

Note that if $\phi \in \dot{\mathfrak{D}}^{p,q}$, then

$$D(\phi)^2 = \|\bar{\partial}\phi\|^2 + \|\delta\phi\|^2 + \|\phi\|^2$$

and

$$\|\bar{\partial}\phi\|^2 = \sum_{IJk} \int_M |\phi_{IJ,\bar{k}}|^2 g^{(IJk)(IJk)} * (1) + \sum_{(IJk)\neq(PQm)} \int_M \phi_{IJ,z^k} \bar{\phi}_{PQ,\,z^m} g^{(IJk)(PQm)} * (1),$$

where the $g^{(IJk)(PQm)}$ are components of the metric tensor on $\mathfrak{A}^{p,q+1}$. Let $\phi^{IJ} = \phi_{KL} g^{(KL)(IJ)}$; then we obtain(for $q>0$)

$$\|\bar{\partial}\phi\|^2 + C_1\|\phi\|^2 \geq C_2\|\phi\|_{\frac{1}{2}}^2 - \sum_{kH} \epsilon_{(kH)}^{kH}\, \epsilon_{(mH)}^{mH} \int_M \phi_{\bar{z}k}^{I(mH)} \bar{\phi}_{\bar{z}m}^{I(kH)} *(1),$$

where H runs over increasingly ordered $(q-1)$-tuples, $\langle mH\rangle$ is the increasingly ordered q-tuple whose elements are $\{m\} \cup H$ and $\epsilon_{(mH)}^{mH}$ is zero if $\langle mH\rangle$ has any repeated integers, otherwise it is the sign of the permutation that sends mH onto $\langle mH\rangle$. Integrating by parts, we obtain

$$\int_M \phi_{\bar{z}k}^{I(mH)} \bar{\phi}_{\bar{z}m}^{I(kH)} *(1) = \int_{bM} \phi^{I(mH)} [\bar{\phi}_{\bar{z}m}^{I(kH)} r_{\bar{z}k} + \bar{\phi}_{\bar{z}k}^{I(kH)} r_{\bar{z}m}] *dr - \int_M \phi_{\bar{z}m}^{I(mH)} \bar{\phi}_{\bar{z}k}^{I(kH)} *(1) + 0(\rho)E(\phi)^2.$$

The boundary condition $n\phi = 0$ implies

$$\sum_k \epsilon_{(kH)}^{kH} \bar{\phi}^{I(kH)} r_{\bar{z}k} = 0 \quad \text{on } bM.$$

Differentiation with respect to $\bar{z}^m$ gives

$$\sum_k \epsilon_{(kH)}^{kH} [\bar{\phi}_{\bar{z}m}^{I(kH)} r_{\bar{z}k} + \bar{\phi}^{I(kH)} r_{\bar{z}k\bar{z}m}] = \lambda r_{\bar{z}m}$$

on bM. Multiplying by $\epsilon_{(mH)}^{mH} \phi^{I(mH)}$, summing on m and using the strong pseudo-convexity we obtain

$$-\sum \epsilon_{(kH)}^{kH} \epsilon_{<mH>}^{mH} \phi^{I(mH)} \bar{\phi}_{\bar{z}m}^{I<kH>} \geq C_3 |\phi|^2$$

on bM. Furthermore

$$\|\delta\phi\|^2 \geq C_4 \Big|\sum_{kmH} \epsilon_{(kH)}^{kH} \epsilon_{<mH>}^{mH} \phi_{\bar{z}m}^{I(mH)} \bar{\phi}_{\bar{z}k}^{I<kH>} *(1)\Big| + 0(\rho)E(\phi)^2.$$

Combining the above we obtain the inequality (*).

To complete the proof of the theorem we use the following inequality which is proved by Fourier transform methods analogous to those in Peetre's thesis.[12] For $a \in \mathbf{R}$, let $bM_a = \{P \in M \mid r(P) = a\}$. Then there exists $\epsilon > 0$ and $C > 0$ such that for any $\phi \in \mathfrak{A}$,

$$\int_{bM_a} |\phi|^2 *dr \leq CE(\phi)^2,$$

where $|a| < \epsilon$. This inequality, together with the usual interior estimates, implies that E is completely continuous with respect to $\|\ \|$. Then the theorem for $q \neq 0$ follows by standard Hilbert space theory. The case $q = 0$ follows from the inequality $\|\Box\phi\| \geq K\|\phi\|$ for $\phi \in \mathfrak{D}^{p,0}$ and ϕ orthogonal to $\mathfrak{K}^{p,0}$. This inequality is established by approximating ϕ with $\Box\alpha$, where $\alpha \in \mathfrak{D}^{p,0}$. Then, using (*) on $\bar{\partial}\phi$ and $\bar{\partial}\alpha$, we obtain

$$\|\phi\|^2 \leq \|\bar{\partial}\phi\|\, \|\bar{\partial}\alpha\| + \|\phi\|\, \|\phi - \Box\alpha\| \leq C\|\Box\phi\|\, \|\Box\alpha\| + \|\phi\|\, \|\phi - \Box\alpha\|$$

which gives the result.

* This work was partly supported by a research project at Brandeis University sponsored by the National Science Foundation (contract G8207).

[1] Kohn, J. J., "Harmonic integrals on strongly pseudo-convex manifolds," *Ann. Math.* (to appear).

[2] Newlander, A., and L. Nirenberg, "Complex analytic coordinates in almost-complex manifolds," *Ann. Math.*, **65**, 391–404 (1957).

[3] Garabedian, P. R., and D. C. Spencer, "Complex boundary value problems," *Trans. Amer. Math. Soc.*, **73**, 223–242 (1952).

[4] Kohn, J. J., and D. C. Spencer, "Complex Neumann problems," *Ann. Math.*, **66**, 89–140 (1957).

[5] Morrey, C. B., "The analytic embedding of abstract real-analytic manifolds," *Ann. Math.*, **68**, 159–201 (1958).

[6] Grauert, H., "On Levi's problem and the imbedding of real-analytic manifolds," *Ann. Math.*, **68**, 460–472 (1958).

[7] Kodaira, K., and D. C. Spencer, "On deformations of complex analytic structures, I–II," *Ann. Math.*, **67**, 328–466 (1958).

[8] Agmon, S., A. Douglis, and L. Nirenberg, "Estimates near the boundary for solutions of elliptic partial differential equations satisfying general boundary conditions. I," *Comm. Pure and App. Math.*, **12**, 623–727 (1959).

[9] Spencer, D. C., "Potential theory and almost-complex manifolds," in *Lecures on Functions of a Complex Variable* (Ann Arbor: University of Michigan Press, 1955), pp. 15–43.

[10] Gaffney, M. P., "Hilbert space methods in the theory of harmonic integrals," *Trans. Amer. Math. Soc.*, **78**, 426–444 (1955).

[11] Nirenberg, L., "Remarks on strongly elliptic partial differential equations," *Comm. Pure App. Math.*, **8**, 648–674 (1955).

[12] Peetre. J., "Théorèmes des régularitès pour quelques classes d'opérateurs différentiels," *Lund.*, (1959).

EXAMPLES FOR DIFFERENTIABLE GROUP ACTIONS ON SPHERES

BY D. MONTGOMERY AND H. SAMELSON*

INSTITUTE FOR ADVANCED STUDY AND STANFORD UNIVERSITY

Communicated June 1, 1961

1. *Introduction.*—The purpose of this note is to prove the following:

THEOREM. *Let G be a compact Lie group, containing more than one element. Then there exists a positive integer k such that G has an infinite number of differentiable actions on the k-sphere S^k (in its usual differentiable structure), no two of which are equivalent.*

Here differentiability is understood in the C^∞-sense; two differentiable actions are equivalent if there exists a diffeomorphism of S^k carrying one action into the other. G is not assumed connected, and may in particular be finite. Actually the actions to be constructed for the proof of the theorem are pairwise topologically inequivalent; that is, there is no homeomorphism of S^k carrying one action into the other. For the proof of the theorem, including the statement of the last sentence, we shall construct, for a given G and suitable k, a sequence of actions with the property that the stationary sets of any two actions are not homeomorphic, by virtue of having different fundamental groups (the stationary set of an action consists of all points left fixed by all elements of the group). Our construction is a modification of one of J. H. C. Whitehead's,[11] which in turn is based on an example of Newman's.[6] In the theorem above, the infinity cannot be more than countable by a result of Palais.[7]

2. *The manifolds Y_i and M_i.*—Our main observations in this section are that Newman's example can easily be modified to yield a sequence of different examples and that the manifolds in question can be taken differentiable.

Newman's example started with a finite simplicial connected two-dimensional complex K, whose fundamental group $\pi_1(K)$ is the "doubled" icosahedral group and which is acyclic (the integral homology groups $H_r(K, Z)$ vanish for $r > 0$). Let $K_i = K \cup \ldots K \cup$ be the one-point union of i copies of K (so that any two of the K have exactly one point in common), for $i = 1, 2, 3, \ldots$. It is well known that $\pi_1(K_i)$ is the free product of i copies of $\pi_1(K)$. Since the minimal number of generators of $\pi_1(K)$ is two, the minimal number of generators of $\pi_1(K_i)$ is $2i$ (cf. reference 4, vol. 2, p. 58). Hence,

LEMMA 1. *If $i \neq j$, then $\pi_1(K_i) \neq \pi_1(K_j)$.*

From standard properties of homology groups we have

LEMMA 2. *K_i is connected and acyclic, for each i.*

We now repeat Newman's construction for any given i:

K_i is imbedded simplicially in some triangulation of the 5-sphere S^5. Transition to the barycentric subdivision makes K_i a full subcomplex; we operate now in this subdivision. Each simplex σ of Star $K_i - K_i$ is uniquely expressible as join $\sigma_a\sigma_b$, with $\sigma_a \in K_i$ and $\sigma_b \subset S^5 - K_i$. The middle section of this join, i.e., the collection of all points of the form $\frac{1}{2}(x_a + x_b)$, with $x_a \in \sigma_a$, $x_b \in \sigma_b$, is a convex cell m_σ, homeomorphic to $\sigma_a \times \sigma_b$. We write M_i for the union of all m_σ, with σ ranging over Star $K_i - K_i$. Newman has shown that the following two lemmas hold.

LEMMA 3. *M_i is a connected 4-manifold, with $\pi_1(M_i) = \pi_1(K_i)$.*

Let Y_i be the closure of that component of $S^5 - M_i$ that does not contain K_i.

LEMMA 4. *Y_i is a simply connected and acyclic, hence contractible, manifold, with boundary M_i.*

We come now to the introduction of differentiability in Y_i. This is accomplished by arguments due to Whitney,[13] Cairns,[1, 2] Whitehead,[12] and Hirsch,[3] using the idea of manifolds with transverse fields. We shall outline a simple direct proof (see ref. 3 in this connection).

LEMMA 5. *There is a homeomorphism of S^5 onto itself which takes M_i onto a differentiable submanifold of S^5, and consequently takes Y_i onto a differentiable manifold-with-boundary.*

Proof: To each $x \in M_i$, written uniquely as $\frac{1}{2}(x_a + x_b)$ as above, there corresponds the line segment $s_x = \{tx_a + (1 - t)x_b: 0 < t < 1\}$. The dependence of s_x on x is continuous, and the various s_x are disjoint. We show first that s_x is transversal to M_i at x in the sense[11] that the angles between s_x and the secants of M_i near x (i.e., the lines through any two points of M_i near x) are bounded away from 0. Suppose not; then one sees easily that near x there are two points of M_i, say x' and x'', such that the line through x' and x'' is parallel to s_x. (The points to observe are that because of linearity one needs to consider only secants one of whose points is outside a fixed small neighborhood of x and that such secants with the second point very close to x are certainly not close to s_x in direction.) Renaming if necessary, one sees that the segment from x_a to x' meets M_i in a second point, namely a point on the segment from x'' to x. But from the nature of the part of M_i in the carrier simplex of x' (which also contains x and x_a), this is impossible.

The segments s_x (directed from x_a to x_b, say) define a continuous vector field in the open set $\bigcup_{x \in M_i} s_x$. We approximate this field by a C^∞-vector field V. Because of the transversality property of the s_x, each trajectory (= integral curve) of V,

starting on M_i, will not meet M_i again for some time. More exactly, for sufficiently small ϵ, the map h of $M_i \times [-\epsilon, +\epsilon]$ into E^5, which sends (x, t) into the point with parameter value t on the trajectory through x, will be a homeomorphism into E^5; here $h(x, 0) = x$. We put $X_i = h(M_i \times (-\epsilon, \epsilon))$, leaving off the end points of the trajectories; this is an open set. It is fairly obvious that the decomposition of X_i into the h-images of the $x \times (-\epsilon, +\epsilon)$ is a differentiable fibering, with the interval $(-\epsilon, \epsilon)$ in its standard differentiable structure as fiber. (One needs the following elementary lemma: Let f, g be two continuous functions on the unit disk D^{n-1} in Eucilidean space E^{n-1}, with $f(x) > g(x)$ throughout. Then the set $\{(x, t): |x| < 1, f(x) > t > g(x)\}$ in E^n is diffeomorphic to $\{(x, t): |x| < 1\}$ with preservation of the projection on the x-coordinate.) The decomposition space X_i' is also a differentiable manifold; and M_i defines a cross section of this fibering, associating to each point of X_i', i.e., to each trajectory, the point of M_i on it. By the standard approximation theorem (ref. 9, p. 25), we obtain an approximating C^∞-cross section, N_i, a C^∞-submanifold of S^5. It is now easy, by moving points on the V-trajectories in X_i, to arrange a homeomorphism of S^5 that is the identity outside of X_i, and sends M_i into N_i, thus completing the proof of lemma 5.

3. *The group actions.*—From now on, we consider Y_i and M_i as endowed with the differentiable structure induced by the homeomorphism of lemma 5. Let D^n be the unit disk in Euclidean n-space E^n, and let S^{n-1}, the $(n-1)$-sphere, be the boundary of D^n, with their standard differentiable structures.

Let the orthogonal group $O(n)$ act on E^n and hence on D^n in the usual fashion. This is of course a differentiable action.

LEMMA 6. *There exists a differentiable structure on $Y_i \times D^n$ such that the action π_i of $O(n)$, defined by trivial action on Y_i and the standard action on D^n, is differentiable.*

Proof: The differentiable structure on $Y_i \times D^n$, derived from that of the two factors, is that of a manifold-with-boundary ($= M_i \times D^n \cup Y_i \times S^{n-1}$) and a corner in the boundary, along $M_i \times S^{n-1}$. By a fairly well-known process, one can smooth the corner:[5] Let E_+ denote the interval $(0, \infty)$, and let E_+^2 be the upper half-plane $\{(x, y): y \geq 0\}$. A neighborhood ("tubular neighborhood") of M_i in Y_i exists, diffeomorphic to $M_i \times E_+$. Similarly, we represent the neighborhood $D^n - \{0\}$ of S^{n-1} as $S^{n-1} \times E_+$, by letting x correspond to $\left(\frac{x}{|x|}, \frac{1}{|x|} - 1\right)$. A neighborhood U of $M_i \times S^{n-1}$ in $Y_i \times D^n$ is then represented as $M_i \times S^{n-1} \times E_+ \times E_+$. One now maps $E_+ \times E_+$ onto E_+^2 by sending $(r \cos\theta, r \sin\theta)$ into $(r \cos 2\theta, r \sin 2\theta)$. The resulting map of U onto $M_i \times S^{n-1} \times E_+^2$ is used to define differentiability along $M_i \times S^{n-1}$. Note that differentiability at points not on $M_i \times S^{n-1}$ is unchanged by this process and that the action of $O(n)$ is differentiable there. But the action is also differentiable along $M_i \times S^{n-1}$, as one sees from the form $M_i \times S^{n-1} \times E_+^2$ for U: only the factor S^{n-1} is affected by the transformations, by our choice of tubular neighborhood of S^{n-1}.

From results of Whitehead[10] and Smale[8] we have

LEMMA 7. *For $n > 10$, the differentiable manifold-with-boundary $Y_i \times D^n$ of lemma 6 is diffeomorphic to D^{n+5}; its boundary consequently is diffeomorphic to S^{n+4}.*

We come now to the construction of the promised examples. Let G be a non-

trivial compact Lie group. There exists an orthogonal representation of dimension $n \geq 10$ which, considered as action on E^n via a homomorphism into $O(n)$, has only the origin as stationary point. By lemmas 6 and 7, we obtain differentiable actions γ_i of G on D^{n+5} and on S^{n+4} for $i = 1, 2, 3, \ldots$; the stationary set of γ_i on $S^{n+4} = M_i \times D^n \cup Y_i \times S^{n-1}$ is $M_i \times 0$. By lemmas 1 and 3, the actions γ_i are pairwise topologically inequivalent, and the theorem is proved, with $k = n + 4$. It is clear that we can require all transformations to be orientation-preserving by using $SO(n)$ instead of $O(n)$.

* The second author was partially supported by NSF grant G-14113.

[1] Cairns, S. S., "Homeomorphisms between topological manifolds and analytic manifolds," *Ann. Math.*, **41**, 796–808 (1940).

[2] Cairns, S. S., "The manifold smoothing problem," *Bull. Amer. Math. Soc.*, **67**, 237–238 (1961).

[3] Hirsch, M., "On combinatorial submanifolds of differentiable manifolds," to appear in *Comm. Math. Helv.*

[4] Kurosh, A. S., *The Theory of Groups*, 2nd English ed. (New York: Chelsea Publishing Company, 1956).

[5] Milnor, J., "Differentiable manifolds which are homotopy spheres," Princeton University, 1959, mimeographed notes.

[6] Newman, M. H. A., "Boundaries of ULC sets in Euclidean n-space," these PROCEEDINGS, **34**, 193–196 (1948).

[7] Palais, *Bull. Amer. Math. Soc.* (to appear).

[8] Smale, S., "Generalized Poincaré conjecture in dimensions greater than 4," *Ann. of Math.* (to appear).

[9] Steenrod, N. E., *The Topology of Fibre Bundles* (Princeton University Press, 1951).

[10] Whitehead, J. H. C., "Simplicial spaces, nuclei and m-groups," *Proc. London Math. Soc.*, **45**, 243–327 (1939).

[11] Whitehead, J. H. C., "On involutions of spheres," *Ann. of Math.*, **66**, 27–29 (1957).

[12] Whitehead, J. H. C., "Manifolds with transverse fields in Euclidean space," *Ann. Math.*, **73**, 154–212 (1960).

[13] Whitney, H., "Differentiable manifolds," *Ann. Math.*, **37**, 645–680 (1936).

DEFORMATION OF PSEUDOGROUP STRUCTURES

By D. C. SPENCER

DEPARTMENT OF MATHEMATICS, PRINCETON UNIVERSITY

Communicated July 3, 1961

In their paper,[3] K. Kodaira and the author have described a general pattern into which the deformation of structures on manifolds, defined by pseudogroups of bidifferentiable transformations, seems to fit; at least, the special types of structure so far investigated (see, for example, refs. 2, 3). The purpose of this note is to describe briefly a method of deformation which fits all the requirements of the general pattern and generalizes the method of the paper;[3] and which applies to structures defined by arbitrary transitive, continuous pseudogroups of local bidifferentiable or biholomorphic transformations of real or complex n-space, respectively. However, as in the case of the structures considered heretofore, the principal results have been obtained for complex pseudogroups only (i.e., pseudogroups of biholomorphic transformations).

Details will be given in a paper to appear in the *Annals of Mathematics*.

1. *Fundamental Sheaves.*—By "differentiable" we shall always mean "differentiable of class C^∞."

Let Γ be a transitive, continuous pseudogroup of local differentiable transformations of n-space (see ref. 4), and let M be a compact Γ-manifold, i.e., the Γ-structure of M is represented by a (locally finite) covering of M by open sets, each of which is covered by a Γ-coordinate, and the transformation from one Γ-coordinate into another belongs to Γ. Then Γ induces over M a pseudogroup of local (differentiable) transformations which, for economy of language, will also be called Γ. For each non-negative integer μ, we have the differentiable fibre bundle $L^\mu \to M \times M$, where L^0 may be identified with $M \times M$ and L^μ, $u \geq 1$, consists of all jets of order μ (in the sense of C. Ehresmann) of transformations of M belonging to Γ. Let $\beta: L^\mu \to M$ be the projection of L^μ onto M sending each jet into its source, and denote by T^μ_β the bundle over L^μ of tangent vectors along the fibres of $\beta: L^\mu \to M$. Let I^μ be the submanifold of L^μ, over the diagonal of $M \times M$, composed of the jets of order μ of the identity map of M. If the diagonal of $M \times M$ is identified with M, the restriction of T^μ_β to I^μ may be identified with a vector bundle R^μ over M. The structure group of R^μ is a (finite dimensional) Lie group $G^{\mu+1}$, and its fibre is $R^n \oplus \mathfrak{g}^\mu$, where $\mathfrak{g}^\mu$ is the Lie algebra of G^μ. In particular, R^μ may be identified, in the case $\mu = 0$, with the tangent bundle of M. Denote by $P^{\mu+1}$ the principal bundle of R^μ, where $P^{\mu+1}$ has fibre and group $G^{\mu+1}$; then R^μ may be identified with the bundle $T(P^\mu)/G_\mu$ obtained (from the tangent bundle $T(P^\mu)$ of P^μ) by identifying points which are transforms of each other under the operations of G^μ on $T(P^\mu)$ induced by the right operations on P^μ.

Let $\mathcal{H}^\mu_{(m)}$ be the sheaf over M of germs of local differentiable deformations (fibre-preserving transformations) of P^μ which depend on a parameter t varying over a neighborhood of the origin O of m-space and reduce to the identity at $t = 0$; and let $\mathfrak{F}_{(m)}$ be the sheaf over M of germs of local transformations of M belonging to Γ which depend on t and reduce to the identity at $t = 0$. We have the projection of $\mathcal{H}^\mu_{(m)}$ onto $\mathcal{H}^0_{(m)}$, where $\mathcal{H}^0_{(m)}$ is the sheaf of germs of all local bidifferentiable transformations of M which depend on t and reduce to the identity at $t = 0$; and we have the injection $\iota^\mu: \mathfrak{F}_{(m)} \to \mathcal{H}^\mu_{(m)}$ of $\mathfrak{F}_{(m)}$ into $\mathcal{H}^\mu_{(m)}$ as sheaf of left operators, where ι^μ is the prolongation of the transformations of $\mathfrak{F}_{(m)}$ into their jets of order μ. Let μ_0, $\mu_0 \geq 1$, be the order of Γ; then, for $\mu \geq \mu_0 - 1$, we have the following exact sequence of sheaves (with distinguished or unit subsheaves which we denote by 1):

$$1 \to \mathfrak{F}_{(m)} \xrightarrow{\iota^{\mu+1}} \mathcal{H}^{\mu+1}_{(m)} \xrightarrow{\mathfrak{D}} \mathfrak{D}\mathcal{H}^{\mu+1}_{(m)} \to 1,$$

where $\mathfrak{D}$ is a differential operator mapping $\mathcal{H}^{\mu+1}_{(m)}$ into a sheaf $J^{\mu,1}_{(m)}$ of germs of "jet forms" of degree 1 depending on t and vanishing at $t = 0$ and where the image $\mathfrak{D}\mathcal{H}^{\mu+1}_{(m)}$ of $\mathcal{H}^{\mu+1}_{(m)}$ in $J^{\mu,1}_{(m)}$ is isomorphic to the quotient $\mathcal{H}^{\mu+1}_{(m)}/\iota^{\mu+1}(\mathfrak{F}_{(m)})$. Then the corresponding exact cohomology sequence is

$$1 \to H^0(M, \mathfrak{F}_{(m)}) \xrightarrow{\iota^{\mu+1}} H^0(M, \mathcal{H}^{\mu+1}_{(m)}) \xrightarrow{\mathfrak{D}} H^0(M, \mathfrak{D}\mathcal{H}^{\mu+1}_{(m)}) \to H^1(M, \mathfrak{F}_{(m)}) \to 1, \quad (1)$$

where, by a theorem of A. Haefliger[1], $H^1(M, \mathfrak{F}_{(m)})$ may be identified with the set of germs of deformations of the Γ-structure of M depending on the parameter t; and

the dependence of the germs of $\mathfrak{F}_{(m)}$ and $\mathfrak{IC}_{(m)}^{\mu+1}$ on t is differentiable if Γ is a pseudogroup of (local) non-analytic differentiable transformations, and holomorphic if Γ is complex, i.e., a pseudogroup of (local) holomorphic transformations. In the first case, $\mathfrak{F}_{(m)}$ and $\mathfrak{IC}_{(m)}^{\mu+1}$ are sheaves of groups, $H^1(M, \mathfrak{F}_{(m)})$ and $H^1(M, \mathfrak{IC}_{(m)}^{\mu+1})$ are both defined, and $H^1(M, \mathfrak{IC}_{(m)}^{\mu+1}) = 1$; hence, in this case, (1) is an exact sequence (in the sense of sets with distinguished elements). In the second case, where Γ is a complex pseudogroup of holomorphic transformations and the germs of $\mathfrak{F}_{(m)}$, $\mathfrak{IC}_{(m)}^{\mu+1}$ depend holomorphically on the point t of complex m-space, $\mathfrak{F}_{(m)}$ is a sheaf of groups, $H^1(M,\mathfrak{F}_{(m)})$ is therefore defined, $\iota^{\mu+1}\mathfrak{F}_{(m)}$ operates on $\mathfrak{IC}_{(m)}^{\mu+1}$ on the left, and $\mathfrak{DIC}_{(m)}^{\mu+1}$ is composed of germs depending holomorphically on t, hence $\mathfrak{DIC}_{(m)}^{\mu+1}$ is a subsheaf of a sheaf $J_{(m)}^{\mu,1}$ of germs of "jet forms" depending holomorphically on t. However, the sheaf $\mathfrak{IC}_{(m)}^{\mu+1}$ of germs of local *differentiable* deformations, depending *holomorphically* on t, of the structure of $P^{\mu+1}$ of complex analytic fibre space, is obviously not a sheaf of groups; and $H^1(M,\mathfrak{IC}_{(m)}^{\mu+1})$ is therefore not even defined. Nevertheless, it is easily verified that the coboundary map

$$H^0(M, \mathfrak{DIC}_{(m)}^{\mu+1}) \to H^1(M, \mathfrak{F}_{(m)})$$

is surjective. Similarly, this map is surjective in the case of a transitive, continuous pseudogroup of real analytic transformations where the germs $\mathfrak{F}_{(m)}$, $\mathfrak{IC}_{(m)}^{\mu+1}$ depend real analytically on the point t of real m-space. Hence, in either the real (analytic or non-analytic) case or the complex (analytic) case, $H^1(M, \mathfrak{F}_{(m)})$ is composed of germs of deformations which are trivial in the differentiable sense.

Next, let $\Sigma^\mu = \oplus_r \Sigma^{\mu,r}$ be the graded sheaf over M of germs of differential forms on M (of class C^∞) with values in R^μ. Then $\Sigma^{\mu,0}$ is the sheaf of infinitesimal transformations of $\mathfrak{IC}_{(1)}^{\mu}$, i.e., we have the surjective map $\mathfrak{IC}_{(1)}^{\mu} \to \Sigma^{\mu,0}$ of $\mathfrak{IC}_{(1)}^{\mu}$ onto $\Sigma^{\mu,0}$ sending the germ $h(t)$ of $\mathfrak{IC}_{(1)}^{\mu}$ into $\partial h(t)/\partial t|_{t=0}$. Let $\Sigma^{\mu+1,r} \to J^{\mu,r}$ be the map of $\Sigma^{\mu+1,r}$ onto the sheaf $J^{\mu,r}$ of "jet forms" of degree r, where the germ $\sigma^{\mu+1}$ of $\Sigma^{\mu+1,r}$ is mapped into the pair $u = (\sigma, \xi)$, $\sigma = \sigma^\mu$ is the projection of $\sigma^{\mu+1,r}$ in $\Sigma^{\mu,r}$, and $\xi = \delta\sigma^{\mu+1}$, where δ is an operator of *formal* exterior differentiation. Namely, let $\sigma^{\mu+1}$, expressed in terms of a local Γ-coordinate $(x^1, \ldots, x^j, \ldots, x^n)$ of M, have the components $\sigma^j_{j_1 \ldots j_\nu}$, $0 \leq \nu \leq \mu+1$; then $\delta\sigma^{\mu+1}$ has the components

$$(\delta\sigma^{\mu+1})^j_{j_1 \ldots j_\nu} = \sum_{k=1}^{n} dx^k \wedge \sigma^j_{kj_1 \ldots j_\nu}, \qquad 0 \leq \nu \leq \mu.$$

We have the map $D: J^{u,r} \to J^{u,r+1}$ which sends $u = (\sigma,\xi)$ into $Du = D(\sigma, \xi) = (d\sigma - \xi, -d\xi)$, where $d\sigma$ has the components

$$(d\sigma)^j_{j_1 \ldots j_\nu} = \sum_{k=1}^{n} dx^k \wedge \frac{\partial}{\partial x^k} \sigma^j_{j_1 \ldots j_\nu}, \qquad 0 \leq \nu \leq \mu,$$

and the components of $d\xi$ are defined in a similar manner. The sheaf $J^\mu = \oplus_r J^{\mu,r}$ has a structure of graded Lie algebra over the real numbers $\mathbf{R}$, defined by a map $J^{\mu,r} \otimes J^{\mu,s} \to J^{\mu,r+s}$ sending $u \otimes v$ into a bracket $[u, v]$ satisfying the following relation

$$D[u, v] = [Du, v] + (-1)^r [u, Dv]. \tag{2}$$

Finally, let Θ be the sheaf over M of germs of Γ-vector fields (or infinitesimal transformations of Γ), and let $i = i^\mu: \Theta \to J^{\mu,0}$ be the injection mapping the germ

θ of Θ into $i(\theta) = (\iota^\mu\theta, \delta\iota^{\mu+1}\theta)$, where $\iota^\mu{:}\Theta \to \Sigma^\mu$ is induced by ι^μ: $\mathfrak{F}_{(1)} \to \mathfrak{IC}^\mu_{(1)}$. If $\mu \geq \mu_0 - 1$, the image of Θ under i is the kernel of the map $D{:}J^{\mu,0} \to J^{\mu,1}$.

We remark that the cohomology $H^*(M, \Theta) = \oplus_r H^r(M, \Theta)$ has a structure of graded Lie algebra over $\mathbf{R}$ which is induced by the structure of Lie algebra of Θ defined by the Poisson bracket of vector fields.

2. *Complex Pseudogroup Structures.*—Let Γ be an arbitrary complex, transitive, continuous pseudogroup and M a compact Γ-manifold. We suppose that the germs of the sheaves $\mathfrak{F}_{(m)}$, $\mathfrak{IC}^\mu_{(m)}$, and $J^{\mu,1}_m$ depend holomorphically on the parameter t of complex m-space $\mathbf{C}^m$, where $J^{\mu,1}_{(m)}$ is the sheaf of germs of $J^{\mu,1}_{(m)}$ depending (holomorphically) on t and vanishing for $t = 0$. Our main result is the following

THEOREM. *There exists a positive integer $\mu_1 = \mu_1(\Gamma)$, where $\mu_1 \geq \mu_0$ (order of Γ), such that, for $\mu \geq \mu_1$:*

(*i*) *The sequence*

$$0 \to \Theta \xrightarrow{i} J^{\mu,0} \xrightarrow{D} J^{\mu,1} \xrightarrow{D} J^{\mu,2} \xrightarrow{D} \cdots \xrightarrow{D} J^{\mu,n} \to 0$$

is exact and hence, by (2), we have the isomorphism (actually "anti-isomorphism" in the sense of reference 3 of the graded Lie algebra $H^*(M, \Theta)$ with the graded Lie algebra of the D-cohomology of sections over M of the sheaf $J^\mu = \oplus_r J^{\mu,r}$.

(*ii*) *The set $H^0(M, \mathfrak{D}\mathfrak{IC}^{\mu+1}_m)$ is the subset of $H^0(M, J^{\mu,1}_m)$ composed of the elements $v(t)$ satisfying the non-linear differential equation (integrability condition)*

$$Dv(t) - \tfrac{1}{2}[v(t), v(t)] = 0. \tag{3}$$

(*iii*) *If $H^2(M, \Theta) = 0$, there exists an effective, complete, complex analytic family of deformations M_t, $t \in \mathbf{C}^m$, $|t| < \varepsilon$, of the Γ-structure of $M = M_0$, where $m = \dim_{\mathbf{C}} H^1(M, \Theta)$, i.e., the number of moduli of M is equal to the dimension of $H^1(M, \Theta)$.*

Let $v(t)$ be an element of $H^0(M, J^{\mu,1}_m)$ satisfying (3). In order to prove (*ii*), it is sufficient to show that each point of M has a neighborhood on which the equation

$$\mathfrak{D}h(t) = v(t) \tag{4}$$

has a solution $h(t)$ which is a section of $\mathfrak{IC}^{\mu+1}_m$ over the neighborhood. The author is indebted to Professor L. Nirenberg for suggesting that the equation (4) can be solved in two steps by writing $h(t)$ as the composition $h_1(t) \cdot h_2(t)$ of two local deformations of $P^{\mu+1}$, where $h_2(t)$ is a deformation of the structure of complex analytic fibre space and $h_1(t)$ is holomorphic, i.e., a deformation in which the complex analytic structure is held fixed.

[1] Haefliger, A., "Structures feuilletées et cohomologie à valeur dans un faisceau de groupoïdes," *Comm. Math. Helv.*, **32**, 248–329 (1958).

[2] Kodaira, K., "On deformations of some complex pseudo-group structures," *Ann. Math.*, **71**, 224–302 (1960).

[3] Kodaira, K., and D. C. Spencer, "Multifoliate structures," *Ann. Math.*, **74**, 52–100 (1961).

[4] Spencer, D. C., "Some remarks on homological analysis and structures," *Proceedings of Symposia in Pure Mathematics (Differential Geometry)*, **3**, 56–86 (1961).

GRAPHICAL ANALYSIS OF MULTI-RESPONSE EXPERIMENTAL DATA USING ORDERED DISTANCES

By M. B. Wilk and R. Gnanadesikan

BELL TELEPHONE LABORATORIES, INC.

Communicated by J. R. Pierce, June 8, 1961

Procedures for the graphical analysis of certain multi-response data by means of appropriate "probability plots" are outlined in this paper. These procedures constitute a generalization and extension of the technique of half-normal plotting which has been advocated by Daniel[1] for analyzing certain single-response data.

These methods may be employed in any multi-response situation in which each individual response could be meaningfully analyzed in terms of single degree of freedom contrasts. They will be described here in the specific framework of (complete) two-level factorials to simplify presentation and because, for this case, a meaningful decomposition into single degree of freedom contrasts is conventional.

Consider, therefore, a situation involving n experimental factors each to be studied at both of two levels. There will then be $N = 2^n$ possible combinations of the levels of all the factors. Suppose that each treatment combination is applied to a separate experimental unit and the response observed.

If the response is a scalar quantity, then the usual analysis of variance proceeds by calculating an orthogonal transformation of the N observations, one for each of the treatment combinations, to obtain the conventional effects (main effects, two-factor interactions, etc.). Thus, in the single response case, if $\boldsymbol{y} = \begin{pmatrix} y_1 \\ \vdots \\ y_N \end{pmatrix}$ represents the N observations from all N treatment combinations and if $\boldsymbol{R}$ is an appropriately constructed $N \times N$ orthogonal matrix, then the usual main effects, interactions and over-all mean are defined by $\begin{pmatrix} m \\ \boldsymbol{x} \end{pmatrix} = \boldsymbol{Ry}$. Here m is a normalized form of the over-all mean of the N observations and the $(N - 1)$ components of $\boldsymbol{x}$ are referred to as the single degree of freedom contrasts for the various treatment effects (see, e.g., Kempthorne[2]). A graphical study of these single degree of freedom contrasts by plotting their ordered absolute values on half-normal probability paper (see Daniel[1]) is often a useful adjunct in analysis of the data.

In many circumstances, several, often qualitatively different, responses are observed on every experimental unit for each treatment combination. Suppose that p responses are observed on each unit, and let $\boldsymbol{y}'_i = (y_{i1}, y_{i2}, \ldots, y_{ip})$ denote this vector of responses for the ith treatment combination ($i = 1, 2, \ldots, N$). Let $\boldsymbol{Y} = \begin{pmatrix} \boldsymbol{y}'_1 \\ \vdots \\ \boldsymbol{y}'_N \end{pmatrix}$ denote the $N \times P$ matrix of observations.

If $\begin{pmatrix} \boldsymbol{m}' \\ \boldsymbol{X} \end{pmatrix} = \boldsymbol{RY}$, where $\boldsymbol{X} = (x_{ij})$ is $(N - 1) \times p$ and $\boldsymbol{m}'$ is $1 \times p$, and $\boldsymbol{R}$ is the same as for the single-response case, then the components of $\boldsymbol{m}'$ are the p

normalized forms of the over-all means for the different responses and the jth column of $\boldsymbol{X}$ consists of the usual single degree of freedom contrasts for the jth response, $j = 1, 2, \ldots, p$. The ith row of $\boldsymbol{X}$, denoted by $\boldsymbol{x}'_i = (x_{i1}, x_{i2}, \ldots, x_{ip})$, has as elements the contrasts for each of the p responses corresponding to the ith treatment effect. Thus, if $i = 1$ corresponded to factor A main effects, then the usual univariate single degree of freedom contrasts for factor A main effect would be x_{11} for response $j = 1$, x_{12} for response $j = 2$, and so on. The rows of $\boldsymbol{X}$, i.e., the $\boldsymbol{x}'_i$, may therefore be called *single degree of freedom contrast vectors.*

It will often be experimentally reasonable to treat the vectors $\boldsymbol{y}_1, \ldots, \boldsymbol{y}_N$ as though they were observations on mutually (statistically) uncorrelated random vectors with the assumption (not critical) that the covariance matrix of all the $\boldsymbol{y}_i$ is the same, say Σ. It would then follow, from these assumptions and the orthogonality of $\boldsymbol{R}$, that the $(N - 1)$ contrast vectors $\boldsymbol{x}'_1, \ldots, \boldsymbol{x}'_{N-1}$ and $\boldsymbol{m}'$ are mutually uncorrelated, each with covariance matrix Σ. Furthermore, even if the original vector observations are not closely p-variate normal, it is likely, through the operation of the Central Limit Theorem, that the contrast vectors would be more closely p-variate normal.

Thus, where no systematic effect exists the corresponding contrast vectors $\boldsymbol{x}_i$ may be reasonably assumed to behave like a random sample from a p-variate normal distribution with mean vector $\boldsymbol{O}$ (null vector) and covariance matrix Σ. When an experimental effect does exist, the corresponding mean vector will be nonnull.

The $(N - 1)$ contrast vectors may be visualized as $(N - 1)$ points in p-dimensions. By the definition of a metric in this space, a length, a distance from the origin, may be associated with each of these contrast vectors. For the case of 2^n factorial experiments these distances may be more usefully interpreted as follows: The vector observations for each of the N experimental units can be represented in the p-dimensional space of responses. Then, each contrast vector is proportional to the vector joining the centroid of half the observations to the centroid of the other half, where the partitions of the observations correspond to the basic definition of the treatment effects summarized in the matrix $\boldsymbol{R}$. The distance between these centroids is thus proportional to the length of the corresponding contrast vector.

The metrics to be considered are nonnegative definite quadratic forms in the elements of the contrast vectors. For a chosen compounding matrix $\boldsymbol{A}$, the distance associated with the contrast vector $\boldsymbol{x}_i$ is $d_i = \boldsymbol{x}'_i\boldsymbol{A}\boldsymbol{x}_i$, $i = 1, 2, \ldots, (N - 1)$.

Some examples of compounding matrices are:

(1) The identity matrix. Then d_i would be the sum of squares of the elements of $\boldsymbol{x}_i$ and this would correspond to the simple Euclidean distance between the centroids (described above) which give rise to $\boldsymbol{x}_i$.

(2) A diagonal matrix of reciprocals of variances (specified or estimated) of the p responses.

(3) The inverse of the covariance matrix (specified or estimated) of the original responses.

Cases (2) and (3) may be particularly appropriate when the responses are measured in widely differing units. However the compoudding matrix is decided upon, it is correct and appropriate, in the general philosophy of the approach taken

in this paper, that subsequent inferences be made conditional on this choice.

Under the null assumption of no systematic effects, the distances d_i (≥ 0), $i = 1, 2, \ldots, (N-1)$, would be distributed as a linear combination of independent central one-degree-of-freedom chi-squared variables. The coefficients in this linear combination are the characteristic roots of $\boldsymbol{A}\Sigma$. (NOTE: The compounding matrix $\boldsymbol{A}$ is left to the judgment of the experimenter, subject only to the restriction that it be nonnegative definite.) Thus, under such a null hypothesis of no effects, the $(N-1)$ distances $d_1, d_2, \ldots, d_{N-1}$ may, as a reasonable approximation, be expected to behave like a random sample from a gamma distribution, with density

$$f(t;\ \lambda, \eta) = \frac{\lambda^{\eta} e^{-\lambda t}}{\Gamma(\eta)}\, t^{\eta-1}, \qquad t > 0,$$

$$= 0 \text{ elsewhere,}$$

where $\lambda > 0$ is a scale parameter, $\eta > 0$ is a shape parameter, and neither λ nor η is known. (The authors feel that 2η may, in some circumstances, be interpreted as the number of essentially independent responses contributing to each d_i.)

If η were known, then a plot of the ordered distances against corresponding quantiles of the gamma distribution (with $\lambda = 1$ and the known value of η) would yield an approximately straight-line configuration when there were no real systematic effects.

Since η is unknown (because Σ is unknown) its value must be estimated. To minimize the influence of possible real effects on this estimation, the estimation of η is based on order statistics. A number L ($\leq (N-1)$) of contrast vectors, which one is interested in studying comparatively, is chosen and the associated distances calculated. A number K ($\leq L$) of contrast vectors which may well not reflect systematic effects, is selected. The M ($\leq K$) smallest distances associated with these contrast vectors, which are thereby even less likely to reflect systematic effects, are considered as the M smallest of a random sample of size K from a gamma distribution. In this situation, the maximum likelihood estimates of η and λ are functions only of the Mth largest distance and the arithmetic and geometric means of the M distances. Tables to facilitate this estimation have been prepared and will be published elsewhere.[3]

Next, using the estimate $\hat{\eta}$ of η, a plot is made of the L ordered distances against the quantiles of the standard gamma distribution ($\lambda = 1$) with $\eta = \hat{\eta}$. Under the null hypothesis of no effects, one would expect to obtain a straight-line pattern with intercept 0 and slope $1/\lambda$. The distances corresponding to real or systematic effects will tend to appear as "too large" deviations from the straight-line pattern. A procedure for obtaining the appropriate quantiles and carrying out the actual plot is in use and will be published elsewhere.[4]

Other departures from the straight-line pattern are identifiable as to cause or source, such as, for example, operation of more than one error covariance matrix.

It will usually be desirable and appropriate to reanalyze the data with different choices of either or both of K and M, as well as according to several choices of the compounding matrix.

The authors wish to thank J. W. Tukey for helpful advice in the exposition of this paper.

[1] Daniel, Cuthbert, "Use of half-normal plots in interpreting factorial two-level experiments," *Technometrics*, 1, 311–341 (1959).

[2] Kempthorne, O., *The Design and Analysis of Experiments* (New York: John Wiley and Sons, 1952).

[3] Wilk, M. B., R. Gnanadesikan, and M. J. Huyett, "Estimation of parameters of the gamma distribution using order statistics," unpublished manuscript.

[4] Wilk, M. B., R. Gnanadesikan, and M. J. Huyett, "Probability plots for the gamma distribution," unpublished manuscript.

*EFFECT OF MITOMYCIN C ON THE GROWTH OF SOME ANIMAL VIRUSES**

BY E. REICH AND R. M. FRANKLIN

THE ROCKEFELLER INSTITUTE, NEW YORK

Communicated by E. L. Tatum, June 28, 1961

Mitomycin C is a specific inhibitor of DNA biosynthesis in bacterial and mammalian cells.[1, 2] The suppression of DNA synthesis by Mitomycin results from destruction of the DNA-template in both mammalian and bacterial systems.[2–4] Thus the effect of Mitomycin on DNA is analogous to those of x-rays and the decay of incorporated P^{32}. Only at very high antibiotic concentrations is the synthesis of RNA and protein affected. The enzymatic synthesis of DNA *per se* is not inhibited by Mitomycin. This follows from the fact that bacteria remain capable of supporting the growth of temperate and virulent bacteriophages in the presence of Mitomycin.[5, 6]

The possibility of selectively destroying biologically active host-DNA provides a unique opportunity for investigating certain genetic and physiological properties of virus-infected cells. Much is known of the interactions between bacteriophages and their hosts,[7] but comparable relationships have not been so clearly described for animal viruses. We have therefore examined the growth of an RNA virus, Mengo encephalomyelitis virus, and a DNA virus, vaccinia, in mammalian cells either in the presence of, or after pre-treatment with, suitable concentrations of Mitomycin C.

Materials and Methods.—Cells: All experiments were conducted with monolayers of L-cells (strain 929), in plastic Petri dishes (60 × 15 mm) containing 5×10^5 cells. The experiments were begun 16 to 20 hours after plating trypsinized suspensions of cells. Cells were maintained and propagated by methods previously described.[4] Monolayers which had been exposed to Mitomycin prior to infection were usually incubated for 16 hours after removal of the compound and before the addition of virus. Companion cultures, which had not been exposed to Mitomycin, served as controls for all experimental manipulations. Other cultures, with cells seeded on cover slips in Petri plates, were used for autoradiography to determine the uptake of appropriate radioactive precursors for nucleic acids in each situation under observation. Thus autoradiographs were obtained on Mitomycin-treated and -untreated cells, both infected with virus and uninfected.

Radioautography: Following incubation in the presence of radioactive thymidine (0.5 μc/ml, usually for 10 hours) or cytidine (0.5 μc/ml, 3 to 6 hours), the cover

slips were removed from the incubation medium and prepared for autoradiography by the method of Doniach and Pelc.[8] Acid-soluble nucleotides were extracted with 2 per cent perchloric acid at 4°C for 60 minutes. Cytidine-labeled DNA was removed, when necessary, with DNase. The film was developed after 3 to 4 days' exposure at 4°C. All radioactive materials were obtained from New England Nuclear Corp., Boston, Mass.

Viruses: The origin and properties of the Mengovirus used have been described.[9] Vaccinia virus (obtained through the courtesy of Dr. S. Dales) was derived from a strain adapted to grow in L-cells.[10] All viruses were assayed by the plaque technique.[9] Infection of L-cells was performed at a multiplicity so that all cells were infected.[11]

Results.—(a) *Mengovirus:* The results of two representative experiments are shown in Table 1. The growth of Mengovirus was not greatly inhibited by any of

TABLE 1

EFFECT OF MITOMYCIN C ON MENGOVIRUS MULTIPLICATION*

Experiments	Dose of Mitomycin C, γ/ml	PFU/cell
No. 1	0	570
	5	470
	15	500
	30	420
No. 2	0	2950
	5	2030
	15	540
	30	530

* Cells were exposed to Mitomycin for 8 hr, and then incubated for 16 hr in Mitomycin-free medium prior to infection with Mengovirus. Infected cultures were incubated in Mitomycin-free medium for 12 hr.

the concentrations of Mitomycin tested. Although very high concentrations (30 to 50 γ/ml) may depress virus yields as much as 80 per cent, this finding has been variable, and virus yields equivalent to those seen in control cultures have been observed at such concentrations of Mitomycin (Table 3).

TABLE 2

EFFECT OF VARIATIONS IN THE EXPOSURE OF L-CELLS TO MITOMYCIN C ON THE GROWTH OF MENGOVIRUS

A. Actively dividing cells were exposed to Mitomycin for 8 hr, and then incubated for 16 hr in Mitomycin-free medium. At this time the cells were infected with Mengovirus and virus allowed to multiply in the absence of Mitomycin. Control cells were infected at the beginning of the period of Mitomycin treatment. During the eclipse phase there was an average of 0.5 PFU/cell.

Concentration of Mitomycin, γ/ml	PFU/cell, 12-hr yield
0	850
5	690
15	360
30	300

B. Mitomycin was added to the input virus and therefore cells were exposed to the drug during adsorption. Mitomycin was also present in the growth medium, i.e., throughout the period of virus growth. The host cells were not exposed to Mitomycin prior to the addition of virus. The control was the same as in part A.

Concentration of Mitomycin, γ/ml	PFU/cell, 12-hr yield
5	1400
15	1100
30	1000

The data shown in Table 1 were obtained under conditions in which the host cells had been exposed to Mitomycin prior to the addition of virus. The presence of Mitomycin throughout the experiment did not affect the results, however, as is seen from the data in Table 2.

TABLE 3

EFFECTS OF HIGH DOSES OF MITOMYCIN C ON THE GROWTH OF MENGOVIRUS IN L-CELLS

Concentration of Mitomycin	Treatment	PFU/cell
0	0 time	5.8
0	24-hr yield	750
30 γ/ml	Present throughout	580
50 γ/ml	Present throughout	920
50 γ/ml	8-hr pulse, infection immediately after pulse	1,310
50 γ/ml	8-hr pulse, infection 16 hr after pulse	230

Virus yields from Mengovirus-infected L-cells vary over a wide range.[11] This may reflect physiological conditions which vary in the cellular population in different experiments. Exponentially growing host cells produce virus yields considerably greater than do stationary cultures. The lower yields of virus sometimes observed in cells which had been pretreated with very high concentrations of Mitomycin may, therefore, be attributable to the 16-hour period of incubation following Mitomycin treatment. During this period, cells whose DNA content had been badly damaged may fail to renew their enzyme systems, thereby decreasing the concentration of intracellular metabolites necessary for virus multiplication so that the reduced capacity for virus production in such cells may be basically metabolic rather than genetic. For this reason experiments were performed in which cells exposed to Mitomycin for 2 hours were infected with Mengovirus in the presence of the antibiotic, and exposure to the drug was continued throughout the viral growth period. The virus yield of such cells was compared with that obtained from others treated with Mitomycin for the usual 8-hour period and infected immediately, or 16 hours after, the termination of Mitomycin exposure. The antibiotic concentrations used were those known to inhibit DNA synthesis (30 γ/ml) as well as RNA synthesis (50 γ/ml). The results are shown in Table 3.

Pulses of Mitomycin C at concentrations above 15 γ/ml for periods of at least 8 hours appear to suppress subsequent DNA synthesis completely, within the limits of resolution of the autoradiographic technique. Following incubation in thymidine-H^3, cells treated in this way showed no radioactivity above background. In our hands this technique would detect a degree of DNA synthesis equal to 0.1–0.2 per cent of normal during the 10-hour period under examination. Thus these cells apparently possessed no DNA capable of replication and therefore, it follows that the production of viral RNA and virus-specific protein does not require the presence of biologically intact, replicating cellular DNA.

The inhibition of cellular DNA synthesis by Mitomycin is not measurably reversed by Mengovirus infection. Indeed, at 15 γ Mitomycin/ml for 8 hours the slight residual incorporation of thymidine into DNA sometimes found in uninfected cells is significantly inhibited in the infected cell. *Thus, in the case of Mengovirus, viral RNA synthesis does not require an associated or preliminary synthesis of DNA, nor does it require the integrity of any particular host genome.*

(b) *Vaccinia:* The experiments of Cairns on the initiation of vaccinia infection suggested that the host-virus relationships in this case might be comparable in some respects to those found for T-2 bacteriophage infection in *Escherichia coli.*[12] For this reason, the data shown in Table 4 are of particular interest. A profound inhibition of vaccinia growth is caused by Mitomycin, either through pre-treatment of the host cell or by its presence throughout the course of infection. *In vitro*

TABLE 4

EFFECT OF MITOMYCIN C ON THE GROWTH OF VACCINIA VIRUS

Concentration of Mitomycin, γ/ml		Yield in PFU/cell, cells pretreated with Mitomycin Experiment 1	Experiment 2	Yield in PFU/cell, cells in Mitomycin throughout Experiment 1	Experiment 2
0	0 time	0.23	0.64	0.23	0.64
0	24-hr yield	18	60	18	60
1	24-hr yield	...	124	...	32
5	24-hr yield	1.2	3.8	1.8	0.72
15	24-hr yield	1.8	1.3	...	...
30	24-hr yield	0.03	1.3	0.01	0.1

The procedure used in these experiments was exactly as in experiments with Mengovirus described in Table 3.

TABLE 5

EFFECT OF MITOMYCIN C ON VACCINIA VIRUS INFECTIVITY

	PFU/ml after 4-hr incubation	PFU/ml after 24-hr incubation
Control	1.14×10^6	5.99×10^5
Mitomycin	1.48×10^6	4.32×10^5

Vaccinia, in Eagle's minimal essential medium with 2 per cent fetal calf serum, was incubated with Mitomycin C at 25°C in the dark. The final concentration of Mitomycin was 10 γ/ml.

incubation of the virus with Mitomycin did not affect its infectivity (Table 5).

The synthesis of DNA peculiar to vaccinia-infected cells can be demonstrated using tritiated thymidine.[12] The label is taken up into acid-insoluble material in the cytoplasm, rather than in the nucleus. Cells were exposed to doses of 5 or 15 γ Mitomycin/ml for 8 hours and then immediately infected with vaccinia. Under these conditions there was no virus synthesis. Cells were exposed to tritiated thymidine from 6 to 8 hours after the start of infection. Uptake of H^3-thymidine into nuclear DNA is reduced to 1–10 per cent of the normal level in both infected and noninfected cells. At 5 γ Mitomycin/ml there is uptake of label into cytoplasmic DNA in only a few cells and at 15 γ/ml there is no uptake into cytoplasmic DNA. Thus Mitomycin prevents synthesis of virus and viral DNA in this case.

The observations discussed above together with those found in cells treated with Actinomycin,[13] suggest that vaccinia growth is indeed related to, and dependent on, nuclear events in the host cell. *A substantially intact host genome and a normally functioning cellular pathway of genetic expression appear to be required for normal vaccinia growth, at least in L-cells.*

Discussion.—The *in vivo* growth of DNA and RNA viruses in neurons of the adult mammalian central nervous system has made it clear that the production of viral DNA and RNA does not require active cellular DNA synthesis. Simon showed that the multiplication of RNA viruses does not depend on a concomitant synthesis of cellular DNA.[14] In these studies inhibitors which prevented DNA synthesis in cultured host cells were used.

The findings reported here and those of Simon suggest that the presence of *biologically intact DNA* is not required for normal RNA virus growth and nucleic acid synthesis. This is noteworthy since the highest level of Mitomycin employed (50 γ/ml for 8 hours) suppresses cellular RNA synthesis as well as DNA synthesis. This finding is not surprising since it may be presumed that most, if not all, cellular RNA synthesis is under genetic control and not independent of DNA. That viral RNA can be replicated in cells which, due to destruction of their genome, no longer are capable of synthesizing their own specific RNA appears to place viral RNA

synthesis in a category different from that of cellular RNA synthesis. Normal DNA-dependent cellular RNA synthesis may represent an enzymatic process which does not necessarily contribute to the production of viral RNA in the infected cell.

Ben-Porat *et al.* reported the production of noninfectious pseudorabies particles in Mitomycin-treated rabbit kidney cells.[15] It is not possible to correlate their results completely with the observations reported here, since the experimental conditions used by Ben-Porat *et al.* probably did not totally destroy the host genome, and their study of virus infection did not include pretreatment of cells with Mitomycin followed by infection in Mitomycin-free medium. Some dependence of synthesis of viral subunits on intactness of host genome can, therefore, not be excluded in this case. Their results suggest that viral DNA synthesis and the expression of at least some viral genetic potentialities could occur in the presence of high, if not totally destructive, concentrations of Mitomycin. This finding resembles that reported for bacteriophages[5, 6] whose growth is not inhibited by Mitomycin. Since the rate of depolymerization of DNA by Mitomycin is slow in relation to the rate of DNA synthesis in phage-infected cells,[4] viral growth and expression of viral genetic traits may occur in the presence of Mitomycin. Thus we conclude that the time required for assembly of mature virus from its newly synthesized constituents permits the destructive action of Mitomycin to be exerted on the genetic material of the particles finally produced. This results in a large proportion of the new particles being noninfectious, presumably due to some interruption in the continuity of their DNA. The parallelism of these phenomena is striking in two DNA viruses, one a bacterial[4] and the other an animal[13] virus.

The results reported in this paper, that in Mengovirus infection viral RNA and protein synthesis are unaffected by Mitomycin, taken with those of Ben-Porat *et al.* on pseudorabies virus[15] and Sekiguchi *et al.* on T-phages,[6] emphasize the highly specific cytocidal action of the antibiotic, based on the destruction of DNA. RNA biosynthesis is affected only to the extent that destruction of the cellular genome removes the governing templates. Introduction of viral DNA into a cell whose genetic apparatus has been badly injured by Mitomycin permits the formation of whatever new RNA may be required for virus-specific protein synthesis. Where genetic specificity resides in RNA, no DNA appears to be required for RNA production.

Cairns has reported[12] that viral DNA synthesis in cells infected with vaccinia could proceed in the cytoplasm and concluded that the virus was virulent and independent of its host. Our data may implicate nuclear participation at some stage in vaccinia growth, presumably that involving synthesis of viral DNA. Mitomycin-treated cells infected with vaccinia showed no uptake of tritiated thymidine. Therefore, the effect of Mitomycin on the growth of this pox virus presumably affects an early stage in its development, and correlates with the absence of the characteristic cytopathic effect which this virus strain normally produces in L-cells.

The authors wish to thank Miss Joan Callender for her excellent technical assistance.

* This work was supported in part by a grant from The National Foundation and by grant C-3610 from the National Cancer Institute, U.S. Public Health Service.

[1] Shiba, S., A. Terawaki, T. Taguchi, and J. Kawamata, *Biken's J.*, **1**, 179 (1958).

[2] Reich, E., A. J. Shatkin, R. M. Franklin, and E. L. Tatum, *Federation Proc.*, **20**, 154 (1961).

[3] Reich, E., A. J. Shatkin, and E. L. Tatum, *Biochim. et Biophys. Acta*, **45**, 608 (1960).
[4] Shatkin, A. J., E. Reich, R. M. Franklin, and E. L. Tatum, *Biochim. et Biophys. Acta* (1961).
[5] Otsuji, N., M. Sekiguchi, T. Iijima, and Y. Takagi, *Nature*, **184**, 1079 (1959).
[6] Sekiguchi, M., and Y. Takagi, *Biochim. et Biophys. Acta*, **41**, 434 (1960).
[7] Stent, G. S., *Advances in Virus Research*, **5**, 95 (1958).
[8] Doniach, I., and S. R. Pelc, *Brit. J. Radiol.*, **23**, 184 (1950).
[9] Franklin, R. M., *Proc. Soc. Exptl. Biol. Med.* (1961).
[10] Hanafusa, T., H. Hanafusa, and J. Kamabora, *Biken's J.*, **2**, 77 (1959).
[11] Franklin, R. M., *J. Biophys. Biochem. Cytol.* (1961).
[12] Cairns, J., *Virology*, **11**, 603 (1960).
[13] Reich, E., R. M. Franklin, A. J. Shatkin, and E. L. Tatum, *Science* (1961).
[14] Simon, E., *Virology*, **13**, 195 (1961).
[15] Ben-Porat, T., M. Reissig, and A. S. Kaplan, *Nature*, **190**, 33 (1961).

MANY-ELECTRON THEORY OF ATOMS AND MOLECULES

BY OKTAY SINANOĞLU

STERLING CHEMISTRY LABORATORY, YALE UNIVERSITY

Communicated by R. M. Fuoss and read before the Academy, April 24, 1961

Orbital theories of atoms and molecules work quite well in a qualitative or semi-empirical way but fail when put to a quantitative test. The error, which is so large that often even molecule formation is not predicted, is generally attributed to electron correlation. Its importance has been stressed in several reviews.[1, 2]

Since electrons affect one another through their instantaneous potentials and not just by their average potentials as in the Hartree-Fock method,[1] we do have a many-electron problem. But what sort of a many-body problem? Does the long range of coulomb repulsions cause all electrons to be involved in one complicated motion? If this were the case to the extent of overcoming the effects of the exclusion principle, shell structure would be wiped out, and an atom or molecule would be more like a drop of electron liquid. Actual shell structure and electron densities are close to those given by the Hartree-Fock method. For example, densities from the latter agree quite well with X-ray results.[3]

The situation of the many-electron problem in atoms and molecules is compared with related many-body problems in Figure 1. Inside nuclei, strong, short-range forces cause only local nucleon pair correlations to dominate. Brueckner theory[4] considers these for the idealized infinite nuclear "matter." Due to the strength of repulsions, each particle moves in an environment it is constantly polarizing. In finite systems,[5] difficulties arise. This "polarized sea" potential is strongly dependent on particle state, so that orthogonal ground-state orbitals cannot be obtained easily. The basis is discrete, and the difficulties of evaluating slowly convergent infinite sums as in ordinary perturbation theory[1] appear.

In the infinite electron gas, Hartree-Fock orbitals being plane waves, there is no electron localization. As we shall see below, correlation is determined by the difference of the instantaneous coulomb potential $g_{ij} = r_{ij}^{-1}$ between two electrons i, j and the average, i.e., Hartree-Fock (H.F.), potential they would exert on one

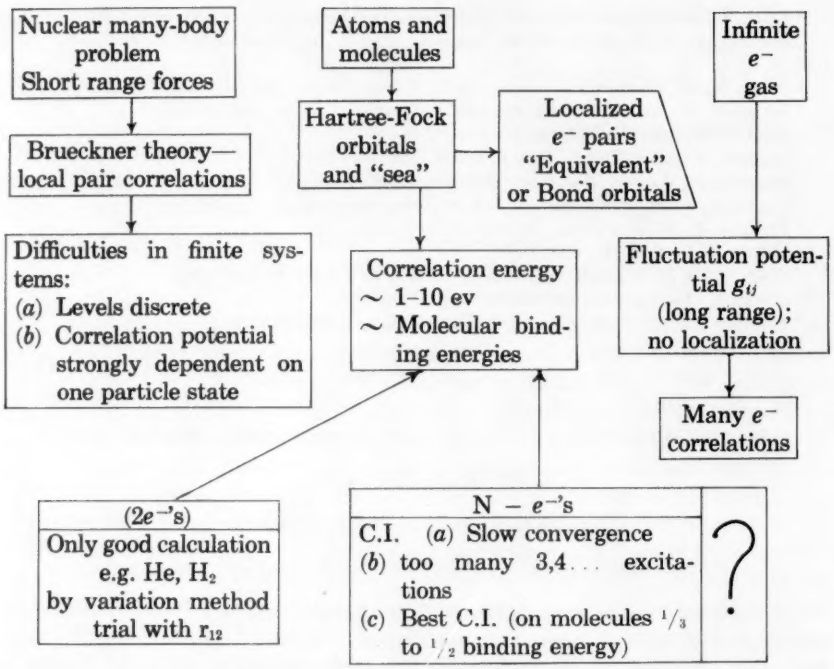
Nuclear many-body problem
Short range forces
Brueckner theory—local pair correlations
Difficulties in finite systems:
(a) Levels discrete
(b) Correlation potential strongly dependent on one particle state
Atoms and molecules
Hartree-Fock orbitals and "sea"
Localized e^- pairs "Equivalent" or Bond orbitals
Infinite e^- gas
Correlation energy
~ 1–10 ev
~ Molecular binding energies
Fluctuation potential g_{ij} (long range); no localization
Many e^- correlations
$(2e^-$'s)
Only good calculation e.g. He, H_2 by variation method trial with r_{12}
N − e^-'s
C.I. (a) Slow convergence
(b) too many 3,4... excitations
(c) Best C.I. (on molecules 1/3 to 1/2 binding energy)
?

FIG. 1.—The situation of the many-electron problem in atoms and molecules and related many-body problems.

another. But due to complete delocalization, this H.F. part, $\bar{S}_i(j) + \bar{S}_j(i)$ is uniform and nearly zero for a very large box, and the fluctuation potential is the full g_{ij} with its long range. Thus *many* electrons correlate at the same time.

Fortunately, in atoms and molecules (except dyes, etc., where metallic behavior is approached), the problem is very different from that of the electron gas. The symmetry, the nuclear wells, and the exclusion principle localize electrons with paired spins in the Hartree-Fock wave function. As shown by Linnett and Pöe,[6] the configuration of maximum probability given by a determinental function, e.g., for Ne, is four electron pairs tetrahedrally arranged. Such spatial arrangements, bonds, etc., are better represented by transforming the H.F. orbitals to "equivalent orbitals" which leave the determinant unchanged.[7]

The only accurate calculations on atoms and molecules so far[8] are still those on two-electron systems based on the classical works[1] of Hylleraas on He, and James and Coolidge on H_2 using trial functions containing r_{12}. This method not having been extended to the case of N electrons, for such systems configuration-interaction (C.I.) is used. The latter is often slowly convergent (except when used for degeneracy or "resonance"), the number of multiple excitations increases very rapidly with N, and best C.I. on small molecules so far has given only about 1/3 to 1/2 of the binding energies.

We have developed an extensive theory for the N-electron atom or molecule (a) to get a quantitative scheme of the order of the difficulty of the He, H_2 case, (b)

to understand the physical behavior of many-electron motion and to relate the "chemical" picture to correlation. In our initial work, rigorous solutions were obtained in perturbation theory.[9] We have now gone far beyond those results and completed the picture in several directions. In this communication, we summarize our latest findings with emphasis on the physical basis and the over-all structure that emerges. The full mathematical theory will be published in the *Journal of Chemical Physics*.

Physical Aspects of Correlation in Atoms and Molecules.—The principal features of the many-electron problem in atoms and molecules are shown in Figure 2. The

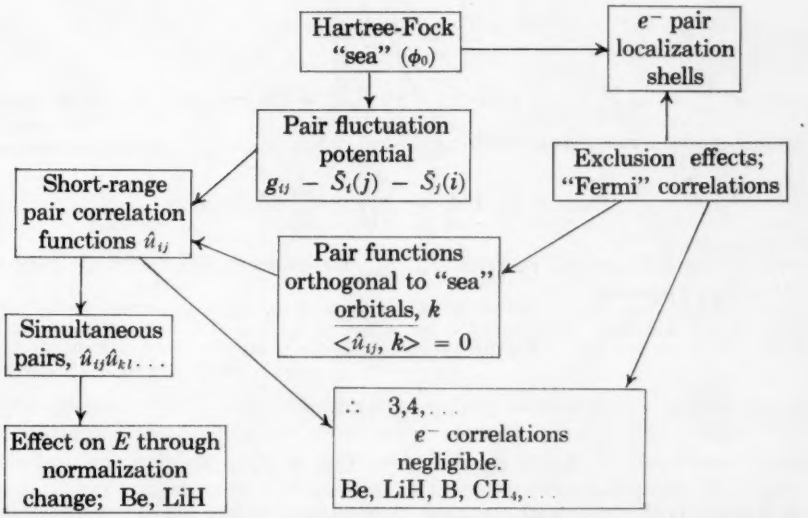
Hartree-Fock "sea" (ϕ_0)
e^- pair localization shells
Pair fluctuation potential $g_{ij} - \bar{S}_i(j) - \bar{S}_j(i)$
Exclusion effects; "Fermi" correlations
Short-range pair correlation functions $\hat{u}_{ij}$
Pair functions orthogonal to "sea" orbitals, k $\langle \hat{u}_{ij}, k \rangle = 0$
Simultaneous pairs, $\hat{u}_{ij}\hat{u}_{kl}\ldots$
$\therefore$ 3,4,... e^- correlations negligible. Be, LiH, B, CH_4,...
Effect on E through normalization change; Be, LiH

FIG. 2.—Main physical aspects of electron correlation in atoms and in molecules with no strong delocalization.

long-range effects of coulomb repulsions are well taken care of by the Hartree-Fock potential and orbitals. We start with the Hartree-Fock solution, ϕ_0. The reason for the choice of this "sea" in which electrons move will become more and more apparent as we go along. The effects of using a polarized "sea" as in the Brueckner method would come up only to quite high orders and would be negligible aside from the cumbersome self-consistency procedures[4, 5] that it would require.

If we write

$$\psi = \phi_0 + \chi \tag{1}$$

for the exact wave function with ϕ_0 the single H.F. determinant and χ the correction for correlation, the energy is separated into an H.F. and a correlation part.

$$E = \frac{\langle \chi, H\psi \rangle}{\langle \chi, \chi \rangle} = E_{\text{H.F.}} + \frac{2\langle \phi_0, (H - E_{\text{H.F.}})\chi \rangle + \langle \chi, (H - E_{\text{H.F.}})\chi \rangle}{1 + 2\langle \phi_0, \chi \rangle + \langle \chi, \chi \rangle} \tag{2}$$

$$E_{\text{H.F.}} = \langle \phi_0, H\phi_0 \rangle,$$

and $$H = \sum_{i=1}^{N} h_i^0 + \sum_{i>j} g_{ij} = H_0 + H_1, \tag{3}$$

with h_i^0 the bare nuclei hamiltonian of electron i and $g_{ij} \equiv 1/r_{ij}$. We separate H into a

$$H_0 = \sum_{i=j}^{N} (h_i^0 + V_i) \tag{4}$$

part for independent electrons in the H.F. potential V_i and a residual "fluctuation" potential part

$$H_1 = \sum_{i>j}^{N} [g_{ij} - \bar{S}_i(j) - \bar{S}_j(i)], \tag{5}$$

writing[9] $\sum_{i=1}^{N} V_i$ as $\sum_{i>j}^{N} [\bar{S}_i(j) + \bar{S}_j(i)]$. An $\bar{S}_i(j)$ is the coulomb plus exchange potential of orbital i acting on electron j. Then

$$E_{\text{H.F.}} = E_0 + E_1 = \sum_{i=1}^{N} \epsilon_i - \sum_{i>j}^{N} (J_{ij} - K_{ij}) \tag{6}$$

with ϵ_i the H.F. orbital energies, J_{ij}, K_{ij} the coulomb and exchange integrals. $(H - E_{\text{H.F.}})$ becomes

$$(H - E_{\text{H.F.}}) = \sum_{i=1}^{N} e_i + \sum_{i>j} m_{ij}, \tag{7a}$$

where $$e_i \equiv h_i^0 + V_i - \epsilon_i$$

and $$m_{ij} = g_{ij} - \bar{S}_i(j) - \bar{S}_j(i) + J_{ij} - K_{ij}. \tag{7b}$$

A Hartree-Fock spinorbital occupied by electron i before antisymmetrization is denoted by i also so that

$$e_i i = 0 \quad \text{from} \quad H_0\phi_0 = E_0\phi_0.$$

Equation (2) becomes

$$E - E_{\text{H.F.}} = \frac{2\langle \phi_0, \sum_{i>j} m_{ij}\chi \rangle + \langle \chi, (\sum_{j>j} e_i + \sum_i m_{ij})\chi \rangle}{1 + 2\langle \phi_0, \chi \rangle + \langle \chi, \chi \rangle} \tag{8}$$

Fluctuation Potential.—Correlation behavior is determined (a) by the pairwise fluctuation potentials m_{ij}, and (b) by the electron distribution in the "sea," ϕ_0, which depends strongly on its antisymmetric character.[6, 7]

An m_{ij} is usually of short range in directions going from orbital to orbital. Take a (1*s*) electron and another in the *Be* atom for example. An electron placed at r_2 sees the average coulomb potential $S_1(r_2)$ of the (1*s*) electron with opposite spin as shown in Figure 3 (taking a Slater (1*s*) orbital with exponent 3.70 as sufficiently close to *H.F.*). The (1*s*) electron is most likely to be found at $r_1 = 0.27$ a.u. (Bohr orbit in Be^{+2}). If it were there instantaneously, electron two would see the $g_{12} = r_{12}^{-1}$, also shown in Figure 3.

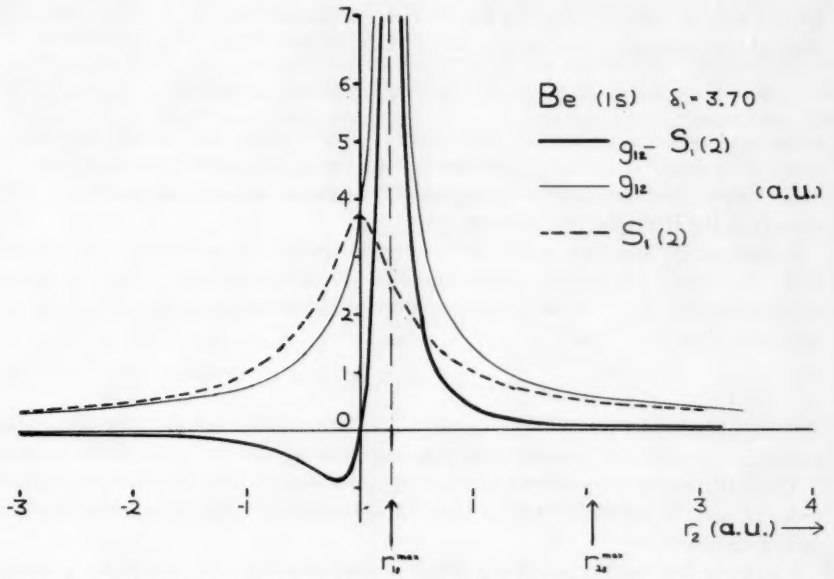

FIG. 3.—Fluctuation potential (g_{12}–$S_1(2)$) as seen by an electron at r_2 due a (1s) electron with opposite spin instantaneously at its Bohr radius and in line with r_2. Note that this potential which determines the correlation, is of short range through $g_{12} = r_{12}^{-1}$ and the Hartree-Fock potential, $S_1(2)$, are long range.

The difference, $g_{12} - S_1(2)$, differing from m_{12} by the constant value 0.39 a.u., is the fluctuation potential, which shows where electron two (r_2) would want to be if electron one were at $r_{1s}^{\max}$. = 0.27 a.u. Both g_{12} and $S_1(2)$ are of long range, but $m_1(2)$ has a short range. It has died off before reaching a distance of 2.1 a.u., about the Bohr radius of (2s) in *Be*. The singularity of g_{12} at $r_{12} = 0$ is the main feature left in m_{12}. Note also the minimum in $m_1(2)$ on the other side of the nucleus. Similar curves and surfaces can be drawn by varying r_1 and θ_{12} (angle between r_1 and r_2) also. These would aid the selection of trial functions to give maximum charge density at the dips and zero at singularity.

The exclusion principle, by putting the third and fourth electrons in a different shell, keeps them at a safe distance from the fluctuation potentials of the $(1s)^2$ electrons. As the discussion of other cases below will show, this phenomenon is quite general and even in more subtle cases leads to local pair correlations as the main effects, making the "collisions" of three, four, . . . electrons usually negligible.

This fact manifests itself in the equation:

$$\chi \sim \chi_e = \sum_{i>j}^{N} \frac{\mathcal{A}}{\sqrt{2}} \left(1,2,3 \ldots N \frac{\hat{u}_{ij}}{ij}\right) \tag{9}$$

where 1, 2, . . . N are the spin-orbitals in ϕ_0 occupied by electrons with the same numerals before the antisymmetrizer $\mathcal{A}$ makes them indistinguishable. The $\hat{u}_{ij}$ is the antisymmetric correlation wave function of i and j which shows how they are thrown out of each other's way by m_{ij}. In the orbital representation, $\hat{u}_{ij}$ contains all double excitations of orbitals i, j from the "sea," ϕ_0. The two electrons cannot

go into regions already occupied by other electrons, and this effect of the exclusion principle is reflected in the orthogonality[9] of $\hat{u}_{ij}$ to the *orbitals* of ϕ_0, i.e.

$$<\hat{u}_{ij}(x_i, x_{zj}),\ k(x_i)>_{xi} = 0 \qquad (k = 1,2, \ldots N) \tag{10}$$

where integration is performed over x_i only. The $\hat{u}_{ij}$ does not contain any single excitations either[9] ($k = i$ or j), because any further adjustment of the orbitals in the "sea" (Brueckner method) is negligible. The major adjustment has been done already in the Hartree-Fock method.

Equations (9) and (10) come out exactly[9] in first-order perturbation χ_1 beyond H.F., i.e., if only part of the energy, equation (8), is minimized.[10] Then $\hat{u}_{ij}$ would be the solution, $\hat{u}_{ij}^{(1)}$, of the first-order part of the Schrödinger equation[11] of two electrons in the H.F. "sea":

$$(e_i + e_j)\hat{u}_{ij}^{(1)} + \hat{m}_{ij}\mathfrak{A}(ij) = 0. \tag{11}$$

$\mathfrak{A}$ antisymmetrizes i and j. The $(\hat{m}_{ij}Bij)$ is $m_{ij}B(ij)$ made orthogonal to all k as in equation (10); thus $\hat{m}_{ij}$ is even more localized than m_{ij}.

We shall now leave equations (9) and (10) quite general and not confine $\hat{u}_{ij}$ to any order of approximation. Various ways of obtaining the pair correlations exactly will be discussed later.

Unlinked Clusters versus Many-Electron Correlations.—The complete χ would contain in addition to equation (9), "clusters" of three, four, etc., electrons at a time ($\hat{U}_{123}$, $\hat{U}_{1234}$, etc.). In addition to these terms, just the substitution of χ_s, equation (9), into the energy, equation (8), introduces three-electron correlations. The analysis is carried out easily with diagrams giving the energy of χ_s as

$$E - E_{\text{H.F.}} \leqslant \frac{1}{D}\left(\sum_{i>j} \tilde{\epsilon}_{ij} + 4\sum_{ijk}\right) \tag{12}$$

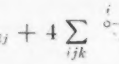

$$\tilde{\epsilon}_{ij} = 2 < \mathfrak{A}(ij),\ m_{ij}\,\hat{u}_{ij} > + < \hat{u}_{ij},\ (e_i + e_j + m_{ij})\hat{u}_{ij} > \tag{13}$$

$$D = 1 + <\chi_s,\ \chi_s> = 1 + \sum_{i>j} <\hat{u}_{ij}, \hat{u}_{ij}> \tag{14}$$

The triangle is the three-electron correlation involving the product of $\hat{u}_{kj}$, $\hat{u}_{ij}$, and m_{ki}. Because of the physical effects described, $\hat{u}_{kj}$ and $\hat{u}_{ji}$ will not both be large in the same region of space, so that only pair energies in equation (12) are significant.

In the recent configuration-interaction study[12] of the Be atom starting with H.F., single and triple excitations were found entirely negligible. But important quadruple excitations appeared—at first sight a surprising result, since the probability of a four-electron "collision" ought to be smaller than that of a three-body one.

Equation (9) represents only two electrons correlating at one time. Actually, it is very likely that when two electrons "collide," somewhere else in the system other binary "collisions" will be taking place independently but simultaneously. To account for these, all possible products of independent pair functions must be added to χ_s; e.g., for Be:

$$\chi_{ss} = \frac{\mathfrak{A}}{2}(\hat{u}_{12}\hat{u}_{34} + \hat{u}_{13}\hat{u}_{24} + \hat{u}_{14}\hat{u}_{23}). \tag{15}$$

As in the theory of imperfect gases, these are "unlinked clusters" and have played an important role in other many-body problems.[4, 13]

If in *Be*, true four-electron correlations, $\hat{U}_{1234}$, are negligible; the coefficients of quadruple excitations should be given only by those of double excitations. In Table 1, such coefficients from equation (15) are compared with those from the

TABLE 1

UNLINKED CLUSTERS VERSUS FOUR-ELECTRON CORRELATIONS IN BE ATOM

Four-excited configuration	Coefficient from 37-configuration wave function*	Calc'd. [Eq. (15)] Unlinked cluster coefficient
$P_1^2(^1S)p_{11}^2(^1S)$	0.00703	0.0073
$P_1^2(^1S)s_1^2(^1S)$	0.00535	0.00547
$P_1^2(^1S)d_{11}^2(^1S)$	0.00159	0.00168
$P_{11}^2(^1S)d_1^2(^1S)$	0.000464	0.000478
Energy contribution	−0.075 ev	−0.074 ev

* From Watson.[12]

37 configuration[12] C.I. The agreement is indeed satisfactory. We have obtained similar results upon examining recent C.I. results[14] on *LiH*.

Effect on Energy.—The energy effect of unlinked clusters such as in Equation (15), is again analyzed with diagrams. One gets from equation (8).

$$E - E_{\text{H.F.}} \leq \sum_{i>j}^{N} \bar{\epsilon}_{ij} \frac{D_{ij}}{D'} + \frac{R}{D'}. \tag{16a}$$

$D' \cong D$ and R contains all triangles, squares, and other joint four- or more-electron correlation effects.

$$D_{ij} = 1 + \sum_{k,l \neq i,j} < \hat{u}_{kl}, \hat{u}_{kl} > + \ldots \tag{16b}$$

As N tends to infinity, D_{ij}/D approaches 1.[4, 13] In atoms and molecules if D is sufficiently different from unity due to some "resonance" as in *Be* (large $2s^2 - 2p^2$ mixing which makes *Be* a metal not an inert gas), unlinked clusters affect the energy by canceling part of D'. This energy change agrees perfectly with the 37 C.I. result in Table 1, showing also that R in equation (16*a*) is negligible as anticipated. Thus,

$$E - E_{\text{H.F.}} \cong \sum_{i>j} \bar{\epsilon}_{ij} D_{ij}/D. \tag{17}$$

One reason for the smallness of many-particle effects is the smallness of $\hat{u}_{ij}$. Even with the $2s^2 - 2p^2$ "resonance" in *Be*, D gets only as large as 1.09. Usually $D \cong D_{ij} \cong 1$. Equation (17) will usually be a good approximation, but if need be, the neglected terms, R, can also be estimated with $\hat{u}_{ij}$ and an upper limit obtained to E.

Exlusion effect in boron.—We have seen how and why three-, four-, and more-electron correlations become unimportant when electrons are localized in radially different regions of space as in *Be* and *LiH*. What about cases, however, which involve say 2*s*, 2*p* electrons which are radially all in the same vicinity?

To see how three-electron correlations are expected to behave in such cases, we examine the boron atom. Almost all of the $(2s)^2$ correlation, $\hat{u}_{34}$, in *Be* is due to $(2p)^2$ mixing.[12] There, $\hat{u}_{34}$ is ^1S, a combination of three $(2p)^2$ determinants. When

a $(2p_z\alpha)$, i.e., spinorbital 5, is put on top of the $(2s)^2$ shell as in boron however, $\hat{u}_{34}$ becomes orthogonal to it, i.e. $<\hat{u}_{34}, 5> = 0$. Instead of the whole sphere, $\hat{u}_{34}$ will now be large only on the xy-plane as shown in Figure 4. To make the three-electron $(2s_\alpha 2s_\beta 2p_z\alpha \equiv 345)$ correlation, *i.e.*, the triangle of equation (12), appreciable, the product $\hat{u}_{34}\hat{u}_{45}$ must be large. But $\hat{u}_{45}$ is large where its fluctuation potential m_{45} and $B(45)$ are large [see equation (11)]. The fluctuation potential, $(g_{45} - S_5(4))$, that electron 4 sees when 5 is at its most likely place (Fig. 4) is shown

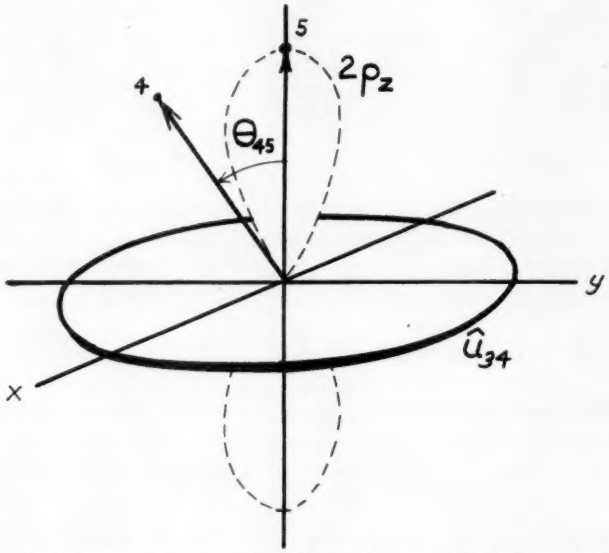

FIG. 4.—Exclusion effect in Boron $(1s^22s^22p_z)$. The two (2s) electrons while correlating are kept away from the $(2p_z)$ electron which has the same spin as one or the other (2s). Thus $(2s)^2$ correlation, $\hat{u}_{34}$, is confined to the vicinity of the xy-plane.

in Figure 5 for a fixed radius.

Note that m_{45}, hence $\hat{u}_{45}$, is very small just where $(\sim 90°)$ $\hat{u}_{34}$ is large. Thus, the product $\hat{u}_{34}\hat{u}_{45}$ will be small everywhere, again exhibiting the combined behavior of m_{ij} and exclusion to make many-electron correlations unimportant.

How to Get the Pair Functions.—Having a sum of pair energies in equation (17), each pair function can be obtained separately in several ways, depending on the magnitude of (D_{ij}/D). These ways and the over-all picture that comes out of our theory is shown in Figure 6.

Each $\tilde{\epsilon}_{ij}$, equation (13), varied subject to orbital orthogonality, equation (10), yields Schrödinger equations of electron pairs in a Hartree-Fock "sea."

$$(e_i + e_j + \hat{m}_{ij})\phi_{ij} = 0 \qquad (18a)$$

where $\phi_{ij} = \mathfrak{B}(ij) + \hat{u}_{ij}$. When this equation is satisfied, $\tilde{\epsilon}_{ij}$ becomes

$$\epsilon_{ij} = <\mathfrak{B}(ij), g_{ij}\hat{u}_{ij}>. \qquad (18b)$$

Minimization of smaller parts[10] of $\tilde{\epsilon}_{ij}D_{ij}/D$ leads to first-order pairs,[9] equation (11). On the other hand, a more complete Schrödinger equation than equation

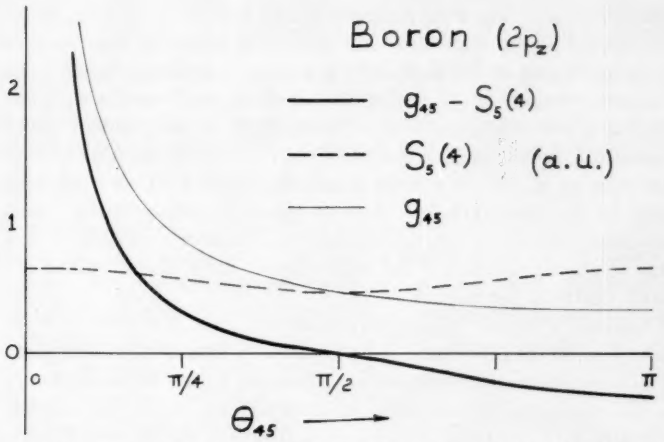

FIG. 5.—Reason for expecting $(2s)^2(2p_z)$ three e^- correlation to be small. The fluctuation potential, $[g_{45}-S_5(4)]$, seen by the (2s) electron, 4, due to electron 5 at the maximum of $(2p_z)$ is *ca.* zero on the xy-plane ($\pi/2$) where $\hat{u}_{34}$ was largest (Fig. 4).

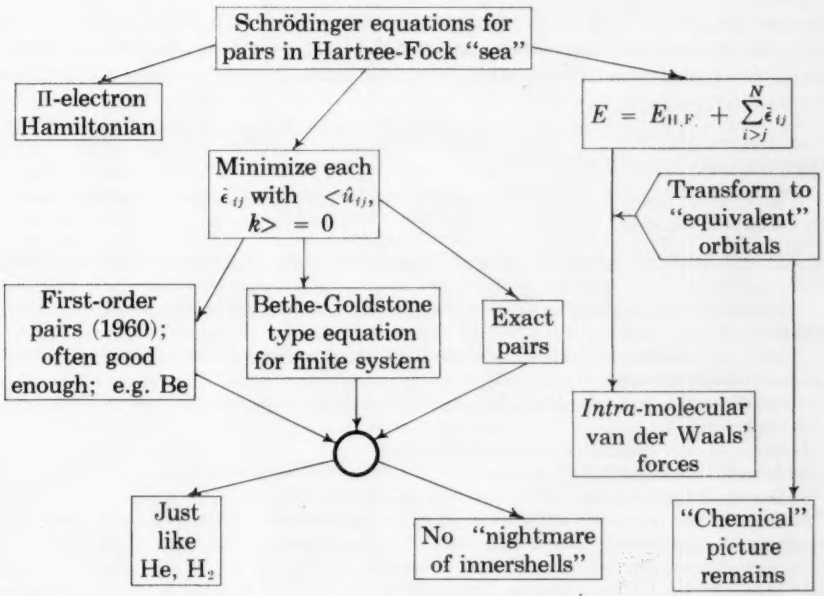
Schrödinger equations for pairs in Hartree-Fock "sea"
Π-electron Hamiltonian
E = E_H.F. + Σ ε̃_ij
Minimize each ε̃_ij with <û_ij, k> = 0
Transform to "equivalent" orbitals
First-order pairs (1960); often good enough; e.g. Be
Bethe-Goldstone type equation for finite system
Exact pairs
Intra-molecular van der Waals' forces
Just like He, H2
No "nightmare of innershells"
"Chemical" picture remains

FIG. 6.—Principle features and ways of using the many-electron theory of atoms and molecules as reported in text.

(18*a*) is obtained by minimizing $\tilde{\epsilon}_{ij}/(1 + <\hat{u}_{ij},\hat{u}_{ij}>)$ instead of ϵ_{ij} alone. Equation (18*a*) differs from the closed form of the Bethe-Goldstone[15]–Brueckner equation in containing $\hat{m}_{ij}$ instead of $\hat{g}_{ij}$. The results we have obtained in this connection should also be useful for finite nuclei.

Now the variational *minimum* principle can be applied to each $\tilde{\epsilon}_{ij}$, equation (13), separately subject to equation (10) and with trial functions that may contain r_{12} explicitly as in *He* and H_2 for shells with a strong "correlation hole."[1] For others, e.g., those with "resonance" as in the $(2s)^2$ of *Be*, a small secular equation need be solved mixing a few configurations. The number of independent pair functions that are needed[9] is much smaller than $N(N-1)/2$ due to the multiplicity of many pair states such as ^3S, ^1D, etc. Only 9 pair functions of which 6 are singlets must be obtained for *Ne*, instead of 45. Because of orbital orthogonality, equation (10), the *minimization* procedure can be applied even to outer shell pairs with no fear of converging to the wrong shell ("the nightmare of inner shells" which plagued the quantum chemistry of the thirties).[16]

The "Chemical" Picture.—Equation (18) for an outer pair with $V_i + V_j - \bar{S}_i - \bar{S}_j = V_{\text{core}}$ (Eq. 7*b*) has the form of a "II-electron Hamiltonian" thus providing a basis for such semiempirical schemes.[17] Moreover, $\tilde{\epsilon}_{ij}$ can be added to $(J_{ij} - K_{ij})$, equation (6), explaining the successes of semiempirical M.O. calculations.

In molecules with no strong electron delocalization, the Hartree-Fock orbitals in ϕ_0 can be transformed[7] into "equivalent orbitals." Then $\sum_{i<j} \tilde{\epsilon}_{ij}$ becomes simply the sum of "bond" correlation energies and "Van der Waals" attractions between non-bonded regions. The latter were discussed semi-empirically by Pitzer.[2] One can use the theory both ways and (a) calculate such Van der Waals forces having C.I. etc. type correlation results starting with Hartree-Fock, or (b) estimate correlation energies of pairs of H.F. orbitals from estimates of bond energies and London dispersion type forces.[2]

Thus the "chemical" picture with its bonds, Lewis-Langmuir octets[6] and orbitals remains *in spite of correlation.*

It is my great pleasure to thank Raymond M. Fuoss and Lars Onsager for the kind interest they showed in this work.

[1] Löwdin, P. O., in *Advances in Chemical Physics* (New York: Interscience Publishers, 1959), vol. 2.

[2] Pitzer, K. S., in *Advances in Chemical Physics* (New York: Interscience Publishers, 1959), vol. 2.

[3] See, e.g., Daudel, R., R. LeFebvre, and C. Moser, *Quantum Chemistry* (New York: Interscience Publishers, 1959).

[4] Brueckner, K. A., in *The Many Body Problem*, ed. C. De Witt and P. Nozières (New York: John Wiley and Sons, 1959).

[5] Bethe, H. A., *Phys. Rev.*, **103**, 1353 (1956).

[6] Linnett, J. W., and A. J. Pče, *Trans. Faraday Soc.*, **47**, 1033 (1951).

[7] See e.g., Pople, J. A., *Quart. Revs. (London)*, **11**, 291 (1957).

[8] The next best calculation is the recent one on Be (reference 12). Here $(2s)^2$–$(2p)^2$ "resonance" is of utmost importance and corrects for much of the correlation.

[9] Sinanoğlu, O., *Proc. Roy. Soc. (London)*, **A260**, 379 (1961).

[10] Sinanoğlu, O., *J. Chem. Phys.*, **34**, 1237 (1961).

[11] As shown in reference 9, for a general pair $\mathfrak{G}(ij)$ is replaced by a pure symmetry state combination.

[12] Watson, R. E., *Phys. Rev.*, **119**, 170 (1960).

[13] Brout, R., *Phys. Rev.*, **111**, 1324 (1958).

[14] Ebbing, D. D., Ph.D. Thesis, Department of Chemistry, Indiana University (June 1960).

[15] Bethe, H. A., and J. Goldstone, *Proc. Roy. Soc. (London)*, **A238**, 551 (1956).

[16] Van Vleck, J. H., and A. Sherman, *Revs. Modern Phys.*, **7**, 167 (1935).

[17] Pariser, R., and R. G. Parr, *J. Chem. Phys.*, **21**, 466 (1953).

RATE-INCREASING ACTION OF CORTICOTROPIN AND OF α-INTERMEDIN IN THE ISOLATED MAMMALIAN HEART

By O. Krayer, E. B. Astwood, D. R. Waud, and M. H. Alper

DEPARTMENT OF PHARMACOLOGY, HARVARD MEDICAL SCHOOL, AND DEPARTMENT OF MEDICINE, TUFTS UNIVERSITY SCHOOL OF MEDICINE AT THE NEW ENGLAND CENTER HOSPITAL, BOSTON

Communicated June 13, 1961

In 1958, we intended to examine the influence of corticotropin upon the fat metabolism of the mammalian heart. In making observations on the isolated heart of the dog, using the heart-lung preparation, it was found that, while not altering the fatty acid content in the blood or the rate of disappearance of glucose, corticotropin exhibited an unusual rate-increasing (positive chronotropic) effect upon the heart beat. More recently, similar results were obtained with α-intermedin, the α-melanocyte-stimulating hormone of the pituitary body. The following is a report on the positive chronotropic cardiac effect of these substances.

Methods and Materials.—Thirty-nine experiments were carried out, eighteen with corticotropin and twenty-one with intermedin. Dogs of either sex and undetermined breed with an average body weight of 11.8 kg (range 8.9–15.8 kg) were used. They were anesthetized with 0.04 gm of sodium pentobarbital per kg body weight except when the animals had been treated with reserpine, in which case half the dose or less was sufficient to produce adequate surgical anesthesia. The Starling preparation was employed with modifications reported by Krayer[1] and by Krayer and Mendez.[2] Defibrinated blood obtained from bleeder dogs under ether anesthesia was used. The total blood volume in the heart-lung preparation at the start of the experiment was kept uniform and amounted to about 1000 ml (range 910–1,200). Heart rates were counted at one or two minute intervals from electrocardiographic tracings recorded with a Grass ink-writing oscillograph. The average temperature of the blood was 38.6°C (range 37.4–39.2), and in the course of the same experiment it did not fluctuate more than ±0.2°C. The average mean arterial pressure was 100 mm Hg (range 90–111) and the average systemic output recorded either by a Shipley-Wilson rotameter or by a Weese flowmeter was 730 ml/min (range 530–850).

The technique described by Krayer *et al.*[3] and Innes *et al.*[4] was used to measure the atrio-ventricular (A-V) propagation time and the functional refractory period of A-V transmission (FRP). Two pairs of stimulating electrodes were attached to the tip of the right atrial appendage. For selected periods during the experiments the heart was driven at a constant rate by stimuli delivered through one pair of electrodes. The driving rate selected was dependent upon the maximal heart rate to be expected after administration of corticotropin or norepinephrine.

The cardiac stores were depleted of intrinsic sympathomimetic catecholamines, mostly norepinephrine, by the subcutaneous administration of reserpine in two dosage schemes, either 0.1 mg/kg given 24 hours before isolating the heart,[5] or, for more complete depletion, 0.5 mg/kg given 48 hours and 24 hours before setting up the heart-lung preparation (Liebman;[6] see also Paasonen and Krayer;[7] Innes and Krayer;[8] Innes *et al.*[4]). Reserpine (3 mg), or guanethidine (3 or 10 mg), was injected to release catecholamines from the normal preparation. To test the response of the isolated heart to norepinephrine, this substance (in the form of the bitartrate) was administered to the heart-lung preparation by continuous infusion using a power-driven syringe. The rate of infusion was 3 μg/min (for details of the method and control results, see Krayer,[9] Krayer and Benforado,[10] Waud and Krayer[11]).

The corticotropin used in most of the experiments was prepared by the oxycellulose method.[12] A small sample of β-corticotropin[13] was put at our disposal by P. H. Bell. The melanophore-stimulating hormone employed in most of the experiments was α-intermedin received from A. V. Schally and prepared by him.[14] The β-intermedin given in two experiments was also donated by Dr. Schally. A fat-mobilizing peptide used in two experiments is referred to as peptide I by Astwood *et al.*[15] The L-norepinephrine bitartrate was generously supplied by Winthrop Stearns, Rensselaer, New York; the reserpine phosphate (lyophilized) and the guanethidine sulfate by

CIBA Pharmaceuticals, Inc., Summit, New Jersey. Unless otherwise indicated all doses of drugs given refer to the base.

Results.—1. *Corticotropin:* When 100 μg of corticotropin was injected into the blood stream of the heart-lung preparation close to the heart and during 1 minute, the heart rate in most experiments began to rise before the end of the injection, and the peak effect was reached in 5 to 8 minutes (Table 1). The rate

TABLE 1

THE RATE-INCREASING EFFECT OF 100 μg CORTICOTROPIN IN THE HEART-LUNG PREPARATION OF THE DOG

Exp. no.	Heart Rate (beats/min) Initial	Heart Rate (beats/min) Increase	Time to maximum, min	Duration of action, min
A-2	162	101	6	90
A-5	132	89	8	70
A-8	148	9	5	..
A-9	128	78	8	>40
A-10	159	1	..	..
A-11	126	104	5	50
A-12	176	79	5	55
A-15	151	4	..	..
A-16	152	51	8	50
A-17	143	0	..	..
Mean	147.7	Mean 51.6		

remained at the maximum for only a few minutes, then gradually decreased and reached a level close to or above the initial rate in 50 to 90 minutes. The intensity of the effect was not predictable. While increases in rate of 100 beats/min or more were observed in some experiments, very little or no effect was seen in others (see Table 1). Although the action was unpredictable even with a dose of 100 μg, in some cases a distinct effect followed a dose of 10 μg (see Fig. 1).

The rate-increasing action of corticotropin was cumulative, and larger effects were seen when additional doses were given before the effect of the first dose had worn off. For example, in the experiment of Figure 1 successive doses of β-corticotropin and of our preparation raised the heart rate from the initial rate of 141 beats/min to the maximal rate of 242 beats/min. However, in hearts that responded little to a dose of 100 μg it was not always possible to cause a marked effect even with larger doses.

On repeated administration of an initially very active dose at the time when the previous increase in rate had subsided, the effect became less from dose to dose and after 3 to 4 doses was impossible to elicit (Fig. 2).

In some experiments, especially when the increase in heart rate was very large (see, for example, Figs. 2 and 3), there was a decrease in systemic output concomitant with an increase in right and left atrial pressures. The pulmonary pressure did not increase. In other cases, no distinct changes occurred in output and atrial pressures. The PR intervals in the electrocardiogram, when measured during the increase in heart rate, were either unchanged (see Fig. 1), increased, or slightly decreased. In two experiments a more rigorous test of the influence of corticotropin upon propagation time of an atrial impulse and upon the functional refractory period of A-V transmission was carried out, using uniform driving rates. As is shown by the data of Table 2, A-V propagation time and functional refractory period were slightly diminished. Infusion of norepinephrine in doses causing less

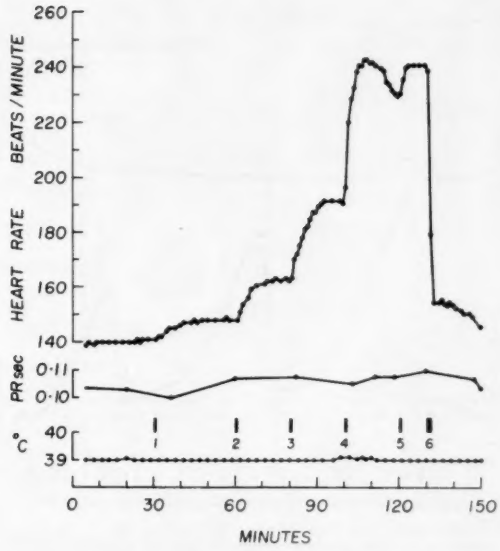

FIG. 1.—The cumulative positive chronotropic action of corticotropin upon the isolated heart. Heart-lung preparation, 4/10/58. (Dog 11.1 kg, female.) From top to bottom: heart rate, PR interval, temperature. Total blood volume, 1200 ml; systemic output, 700 ml/min. (Weese flowmeter). Mean arterial pressure, 99 mm Hg. Supply level, 117 mm. At 1 and 3, injection (in 1 minute) of 10 and 30 μg of β-corticotropin. At 2, 4, and 5, injection of 10, 30 and 30, μg of corticotropin. At 6, injection (in 2 minutes) of 0.8 mg of veratramine.

TABLE 2

THE EFFECT OF CORTICOTROPIN (ACTH) AND OF NOREPINEPHRINE (NE) INFUSION UPON A-V PROPAGATION TIME AND FUNCTIONAL REFRACTORY PERIOD OF A-V CONDUCTION (FRP) IN THE HEART-LUNG PREPARATION OF THE DOG

Exp. no.	Driving rate (beats/min)	ACTH, μg	NE, μg/min	Heart Rate (beats/min)		A-V Propagation Time, msec		FRP, msec	
				Before	At peak	Before	At peak	Before	At peak
A-16	200	100	..	152	203	170	158	268	259
	200		1.72	142	162	210	100	298	238
	200		3.0	142	180	210	93	298	222
A-18	240	300	..	160	220	188	158	203	198
	240		0.29	156	160	182	166	208	203
	240		3.0	156	187	182	115	208	176

increase in heart rate than the selected doses of corticotropin were more effective in decreasing A-V propagation time and functional refractory period of A-V transmission.

In three experiments, A-5, A-6, and A-8, a dose of 3 mg of reserpine was administered after corticotropin. In all three experiments the increase in rate caused by reserpine was accompanied by a decrease of PR interval, atrial pressures, and heart volume, and an increase in the competence of the heart. In experiment A-5 after 100 μg of corticotropin and in A-8 after 300 μg, the rate increased 89 and 97 beats/min respectively, while in both cases reserpine caused an increase of only 38 beats/min. The positive chronotropic action of corticotropin was obtained also in the

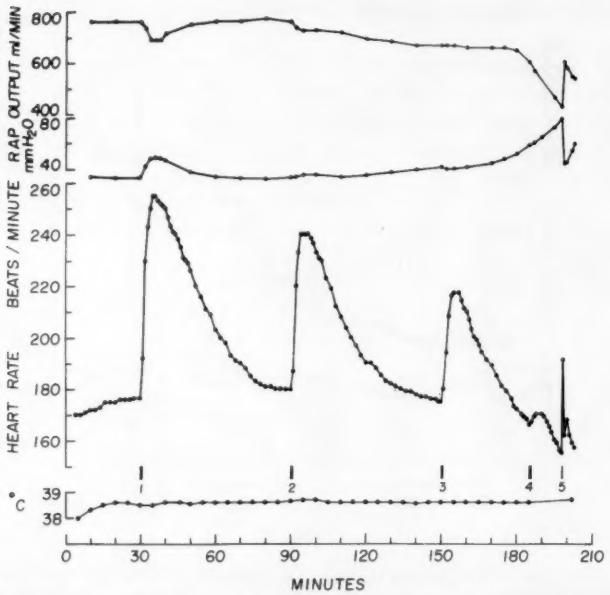

FIG. 2.—The diminution of the positive chronotropic effect of corticotropin upon repeated administration to the isolated heart. Heart-lung preparation, 6/25/58. (Dog 9.6 kg, male.) Total blood volume, 1120 ml; systemic output, 770 ml/min; (Weese flowmeter). Mean arterial pressure, 111 mm Hg. Supply level, 124 mm. From top to bottom: systemic output, right atrial pressure, heart rate, temperature. At 1, 2, 3, and 4, injection (in 1 minute) of 100 μg of corticotropin. At 5, injection (in 4 seconds) of 30 μg of norepinephrine.

presence of atropine sulfate (1:100,000 w/v) or hexamethonium (1:100,000 w/v). It was antagonized by veratramine (see Fig. 1).

Three experiments were carried out with corticotropin in the heart-lung preparation from dogs pretreated with reserpine (0.1 mg/kg, 24 hr before isolating the heart). The initial rates of these hearts were 103, 122, and 142 beats/min respectively; and the corresponding increases in heart rate, caused by 100 μg of corticotropin, were 4, 27, and 11 beats/min. Because of the variability of the response these limited data do not permit a quantitative comparison with the response of the normal heart; they suggest, however, that reserpine pretreatment of this intensity does not abolish the increase in rate.

2. *Intermedin:* α-Intermedin was used in 21 experiments (β-intermedin and peptide I were given for comparison in two experiments each; they possessed the same activity but appeared to be less potent). α-Intermedin in doses of 1 μg and 3 μg had slight but distinct rate-increasing effects, in one experiment each. In all other experiments doses of 10 μg or more were given. In eleven experiments with 10 μg the results were similar to those obtained with 100 μg of corticotropin. As Table 3 shows, the onset of action, the peak effect, and the time required for the maximal effect were of the same order of magnitude. The duration of action appeared to be longer after 10 μg of α-intermedin than after 100 μg of corticotropin (compare Tables 1 and 3). In four experiments (I - 6, 8, 14, and 20) the duration

TABLE 3

RATE-INCREASING EFFECT OF 10 μg α-INTERMEDIN IN THE HEART-LUNG PREPARATION OF THE DOG

Exp no.	Heart Rate, beats/min Initial	Increase	Time to maximum, min	Duration of action, min
I-1	121	109	13	130
I-5	121	6	(18)*	..
I-6	138	4	5	..
I-7	115	3	(20)*	..
I-8	133	18	9	..
I-10	138	106	10	70
I-11	151	45	13	100
I-13	114	2	7	..
I-14	132	28	(20)*	..
I-16	179	77	12	105
I-20	131	36	14	..
Mean	139.9	Mean 39.5		

* Indicates the time when an injection of 100 μg was given. The 7 experiments for which no duration of action is given are the normal experiments of Table 4 in which an additional dose of 100 μg was administered.

of action of a subsequent dose of 100 μg was 80, 100, 80, and 150 minutes, respectively. Cumulative action of closely spaced successive doses (see Fig. 3, right) and weakening of the effect of repeated doses after the previous effect had subsided

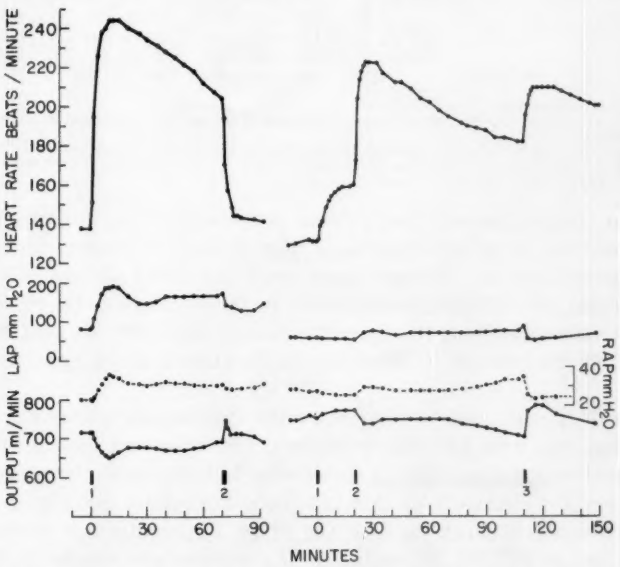

FIG. 3.—The positive chronotropic effect of α-intermedin upon the isolated heart. Heart-lung preparations. From top to bottom: heart rate, left atrial pressure, right atrial pressure, systemic output (Weese flowmeter). Left: 3/28/61 (Dog 12 kg, male). Total blood volume, 1020 ml; systemic output, 713 ml/min. Mean arterial pressure, 100 mm Hg. Temp. 38.8–38.9°C. Supply level, 110 mm. At 1, injection (in 1 minute) of 10 μg of α-intermedin. At 2, injection (in 2 minutes) of 0.8 mg of veratramine. Right: 4/4/61 (Dog 12.5 kg, male). Total blood volume, 1645 ml; systemic output, 748 ml/min Mean arterial pressure, 100 mm Hg. Temp. 38.5–38.7°C. Supply level, 114 mm. At 1, injection (in 1 minute) of 10 μg and at 2, of 100 μg of α-intermedin. At 3, injection (in 1 minute) of 3 mg of guanethidine.

were as described for corticotropin. Likewise, as may be seen in Table 3, the same difficulty of predicting the response was encountered.

The increased rate caused by α-intermedin was accompanied in some experiments by a slight decrease in right atrial pressure; in most experiments there was no change or a slight progressive increase in right and left atrial pressure; systemic cardiac output remained unaltered or decreased slightly. In a few experiments the right and left atrial pressures increased conspicuously while the systemic output decreased and the heart volume increased (Fig. 3, left). The PR intervals were either not changed or slightly shortened.

The influence of reserpine-pretreatment (2 × 0.5 mg of reserpine/kg) was examined in 7 experiments. The responses are compared in Table 4 with those

TABLE 4

HEART RATE INCREASE CAUSED BY α-INTERMEDIN IN THE HEART-LUNG PREPARATION OF NORMAL AND RESERPINE-PRETREATED DOGS

			Heart-Lung Preparation		
Dogs	Dose, μg	n subscript Exp.	Initial rate av (range), beats/min	Rate increase av (range), beats/min	Maximum rate av (range), beats/min
Normal	10	11	134 (114–179)	42 (2–109)	175 (116–256)
		4	150 (121–179)	84 (45–109)	232 (196–256)
		7†	126 (114–138)	14 (2–36)	140 (116–167)
	(10) + 100	7†	126 (114–138)	46 (7–112)	172 (122–243)
Reserpine-pretreated*	10	7	130 (112–149)	25 (2–59)	155 (116–199)
		3	138 (125–149)	32 (3–59)	170 (128–199)
		4‡	124 (112–138)	20 (2–44)	144 (116–173)
	(10) + 100	4‡	124 (112–138)	68 (9–136)	191 (145–265)

n = number of experiments.

* Reserpine pretreatment consisted in subcutaneous injection of 0.5 mg/kg 48 hours and 24 hours before setting up the preparation.

†, ‡ The additional dose of 100 μg of α-intermedin was given to the heart-lung preparation of 7† of the normal and 4‡ of the reserpine-pretreated dogs 15–25 minutes after the 10 μg dose. The maximal effect of 10 μg had then been reached or passed.

observed in normal hearts. The evidence indicates that the rate-increasing effect of α-intermedin is to be seen even when there is almost complete depletion of the stores of norepinephrine. In two experiments (I-9 and I-12) the effect of 10 μg lasted 120 and 130 minutes, respectively; in three others (I-17, 18, and 19) the increase in rate caused by 100 μg had subsided after 100, 75, and 85 minutes. Hence, neither the intensity of effect nor the duration of action appear to be modified.

In the experiments with α-intermedin the catecholamine-releasing substance, guanethidine, was used for the comparison. In all of ten experiments without reserpine-pretreatment in which α-intermedin had previously been given, guanethidine caused the changes typical of catecholamine release (see Fig. 3). In seven of the experiments, in which the dose was 10 mg, the average rate increase was 100 beats/min (range 70–150), as compared to 110 beats/min (range 91–121) in five normal control experiments in which no other substance had been administered. In four heart-lung preparations from reserpine-pretreated dogs guanethidine had no effect; 10 mg caused an average rate increase of 6 beats/min (range −2 to +12).

3. *Subsensitivity to norepinephrine:* In several experiments during this investigation, after a large effect upon the heart rate from corticotropin or α-intermedin had worn off, the rate-increasing action of single doses of norepinephrine appeared to be reduced in intensity and duration. The decreased sensitivity to

norepinephrine was especially clear in three experiments with α-intermedin in which continuous infusion was used in the heart-lung preparations from dogs pretreated with reserpine. The phenomenon is illustrated in Figure 4. The infusion of 3 μg/min of norepinephrine in this experiment had no influence at all upon heart rate. By contrast, the force of contraction was greatly increased, as indicated by the increased output and the simultaneous decrease in right and left atrial pressure. However, the pacemaker of the heart was capable of responding to norepinephrine with an increased rate, as shown by the administration of guanethidine which raised the heart rate and improved still further the volume work of the heart.

It is known that the response of the heart to the rate-increasing effect of epinephrine and norepinephrine in the heart-lung preparation decreases with time.[11] Yet in the present experiments, the marked reduction in sensitivity of the pace-

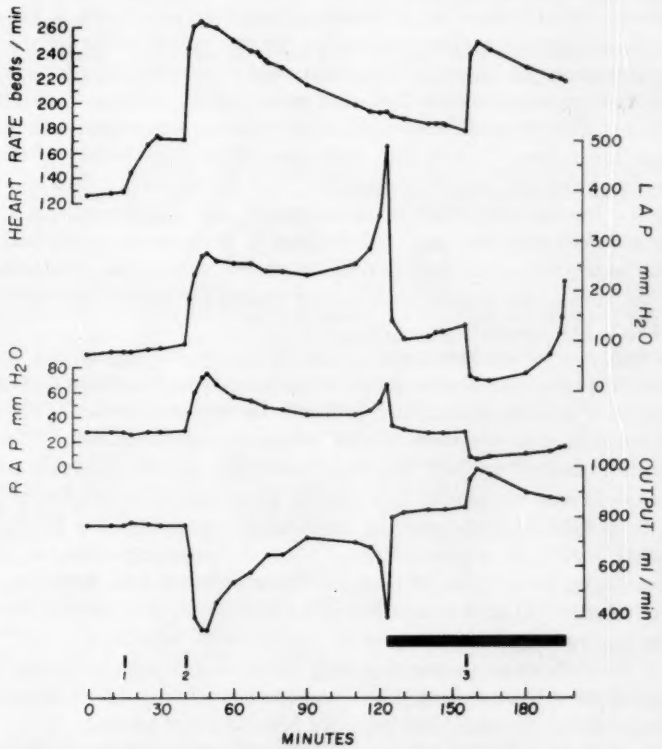

FIG. 4.—Effect of α-intermedin and norepinephrine upon the isolated heart. Heart-lung preparation, 4/21/61. (Dog 11 kg, male. Pretreated with reserpine 0.5 mg/kg, subcutaneously, 48 and 24 hours before isolating the heart.) Total blood volume, 1040 ml. Mean arterial pressure, 97 mm Hg. Supply level, 110 mm. Temp. 39°C. From top to bottom: heart rate, left atrial pressure, right atrial pressure, systemic output (Shipley-Wilson rotameter). At 1 and 2, injection (in 1 minute) of 10 and 100 μg of α-intermedin. respectively. At 3, injection (in 1 minute) of 10 mg of guanethidine. Black bar at right bottom, continuous infusion of norepinephrine 3 μg/min. For further explanation, see text.

maker may well have depended in part upon the preceding influence of α-intermedin, since in the three experiments the decrease in sensitivity appeared to be inversely related to the strength of the positive chronotropic action of α-intermedin. Further experiments are needed to verify whether or not subsensitivity to the positive chronotropic action of norepinephrine is a later effect of corticotropin and α-intermedin. The selectivity of the phenomenon is underlined by the fact that the effect of norepinephrine upon force of contraction was not suppressed.

In the heart-lung preparation from dogs pretreated with reserpine, as in the experiment of Figure 4, guanethidine alone had no rate-increasing activity and, in a dose of 3 mg or more, it decreased force of contraction. Its effect, as was discovered in the course of these experiments with α-intermedin, is due to its ability to render the heart hypersensitive to *administered* norepinephrine, the synergistic action extending to the effect upon force of contraction as well as to the rate-increasing effect.

Discussion.—Apart from the sympathomimetic amines there is no group of pharmacological agents capable of increasing the rate of beat of the isolated, acutely denervated mammalian heart. Other substances possessing this property, such as the reserpine-type rauwolfia alkaloids and guanethidine, owe their activity to the release of intrinsic sympathomimetic amines. In this latter group, therefore, the effect upon heart rate is linked with other properties characteristic of epinephrine and norepinephrine, i.e., an effect upon the force of contraction and upon impulse conduction. Because the effect of corticotropin and α-intermedin is almost exclusively an effect upon the rate and, at least in the case of α-intermedin, is not altered by nearly complete depletion of the stores of intrinsic sympathomimetic amines, the substances cannot be releasing agents for norepinephrine or related compounds.

In the past the sympathomimetic amine, tyramine, has repeatedly been implicated for epinephrine-like cardiac action of tissue extracts,[16] in which it accumulated in the course of protein degradation, probably by bacterial action. The available evidence suggests that tyramine acts by releasing catecholamines. The methods of preparation make it unlikely that small molecules such as tyramine are present in corticotropin or α-intermedin. Moreover, the quantitative studies of Liebman[6] exclude the possibility that tyramine could have been responsible for the positive chronotropic action of α-intermedin. Under the same experimental conditions in the heart-lung preparation of dogs heavily pretreated with reserpine, the continuous infusion of 150 μg of tyramine/min for 10 minutes or more, in 5 experiments, caused an average heart-rate increase of only 14 beats/min (range 2–36).

One of the difficulties in working with corticotropin and α-intermedin is the variability of the rate-increasing effect from one heart-lung preparation to the next. No explanation for the capricious behavior is available at present.

It is of especial interest that these particular peptides exert the cardioaccelerator effect because they are among the ones which have been found to evoke metabolic effects in other animals. Corticotropin, which has intrinsic melanophore-expanding activity, is the most active factor in pituitary extracts causing release of free fatty acids from adipose tissue when tested in mice,[17, 18] or on isolated depot fat from rats in vitro.[19] The two intermedins[20] and peptide I are potent in this respect in the rabbit and peptide I also causes lipemia in this species.[15] α-Intermedin is a

tridecapeptide with the same sequence of amino acids as the C-terminal end of corticotropin, while β-intermedin from ox or pig shares 10 of its 18 amino acid residues with corticotropin.[21-23]

Whether or not these and related peptides and the diverse effects that they are being found to have are of physiological importance can only be decided by further work. Nonetheless these peptides are probably merely other examples of what might prove to be a large class of pharmacologically interesting substances.

Summary.—A preparation of corticotropin and α-intermedin were found to exhibit an unusual heart rate-increasing action in the heart-lung preparation of the dog. The effect was unpredictable from one experiment to the next but was often very striking. The chronotropic action was not linked to effects upon impulse propagation and force of contraction as in the case of the sympathomimetic amines. α-Intermedin was shown to have the same effect in normal heart-lung preparations and in those almost completely free of intrinsic sympathomimetic amines, obtained from dogs heavily treated with reserpine.

Note added in proof: After this paper had gone to press, Dr. K. Hofmann generously put at our disposal a sample of his synthetic α-intermedin (Hofmann, K., H. Yajima, and E. T. Schwartz, *J. Am. Chem. Soc.*, **82**, 3732 (1960)). In the four experiments carried out so far in the heart-lung preparation of the dog, the activity of the synthetic substance was qualitatively similar to that of the natural polypeptide.

We should like to thank P. H. Bell for supplying the pure β-corticotropin, and A. V. Shally for the α- and β-intermedin. The reserpine and guanethidine were generously donated by CIBA Pharmaceutical Products, Inc., Summit, New Jersey.

The expert technical help of Miss Gabriele Schröder and W. Mosimann is gratefully acknowledged.

This work was supported by Grants A-612, 2A-5166, and H-2205 from the National Institutes of Health, and by funds received from the Eugene Higgins Trust; it was initiated when one of the authors (E. B. Astwood) was a Visiting Professor in the Department of Biological Chemistry at Harvard Medical School. While participating in this investgation D. R. Waud was a Fellow of the Life Insurance Medical Research Fund and M. H. Alper was a Postdoctoral Trainee under the U. S. Public Health Service Training Grant 2G-165.

[1] Krayer, O., *Arch. exp. Pathol. Pharmakol.*, **162,** 1 (1931).

[2] Krayer, O., and R. Mendez, *J. Pharmacol. Exptl. Therap.*, **74,** 350 (1942).

[3] Krayer, O., J. J. Mandoki, and C. Mendez, *ibid.*, **103,** 412 (1951).

[4] Innes, I. R., O. Krayer, and D. R. Waud, *ibid.*, **124,** 324 (1958).

[5] Waud, D. R., S. R. Kottegoda, and O. Krayer, *ibid.*, **124,** 340 (1958).

[6] Liebman, J., *ibid.* (in press).

[7] Paasonen, M. K., and O. Krayer, *ibid.*, **123,** 153 (1958).

[8] Innes, I. R., and O. Krayer, *ibid.*, **124,** 245 (1958).

[9] Krayer, O., *ibid.*, **98,** 427 (1950).

[10] Krayer, O., and J. M. Benforado, *Pflüger's Arch. ges. Physiol.*, **260,** 177 (1955).

[11] Waud, D. R., and O. Krayer, *J. Pharmacol. Exptl. Therap.*, **128,** 352 (1960).

[12] Astwood, E. B., M. S. Raben, R. W. Payne, and A. B. Grady, *J. Am. Chem. Soc.*, **73,** 2969 (1951).

[13] Bell, P. H., *J. Am. Chem Soc.*, **76,** 5565 (1954).

[14] Schally, A. V., and R. Guillemin, *Texas Repts. Biol. and Med.*, **18,** 133 (1960).

[15] Astwood, E. B., R. J. Barrett, and H. Friesen, *Science*, **133,** 1364 (1961).

[16] Grabe, F., O. Krayer, and K. Seelkopf, *Klin. Wochschr.*, 1381 (1934).

[17] Rosenberg, I. N., *Proc. Soc. Exptl. Biol. Med.*, **82,** 701 (1953).

[18] Astwood, E. B., M. S. Raben, I. N. Rosenberg, and V. W. Westermeyer, *Science*, **118,** 567 (1953).

[19] Hollenberg, C. H., M. S. Raben, and E. B. Astwood, *Endocrinology*, **68,** 589 (1961).

[20] Raben, M. S., R. Landolt, F. A. Smith, K. Hofmann, and H. Yajima, *Nature*, **189,** 681 (1961).

[21] Harris, J. I., and P. Roos, *Nature*, **178**, 90 (1956).
[22] Harris, J. I., and A. B. Lerner, *Nature*, **179**, 1346 (1957).
[23] Harris, J. I., *Brit. Med. Bull.*, **16**, 189 (1960).

---

*RESPIRATORY ENZYME CHANGES DURING FROG EMBRYOGENESIS**

BY CALVIN A. LANG† AND PHILIP GRANT‡

DEPARTMENT OF PATHOBIOLOGY, SCHOOL OF HYGIENE AND PUBLIC HEALTH, THE JOHNS HOPKINS UNIVERSITY

Communicated by E. V. McCollum, June 29, 1961

Marked differential changes in several respiratory enzyme activities have been demonstrated in the mosquito during its post-embryonic life span.[1] Of particular interest was the finding that the ratio of DPNH-cytochrome *c* reductase to TPNH-cytochrome *c* reductase was about 2 during the growing stages and increased to over 20 in the adult stage. This latter ratio was the result of both an increase in the DPNH-linked enzyme and a decrease in the TPNH-reductase activities. We were curious as to whether similar changes in these enzyme patterns occur during frog embryogenesis and are related to known physiological and morphological events.

Many studies have been reported on respiration rates of whole amphibian embryos and brei preparations as measured by oxygen uptake and individual enzymes. To our knowledge, however, the activities of several respiratory enzymes during embryogenesis have not been measured in the same sample. To this end the activities of DPNH-, TPNH-, and succino-cytochrome *c* reductases and cytochrome oxidase were determined in frog embryos of different developmental stages.

Materials and Methods.—Eggs were obtained from *Rana pipiens* females by the usual method of pituitary injection.[2] Fertilized eggs, in groups of approximately 100, were placed in finger bowls containing charcoal-treated tap water and allowed to develop at 17–19°C. At various time intervals, samples were taken, and the jelly was removed. Embryos of stages 1–15 (Shumway)[3] were used with the vitelline membrane intact, but this membrane and perivitelline fluid were removed from embryos of stages 16–25. The above procedure was replicated using several batches of eggs obtained from eight different frogs. In each experiment samples from early, middle, and late stages of development were analyzed.

Ten embryos were homogenized in 1.0 ml of 0.25 *M* sucrose using a loose-fitting Ten Broeck homogenizer, and the homogenate was centrifuged at 600 × *g* for 10 min. The resultant residue was washed twice with sucrose, and the washings together with the original supernatant fraction were saved for analysis. The above sample preparation was carried out at 0–4°C and kept at this temperature until assayed. Microscopic examination indicated that a few homogenates (usually of stages 20–25) contained a small number of whole cells, and all preparations were completely free of yolk granules.

Each sample was assayed for the different enzymatic activities and protein content. The cytochrome *c* reductases were determined spectrophotometrically at 23–25°C using the method of Lehman and Nason,[4] and the reduction of cytochrome

c measured at 550 mμ in the presence of DPNH, TPNH, or sodium succinate was used as a measure of the different reductases. Cytochrome oxidase was assayed by the method of Cooperstein and Lazarow;[5] cyanide controls were run for each sample. A unit of both reductase and oxidase activity was defined as a change of 0.001 optical density units at 550 mμ per min, and the initial rate of change was determined and was proportional to protein concentration determined by the method of Lowry *et al.*[6] Conditions of substrate saturation were used in the enzyme assays, and all results were corrected for the endogenous rate which was generally less than 20% of the total activity. Cytochrome *c* and the reduced pyridine nucleotides were of greater than 90% purity and obtained from the Sigma Chemical Company.

Results.—Since the enzymatic activities are expressed in terms of milligram protein, it was necessary to determine the protein content of the samples during development. The data in Figure 1 indicate that the protein content, 410 ± 15

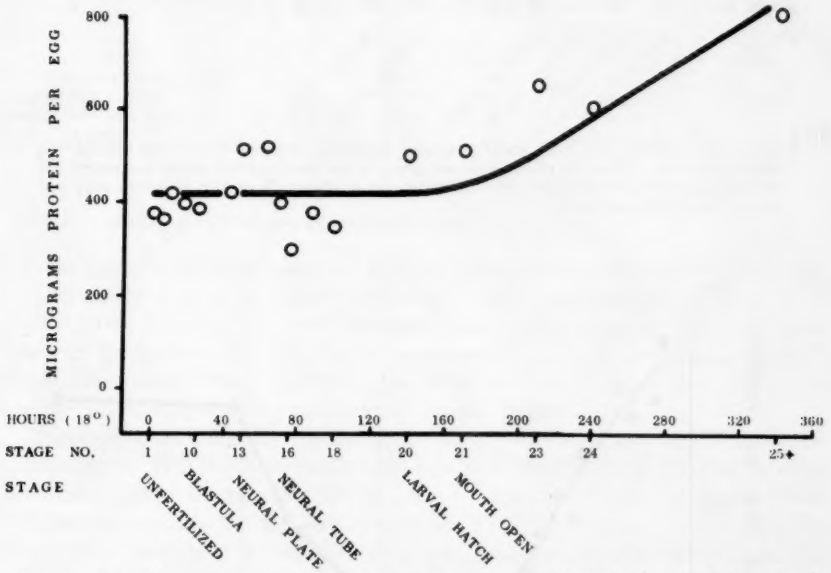

FIG. 1.—Protein concentration during frog embryogenesis. Method of analysis is given in the text. Each point represents the average value of 3–6 samples with the exception of stages 24 and 25 in which only one sample each was analysed.

mcg per embryo, is constant until hatching. From that time through stage 25 the content increases. Consequently differences in specific activity during embryogenesis are due to changes in enzymatic activity rather than protein concentration. Since the protein level is constant, the index, units per embryo, can also be used as an expression of specific activity.

The reductase activities are presented in Figure 2. DPNH-cytochrome *c* reductase was high in the unfertilized egg and in the early embryonic stages, declining slightly from stages 1 to 14. From stages 15 through 18, however, the activity decreased 75 per cent and continued at this low level until hatching, stage 21.

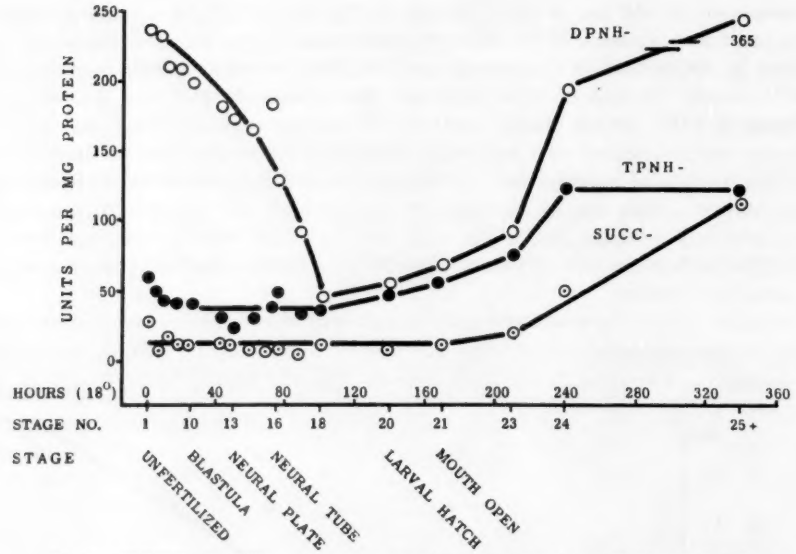

FIG. 2.—DPNH-, TPNH-, and succino-cytochrome *c* reductase activities during frog embryogenesis. Methods of analysis are given in the text. Each point represents the average value of 3–6 samples with the exception of stages 24 and 25 in which only one sample each was analysed.

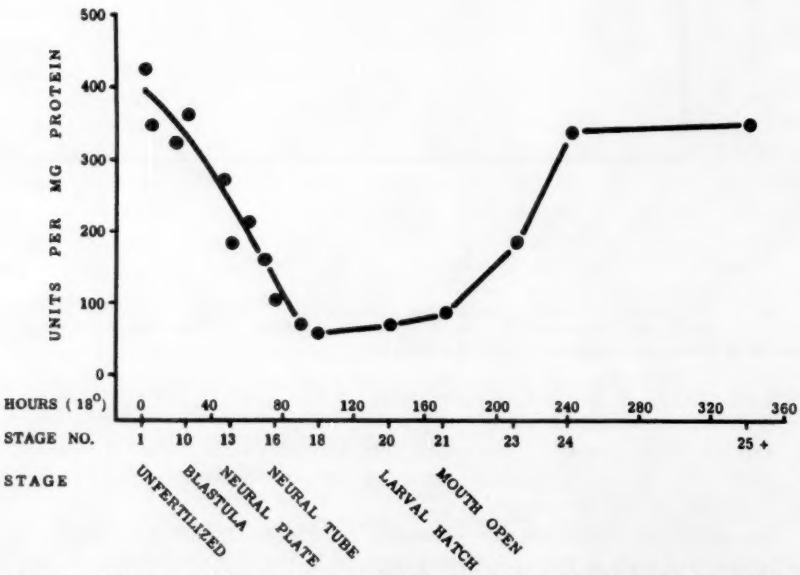

FIG. 3.—Cytochrome oxidase activity during frog embryogenesis. Methods of analysis are given in the text. Each point represents the average value of 2–6 samples with the exception of stages 24 and 25, in which only one sample each was analysed.

Henceforth the activity increased and at stage 25 was higher than the initial value. A similar pattern was observed for cytochrome oxidase as shown in Figure 3, except that the increase in post-embryonic stages was less. The marked decreases in activity of these two enzymes during neurulation (stages 15–18) were observed consistently in separate batches of eggs from five different females.

The TPNH-cytochrome *c* reductase level was lower than that of the DPNH-enzyme and remained constant until the time of hatching, when it increased almost threefold at stages 24 and 25. Succino-cytochrome *c* reductase activity was barely detectable during embryogenesis but likewise increased after hatching.

In view of the variation observed between batches of eggs, the validity of the slight decrease in DPNH-cytochrome *c* reductase and cytochrome oxidase during early embryogenesis was questioned. The data for these two enzymes were grouped as shown in Table 1 and analyzed by standard statistical procedures. It was found

TABLE 1

CYTOCHROME REDUCTASE AND OXIDASE DURING FROG EMBRYOGENESIS

Stage	Stage (no.)	Age (hr)	No. of samples	DPNH-cyt. *c* reductase (Units/mg. protein)	Cytochrome oxidase (Units/mg. protein)
Unfertilized: mid-gastrula	1–11	0–35	23	221 ± 13.0*	366 ± 24.5
Late gastrula: rotation	12–15	37–75	16	172 ± 10.0	208 ± 15.2
Neural tube and tail bud	16–17	72–94	9	117 ± 24.4	94.4 ± 13.3
Muscular response: hatching	18–21	93–173	12	54.8 ± 4.69	70.9 ± 8.25
Larval	22–23	192–216	5	87.0 ± 13.4	179 ± 50.3
	24	240	1	190	334
	25	334	1	365	344

* Mean, ± standard error of the mean except stages 24 and 25.

that the initial DPNH-cytochrome *c* reductase level up through gastrulation (stages 1–11) is different from that in stage 12–15 ($P < 0.01$) and in stages 16–17 or 18–21 ($P < 0.001$). Similarly the cytochrome oxidase concentration in the same initial stages is significantly decreased in the subsequent stages (all having a $P < 0.001$). These data demonstrate, therefore, that these two enzymatic activities decrease slightly during stages 1–15 and markedly during stages 15–18.

The relative activities of DPNH-cytochrome *c* reductase and cytochrome oxidase in reference to TPNH-cytochrome *c* reductase are shown in Table 2. During early development until neural tube closure (stages 1–15) the DPNH-reductase activity is approximately 5 to 6 times greater than the TPNH-reductase activity. During neural tube closure and tail bud formation (stages 16 and 17), the DPNH-reductase

TABLE 2

RELATIVE CYTOCHROME REDUCTASE AND OXIDASE ACTIVITIES DURING FROG EMBRYOGENESIS

Stage	Stage no.	Age (hr)	Relative Activity*: DPNH-cyt. *c* reductase	TPNH-cyt. *c* reductase	Cytochrome oxidase
Unfertilized: mid-gastrula	1–11	0–35	5.01	1.00	9.25
Late gastrula: rotation	12–15	37–75	6.30	1.00	8.22
Neural tube and tail bud	16–17	72–94	2.68	1.00	2.17
Muscular response: hatching	18–21	93–173	1.18	1.00	1.53
Larval	22–24	192–240	1.25	1.00	2.55
	25	334	3.04	1.00	2.86

* Data represent averages of 6–23 samples per group except for stage 25 which is a single sample.

was only 2 to 3-fold greater, and from tail bud until post hatching (stages 18–24), the two reductase activities were approximately the same. Although an increase in DPNH-reductase activity is shown at stage 25, its significance is questionable since only one determination was made. The relative activity of cytochrome oxidase changed in a similar manner. It is of interest that succino-cytochrome *c* reductase was less than 10–30 per cent of the TPNH-reductase activity throughout development.

Factors affecting enzymatic activities: The observed changes in enzymatic activity may be attributable to various factors. In addition to obvious changes in apoenzyme content, differences in the intracellular distribution and structural organization may alter the measurable activity. It is also possible that activators and inhibitors may be present and will affect activity in a manner similar to that due to changes in amount of enzyme. A series of experiments was undertaken in an attempt to resolve some of the more obvious factors which may be responsible for the observed activity changes. In these experiments samples of high activity (stages 12 and 13) were compared with those of low activity (stages 17 and 18).

The reductase activities were unaffected by homogenization in water, 0.25 *M* sucrose, or 0.50 *M* sucrose; or by the addition of the surfactant, Triton X-100. However, freeze-thaw treatment of homogenate and subcellular fractions resulted in a lowering of reductase activities, and storage of the homogenate at 0°C for 30 hr or 23°C for 4 hr produced a 60 per cent reduction of DPNH- and TPNH-cytochrome *c* reductase activities.

To determine whether activators or inhibitors were present, homogenates prepared from stages of high and of low activity were combined and compared with their individual activities. The results revealed that the mixture expresses a summation of the individual activities. Since treatment of these samples by techniques designed to demonstrate the influence of structural organization, latency, and activators or inhibitors were ineffectual, the data suggest that changes in apoenzyme content are responsible for the activity changes.

Distribution of activity in the embryo: One objective of the localization experiments was to determine a possible relationship between the marked decrease in enzymatic activity and the morphological change occurring during neurulation. In addition, information on the distribution of activity in the embryo would be obtained. Samples of embryos of stages 13, 16, and 18, which include the period of neurulation, were dissected as follows: The dorsal region was separated from the ventral, yolk-filled area, and both sections of the same eggs were compared to whole eggs. The dorsal region of stage 13 consisted primarily of the neural plate whereas the dorsal section of stages 16 and 18 included head, neural tube, and somites. Each sample was analyzed for DPNH- and TPNH-reductase activities. The results are shown in Table 3.

The specific activities (units per milligram protein) of both enzymes were higher in the dorsal regions of all stages than in either the ventral section or the whole embryo. This greater concentration of activity is consistent with the fact that at this developmental stage the most active portion of the embryo from a morphogenetic viewpoint is the dorsal region which contains the neural tissue. However, the enzymatic activities found in each region (units per embryo) are approximately equal and indicate that the low specific activity found in the ventral areas is due

TABLE 3

DISTRIBUTION OF CYTOCHROME *c* REDUCTASES IN THE FROG EMBRYO

Stage no.	Sample	Cytochrome *c* reductases			
		DPNH- (Units/mg. protein)	TPNH- (Units/mg. protein)	DPNH- (Units/embryo)	TPNH- (Units/embryo)
13	Whole	67	14	56	12
	Dorsal region* (neural plate)	137	91	19	11
	Ventral region*	103	30	24	6
16	Whole	28	20	22	16
	Dorsal region (neural tube and brain)	98	60	12	7
	Ventral region	32	25	11	9
18	Whole	14	7	12	4
	Dorsal region (neural tube, head, and somites)	96	36	11	4
	Ventral region	36	0	7	0

* Vitelline membranes and perivitelline fluids were removed.

to a higher protein content rather than lower activity. Since the ventral region has a greater concentration of yolk, the high protein content in this region may be due to soluble yolk protein which would be included in our sample preparations. It is possible, therefore, that the concentration of enzymatic activity per milligram protein of completely yolk-free embryos may be actually the same.

Intracellular localization: The intracellular distribution of the reductases was determined in stages 12, 13, and 18. Differential centrifugation procedures using 0.25 *M* sucrose were employed to obtain nuclear, mitochondrial, microsomal, and supernatant fractions. These data, in general, reflect a distribution common to that reported for mammalian tissues; namely, DPNH- and succino-cytochrome *c* reductase were concentrated in the mitochondrial fraction, and TPNH-cytochrome *c* reductase, in the microsomal fraction. The data are insufficient to evaluate any changes in distribution during development.

Discussion.—Embryonic development cannot be defined easily by usual biochemical parameters. Deoxyribonucleic acid content and cell number, for example, are described by an increasing curve of exponential nature.[7] On the other hand the total nitrogen[8] and protein concentration remains constant during frog embryogenesis. Our data on DPNH-cytochrome *c* reductase and cytochrome oxidase activities in terms of units per milligram protein present still another pattern. This activity curve decreases during the early developmental stages, falls markedly during neurulation, and remains at a low level until larval emergence when the activity increases and attains a magnitude at least as high as the initial values. This decrease in two enzymes of metabolic importance is particularly unusual, for the general pattern of enzyme development during embryogenesis is an increasing curve. This emphasizes the possible importance of losses as well as gains in enzymatic activity as a phenomenon of embryonic differentiation.

Previous studies of respiratory enzymes in the amphibian embryo have been concerned primarily with cytochrome oxidase and succinoxidase. Since succinoxidase is an over-all measurement of an electron transport pathway in contrast to succino-cytochrome *c* reductase as determined in this study, comparison is difficult. Spiegelman and Steinbach[9] found that cytochrome oxidase was constant throughout development of *R. pipiens*, whereas Boell and Weber[10] observed an increasing activity in *Xenopus laevis*. This discrepancy may be due to differences in experimental procedure or biological species. Although both groups used manometric

methods of assay with *p*-phenylenediamine and cytochrome *c* as substrates, the former prepared their samples at temperatures "below 25°C" and assayed at pH 6.5. No data were presented to indicate the validity of these conditions.

Our cytochrome oxidase data which describe a different pattern from either of the forementioned, may perhaps also be explained by differences in assay method. The microspectrophotometric method employed by us is sensitive, utilizes a non-autoxidizable and naturally occurring substrate, has a small endogenous rate correction, and requires less than two minutes' exposure of the samples to room temperature. This procedure enabled the rapid determination of initial oxidation rates and avoided the possible inactivating effects of incubation at 25° or higher, an intrinsic characteristic of the manometric methods used above. Our own data on other tissues, as well as that of others,[11] indicate that cytochrome oxidase activity is rapidly destroyed in less than one hour at 25°, but is stable for at least six hours at 0°.

In order to measure total activity of the various enzymes, which are localized in different intracellular fractions, homogenates instead of mitochondrial preparations were studied. However, these homogenates were cleared of cell wall debris, nuclei, and yolk granules to remove as much metabolically inactive material as possible. Preliminary experiments comparing cleared homogenates with dissected components of the egg, such as the jelly coat and perivitelline membranes and fluid, and with whole egg homogenates indicated little if any difference in activity.

One objective of this investigation was to examine the relative contribution of several individual respiratory enzymes to electron transport. According to the results, the main pathway appears to be via DPNH-cytochrome *c* reductase and cytochrome oxidase, for the activities of TPNH- and succino-reductase are very low throughout embryogenesis. The rate-limiting step under our assay conditions of substrate saturation is probably between DPNH and cytochrome *c* except during stages 16 and 17 (see Table 1) when the DPNH-reductase and cytochrome oxidase activities are approximately equal. We were unable to demonstrate pyridine nucleotide transhydrogenase activity using depleted mitochondria or DPN-analogues.

The U-shaped enzyme curves described by DPNH-cytochrome *c* reductase and cytochrome oxidase in Figures 2 and 3 are analogous to those found in our earlier experiments on the mosquito pupa. This metamorphic insect stage is a period of active differentiation and has some other similarities to the frog embryo. Although a correlation between the ratio of DPNH- to TPNH-reductase and growth stages was observed in the mosquito, the significance of the ratio changes in regard to the various differentiation processes of frog embryogenesis is difficult to interpret.

The significant and considerable decrease in DPNH-cytochrome *c* reductase and cytochrome oxidase activities during neurulation is of particular interest. It could be assumed on the basis of the failure to demonstrate latency or inhibitors and activators and the presence of excess amounts of substrates and cofactors in the assay medium that the observed activities are due to changes in apoenzyme concentration. Although such a conclusion requires some temerity and may be proved to be fallacious upon further investigation, it seems reasonable at the present time.

The decreases correlate very well with the fall in oxygen consumption of *R. pipiens* breis during the same developmental period as described by Spiegelman

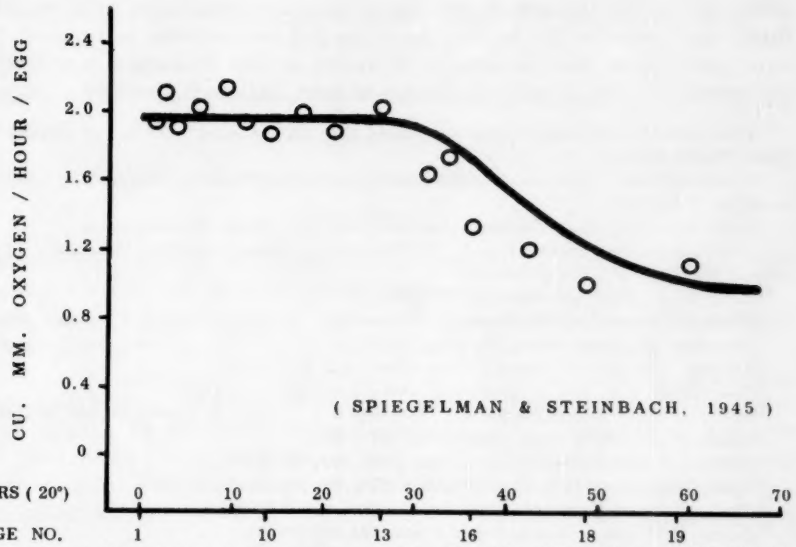

FIG. 4.—Respiration rates during frog embryogenesis. The data of Spiegelman and Steinbach[9] have been replotted but are otherwise unaltered.

and Steinbach[9] and shown in Figure 4. In their experiments the frog embryos were incubated at a temperature the same as ours. Our findings may provide a partial explanation for the diminished oxygen uptake. A different oxygen consumption curve was observed by Gregg and Ray[12] who used embryos incubated at temperatures ranging from 8–25°C. Their curve indicated a low oxygen-consumption rate during early embryogenesis and might be explained by the data of Hopkins and Handford,[13] which demonstrated that oxygen uptake is reduced markedly in cold-reared early embryos.

According to the present results, the enzymatic pathways for producing energy by means of electron transport and oxidative phosphorylation are at a low level during later embryogenesis. It is interesting to note, however, that this low activity appears to be concentrated in the dorsal region, which is a morphogenetically active center during this period of neural tube closure and initiation of muscular activity. Whether or not the decrease in energy-producing enzymes can be interpreted as a diminished requirement for energy during this embryonic period is an open question.

The results presented are of a preliminary nature. Elucidation of the biochemical mechanisms involved must await further experimental inquiry.

Summary.—The enzymatic activities of DPNH-, TPNH-, and succino-cytochrome *c* reductases and cytochrome oxidase were determined in homogenates of *Rana pipiens* of different stages of embryonic and early larval development. Similar U-shaped activity curves were observed for DPNH-cytochrome *c* reductase and cytochrome oxidase, and the lowest activity levels occurred during the period from neurulation to larval hatching. These changes coincide with oxygen consumption data obtained by others. TPNH- and succino-cytochrome *c* reductase

activities were low throughout embryogenesis and increased after larval hatching. Other results describe the localization of the different activities and provide presumptive evidence that the activity differences are due to changes in apoenzyme concentration. The possible significance of these findings is discussed.

* This work was supported in part by grants from the National Institutes of Health, U.S. Public Health Service.

† Present address: Department of Biochemistry, School of Medicine, University of Louisville, Louisville 2, Kentucky.

‡ Senior Research Fellow, National Cancer Institute, U.S. Public Health Service.

The following abbreviations are used: DPNH, reduced diphosphopyridine nucleotide; TPNH, reduced triphosphopyridine nucleotide.

[1] Lang, C. A., *Exptl. Cell Research*, **17,** 516 (1959).

[2] Rugh, R., *Experimental Embryology* (Minneapolis: Burgess Publishing Company, 1948).

[3] Shumway, W., *Anat. Record*, **78,** 139 (1941).

[4] Lehman, I. R., and A. Nason, *J. Biol. Chem.*, **222,** 497 (1956).

[5] Cooperstein, S. J., and A. Lazarow, *J. Biol. Chem.*, **189,** 665 (1951).

[6] Lowry, C. H., N. J. Rosebrough, A. L. Farr, and R. J. Randall, *J. Biol. Chem.*, **193,** 265 (1951).

[7] Grant, P., *J. Cellular Comp. Physiol.*, **52,** 227 (1958).

[8] Gregg, J. R., and R. Ballentine, *J. Expti. Zool.*, **103,** 143 (1946).

[9] Spiegelman, S., and H. B. Steinbach, *Biol. Bull.*, **88,** 254 (1945).

[10] Boell, E. J., and R. Weber, *Exptl. Cell Research*, **9,** 559 (1955).

[11] Layne, E. C., and A. Nason, *J. Biol. Chem.*, **231,** 889 (1958).

[12] Gregg, J. R., and F. L. Ray, *Biol. Bull.*, **113,** 382 (1957).

[13] Hopkins, H. S., and S. W. Handford, *J. Exptl. Zool.*, **93,** 403 (1943).

SYMPOSIUM ON RESEARCH FRONTIERS IN SOLAR ENERGY UTILIZATION

By Invitation of the Committee on Arrangements for the Annual Meeting

Presented before the Academy, April 24, 1961

Farrington Daniels, *Chairman*

CONTENTS

Introduction—Survey of Research Fields and Needs *Farrington Daniels* 1245
Solar Energy in the Exploration of Space . . . . . .
. . . . . *Hugh L. Dryden and A. E. von Doenhoff* 1253
Research on the Use of Solar Energy Made in the Soviet Union . . .
. . . . . *V. A. Baum* 1262
Solar Collectors, Selective Surfaces, and Heat Engines . . *H. Tabor* 1271
Fundamental Problems in Solar Distillation . . *George O. G. Löf* 1279
The Storage of Heat and Electricity. . . . . *Bertrand A. Landry* 1290
Photochemical Utilization of Light Energy. . . . *Eugene Rabinowitch* 1296
Photoelectricity. . . . . *Paul Rappaport* 1303

INTRODUCTION—SURVEY OF RESEARCH FIELDS AND NEEDS

By Farrington Daniels

Solar Energy Laboratory, University of Wisconsin

The purpose of this symposium is to encourage research which may lead to new ways of using the sun's energy. Economic restrictions based on present American practice will not be considered. Another symposium at Rome in August, sponsored by the United Nations will be concerned with practical applications. Immediate use of solar energy will not come soon in industrialized countries, but it could come now in nonindustrialized countries where fuel is scarce and electricity is expensive.

This symposium is organized to bring out new ideas rather than to record the progress of the past. It involves many different sciences and thus it is appropriate that it be sponsored by the National Academy of Sciences.

At present, there is plenty of combustion fuel and food in the industrialized countries but the abundance may well be temporary. The population expansion and the increasing demands for more power per person in both industrialized and nonindustrialized countries are hastening the time when substitute sources of energy must be developed. We should undertake research now to meet these future demands.

There is an ample supply of solar energy and 15 square feet of it is equivalent to about 1 kw of heat or to 50 watts of electricity if the conversion of heat to electricity is 5 per cent efficient.

Solar energy is certain to work. There is no scientific nor technological gamble

as there was in the development of atomic energy and as there is now in the development of thermonuclear energy. The problem is one of economics and adaptability. Attempts to use the sun in the past to run machines were not continued in competition with cheap combustion fuel. But now we have new reasons for reexamining the situation and encouraging the efforts of scientists and engineers. We have new materials to work with, such as inexpensive sun-permanent plastics, and new semiconductors of high purity; and we realize, as we have not realized before, the opportunity which exists for helping the nonindustrialized countries. Another reason for emphasizing research in solar energy is that it can be undertaken effectively by small nations without heavy expenditures of funds and without new and highly specialized techniques.

In the United States, very little effort has been devoted thus far to solar energy research. Recently, however, the program for space exploration has led to large investments in finding new ways to use the sun's energy directly. These are discussed in this symposium by Dr. H. L. Dryden and Dr. A. E. Von Doenhoff. Years ago, the government's development of Diesel engines for submarines led to the later use for railroad trains, and its development of atomic energy led to new sources of industrial power. The government's large scale support of solar energy research for space studies is likely to speed the practical use of the sun's energy on earth.

We are fortunate to have participating in our general symposium Dr. V. A. Baum, who summarizes research on solar energy in the USSR.

Future Solar Fuels.—Let us first consider likely fields for long-range research anticipating the time when our fossil fuels may no longer be sufficient for our needs. As emphasized already, these discussions are not limited to practical plans for present application.

The arid regions of our southwestern states and the large deserts of the Sahara and of northern Chile could supply enormous quantities of energy as heat, electricity, and transportable chemicals. At five per cent conversion, a square mile of sunshine could give about 90,000 kw of electricity. In these regions, raw starting materials will be limited. They must be almost free and automatically transportable. One naturally turns to water and carbon dioxide which were the starting materials for all our present fuel. One can imagine drawing large volumes of desert air through absorption towers of silica gel or other desiccants to take up the moisture and then recovering the water as liquid by heating with focused solar energy and condensing the water vapor. The water can be converted by electrolysis with solar-generated electricity into hydrogen, which can be transported in pipe lines beyond the 300- or 400-mile present limit of electric transmission lines.

The hydrogen can be combined with carbon dioxide to give useful and transportable organic chemicals and fuels such as methanol. The carbon dioxide can be obtained by drawing large volumes of air (0.03 per cent CO_2) through towers of oxides or carbonates and recovering pure carbon dioxide at high pressures by heating with focused sunlight. Here again research is needed.

Another approach is to combine hydrogen from solar-electrolyzed water with atmospheric nitrogen to give ammonia by the Haber process. Ammonia can be transported in pipes or tanks and it can be oxidized to nitric acid. It can be partially oxidized to give concentrated solutions, 70 per cent of ammonium nitrate

in liquid ammonia, with pressures of ammonia which at room temperature are less than one atmosphere. These solutions can be transported and they could be used for monopropellants in rockets and other devices. It may be worth-while to explore the possibility of using this concentrated solution of ammonium nitrate in ammonia as an engine fuel injected intermittently. The small volume of liquid injected without air and without mixing devices expands on thermal decomposition to a large volume of gas consisting of nitrogen and steam. Investigations of its safety will be needed.

Solar Collectors.—For most purposes, it is necessary to use the solar energy at elevated temperatures. In one type of solar collector, flat, black plates in a fixed, inclined position facing south are covered with one or more transparent sheets of glass or plastic which hold back the infrared radiation of the heated plate and trap the heat. It is possible to obtain temperatures in the neighborhood of 100°C. In another type, movable focusing collectors are used to give much higher temperatures on a small receiving surface. Large parabolic mirrors made with optical precision can give concentration ratios of over 5,000 and temperatures above 3,000°C. Cheaper parabolic collectors may be easily made of plastics and aluminized mylar to give concentration ratios of around 200 and temperatures in the neighborhood of 500°C. Cylindrical focusing collectors give lower temperatures.

There are many research problems involved in the improvement of these collectors. The aluminized plastic collectors usually have efficiencies of only a little better than 50 per cent due to microimperfections in the reflecting surface, macroimperfections in the collector area, and distortions in the shape of the collector. Practical ways of greatly improving the reflectivity and focusing are needed. New methods for making molds and applying the plastics and reflecting surfaces should be studied. Practical and inexpensive ways of mounting the focusing collectors and tracking the sun are needed. The structural mountings have to withstand strong winds, and the collectors need to be easily cleaned from dust accumulation.

Thin, transparent plastic coverings are much cheaper than glass and are more easily transported and mounted. Older plastics deteriorated after a year or more of exposure to sunlight, but new plastics are now available which will withstand many years of weathering. In one type, an ultraviolet-absorbing dye is incorporated in the plastic to screen out light which produces photodecomposition. Plastic sheets of completely fluorinated organic material are now available which are estimated to withstand sunlight and weathering for 20 years.

Solar Heating.—The simplest use of solar heating is in cooking. Plastic cookers four feet in diameter with a framework of light steel tubing (electric conduit tubing) are capable of bringing a liter of water to boiling in 15 min. They have been tested in Mexico. There are problems of technical performance, economic cost, and social acceptance. Anthropologists have been helping with the field tests.

The natural disadvantage of a solar cooker is that it cannot be used indoors or in cloudy weather or in the evening. There is a strong incentive to try to develop a practical device which can be exposed to the focused sunlight for an hour or two and in which the heat can be stored for transfer and use in the kitchen a few hours later.

Solar water heating is now used in Florida and Japan and elsewhere. Metallic water pipes are soldered to the back of a flat, black metal sheet on the roof. A

double metallic sheet has been developed with welded seams which are expanded with hydraulic pressure to give water channels with the maximum heat transfer and the minimum labor of installation. An inexpensive portable water heater of plastic is available.

Solar heating, with provisions for stored heat, has been tried in only a few experimental houses. Circulating air or water may be used. The capital investment for long heat storage is high and supplementary heating with fuel is advised in cold or cloudy areas. Another problem is that of making a collecting surface of several hundred square feet architectually acceptable.

There is a widespread need for research on the solar heating of small houses with inexpensive plastic collectors in areas where fuel is scarce. One of the problems is the circulation of air when standard electric power is not available.

The solar drying of hay and agricultural crops is another field which merits research attention.

From the point of view of conserving our national resources, valuable fossil fuels should not be used for low-temperature heat and for manufacturing operations if there is an opportunity to use solar heat. These fuels should be used for high-temperature engines or as a source of petrochemicals.

Selective Radiation Surfaces.—In solar heating, it is desired to keep the heat losses as low as possible and thus permit attainment of higher temperatures. Dr. H. Tabor, who pioneered in the development of selective radiation surfaces, discusses the possibilities. Some thin, black coatings of the order of 10^{-5} cm thick, overlying bright reflecting metallic surfaces have high absorptivity for the solar radiation and yet, when heated, do not emit much radiation because in the neighborhood of 10 μ the wave length is many times the thickness of the black surface coating. A permanent surface with about 85 per cent absorptivity of solar radiation and 20 per cent of infrared emissivity is produced by electroplating with bright nickel and then with a very thin layer of copper. The copper is oxidized in air by heating in an oven, or by focused sunlight, to produce the black oxide. Nickel and cobalt oxides are also satisfactory, and for temperatures of 1000°C cobalt oxide on platinum is good.

There are many problems to be solved. The basic theory and the effect of particle size need further study. Organic materials cannot be used at high temperatures because they burn up. For use in space vehicles, where there is no oxygen, the black oxide must not dissociate appreciably, because when an atom of oxygen is lost it is not replaced, as it is in air. Both the dissociation constant and the rate of dissociation are involved.

Storage of Heat.—Because of the intermittent nature of sunlight, it is necessary for most purposes to store the heat. Dr. B. A. Landry discusses research opportunities in the storage of heat and power. Large water tanks may be used for heat storage. Pebble beds are good because they have such effective heat exchange with a stream of air flowing through them and because they have low heat conductance through the limited areas of contact between spheres. Moreover, they are simple and inexpensive to construct and maintain.

Large shallow ponds of water under suitable conditions can be heated to high temperatures after many days of solar heating, and they hold their heat so that they may be used night and day for continuous operation of low-temperature tur-

bines. Dr. Tabor and others are working on these power ponds.

Chemical systems are capable of large heat storage because the heats of reaction are considerably greater than the heat which is stored by heat capacity alone. It is necessary to have a reversible reaction which proceeds with the absorption of heat at a high temperature and with emission of heat at a lower temperature. Hydrated sodium sulfate loses its water of crystallization, for example, at temperatures above 32.3°C and rehydrates with the evolution of about 50 calories per gram at temperatures below this. Studies of nucleation are necessary for the continuous operation without developing supersaturation over thousands of cycles. Many other chemical reactions should be explored. It is necessary to have a reaction which will reverse itself over a temperature range that is not too large, and yet it is desirable to choose a reaction which evolves a large amount of heat. These two requirements tend to be incompatible. The range of possibilities is increased by accepting the complication of a two-vessel system in which the products are separated by heating and then stored, to be recombined by mixing at a later time. For example, water may be driven out of calcium hydroxide at a high temperature to give calcium oxide and the reaction reversed later at a lower temperature.

Solar Cooling.—At present, refrigeration and air conditioning usually require electric power and expensive equipment. A large demand would develop if solar cooling could be made practical. Solar air conditioning would require a solar collector on the roof about equal in area to the floor space to be cooled. The absorption-desorption principle is simple. A volatile material is vaporized out of a solution by solar heating and is condensed under pressure in another part of a closed system. The solution is then allowed to cool and the condensed liquid is reabsorbed. In vaporizing, the liquid cools the insulated box in which it is contained. Intermittent operation, involving the vaporization of the liquid from the condenser to the solution, is the simplest procedure, but a continuous operation can be readily arranged with pumps and a more complicated system. One system uses ammonia driven out from water with a focusing solar collector. Other systems use low-boiling freons dissolved in high-boiling ethers. Extensive physical chemical measurements have just been completed by Dr. G. C. Blytas on concentrated solutions (up to 70 per cent) of sodium thiocyanate dissolved in liquid ammonia. Such highly concentrated solutions have some of the properties of fused salts. The vapor pressures are low, thus simplifying the construction of the equipment. Experiments are underway to use this system for solar cooling. Many other solutions should be studied for absorption-desorption cooling.

Another approach to solar cooling is by the evaporation of water or a more volatile liquid, using absorption in silica gel, lithium bromide, or other drying agent, followed by rejuvenation of the desiccant with solar heating.

Salt Water Distillation.—Solar distillation is one of the ways being investigated for the production of fresh water from salt water. The principles are thoroughly discussed in this symposium by Dr. G. O. C. Löf, and some estimates for use in the USSR are given by Dr. Baum. One of the problems is to cover a large area with transparent enclosing material at a sufficiently low price. Sloping, condensing roofs of glass plates or plastic condense and collect the pure water. In another system, air is swept over the solar-heated water and the moisture is condensed out in a water-cooled condenser. In some cases, multiple stills can be used if the

temperature of the salt water is high enough, thus using some of the heat of condensation to help evaporate more water. Inclined cloth wicks saturated with flowing salt water have been used. Often in crowded communities flat land is not available and stills, which can be set on sloping hills, are preferred.

Heat Engines.—Although steam can be readily generated by focused solar heat, small steam engines of 1 kw and less are very inefficient. Dr. Baum describes solar steam engines briefly. A hot air engine operated with focused sunlight was proposed by Ericsson nearly a century ago. Stirling hot-air engines operated by solar energy are being planned for space use. An improvement is being studied by Finkelstein, Utz, and Braun in which the solar energy is focused directly into the interior of the engine chamber through a transparent window, thereby eliminating one of the chief difficulties in getting sufficient heat transfer through the opaque engine head and its accompanying air films. Small hot-air engines appear to be capable of higher efficiencies than small steam engines and they are simpler to operate. Still greater improvements in heat engines might be made if a radiation-absorbing gas similar to iodine can be used instead of air.

Solid Converters of Solar Radiation into Electricity.—Thermocouples are extensively used in research and industry for converting heat into electricity, and photographic exposure meters are widely used for converting sunlight into electricity. The problem has been to increase the efficiency of the conversion into electricity. This problem has been largely solved in the last five to ten years through basic research in solid-state physics on semiconductors. The efficiencies in both thermoelectricity and photovoltaic electricity have been increased by a factor of more than ten. The advances depend on theories of semiconductors and on the use of new techniques for producing highly purified materials and adding specific impurities.

Thermoelectric converters require two different materials which give a high thermoelectric force when one junction is hot and the other is cold. The materials need to have high electrical conductance, low thermal conductance, and high melting points. Elements such as bismuth, lead, germanium, combined with arsenic tellurium, selenium, sulfur, and oxygen containing added impurities are among the materials now being studied. One of the problems is the permanence of the thermoelements at high temperatures. There is a tendency for the impurities to diffuse from regions of high temperature to regions of low temperature. Also there is the problem of maintaining good mechanical stability and electrical contact in spite of strains caused by many thermal expansions and contractions of unlike materials.

A considerable effort is being devoted to research and development of thermoelectric devices which will have high efficiencies combined with long life. Dr. R. R. Heickes and Dr. L. Dykstra of the Westinghouse Electric Corporation reported on progress in this field at the symposium. An expanded report of their work will be published elsewhere.

Temperatures around 500°C now make possible the conversion of heat into electricity with about five per cent efficiency. Considerably higher efficiencies have been reported for short periods of time. There is evidence for a theoretical limit of efficiency in one thermoelectric unit of 19 per cent.

Thermoelectric units have been operated with focused solar radiation, and the

pumping of water and charging of storage batteries have been demonstrated. Temperatures of 500°C on surfaces of about 25 square inches are easily obtained with parabolic focusing collectors six feet in diameter made of plastics and aluminized mylar. One of the problems involves the fact that the thermoelectric units produce direct-current electricity most conveniently at low voltage and high amperage under conditions which are not well suited for the efficient operation of small motors. One solution is to charge storage batteries in parallel and discharge them in series. Other solutions are needed.

Rapid progress has been made at the Bell Telephone Laboratories and elsewhere in the development of photovoltaic silicon cells which convert about ten per cent of sunlight directly into electricity without the consumption of any materials. Unfortunately the solar cells are quite expensive because they involve high purification, growth of single crystals with the introduction of specific impurities, and the cutting of the crystals with diamond saws. If a way can be found to use polycrystalline cells produced by vapor plating or electroplating with good electrical conductivity between the small crystals and the electrodes, the cost should be greatly reduced. Dr. P. Rappaport of the Radio Corporation of America describes the problems and the opportunities of photovoltaic cells.

Another way of obtaining electricity from solar energy is through thermionic converters. Electrons are driven out in an evacuated space from an electron-emitting surface at very high temperatures and collected on a cooled metallic surface which is very close to it. It is necessary to focus the sunlight to give temperatures of about 1,500°C, and although these temperatures can be achieved with optically perfect parabolic mirrors, they cannot easily be produced with the cheaper plastic collectors.

Storage of Energy.—The pumping of water to a higher level and storage in a reservoir for later use with a water turbine constitutes perhaps the simplest way of storing energy. On a large scale, these operations are very efficient, but in fractional kilowatt units they are less than 50 per cent efficient. Elevated reservoirs supported on structural frame work are too expensive, but in hilly country or where reservoirs can be easily placed at different levels, they may be practical.

Electric storage batteries, such as are used in automobiles are mass produced and inexpensive. Batteries for storing solar energy do not have to meet the difficult requirements of portability and heavy drains required of automobile batteries, but they do have to be subjected regularly to nearly complete discharges every day, which shortens their life. Further research is needed for producing storage batteries of low capital cost and long life.

The electrolysis of water and storage of hydrogen is inexpensive and it is about 70 per cent efficient. Hydrogen can be stored in water-displacement reservoirs, in caves, in plastic bags, and in pressure tanks. The best way would be to take up hydrogen reversibly in a solid or liquid chemical. Research is needed to find suitable organic or inorganic substances which will take up large quantities of hydrogen reversibly. In principle, the hydrogen can be stored, transported, and used, perhaps in balloons, for small trucks and tractors operating on fuel cells or internal combustion engines. Research is needed for all of these applications. The hydrogen must be converted into power with high efficiency because it is so expensive when produced by the sun with photovoltaic cells, thermoelectric de-

vices, or heat engines and dynamos.

A great deal of research is now going into fuel cells in which the materials of an electrochemical battery are fed into the battery as fast as they are consumed. The hydrogen-oxygen fuel cell is one of the more promising types and it is particularly well suited for solar use.

Thermally-regeneratable galvanic cells offer another means of producing electricity with solar heat. A chemical product results from the operation of a fuel cell, and this material is then reconverted to the reacting materials by thermal decomposition at a high temperature produced by focusing collectors.

Photochemistry.—The storage of the sun's energy through direct photochemical reactions offers challenging opportunities for research. We are just beginning to understand the mechanisms by which our foods and fuels have been made through photosynthesis in growing plants.

Three years ago, a committee was appointed by the National Academy of Sciences–National Research Council to encourage research on the "Photochemical Storage of Energy." The report of this committee has now been published and it points out the difficulties of the problem. Very few photochemical reactions are available which meet the necessary requirements of an energy-absorbing photochemical reaction that responds to most of the visible sunlight with a quantum yield near unity (i.e., one molecule reacting for each photon of light absorbed) and that can be reversed at will in the dark with the evolution of energy. The reverse reaction should proceed at just the right rate, not so fast as to give up its energy prematurely and yet fast enough to be practically useful. Moreover, it should store at least 50 to 100 calories of energy per gram. The products of the photochemical reaction may be quickly separated and mixed later when desired, or they may be kept inactive at room temperature and brought to rapid reaction by raising the temperature.

It is interesting to realize that whereas an agricultural crop in temperate climates gives two or three tons of dry organic material per acre per year, it is *theoretically* possible to produce three tons of product *per day* by an acre of sunlight if one-tenth of the solar energy is absorbed and used, if the reaction procedes with a quantum efficiency of unity, and if the product has a molecular weight of 100. No such photochemical reaction is now known.

Solar energy can be stored much more usefully in the form of electrochemical products which combine later, in the dark, at a suitable rate. If the products release electrons at one electrode and take up electrons at the other electrode, they can deliver the energy of recombination in the form of an electric current rather than in the form of heat. Professor E. Rabinowitch discusses the areas where further research might be directed in order to try to find suitable solar-produced photochemical reactions for the storage and later released of electricity or heat.

Conclusions.—We do not expect important and revolutionary practical applications of solar energy to come immediately, but we do expect them in the future.

Modest beginnings can be made now in the development of small units for economically less developed areas, and it is important to encourage basic and applied research which will help to develop practical, direct uses of the sun's energy.

SOLAR ENERGY IN THE EXPLORATION OF SPACE

By Hugh L. Dryden* and A. E. von Doenhoff†

NATIONAL AERONAUTICS AND SPACE ADMINISTRATION

All space vehicles require some source of power for operation of the instruments and the radio communication equipment which makes possible the remote recording of the data obtained. Current satellites and space probes require relatively low power; for example, Pioneer V, whose data were recorded at distances up to $22^1/_2$ million miles from the earth, carried out its mission with a power of 30 watts.

Many satellites use chemical energy stored in nickel-cadmium or silver-zinc base batteries, which have a limited life dependent on the battery weight and power requirements. Others, such as Vanguard I, use solar power, giving much longer life. Vanguard I is still transmitting after three years in orbit.

Many of the hurdles that have stood in the way of the use of solar energy for generating electric power on the earth's surface are absent in the case of space vehicle applications The difficulties of earth stations have been associated primarily with the prolonged periods of cloud cover, the relatively long periods of complete darkness at night, and the bulkiness and unwieldiness of the solar energy collectors. To provide a continuous flow of power under these conditions requires a large energy storage device. Since earth satellites may enter the earth's shadow, energy storage is also required in space applications of solar power, but the requirements can be met with less difficulty because of the shorter periods of darkness.

Solar Cells versus Chemical Batteries.—It is of some interest to make a brief comparison of solar energy devices with chemical sources. At the position of the earth's orbit, the solar radiation density is about 0.140 watts per square centimeter or 130 watts per square foot. The most frequently used conversion device is the photovoltaic silicon cell usually called simply a solar cell. These cells have relatively low efficiency because of losses of energy by reflection and transmission. It is reasonable to expect an output of about 10 watts per square foot from an oriented solar array. One specific design for a future spacecraft indicates a total weight of the complete solar power system of about 2 pounds per square foot. The net specific output is then approximately 5 watts per pound. By comparison, a silver-zinc chemical battery stores energy with a specific weight of about 50 watt-hours per pound. Since the weight of a battery is proportional to the total energy stored, whereas the weight of the solar cell source is more nearly proportional to the rated power, it is clear that a solar energy source would be far superior to a chemical battery when the power is to be used for a long time. For example, in the case cited, the solar cell array would be lighter than the silver-zinc battery if the power is required for a time longer than 10 hours.

Power Requirements for Spacecraft.—An indication of the important part played by solar energy in the exploration of space may be found from a review of the estimated electric power requirements for some present and future space vehicles given in Figure 1. Some typical spacecraft or missions and the associated power levels are given as a function of actual or probable initial launch date. Pioneer V and Tiros I were each fitted with a large number of photovoltaic silicon cells that

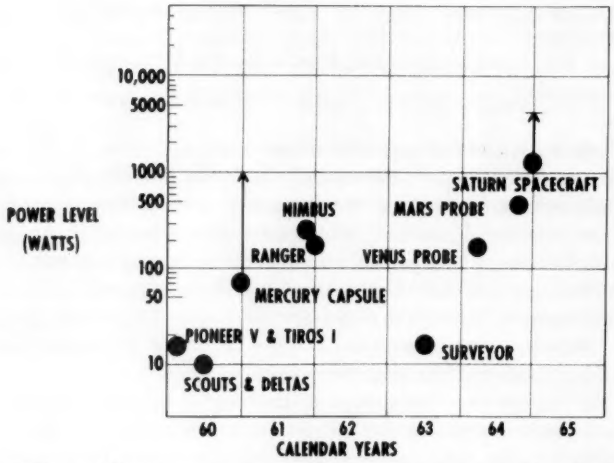

FIG. 1.—Estimated electric power requirements for various spacecraft and missions.

developed about 20 to 30 watts. The Scout and Delta boosted vehicles require 10 watts or less. The one-man Mercury capsule is intended to be a relatively short-lived vehicle. Because of the limited total energy requirement, the average power of 70 watts can most conveniently be supplied by about 150 pounds of silver-zinc primary batteries. The Nimbus meteorological satellite will require an average power of about 250 watts which will be derived from a solar cell array. The Ranger spacecraft to be launched on lunar landing missions will be fitted with over 4,000 solar cells mounted on panels. These cells will develop a little over 100 watts. They will be used for the approximately 3-day transit period from the earth to the moon. When the spacecraft is near the moon, a small capsule will be detached and landed nondestructively. Techniques have been developed that will permit reception of signals from the capsule which will transmit at a level of $^1/_4$ watt of radiated power. The power required by the transmitter is small enough for it to be operated several days with a few pounds of batteries. The Surveyor spacecraft is, like Ranger, to be launched on lunar landing missions. It is however, a more sophisticated second-generation vehicle. The power level of 15 watts shown is the average power desired after a "soft" lunar landing. The power requirements during transit are much as for Ranger and will be supplied by solar cells. The Venus and Mars probes (Mariner spacecraft) will have a configuration much like Ranger. The solar panels for the Mars probe must, however, be somewhat larger both because of the large communication distances involved and because of the decreased solar intensity at the distance of Mars from the sun. As is shown in Figure 1, it is estimated that the Saturn spacecraft power requirements will be substantially larger than for the Ranger and Mariner series spacecraft. This review, then, indicates that most of the spacecraft to be launched within the next few years will use power from the sun.

Energy Storage Requirements.—In designing a power system for a space vehicle, it is frequently desirable to have power available when the vehicle is in eclipse. It is

also desirable that the size of the solar cell array or other solar collector be determined by the average power demand rather than the peak power demand. Both of these requirements indicate the need for an energy storage device, which is usually a group of chemical batteries, charged from the solar cells while in the sunlight. For earth satellites, the size of the storage device is dictated by the maximum time the satellite can be expected to be in the earth's shadow. Figure 2 is a plot of the

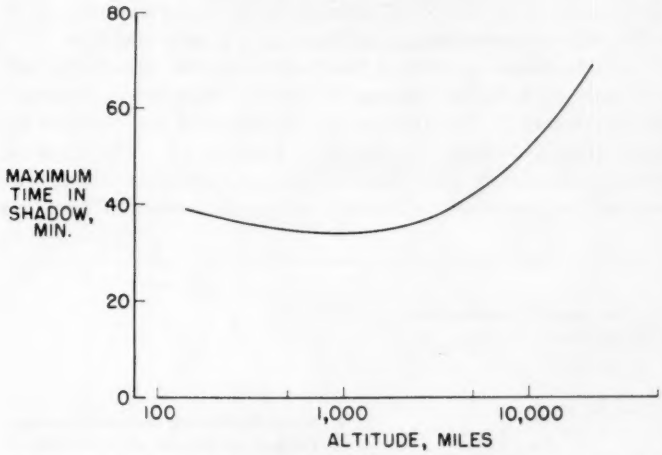

FIG. 2.—Energy storage for passage through the earth's shadow. Maximum shadow time versus altitude for earth satellites.

maximum time in shadow against altitude for circular geocentric orbits. It is seen that for altitudes up to 5,000 miles the maximum shadow time stays relatively constant at about 35–40 minutes. For very high orbits, for example, the so-called 24-hour orbit, the maximum time in shadow increases to 69 minutes.

The energy storage problem is particularly severe for long-lived near-earth satellites. A satellite in a 300-mile orbit has a period of about 90 minutes. This means that it encircles the earth about 6,000 times in the course of a year. A secondary battery with an extremely long cycle life must be chosen for such an application. At the present time, rechargeable nickel-cadmium batteries seem best suited for this purpose. A detailed analysis considering many of the significant factors that determine battery life is given by Thomas.[1] Obviously, many factors in addition to number of cycles are involved, such as the maximum permissible overcharging current and the minimum overcharge required. At the present time battery characteristics are not known well enough to predict the permissible depth of discharge as a function of battery operating conditions with a high degree of precision. However, it is clear that conditions in a low orbit are particularly severe and that the battery can only be used to a relatively small fraction of its total capacity if a long battery life is to be attained. A nickel-cadmium battery can store approximately 14 watt hours per pound. If to obtain adequate battery life it is necessary to limit the discharge to 10 per cent of capacity, then the effective specific battery weight is 1.4 watt hours per pound.

Solar Cell Deterioration.—Solar cells have proved to be reliable devices. Some evidence has, however, been accumulated which indicates that the service life of these cells may be severely limited, if the cells are subjected to irradiation by high-energy particles. Some basic work on this subject has been presented by Loferski and Rappaport.[2] It was shown that the solar output was reduced to 75 per cent of its initial value by irradiation with (1) 5×10^{13} electrons per square centimeter having an energy of 1.7 mev; (2) 3.5×10^{10} protons per square centimeter with an energy of 17.6 mev; or (3) 4.4×10^{9} alpha particles having an energy of 40 mev.

At the time this work was done, insufficient data were available on the Van Allen belts to be able to assess the effect of this radiation on the life of solar cells. More recently a study of radiation damage in satellite solar power systems has been carried out by Denney.[3] The evidence on the nature of the effects to be expected was obtained from a study of the data from Explorer VI. The Explorer VI data are particularly valuable because radiation intensity and solar cell charging current were measured simultaneously. Figure 3 shows the measured variation in solar

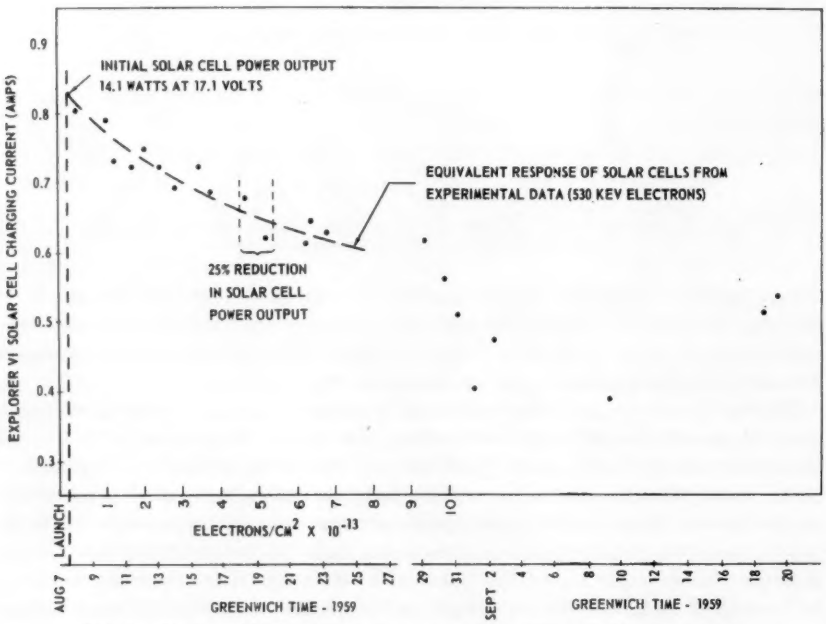

FIG. 3.—Explorer VI charging current versus time (Fig. 6 of Denney paper).

cell charging current with time for Explorer VI. On the basis of a detailed analysis,[3] Denney indicated that the primary effective radiation in this particular case was the electron flux. On the basis of an ingenious qualitative argument, he indicates that the radiation damage suffered by the cells on Explorer VI would be equivalent to that of an equal flux of 530 kev electrons. It is seen that the degradation in the performance of the cell is equivalent to that calculated on the basis of the laboratory tests. It seems likely that the reason for the ultimate failure of the power system

on Explorer VI was radiation damage to the solar cells. It seems significant that a 25 per cent reduction in solar cell output occurred in a period of only 11 days.

This rapid degradation in the solar cell performance on Explorer VI appears to be contradicted by the experience with Vanguard I which is still transmitting after 3 years in orbit. Denney offers the following explanation: typical solar cell voltage characteristics are shown in Figure 4. Increasing the temperature of a

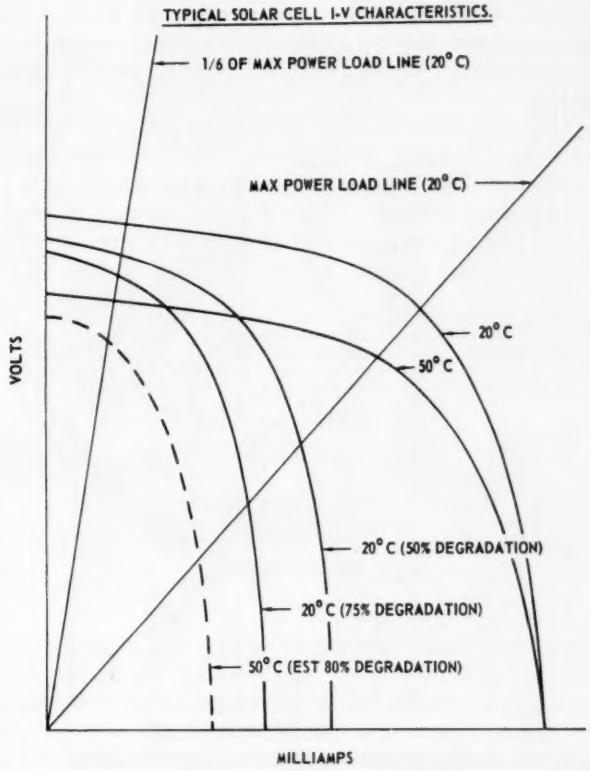

FIG. 4.—Solar cell voltage characteristics (Fig. 9 of Denney paper).

solar cell decreases the open circuit voltage but changes the short circuit current very little. The effect of radiation damage, however, is to decrease the open circuit voltage only slightly and to cause a very large decrease in the short-circuit current. A load having an internal impedance corresponding to the maximum power point would suffer a very large decrease in power absorbed as the cells deteriorated. If, on the other hand, the load impedance were much higher than that corresponding to maximum power in the original cell condition, the relative decrease in power absorption with cell degradation is very much less. This, in fact, was the case for Vanguard I. The transmitter absorbed only about one-sixth of the power available from the cells at launch. It is estimated that in spite of the heavy cover glasses over the cells, they have suffered approximately 80-per cent degradation. It

nevertheless appears reasonable that the transmitter should continue to function for some time. This is one of the rewards of a very conservative design philosophy.

A Solar Turbo-Electric System.—In addition to the photovoltaic cells there are, of course, a number of other methods of utilizing solar energy to obtain electric power. Most of these transform the solar energy into heat and then convert to electric power. Direct conversion devices such as the thermoelectric converter and the thermionic diode are of particular interest because they involve no moving parts. Development of these devices, however, has not progressed to the point where they are considered ready for application to specific missions in a solar device. The NASA is, however, developing a solar turbo-electric power source known as the Sunflower project.

One of the interesting features of this development is the method of energy storage. Energy is stored as heat. In particular, it is stored as the heat of fusion of a substance. This has the advantage of providing an essentially isothermal heat source for dark-period operation. The heat of fusion and the melting point for thermal storage materials to be used with solar heated systems are shown in Figure 5. It may be recalled that primary batteries stored energy with the specific weight

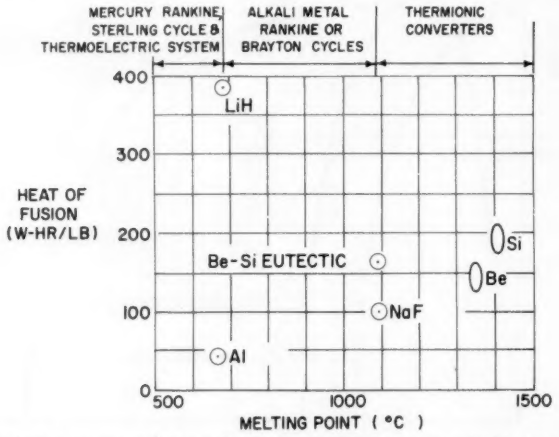

FIG. 5.—Heat of fusion versus melting point for various substances suitable for thermal storage.

of about 50 watts hours per pound. A nickel-cadmium battery had a specific storage capacity with a deep discharge of about 14 watt hours per pound and an effective multiple-cycle specific capacity of 1 to 3 watt hours per pound. The heat of fusion of lithium-hydride is shown to be 390 watt hours per pound. However, the heat of fusion must be multiplied by the thermal efficiency of the conversion cycle to obtain a proper comparison. A reasonable value for the thermal efficiency of the turbo-generator is about 10 per cent. Consequently, the comparative number for lithium-hydride would be 39 watt hours per pound. Even after allowance is made for the weight of the container, the effective specific energy storage weight of the lithium-hydride system is substantially lower than that of storage batteries.

The use of thermal storage is also advantageous for a mechanical conversion system because it permits the machinery to run continuously at constant power out-

put even during the shadow portion of an orbit. This mode of operation eliminates some severe difficulties associated with repeated starting and stopping of the system. It is indeed fortunate that not only does lithium-hydride have a high heat of fusion but also that the melting point is almost ideally suited to the use of mercury as a working fluid in a turbo-generator.

An artist's conception of the Sunflower solar turboelectric power unit is shown in Figure 6. This device is designed to generate 3 kilowatts of electric power con-

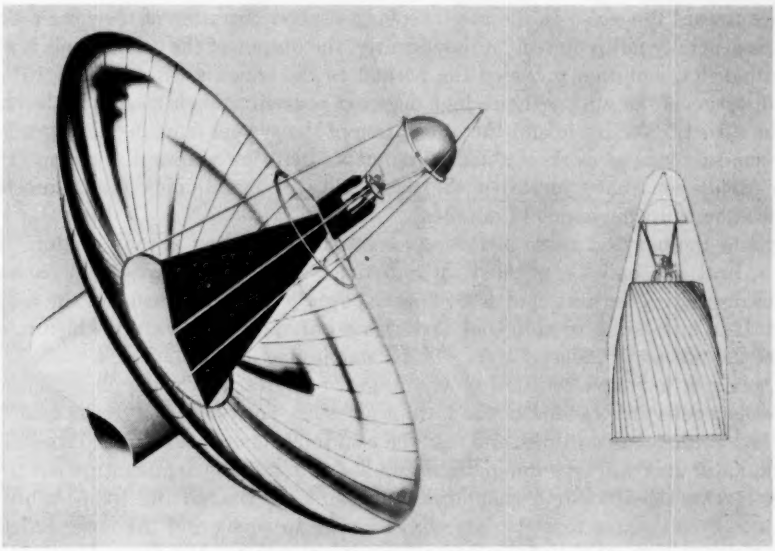

FIG. 6.—Solar turbo-electric power unit, Sunflower I.

tinuously for any circular orbit between 300 miles and 22,000 miles altitude. It is planned to be able to demonstrate a 90-day service life by 1963.

The system consists of an erectile parabolic mirror having a diameter of 32 feet in the unfolded condition. This mirror focuses the sun's rays onto the combination boiler and heat storage unit. As indicated previously the heat storage material is lithium-hydride. When the lithium-hydride solidifies it boils mercury in a tubular heat transfer unit. The hot mercury vapor then passes through the turbine and is condensed in the radiator panels. The liquid mercury is then pumped back to the boiler by a small centrifugal pump mounted on the same shaft as the turbine. In fact, the turbine, generator, and pump all operate on a common shaft supported by two mercury lubricated bearings.

The design of the large parabolic mirror poses some difficult problems. These are mainly concerned with conflicting requirements of lightweight construction and optical accuracy. In order to achieve reasonable collection efficiency, it is necessary that the collector concentrate the light in a relatively small area. If the temperature of the target is fixed as in the present case, the amount of heat reradiated out to space is directly proportional to the hot exposed target area and to the fourth power of the target temperature. The present target temperature is

approximately that of melting lithium-hydride or about 690°C. At this temperature calculations indicate that a reasonable collection efficiency can be obtained if the area of the "hot spot" of the mirror is less than one-half per cent of the total mirror area. Fortunately, this requirement puts only a modest demand on the optical quality of the mirror. For higher temperatures, such as might be required in systems using some of the alkali metal vapors as working fluids, the degree of concentration required to achieve the same collection efficiency is considerably more.

Another characteristic that deserves attention is the need for orientation of the device toward the sun. In the case of solar cells, concentration of the solar radiation is generally not required. Consequently, the output of the solar panels is not sensitive to orientation provided the normal to the panel is within about 15° of the direction of the sun. When a high degree of concentration is used as in the case of the solar turbo-electric unit the orientation of the system must be fairly precise. The sun subtends an angle of about 32 minutes when viewed from the earth. Design calculations have indicated the desirability of maintaining a sun-directed orientation to within about 15 minutes.

One of the heaviest items in the power conversion system is the radiator. In space, heat can only be rejected by radiation. The heat dissipated, of course, varies directly as the area, and as the fourth power of the temperature of the radiator. It is interesting to note that there is an optimum temperature which minimizes the necessary radiator area. If the simplifying assumptions are made that the machine, having a constant power output, operates with a thermal efficiency which is a constant fraction of the Carnot efficiency corresponding to the heat input and output temperatures, and that the heat input temperature is held constant, the radiator area will be a minimum for an absolute radiator temperature equal to three-fourths the absolute heat input temperature. If the radiator temperature is too low, then its area must be increased in order to counteract the lower radiant heat transfer coefficient. If the radiator temperature is too high, then the thermal efficiency of the device decreases to such an extent that it more than makes up for the higher radiant heat transfer coefficient at the higher temperature.

Another factor of importance in the design of the radiator is that of meteoroid damage. An indication of the importance of the problem can be obtained from Figure 7. This plot of the magnitude of the meteoroid against the number of hits to be expected per year of a given magnitude or larger is derived from the estimates presented by Whipple.[4] A tenth-magnitude meteoroid may be expected to penetrate about 10 millimeters of aluminum. A fifteenth-magnitude meteoroid can be expected to penetrate about 2 mm of aluminum. With an exposed radiator area of 100 square feet corresponding to one hit per year of an eleventh order or larger meteoroid, it is evident that the meteoroid damage problem will have a dominating influence on the weight of the radiator. The problem will become increasingly severe for larger power systems. The importance of obtaining more accurate and complete data on the number and size of meteoroids present at various locations in space is very clear.

Design calculations indicate that a 3-kilowatt solar turbo-electric unit can be built with a weight of less than 1,000 pounds and that it can be folded into a space compatible with a spacecraft designed for the Centaur launch vehicle.

Summary.—For amounts of power from a few watts to a few hundred watts,

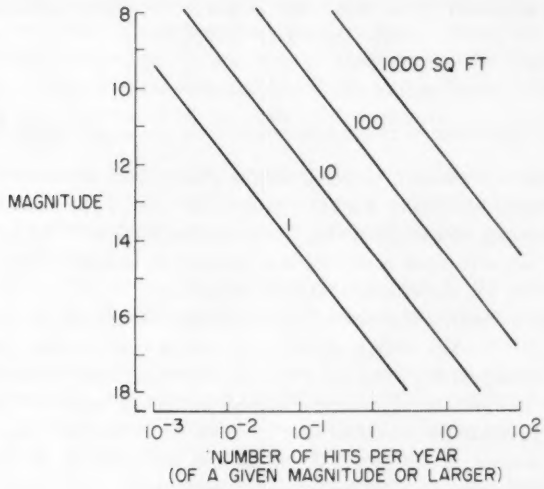

FIG. 7.—Influx of meteorites.

silicon solar cells seem to be a reliable, convenient source of power in space. Such power levels appear adequate for minimum communication needs for missions as far as Mars. The generation of larger amounts of power from a solar turbo electric system, such as Sunflower I, appears feasible but remains to be demonstrated. For power levels of many kilowatts or megawatts as may be required for electrical propulsion, nuclear energy sources and appropriate conversion systems will probably be required.

* Deputy Administrator.

† Lunar and Planetary Program (Spacecraft Technology).

[1] Thomas, U. B., "Battery considerations for a communications satellite," presented at the ARS Space Power Systems Conference, Santa Monica, California, September 30, 1960. (ARS 1308-60.)

[2] Loferski, J. J., and P. Rappaport, "The effect of radiation on silicon solar-energy converters," *RCA Review*, 19, no. 4 (1958).

[3] Denney, J. M., "Radiation damage in satellite solar cell power systems," presented at the ARS Space Power Systems Conference, Santa Monica, California, September 30, 1960. (ARS 1295-60.)

[4] Whipple, F. L., "The meteoritic risk to space vehicles," in *Proceedings of the VIIIth International Congress, Barcelona*, October 6–12, 1957 (Vienna: Springer-Verlag, 1958) pp. 418–428.

RESEARCH ON THE USE OF SOLAR ENERGY MADE IN THE SOVIET UNION

By V. A. Baum

SOLAR ENERGY LABORATORY OF THE POWER INSTITUTE OF THE USSR ACADEMY OF SCIENCES

The features of the modern power industry which have developed over almost 150 years will soon undergo very great changes, in view of the need to utilize new sources of energy and new methods for transforming energy. The power industry of the economically advanced countries is at present so immense that it is essential to begin preparing for the changes well in advance.

Recently solar radiation has come to be regarded as one of the new promising sources of energy.[1–6] Yet only a short while ago a very modest part had been accorded to it in the future power balance. However, in view of the achievements in physics, the production of new specialized materials, and the possibilities of modern industry, it can be expected that in the near future solar energy can be a supplementary source of energy. Then, as the methods of its utilization are perfected, it could come to play an ever-increasing role.

The problem of utilizing solar radiation could be formulated as studying the interaction of the radial energy of the sun with live and dead matter and determining possible ways for the practical use of this interaction. However, when the problem is formulated in such a general way, the volume of research becomes too large and indefinite. It is expedient to conduct the research first in those directions which could be expected to produce the most important practical results in the shortest space of time. From this point of view, we believe the primary directions of research should be the following: (1) Studies of the Earth's climate and the extent to which it could be controlled. These studies would include both the elaboration of methods for controlling climatic conditions in large territories and also the changing of micro-climates. (2) Studying photochemical processes, particularly photosynthesis, both for the purpose of increasing crop harvests and for determining the possibility of creating artificial chemical systems for obtaining food products and energy. (3) Studying photoelectric and thermoelectric processes in order to create economically-acceptable devices for transforming the energy of solar radiation into electricity. (4) Studying the processes of heat and mass transfer in different solar installations. (5) Investigations connected with designing and manufacturing special materials and their products with definite properties (materials for photo- and thermo-elements, transparent and metal films, selective coverings, and so on). (6) The search for new methods of transforming and utilizing solar energy. (7) At the same time, engineering work should be continued on designing prospective solar installations and calculating their technological and economic characteristics.

These subjects, though different in their scientific and practical value as well as in the methods and scale of research are closely interlinked.

In the Soviet Union there are many institutes whose work is connected to a greater or lesser extent with the problems of using solar energy. These are the institutes which study the theoretical and practical problems of photosynthesis, photochemistry, the physical and chemical properties of semiconductors, the

production and testing of semiconductors and other materials, the climate of the Soviet Union, and questions of heat and mass transfer. However, in addition to institutes, classified according to methods of research or the field of science in which they work, it is also considered expedient to have laboratories working on problems as a whole or on their separate major aspects if practical results are likely to be obtained.

In the Soviet Union there exist, in addition to the Helio Laboratory of the Power Institute of the Soviet Academy of Sciences, similar laboratories or groups in some of the southern republics for which separate aspects of the problem have an economic significance.

From the work done during the last 3–4 years by the Helio Laboratory of the Power Institute of the Soviet Academy of Sciences, the following projects could be mentioned:

The information collected on the number of hours of sunshine and radiation (and in some cases also the temperature and wind velocity), as well as the data on the efficiency of different solar installations, serve as the basis for the determination of the prospects of utilizing solar energy in a given area.

The Helio Laboratory has attempted to determine by statistical methods on the basis of a large number of climatic studies the correlation between the number of hours of sunshine τ_0 and the possible number of hours during which solar installations could operate τ, as well as the correlation between solar radiation $\mathfrak{Z}_0$ and the amount of energy which could possibly be used $\mathfrak{Z}$ (ref. 7, pp. 18–26). This dependence was determined for eight places in the southern part of the Soviet Union for certain types of solar installations. For instance, for a solar heating station it was determined that $5 \cdot 10^4 < \mathfrak{Z}_0 < 3 \cdot 10^5$ kg cal/m^2 month. The equation would be $\mathfrak{Z} = 1.1 + 0.266\ \mathfrak{Z}_0 + 0.00118\ \mathfrak{Z}_0^2$, where $\mathfrak{Z}$ is the heat output per square meter of mirror surface a month and $\mathfrak{Z}_0$ the total radiation per square meter for a month. The deviations from this equation for different geographical places are not considerable, the correlation coefficient r being equal to 0.95.

The transformation of solar radiation into mechanical or electrical energy is one of the main questions. So far, it is realistic to speak of three ways of transformation: by means of the ordinary steam system, by solar thermoelectrogenerators, and by solar photoelectric batteries.

To obtain capacities from 1,000 to 3,000 kw in a single installation, it is at present most economically advantageous to use the conventional steam system which we have elaborated in detail. When solar radiation is transformed into the heat of steam, the efficiency is about 55–65 per cent, and when transformed into electricity, about 12–15 per cent. These installations could be regarded as prototypes of a power unit for reclaiming arid and semiarid ones and creating oases where they could be utilized for producing electricity, for distilling or pumping water, and for other purposes.

Calculations made in the Helio Laboratory have shown that a steam engine of a capacity of about 1–2 kw can hardly have an efficiency of more than 1 per cent. This is due to the fact that when the size of steam machines is decreased the comparative heat losses are greatly increased as a result of the heat transfer between the steam and walls of the cylinder of the machine. It is also known that even a small admixture of noncondensing gases (air for instance) added to the steam

greatly reduces the heat transfer coefficient from the steam to the wall. The Helio Laboratory conducted experiments on the condensation of steam from a moving air-vapor mixture. The following dependence was obtained[8] for Re 1,300–40,000 with the amount of steam in the mixture from 3 to 95 per cent (volumetric):

$$\Pi = \frac{Gd}{(D_t + D_m)p_m} = 13.0\, Re^{-0.2} \left(\frac{p_s}{p_m}\right)^{1.2} \left(\frac{p_s - p_w}{p_m}\right)^{0.105},$$

where D_t and D_m are the coefficients of turbulent and molecular diffusion taken in regard to the partial pressures, G is the density of the steam flow in the direction of the condensation surface, d is the diameter of the pipe along which the mixture is moving, p_s, p_w, and p_m are the partial pressures of the steam, the steam near the condensation surface, and the air-vapor mixture, and Re is the Reynolds number.

The coefficient of turbulent diffusion is determined on the basis of previous work.[9] For preliminary calculations, when $700 < Re < 1{,}300$, the following equation could be used.

$$\Pi = \left(2\frac{p_s}{p_m} - 0.06\right)\left(\frac{p_s - p_w}{p_m}\right)^{1.105}.$$

Using this relation, maybe it would in some cases be possible to improve somewhat the efficiency of small steam machines.

Experiments carried out in the United States on building small steam engines have shown that their efficiency is low.[10] This task is evidently a very difficult one. But it is probably too early to give the matter up altogether.

The experiments in building solar thermoelectric generators showed that they have a much higher efficiency of transforming solar energy into electricity than small steam machines (ref. 4, pp. 7–23). The intensive search for semiconductors gives grounds for hoping that in the near future it will be possible to make solar thermoelectric generators of a capacity of 1–3 kw with an efficiency of about 5–8 per cent which would be economically acceptable in some areas for such purposes as the pumping of water.

The investigations connected with creating solar thermoelectrogenerators were conducted in the Helio Laboratory in the following directions: choosing and investigating materials for thermal couples (ref. 7, pp. 78–87 and 99–110), the search for methods for distributing evenly the heat flow passing through separate elements of the battery (ref. 7, pp. 88–98), a study of the optimal conditions for the work of such devices, designing mechanisms for following the sun, and engineering methods of calculation.[11]

Recently our Helio Laboratory has investigated at various temperatures the thermoelectric properties of the following binary compounds of tellurium: FeTe, CoTe, GeTe, PdTe, AgTe, Ag_3Te_2, Ag_2Te, InTe, In_2Te, SnTe, Sb_2Te_3, PbTe, $BiTe_3$.

On the basis of measurements of the Hall effect, the electric conductivity σ and the thermoelectric force α, a calculation was made for the density of current carriers, their mobility, and their effective mass.[12] These investigations are important for practical purposes, since the evaluation of the effectivity of the materials in regard to α, σ, and the heat conductivity λ measured at room temperature could lead to large errors. The value of $z = \sigma\alpha^2/\lambda$ for some materials depends

very little on the temperature of the hot junction, but for others it decreases very sharply. Figure 1 shows for some tellurium compounds with different admixtures the dependence of σ, α, λ, and z on the temperature of the hot junction.

Here σ is the electric conductivity of the material 1/ohm cm; α is the thermoelectric force V/C°, and λ is the heat conductivity W/cm C°.

It is to be noted that in Figures 1–6, λ is given in heat units kg cal/m hr C°,

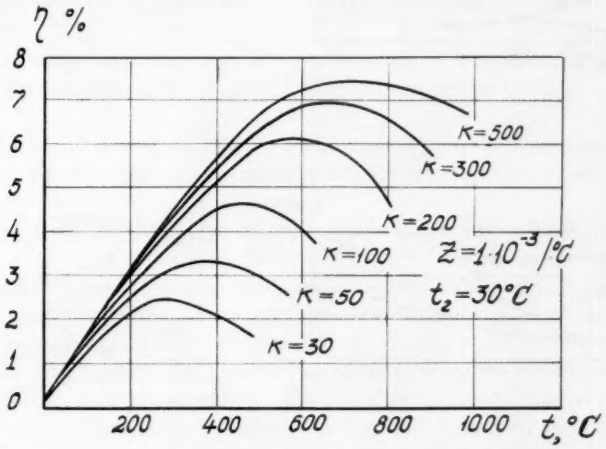

FIG. 1.—Efficiency of a thermoelectric generator at different temperatures and solar radiation concentrations.

and to calculate z, the heat conductivity λ must be taken in W/cm C°.

At given temperatures of hot and cold junctions of electric batteries, an increase in the coefficient of concentration $K = F_{bat}/F_{mir}$ (where F_{bat} = surface of battery heated by rays in m² and F_{mir} = surface of mirror in m²) leads to an increase in the efficiency of the solar thermoelectrogenerator, since at an equal amount of energy received by the battery its heat losses through convection and radiation are lessened because the surface of the batteries heated by the rays is decreased. At a given coefficient of concentration, there exists a maximum temperature of the hot junction, since the heat losses by radiation and convection from the battery grow faster than the quantity of heat transformed into electricity does. However, even at such small concentrations as $K = 500$, this maximum temperature is considerably higher than the melting point of the existing materials.

Figure 2 shows the results of calculations of the efficiency of a solar thermoelectric generator η depending on the temperature of the hot junction and the coefficient of ray concentration K for a conditional case where $z = 0.001$ (constant).

The Helio Laboratory is continuing to work on methods of construction. This is one of the most complicated and important problems in creating thermal batteries, since many of the materials investigated proved fragile and unstable. At working temperatures, they warp and crack. In view of this, as well as because of intercrystalline corrosion, their electric resistance increases in time. Measurements were also made of the coefficient of linear expansion of materials during heating which wholly satisfies the practical requirements.

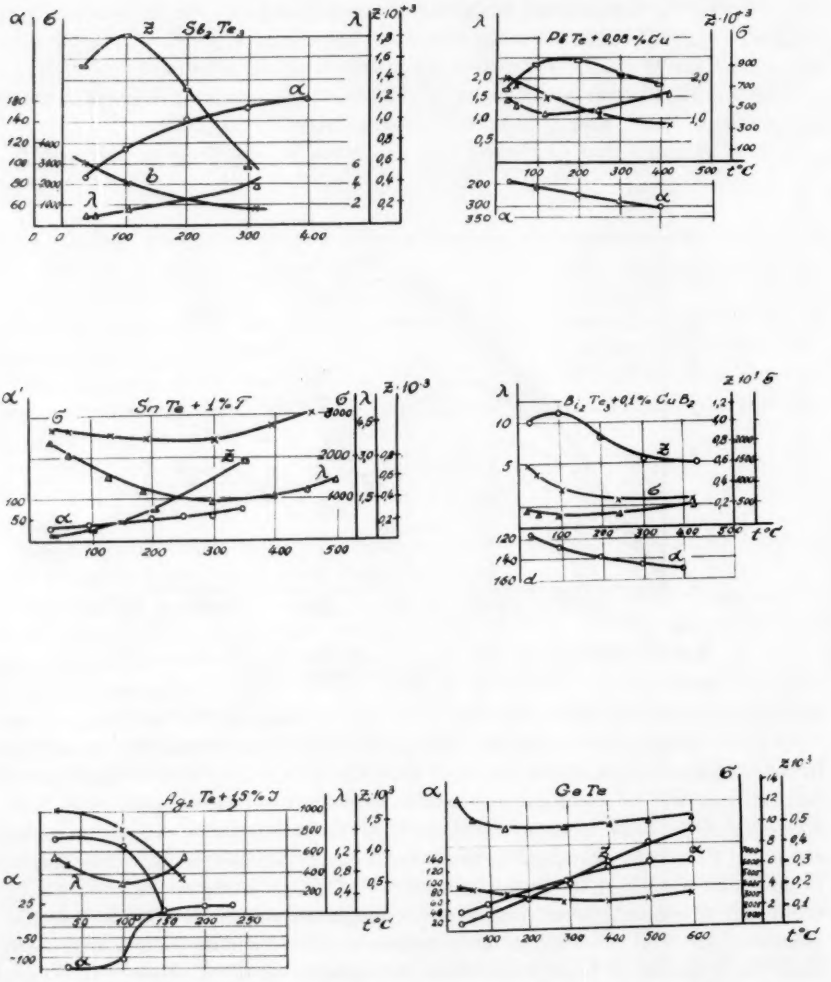

FIG. 2.—Thermoelectric behavior of selected systems. Abscissa is temperature difference; ordinate α is thermo-electric force and ordinate λ is thermal conductivity.

The Helio Laboratory also studied the creation of conditions in thermal generators such that the hot junctions of all elements of the battery have the same temperature at a given temperature of the cold junctions. These requirements can be approximated as follows: (*a*) by making thermoelectric batteries with a special form of hot surface or with thermo-elements of different length (an approximate method of determining this form was examined by D. Tepliakov[13]); (*b*) by the use of massive plates which by means of heat conductivity smooths the heat flow on the hot side of the battery (thus it was that A. Okhotin built an experimental solar thermoelectrogenerator); (*c*) by making the surface of the reflectors in a special form. R. Aaparasi, for instance, designed a special mirror that creates

in the focal plane a more equal flow than is created by a paraboloid mirror. The equation for this mirror in polar coordinates is

$$\rho = C_0 \frac{1 - K - \varphi \tan \frac{\theta}{2}}{1 + K + \varphi \tan \frac{\theta}{2}} \frac{1}{\varphi + K \sin \theta},$$

where φ is the angle of divergence, $K = \sqrt{1 + \tan^2 \theta}$, θ is determined from the equation for the focal distance $f = \rho \cos \theta$, C_0 is determined on the basis that $\theta = 0$; $\rho = \rho_0$.

Mirrors which give a smoothed flow of radiant energy on the focus are important also for designing solar photoelectrogenerators with an increased concentration of solar radiation.

The silicon photocells with a high efficiency made at first in the United States[14, 15] are of great interest in those cases when the cost of the electricity produced is irrelevant, as for instance for man-made space bodies. These photocells are now produced in many countries. However, for the ordinary consumer they are too expensive. It would seem that the problem of creating economically acceptable solar photoelectric generators had reached an impasse, since their working temperature should not exceed about 100°C. However, experiments carried out in the Soviet Union have shown that by increasing the light falling on the photocells it is possible to increase its output considerably if it is cooled artificially.[16, 17] Thus, in some cases we have succeeded in increasing the output of a photoelement 70 times by increasing the light falling on it 160 times. Under certain conditions it is profitable to concentrate the rays, since the cost of a unit of surface of the photocells is several hundred times greater than that of mirrors. We believe that by using concentrating mirrors, cooling the photoelements, and improving the tapping of the current, it would be possible to solve the problem of creating an economically acceptable device for obtaining electricity from solar energy.

Several small experimental designs of photoelectrogenerators were made by the Helio Laboratory in 1960.

The photoelectrogenerator consisted of a photobattery with a surface of 100 cm^2 which worked from concentrated solar energy reflected from an aluminum mirror with an effective surface of 1.2 m^2. The reflection coefficient of the mirror was equal to about 0.7. The photobattery was placed in a chamber with a glass lid. Water passing through the chamber cooled the face surface of the photobattery. The useful capacity of this device, at a radiation of $J_0 = 700$ kg cal/m^2 hr, was about 10 watt. Without the mirror, the photobattery would have given a useful capacity of 0.5 watt, that is, one twentieth as much.

In some of the problems connected with the use of solar radiation, the so-called selective surfaces are of very great significance, and so a great deal of attention was devoted this research.[18] The Helio Laboratory examined the theoretical aspects of this problem and conducted experiments on creating selective surfaces for solar heating installations. It proved feasible to introduce a concept of an ideal selective surface which in the range of waves from $\lambda = 0$ to $\lambda = \lambda_0$ is, for instance, absolutely black $A = 1$, and in the range $\lambda = \lambda_0$ to $\lambda = \infty$ is absolutely

white. As has been done in a number of similar works,[19] we shall call λ_0 the threshold length.

For an ideal surface, λ_0 must be such that the ratio between the quantity of absorbed radiation and the quantity of lost energy should be optimal. If, for instance, solar radiation of an absolutely black body at a temperature $T_1 = 6{,}000°\text{K}$, then we find that λ_0 can be determined in microns from the following formula

$$\lambda_0 = \frac{C_2\left(\frac{T_1 - T_2}{T_1 T_2}\right)}{\ln M + 4 \ln \frac{T_1}{T_2}},$$

where $M = \frac{1}{\mathfrak{Z}_0}\sigma_0(T_2^4 - T_0^4)$, C_2 is the second constant of Planck's law equal to 0.01438 m deg, $T_1 = 6{,}000°\text{K}$, T_2 is the temperature of the selective surface in °K, T_0 is the temperature of the ambient in °K, $\sigma = 4.9 \times 10^{-4}$ the radiation coefficient of an absolutely black body, and $\mathfrak{Z}_0$ is the solar radiation near the earth's surface in kg cal/m² hr.

Table 1 gives the results for calculations of λ_0 depending on T_2 and $\mathfrak{Z}_0$.

TABLE 1

$\mathfrak{Z}_0$ $\left(\frac{\text{kg cal}}{\text{m}^2\ \text{hr}}\right)$	T_2-temperature of surface in °K			
	600	500	400	350
700	1.91	2.34	3.04	3.61
810	1.93	2.37	3.08	3.66
1000	1.95	2.40	3.14	3.73

It can be seen that the value of $\mathfrak{Z}_0$ has little influence on λ_0.

The λ_0 was also determined graphically on the basis of real solar radiation and it can be seen that the results obtained coincide fairly well with those given in Table 1.

In order to compare the selective absorbing surface with the blackened surface, a number of calculations were done. The efficiency of the heater with a blackened surface decreases much more quickly than that of a heater with a selective surface. The results of the calculations also showed that for improving the efficiency of a heater with a selective surface, it is very important to try to decrease the heat losses by free convection in the air.

Experiments with black selective surfaces were carried out by covering different freshly-polished surfaces of metallic plates with electroplating methods and by spraying with nitrate paints. On the basis of these experiments, it can be concluded that the optimal thickness of the covering layer lies between 0.2 and 0.5 microns if produced by electroplating methods, and the optimal weight of a sprayed black nitrate paint is between 0.2 and 0.4 mg/cm².

The results of some experiments are given in Tables 2–5, in which ε is the fraction of emission and α_s is the fraction of absorptivity compared to those of an ideal black body.

On the basis of existing experiments and calculations, the Helio Laboratory determined the technical characteristics of the different methods of distilling salt water with the help of solar energy.[21, 22] The capacity of solar distillers of the

TABLE 2

STAINLESS STEEL COVERED BY A LAYER OF COPPER OXIDES

Thickness of layer in microns		
0.15	0.18	0.71
0.23	0.2	0.78
0.3	0.22	0.8
0.35	0.24	0.86
0.4	0.26	0.87

TABLE 3

ALUMINUM COVERED BY A LAYER OF COPPER OXIDES

Thickness of layer in microns	ε	α_s
0.39	0.2	0.62
0.54	0.27	0.68
0.9	0.38	0.82
1.09	0.41	0.82
1.3	0.43	0.84

TABLE 4

STAINLESS STEEL COVERED BY A LAYER OF COPPER OXIDES

Thickness of layer in microns		α_s
0.168	0.19	0.81
0.237	0.25	0.84
0.34	0.30	0.86
0.38	0.31	0.88
0.475	0.35	0.90
1.04	0.40	0.93

TABLE 5

ALUMINUM SPRAYED WITH BLACK NITROPAINT

Weight of sprayed paint in mg/cm²	ε	α_s
0.25	0.34	0.83
0.29	0.39	0.88
0.34	0.43	0.90
0.57	0.60	0.93
0.87	0.70	0.94

hot-box type was determined by a computing machine, and the results given in graphic form, showing its dependence on solar radiation, the ambient temperature, and the quality of the glass. The capacity of a distiller was determined from such a big solar station as was described in references 4 and 23. I shall mention only a few of the characteristics of this station. It consists of a tubular screen-boiler with a surface of 15×9 m². The rays of the sun are reflected from 1,300 flat mirrors having a total surface area of 20,000 m². The amount of steam obtained in the boiler could be calculated by taking the efficiency of the boiler to be 60–65 per cent and the efficiency in the production of electricity as 15 per cent.

For the conditions of Tashkent, where the annual amount of solar energy falling on a surface perpendicular to the rays amounts to 1,700,000 kg cal/m² hr, we obtain the following results:

1. If all the steam produced by the boiler is channeled into an 8–9 stage distiller, then the annual productivity of the installation will amount to about 1.6×10^5 tons of distillate from water containing any amount of salt.

2. If the steam from the solar boiler is used for a condensation turbine, its generating capacity will be 2,500 kw. If this electricity is used to purify water by means of an electro-ionic purifier, the following quantity of water containing about 350 mg of salt per liter will be obtained.

Initial salt content in water (mg/liter)	885	4,635	10,000	35,000
Annual productivity of installation in tons	7×10^6	1.8×10^6	0.85×10^6	0.28×10^6

The productivity of a hot box distiller with a surface of 20,000 m² would be about 1.7×10^4 tons of distillate a year.

In recent years, considerable attention is being paid in many countries to the utilization of solar energy. Substantial results have been obtained. Of course, there are still many difficulties which have to be overcome. But they are not difficulties of principle.

Just imagine for a moment that mankind had based his power industry on solar radiation, not fuel, and then the proposal to use different kinds of fuel was put forward. Probably, there would have been very many objections.

One could imagine that one of the most important arguments in defense of solar energy would be formulated as follows:

Solar radiation is a "noble" form of energy and it was under its influence that life originated and continues to develop on earth; therefore its use, no matter on what scale, could represent no danger or inconvenience for either the flora or fauna of the world. The use of any other kind of fuel would inevitably be connected with the poisoning of the atmosphere, water, and land. Fuel should be used only where there are no other possibilities of obtaining energy, and in the sunny regions of the world the energy of the sun should be used.

[1] Trofimov, K., *Ispolzovanie solnechnoi energii* (Using of Solar Energy), collection of papers, IV, Tashkent, USSR, 1935.

[2] *Proceedings of the Symposium on Wind and Solar Energy*, New Delhi, 1954 (UNESCO, 1956).

[3] Daniels, F., and J. Duffie, *Solar Energy Research* (Madison: University of Wisconsin Press, 1955).

[4] *Ispolzovanie solnechnoi energii* (Using of Solar Energy), collection of papers, I, Academy of Sciences of the USSR, 1957.

[5] *New Sources of Energy and Economic Development*, United Nations, New York, 1957.

[6] Proceedings of the World Symposium on Applied Solar Energy, Phoenix, Arizona, 1955. Transactions of the Conference on the Use of Solar Energy, Tucson, Arizona, 1955.

[7] *Ispolzovanie solnechnoi energii* (Using of Solar Energy), collection of papers, II, Academy of Sciences of the USSR, 1960.

[8] Baum, V., and P. Brdlik, *Teploenergetica*, No. 1, 1957, Moscow.

[9] Baum, V., *Izvestia Academii Nauk*, OTN, No. 2, 1952, Moscow.

[10] Hsu, S. T., and B. S. Leo, *J. Solar Energy*, **2**, No. 3–4, p. 7 (1958).

[11] Baum, V., and A. Okhotin, *Ingenerno-phys. Journ.*, No. 11, 1959, Minsk.

[12] Telkes, M., *Solar thermoelectrogenerators*, see references 3 and 6.

[13] Tepliakov, D., *Ingenerno-phys. journ.*, No. 4, 1958, Minsk.

[14] Chapin, Fuller, and Pearson, *J. Appl. Phys.*, **25**, 676 (1954).

[15] Chapin, Fuller, and Pearson, *Bell Lab. Rec.*, **33**, 241 (1955).

[16] Vavilov, V., Malovetskaja, and Galkin, *Atomic Energy*, No. 5, 1958, Moscow.

[17] Baum, V., R. Borovikova, and A. Okhotin, *Ingenerno-phys. Journ.*, No. 8, 1960, Minsk.

[18] Tabor, H., see reference 6, vol. 2, part 1, sect. A.

[19] Trivich, D., and P. Flinn, see reference 3.

[20] Ge Sing-shi, see reference 7, pp. 133–141.

[21] See reference 7, pp. 122–132.

[22] Baum, V., *Solar Distillers* (to be published).

[23] Baum, V., Aparasi, R. R., and Garf, B. A., *J. Solar Energy* (1957).

SOLAR COLLECTORS, SELECTIVE SURFACES, AND HEAT ENGINES

By H. Tabor

NATIONAL PHYSICAL LABORATORY OF ISRAEL

From time to time I ask myself, as a physicist, why I should be working on the conversion of solar energy to power by thermal means instead of concentrating on the more logical photonic processes. Perhaps the answer is that at the end of the First World Symposium on Solar Energy, held in 1955, most observers had the feeling that—in the existing state of the art—the accent was to be on thermal processes and this despite the magnificent breakthrough in the silicon photocell by the Bell Telephone team.

It seems, alas, that after six years, the situation has not changed radically as far as practical applications are concerned, though some excellent basic work in photochemistry and photoelectricity is being pursued that will, we hope, ultimately pay off.

In the thermal processes, very fundamental discoveries are hardly to be expected, except perhaps in the field of thermoelectrics (in the widest sense of this word); yet the last few years have shown that considerable progress is possible by the application of modern scientific method to a classical problem and that there is still room for further progress before the fundamental limitations of thermodynamics call a halt.

This paper will indicate very briefly some of the areas where progress has been made in thermal conversion of solar radiation and pointers for future work.

Thermal Research Program.—The power output of a thermal solar installation is the product of three factors: the solar intensity, the collection efficiency, and the heat engine conversion efficiency. A research program on solar power must study these three factors and attack those points where there appears to be most room for improvement.

Figure 1 illustrates this line of reasoning and shows the major areas where research is being pursued. Shown boxed are five subjects under study at the National Physical Laboratory of Israel. (The dotted boxes indicate other areas studied of lower priority.) Time will permit a glance at only three of them.

(a) *Selective surfaces:* I start with recent research on selective surfaces for this was the point from which solar energy started in our laboratory. Although the general concept of selective surfaces (i.e., surfaces that are good absorbers in the solar spectrum but good reflectors, i.e., poor emitters, for longer wavelengths) has been recognized for some years, it is only recently that we have been able to tackle the basic problem of why and how a surface is selective.

There are two kinds of selective surface: those in which a smooth low-emissivity metal base is covered by a thin surface layer which is visibly dark but substantially transparent in the infrared and those which are entirely metallic, so that the emissivity is low, but where, because of color or a finely divided structure, the absorptivity in the visible spectrum is low. Polished zinc is an example of the second kind: it absorbs about 55 per cent of the solar spectrum, but has quite a low emissivity. The absorption to sunlight is not high enough to be practical,[1] and in fact, there are so far almost no practical surfaces of the second kind in use.

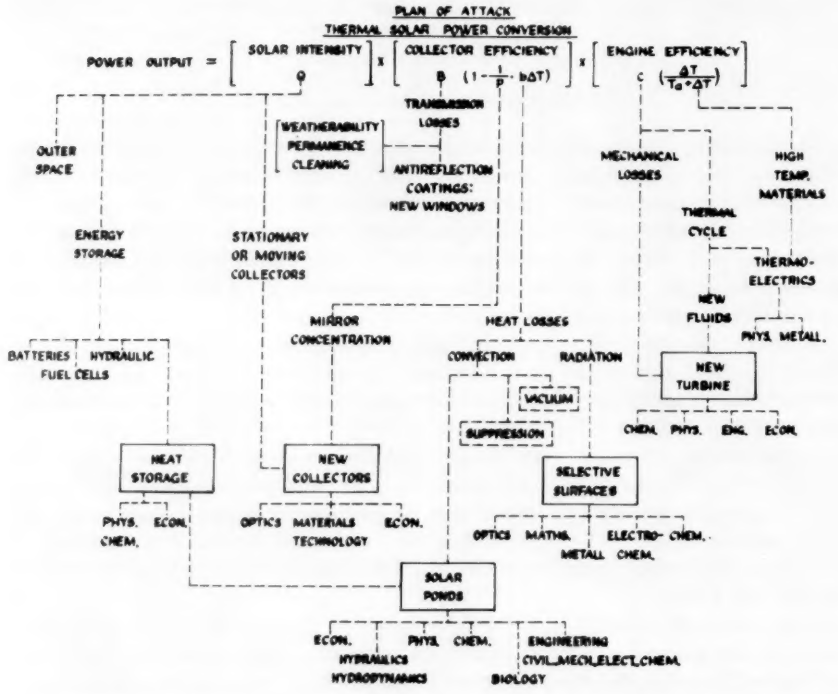

FIG. 1.—Solar energy investigations at the National Physical Laboratory of Israel.

Some recent work in our laboratory on what was at first thought to be finely divided nickel deposited electrochemically (absorptivity of 90 per cent) was shown to be predominantly nickel oxide and hydroxide, making it a selective surface of the first kind. Copper oxide surface layers have been studied at the University of Wisconsin, at MIT, and in our laboratory. Absorptivities of about 90 per cent with emissivities of 10–20 per cent have been recorded, but higher absorptivities are very difficult to obtain. Since 1954, we have been interested in nickel-black, produced by electrodeposition of a complex of nickel and zinc sulfides, and this process is now in commercial use. One of the really interesting features of this process is that there are so many variables—pH, current density, buffers, temperature—that the possibilities of getting a desirable end product are increased. (On the other hand, the problem of control, in an industrial process, is correspondingly more difficult and considerable know-how is required to carry out the process.)

Two observations were made very early: one, that optical interference played an important part in the process, and the absorptivity could be increased by arranging for a zero or near-zero reflectance by destructive interference at an optimum point in the solar spectrum, and two, that the optical properties could be altered by, for example, changing the current density during deposition, so that, in fact, a multilayer deposit was produced. (There is reason to believe that even a single layer deposit is not uniform in composition with depth.) Micro-analytical tech-

niques have had to be developed for studying as little as $^1/_2$ mg of material in thicknesses as little as 100 Angstroms. Reliable information on nonhomogeneity in depth is not yet available.

The following table gives an example of the results obtained for two deposits from the same bath for layers thick enough for the optical properties not to be influenced by the base metal.

Current density	0.5 ma/cm²	1.5 ma/cm²
Per cent nickel	33.5	15
Per cent zinc	26	56.5
Per cent sulfur	13	12.5
Per cent unaccounted (probably oxides and hydroxides)	27.5	16
Optical constants* $n - ik$	1.85–0.83 i	1.68–0.35 i

* $n - ik$ represents the complex refractive index where n is the real part of the refractive index and k is the extinction coefficient.

It had also been observed that a two-layer system (i.e., where the current density was suddenly changed in the course of plating) seemed to give better results than a single layer, and this was to be expected from thin-film optics theory. Very recently, Mr. H Weinberger, a member of our staff, has been able to work out the conditions of destructive interference for absorbing layers on metal substrates, and while a zero reflectivity for a single layer imposes very narrow limitations on the optical properties of the layer and the substrate, a double layer provides a double infinity of choice for the optical properties of the layers. Clearly, a double or multiple layer also gives more chance of destructive interference over a wide range of wavelengths (i.e., over the whole solar spectrum).

Figure 2 shows the reflectivity of two different nickel-black surfaces, one on

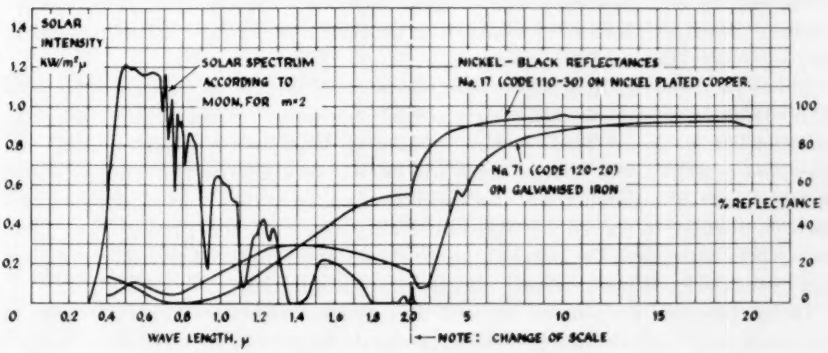
SOLAR INTENSITY KW/m²μ
SOLAR SPECTRUM ACCORDING TO MOON, FOR m=2
NICKEL-BLACK REFLECTANCES
No. 17 (CODE 110-30) ON NICKEL PLATED COPPER.
No. 71 (CODE 120-20) ON GALVANISED IRON
% REFLECTANCE
WAVE LENGTH, μ
NOTE: CHANGE OF SCALE

FIG. 2.—Solar radiation, and reflectance of selective surfaces.

nickel-plated copper and one on galvanized iron, superimposed on a plot of standard sunshine for an air-mass $m = 2$. The computed absorptances for this solar spectrum are 0.901 for Index No. 17 and 0.886 for Index No. 71, while the emissivities are 0.05 and 0.112 respectively.

This research is proceeding with the view to learning more about the basic structure of selective surfaces, their optical constants, and their use in combination to provide any particular optical behavior. One important auxiliary aspect of

research is on the stability of such surfaces, particularly with respect to elevated temperatures.

The benefits from selective surfaces vary in magnitude. For flat-plate collectors, the heat loss for a selective black ($e = 0.1$) and one cover glass is slightly less than for a conventional black and two cover glasses. The selective surface thus saves one cover and the associated transmission losses. For focusing collectors, multiple cover glasses are often difficult to execute, and the use of a selective coating can be very significant. Thus, a calculated example for a concentration factor of three—for a collector used to drive a heat engine—shows that replacing a normal black by a selective black increases the power output by 81 per cent. In outer space, where there are no convection losses, a low emissivity absorber is very significantly better than a conventional black.

Selective surfaces have applications other than for solar collectors. For many years, the University of California Radiation Laboratory under Professors Dunkle and Gier have studied selective spectral characteristics with a view to being able to determine equilibrium temperatures of surfaces subject to solar radiation (aircraft, space probes, etc.). Another application has been in studying the radiation balance of the earth where selective black surfaces have been used on a satellite to distinguish between albedo from the earth and long-wave ground radiation.

Where selective black surfaces are used in terrestrial collectors, the radiation heat loss generally becomes smaller than the convection loss. The latter then becomes extremely important. Ways of reducing this loss are discussed in the next section.

(b) *New collectors:* As far as flat plate collectors are concerned, there is not much to report. The problem is predominantly one of materials technology.

Progress in new plastics is encouraging, especially the transparent polyvinylfluoride, which exhibits good weathering properties and a low refractive index, i.e., low reflection losses.

It has been pointed out that where plastic windows are so thin as to be substantially transparent to heat waves, the "hothouse" effect of the flat-plate collector can be lost. Thus, it has been shown that such a collector using one glass, one plastic, and a normal black will have a very inferior performance if the plastic is heat-transparent; but if a selective black ($e \sim 0.1$) is used, the performance is slightly improved by the heat-transparency of the plastic. Du Pont researchers have found the loss of hothouse effect important for plastic solar distillers and have developed plastics less transparent in the infrared.

In the previous section, we showed that thermal radiation—which represents the major source of heat loss in a collector—could be reduced by an order of magnitude by use of selective black surfaces and in such cases the convection loss becomes the dominant loss term.

Free convection is governed by the Grasshof number, which, among other terms, contains L^3, where L is a characteristic dimension of the air space.

Some years ago we experimented with the possibility of reducing convection losses in flat-plate collectors by dividing the air gap between receiver and glass cover into small cells where the Grasshof number would be low enough (below about 2,000) to suppress convection. The results were discouraging: some benefit was observed with normal blacks but not with selective blacks. This is because

the walls of the cells are nonmetallic (to avoid thermal short-circuit) and are therefore, generally, of high emissivity. Thus: (*a*) they must not touch the hot receiver plate, as in that case *they* become the emitters; (*b*) even if they do not touch, a temperature gradient must exist and thermal radiation from the walls finally escapes from the tops of the cells. Very thin plastic (transparent to I-R) can be used, but mechanically the cells are weak. If they are also transparent in the visible, the cell walls do not cause loss of solar transmission to the blackened surface.

We finally postponed further work in this field, but I understand from Professor Dunkle (now in Australia) that he is pursuing this further, and we await his progress with interest.

The Grashof number (for air) contains ρ^2, where ρ is the density of the air. If, therefore, the air pressure is reduced to a small fraction of an atmosphere, convection will be suppressed in most practical cases. Partial vacuum is not practical for flat-plate collectors, but it is possible for cylindrical-type focusing collectors. A partial vacuum is far easier to achieve and *maintain* than the very high vacuum required for suppression of *conduction* in an air gap.

Figure 3 shows some measurements of heat losses for a flat collector placed diametrically in a glass tube.

It is seen—from the results in the boxed insert—that though a reduction of air pressure is not very useful with a normal black surface, when it is used with a selective surface the benefit is very considerable.

Many years ago, Professor Hottel pointed out that if a flat-plate collector had, say, six (or more) windows—with suitable anti-reflection surfaces—then it could be used to operate a heat engine with a reasonably satisfactory over-all performance. Unfortunately, we still do not have cheap anti-reflecting surfaces, and even without them, a flat-plate collector today with six glass or plastic windows would be expensive. This leads to the question whether a mirror-type collector might not have a lower specific unit cost than a flat-plate collector, particularly at higher operating temperatures. So long as metal or glass mirrors are considered, the answer is negative, but with the possibilities presented by vacuum-coated aluminized plastics, the answer may be affirmative. One condition would appear to be that the mirror be stationary. This has led to a study of the optics of stationary mirrors and the interesting result that a mirror with no diurnal movement (but requiring periodic seasonal adjustment) can give an optical concentration of about three times. Although this is not high, it can, together with a selective receiver, yield working temperatures (i.e., optima, when coupled to a heat engine) of about 150°C.

We are now in the middle of work on a collector of this type that we hope will be less expensive than a flat-plate collector. It involves a cylindrical mirror using aluminized plastic, mounted horizontally with the axis in an east-west direction, and an angle of acceptance of 12–14°, i.e., an ability to "see" the sun for 7 hr. on the solstice days and longer periods on other days. We hope to be able to report performance data and technical features for the UN Conference on New Sources of Energy in Rome in August.

(c) *The turbine:* Without doubt, one of the major difficulties in solar power installation, particularly in small units of, say, a few horsepower, has been the

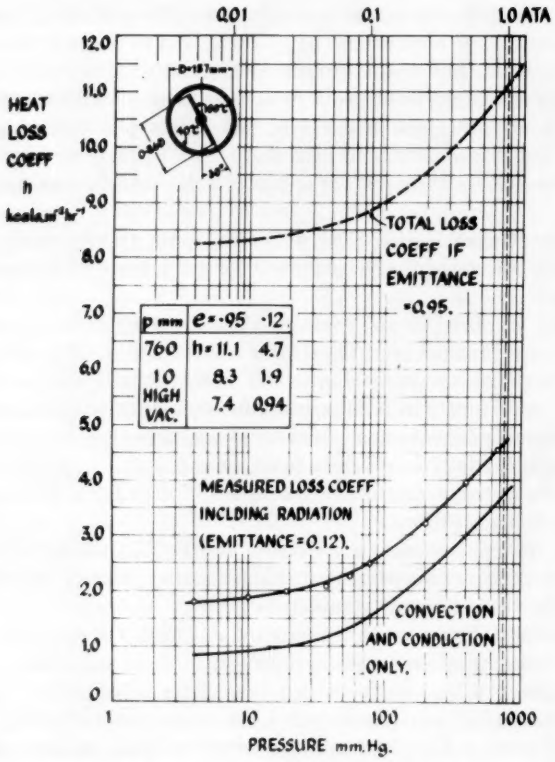
0.01
0.1
1.0 ATA
HEAT LOSS COEFF h
TOTAL LOSS COEFF IF EMITTANCE =0.95.
p mm | e=·95 | ·12
760 | h= 11.1 | 4.7
10 HIGH VAC. | 8.3 | 1.9
7.4 | 0.94
MEASURED LOSS COEFF INCLDING RADIATION (EMITTANCE=0.12).
CONVECTION AND CONDUCTION ONLY.
PRESSURE mm.Hg.

FIG. 3.—Heat losses for a flat collector in a glass tube.

nonavailability of a suitable external-combustion prime mover. Both turbines and engines in small sizes are of low efficiency, particularly if only moderate temperatures are available for their operation (which is the case if nonmoving solar collectors are employed), and the cost of the collector becomes the dominant cost item. Anything done to raise the efficiency of the heat engine, even at considerable cost, may result in a cheaper (as well as more compact) over-all power package.

Hsu and Leo have reported on four very simple fractional horsepower steam turbines with efficiencies of 1–2 per cent. The Italian Somor engine—operating at 60°C—has been reported as having an efficiency of 3 per cent. A thermoelectric converter, operating at 400°C has given 4 per cent conversion efficiency, while the 100 hp steam engine used by Shuman in 1913 had an efficiency of 10 per cent. Were the same engine scaled down to a few horsepower, its efficiency would fall to a few per cent.

The heat engine therefore seemed to us to be an area with great potential for improvement. For a source temperature of, say, 150–200°C and a sink at, say 30°C, the Carnot efficiencies are 28.4 to 35.9 per cent. This is an order of magnitude better than the efficiencies previously quoted.

It is, perhaps, an indictment of engineering education at least until a few years ago—that engineers would instinctively think of steam when an external combustion prime mover was discussed. Thus, although engines and turbines using vapors other than steam have appeared in the literature, they do not seem to have received the attention that they deserve. Thanks are due to D'Amelio for reminding us of the possibilities of heavy vapors as an alternative to steam.

We have given this matter considerable thought and the results are very gratifying: there is no difficulty in obtaining efficiencies of 15–20 per cent for turbines of a few horsepower size, operating at temperatures of 150–200°C.

There is not enough time to go into all the details and a fuller description will be published for the Rome UN Conference. But the basis will be sketched.

Steam is unsatisfactory for small engines because an engine cannot exploit the full expansion of steam down to condenser temperatures. Although a turbine can exploit this expansion, small turbines are inefficient because multistaging is impractical, and a single-stage De Laval type has to operate at high speed and has high disc and windage losses.

For a vapor turbine, it may be shown that the speed can be reduced inversely as the square root of the molecular weight, MW, of the vapor used. If the MW is over a hundred, and preferably over several hundred, then a simple single-stage impulse turbine of good performance can be constructed. It is shown, in fact, that (for terrestrial applications) the fluid used must satisfy four conditions:

(1) MW over a hundred, preferably over several hundred;

(2) Boiling point not below 100°C (as this would cause a high condenser pressure and high disk losses) and not over 150°C (as this would involve too high a vacuum in the condenser);

(3) Chemical and thermal stability;

(4) A suitable temperature-entropy diagram. It was found very early that the high-molecular-weight fluids had a bad-shape T-S diagram, which appeared to get worse as the molecular weight was increased, but that a few fluids, like CCl_4 and C_6H_5Cl had very good shapes. A former staff member, Dr. Goldstein, showed that the shape of the T-S diagram was to a first approximation, a function of the number of atoms in the molecule, not their kind, and that this number should be about 5–10 for an ideal T-S diagram. The fluid chosen should therefore have few atoms in the molecule but heavy ones. Unfortunately, such compounds in the correct boiling point range, are few, and most of them are chemically or thermally unstable. Chlorobenzene has shown remarkable stability tested up to 250°C in contact with various metals. Indeed it was the only fluid out of a larger number studied that satisfied all four conditions, and it is being used in our experimental turbine. First tests on an experimental turbine of 2–10 kw show that the computed efficiencies will be achieved in practice.

Time does not permit me to describe some thermodynamic manipulations which make it possible to "correct" a bad T-S diagram and which thus greatly widen the choice of possible fluids. Fluids with MW up to 400 have been found that

should give rise to an extremely elegant turbine design: our next experimental model will, we hope, use such a fluid.

Clearly an increase in efficiency by a factor of three or more over previous prime movers means smaller collectors—which in any solar power installation represent the major item of cost—and a small power package producing power for 5 cents per kw-hr seems feasible. (This is a low price for power from isolated generators.)

The Future.—Selective surfaces, optically speaking, are not far from ideal, particularly for terrestrial applications where lower emissivities cannot be exploited, but further bas c studies will lead to better properties and to other applications such as "tailor-made" I. R. filters. Better and easier methods of production are needed and improving chemical and thermal stability is important.

Further improvements in collectors would seem to be dependent primarily on advances in materials technology. More attention should be given to such matters as antireflection surfaces, weatherability of plastics, design of simple stationary collectors with a moderate concentration and low in price and easy to transport. Research on means for suppressing convection seems important in view of the progress in reducing radiation heat losses.

Small prime movers could be efficient if suitable working fluids were available. Thus research on fluids with MW of several hundred or even a thousand, boiling points of 100–150, freezing points below 0°C, and complete stability in the presence of constructional materials would, if successful, make small mechanical prime movers efficient.

A fundamental problem to be tackled for all terrestrial collectors is the question of how to keep them clean. It should not be beyond our ingenuity to find plastics to which dust will not stick, or other methods of preventing dust settling. In areas with long rainless periods, the transmission through a tilted glass can drop to half in a few weeks if not cleaned; and whereas cleaning is possible for small units (such as are used for water heating), it becomes an onerous task for large area collectors.

Time does not permit discussion of large area collectors of extreme interest, i.e., solar ponds based upon the use of a density gradient or employing vast plastic covers. This is a most fascinating field for future research, since it may lead to the possibility of solar power stations in the megawatt class, but they are intended, of course, for developing underdeveloped regions where large areas of space can be allocated for solar power production and yet where a demand for the power is now present or shortly will exist.

[1] Some years ago we studied the question of increasing the absorptivity by corrugating the surfaces in the form of vees, particularly if the surface of the material were specularly smooth. Thus if every incident ray is reflected n times before emerging from the vee, the effective absorptivity is

$$\alpha_e = 1 - r^n = 1 - (1 - \alpha)^n$$

so that for $\alpha = 0.55$ and $n = 3$ the effective absorptivity is over 90%. The effective emissivity of the vees for *low* emissivities can be shown to be just less than Se, where S is the periphery of the vee and e the emissivity of the surface. Thus for a 60° vee the emittance is approximately twice that for the material itself. A 60° vee will also give three reflections for *normal* incident beams, but less if the beam is displaced. I understand that French researchers have pursued this subject further.

FUNDAMENTAL PROBLEMS IN SOLAR DISTILLATION

By George O. G. Löf*

The distillation of sea water is one of numerous applications of solar energy readily workable from the technical standpoint but difficult from the economic point of view. The problem of producing a commodity by some sort of process equipment at a cost less than 20¢ per ton is very formidable.

As a consequence, most of the recent development work has been directed toward reducing the construction cost of solar distillation equipment through use of cheaper materials, simpler design, and other measures. Less effort has been devoted to *technical* improvements which might increase distiller efficiency and reduce the necessary size of a unit for a certain water production capacity. There has been even less work in the study of the basic principles in the solar distillation process. It is with these two technical areas that this paper is concerned. Some of the recently reported studies and a few of the current efforts along these lines are reviewed. The manner in which these technical developments may influence the *economics* of the solar distillation of sea water is indicated.

Solar Distillation Methods and Equipment.—Before the significance of the new solar distillation research work is explained, the characteristics of the process and its equipment should be briefly examined.

The basin-type solar still, shown diagrammatically in Figure 1, consists princi-

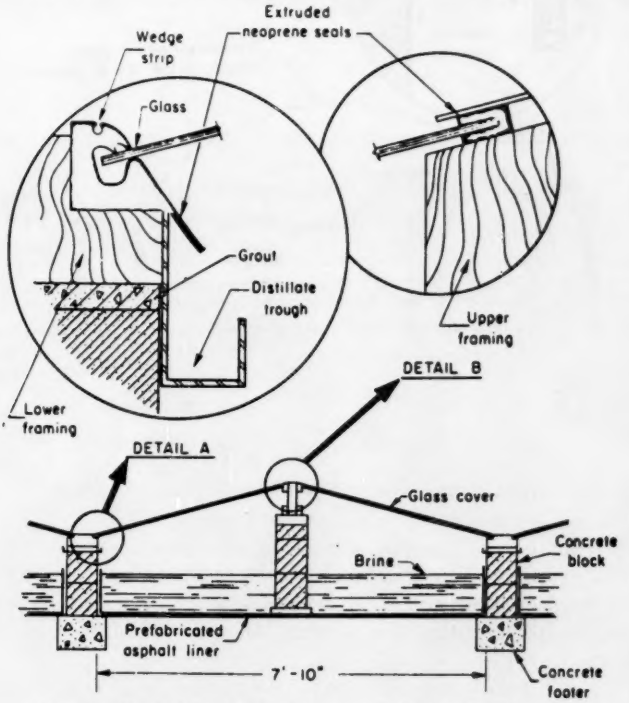

Fig. 1.—Typical section of glass-covered deep-basin solar still.

pally of a shallow black basin or pond covered by sloping transparent surfaces of glass or plastic. With salt water in the pond, slow evaporation takes place from the water surface due to the heating by solar radiation absorbed on the basin bottom. The cover is cooled by the atmosphere, so condensation of pure water occurs on the inside of that surface, the distillate being collected in small gutters or troughs at the low edges of the transparent cover. The figure shows the design of an experimental, glass-covered solar distillation pilot plant constructed in Florida about two years ago.[1] Factors differentiating it from earlier designs are a deeper water layer, approximately 1 foot, and construction directly on the ground rather than on an elevated platform. Conservation of heat from the distiller bottom is made possible by the large ground area covered and the negligible downward conduction loss. The principal virtue of the deep-basin design is in its simple and cheap construction. Water production, at a rate of about 0.1 gal per sq ft on a sunny day, is fairly uniform through the 24-hr period.

Figure 2 is a sketch of a basin-type still provided with a plastic film cover sup-

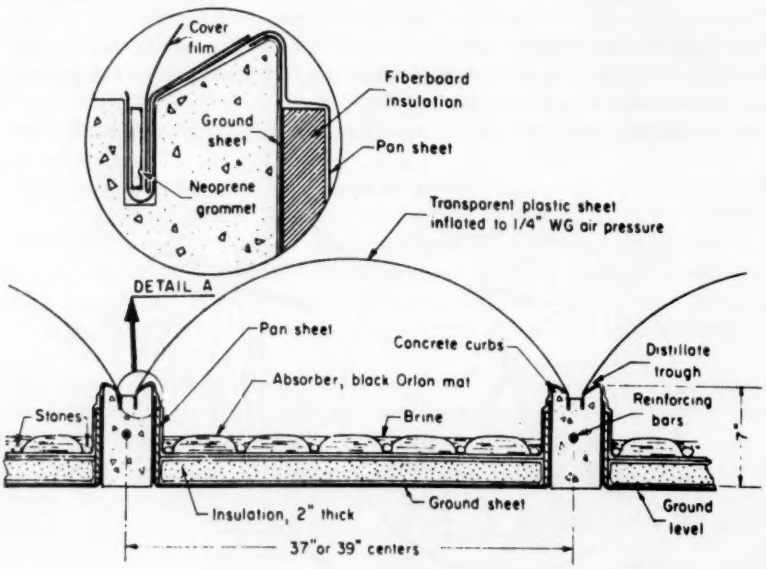

FIG. 2.—Cross-section view of air-supported plastic still.

ported by slight internal air pressure from a small blower.[1] Operation of the still is similar to the one previously described, with the exception that this design responds much more rapidly to changes in solar radiation and atmospheric temperature. The shallow layer of water achieves a higher temperature during midday hours than the deep-basin still, and the unit operates at a high rate during this part of the day. Because it cools at night, the total 24-hr productivity is comparable to the deep-basin output.

Figures 3 and 4 are photographs of the two previously described pilot plant installations in Florida.

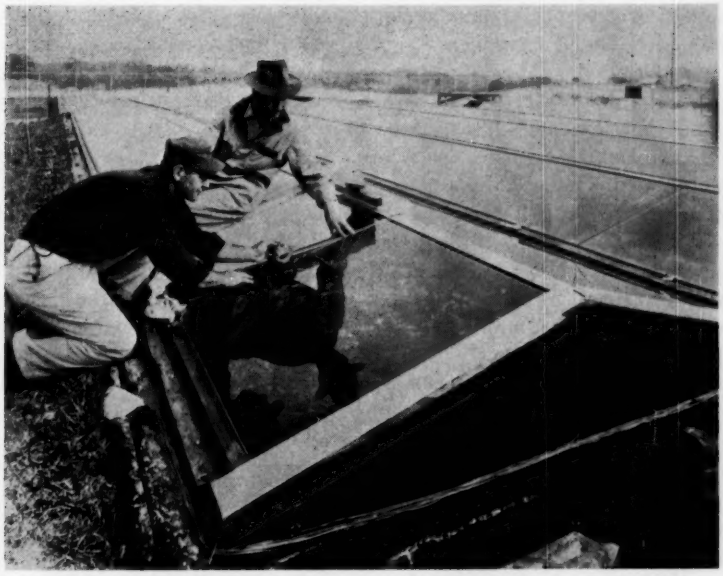

FIG. 3.—Glass-covered deep-basin solar distiller at Daytona Beach, Florida.

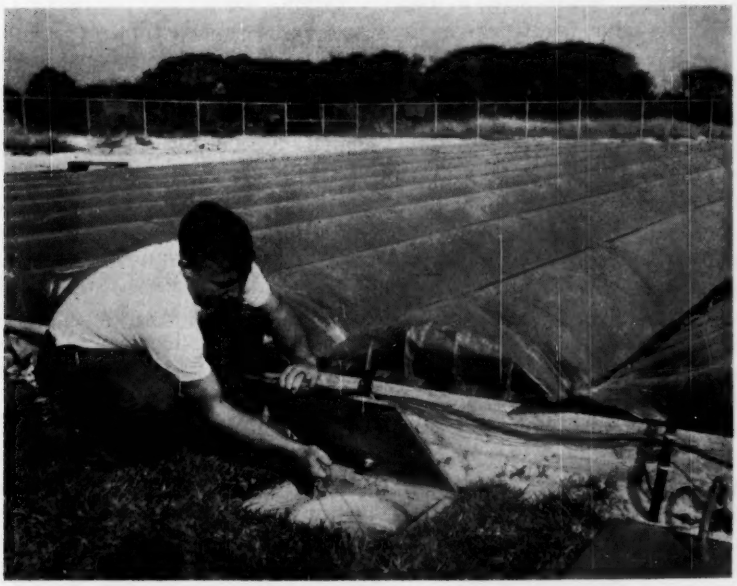

FIG. 4.—Air-supported plastic still at Daytona Beach, Florida.

Numerous experimental modifications of this basic type solar distiller have been made. Those having received most attention are the following:

1. In the tilted, wick-type distiller, the black "basin" is tilted to an angle approximately equal to the latitude, so that the evaporating surface is nearly normal to the sun rays at noon. The surface thus receives more solar radiation per square foot of area, and the distillate yield rises. To make a tilted water surface possible, the water pond is replaced by a black fabric which serves as a wick, the salt water being fed to this towel-like surface so that it is saturated at all times. Sufficient sea water is allowed to flow through the wick to prevent accumulation of salts in the fabric. A glass or plastic cover, serving as the condenser, is placed within an inch or two of the evaporating surface, and a trough at the lower edge of the cover collects the distillate. Insulation on the back of the unit reduces thermal losses.

2. In the forced convection still with external condenser, air is circulated through the vapor space of a basin-type still, leaving the unit at a relatively high humidity and temperature. If this air is then passed through a condenser cooled by sea water, distilled water can be separated from the air stream, which can then be recirculated to the distiller basin. Under proper conditions, a greater yield of distillate can be obtained with this system than with a conventional type still of the same area. This is apparently due to more effective vaporization of water from the liquid surface and a lower loss of heat to circulating air. The advantage of higher yield must of course be balanced against the requirements for a separate condenser and other accessories.

3. Numerous types of multiple-effect solar stills have been suggested, but none has received appreciable experimental success with solar energy input. Since raw solar energy has no cost, the usual incentive for multiple-effect operation, i.e., fuel economy, is not involved in solar distillation. Only if equipment costs can be reduced per unit of water-production capacity can the multiple-effect solar still have an advantage over single-effect. In all of the proposed designs, there is an additional surface of some type for each added effect, serving the purpose of condensing vapor on one side and evaporating liquid on the other side. Thus, the cost of this surface and its structural requirements, along with any necessary auxiliaries must be weighed against the cost of additional area of single-effect solar stills.

A multiple-effect solar still involves a series of evaporating chambers, each operating at a lower temperature than the one preceding. But instead of the total pressure being successively lower, stage to stage, the partial pressure of the water vapor in the air-vapor mixture becomes progressively lower. Thus, if a limited quantity of salt water is supplied to the cooler side of a vapor-condensing surface, the heat of condensation is transferred to the salt water, which partially vaporizes. This vapor, after flowing across a small air space, can then be condensed on another surface, which is in turn cooled by salt water evaporating on the other side. Temperatures in such a system are necessarily lower than in a steam-heated evaporator, so there appears to be a rather low limit to the number of possible stages—perhaps three or four. Most of the proposed designs involve wick-type systems and plastic film surfaces for condensation-evaporation transfer.

4. It is possible to generate steam in some type of solar boiler and then supply the steam to a conventional evaporator plant. This system would not be substantially different from a conventional evaporating plant except that the sun would

replace fuel as the source of heat. The economics of this process depend on the relative cost of steam from a solar boiler and a conventional fuel-fired boiler. Because of the low load factor in a solar plant (maximum use about 10 hr per day) and the intrinsically higher costs, there is little interest in this system.

Quantitative Aspects of the Solar Distillation Process.—Several recent studies have contributed materially toward a full understanding of the complex processes taking place in a basin-type solar still. Eibling, Bloemer, and Löf[3] have made an analytical study of the full set of variables affecting solar distiller operation. The following summary of their results illustrates one of the ways in which research can yield exceedingly useful information and technical improvements in a field long dominated by empirical efforts. Studies have also been made by Baum along very similar lines.

Figure 5 shows diagrammatically the principal energy exchange mechanisms in a

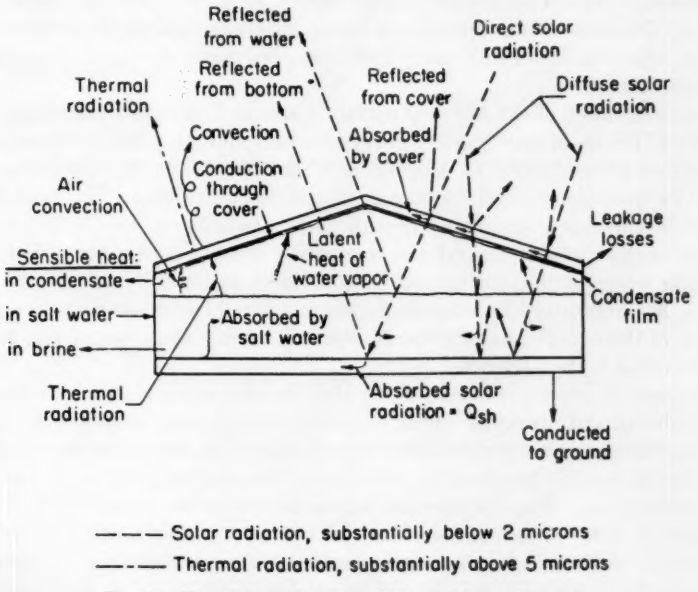

FIG. 5.—Energy-flow diagram of a basin-type solar still.

basin-type solar distiller. Solar radiation, direct and diffuse, is absorbed on the black bottom of the basin. There are several reflection losses, however, from the cover surfaces, the water surface, and the bottom itself. There may also be some absorption of solar energy in the distiller cover. Energy absorbed on the basin bottom is then largely transferred to the salt water by conduction and convection. A small fraction of the absorbed heat may be lost by conduction into the ground. At the water surface, energy is transferred to the cover by three mechanisms. The principal means is by vaporization of water from the liquid surface; by diffusion and convection, the vapor is transferred to the cover, where its latent heat is liberated by condensation. Some heat is also transferred to the cover by free convection of the air in the distiller. Thirdly, heat is radiated from the water surface to the

cover where it is largely absorbed. The cover, may, however, be partially transparent to thermal radiation, and some may pass directly through into the surroundings.

Heat conducted through the cover surface is transferred to the atmosphere by radiation and convection. Additional thermal flows may be as sensible heat in the entering sea water and sensible heat in the brine and distillate leaving the distiller. Leakage of vapor and liquids may also involve thermal losses. A final energy term is the change in enthalpy of the basin contents during a particular time interval. This may be an important item because of unsteady state operation due primarily to highly variable solar radiation rate.

The energy transfer relationships outlined above show that the direct, solar-heated distiller is not a simple device from the point of view of the processes taking place within it. The mechanism of transfer of water from salt water surface to condensing surface is particularly complicated. In addition to questions of conduction and diffusion resistances, there are problems concerning eddy diffusion, degree of approach to saturation at the two surfaces, buoyancy effects due to density differences, and others.

In an evaluation of the effects of certain design and operating variables in a solar distiller of the basin type, various energy transfer and mass flow relationships were formulated as completely as possible, and the specific effects of changing certain variables were determined by means of computer analysis. The procedure involved setting up a complete, over-all energy balance on the entire distiller, a second energy balance around the condensing surface, and a mass flow balance equating water production rate to its equivalent in terms of a convection coefficient. Approximately 20 design and operating variables appeared in the equations. Details of the equations and their solution are beyond the scope of this paper but may be found in the reference.

The general procedure for handling the machine computations involved fixing all the design and operating variables except one and then determining the effects of changing that one variable over a broad range. In each case, the effects of the variable on distiller productivity, salt water temperature, and cover temperature were determined. Some of the more significant results are shown in Figures 6 to 11. In general, these determinations show that distiller productivity increases with a rise in solar radiation intensity, atmospheric temperature, and (Fig. 11) the closeness of approach to temperature and vapor pressure equilibrium at salt water surface and condensing surface. To achieve high distiller productivity, it is seen that wind velocity should be minimized, condenser surface should be as small as practical, and the reflectivity of the surfaces in the still should be as low as possible (Figs. 8–10).

The results obtained from this analysis showed a few unexpected trends. The high dependence of distiller productivity on atmospheric temperature and wind velocity was not anticipated nor was the sensitivity of the productivity to changes in the ratio of condenser area to evaporating area. It was somewhat surprising to see how important the degree of approach to equilibrium is in affecting productivity. In nearly all of the figures, it is also interesting to observe that high productivity is associated with comparatively high operating temperatures but that the temperature difference between salt water surface and the cover surface changes only slightly.

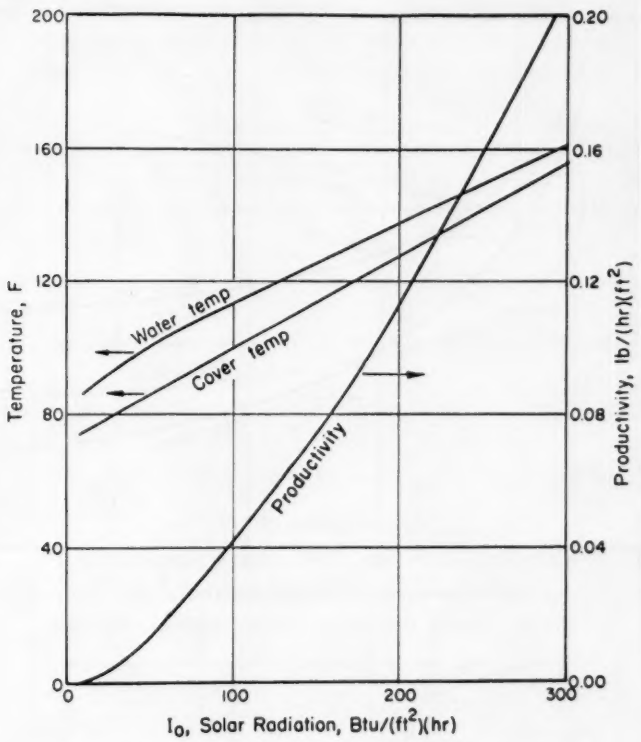

FIG. 6.—Effect of solar radiation on solar distiller performance.

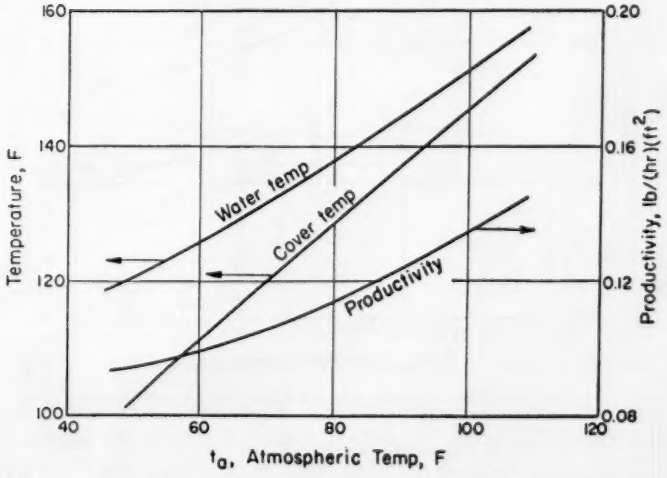

FIG. 7.—Effect of atmospheric temperature on solar distiller performance.

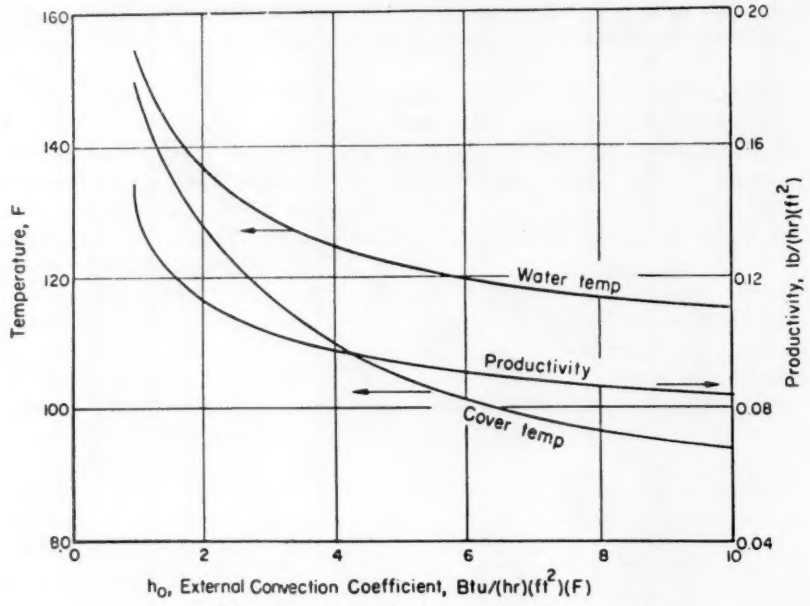

FIG. 8—Effect of wind velocity on solar distiller performance.

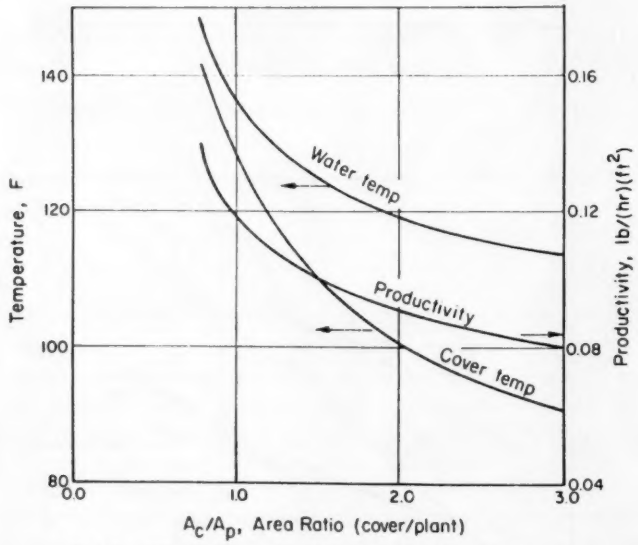

FIG. 9.—Effect of cover area on solar distiller performance.

Another illustration of the potential benefits of fundamental studies in the solar distillation process is the work of Grune, Thompson, Collins *et al.*[2] In a paper soon to be presented, methods for predicting the rate of production from natural-con-

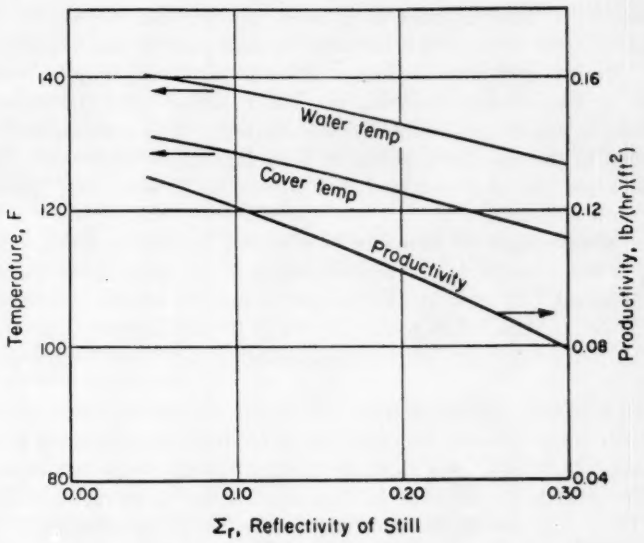

FIG. 10.—Effect of reflectivity on solar distiller performance.

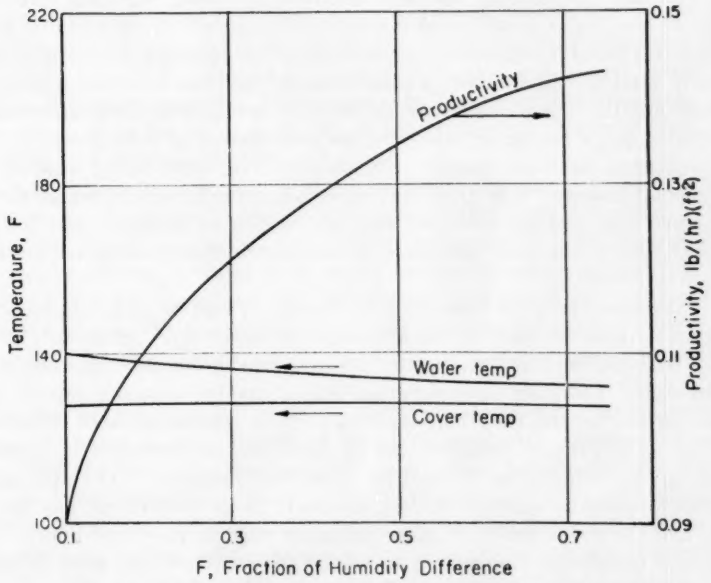

FIG. 11.—Effect of approach to equilibrium on solar distiller performance.

vection and forced-convection solar stills, based on analysis of heat and mass transfer processes within the enclosure, are developed. It is postulated that the rate of production in natural-convection stills is controlled by the rate of diffusion of water vapor from the basin through the stagnant air films to the cover. It is shown that

the resistance to vapor diffusion in a small experimental still varies as the two-thirds power of the product of a modified Grashof number and a modified Prandtl number. The product of these dimensionless groups is roughly proportional to the difference in temperature between the water surface and the cover. Hence, productivity in this natural-convection still was found to be approximately inversely proportional to the two-thirds power of the temperature difference. The inverse relationship was also observed by Löf, Eibling, and Bloemer, but apparently not with the same exponent.

If these relationships are found to be generally applicable to solar distillers of this type, a considerably better understanding of the internal circulation process may be obtained. In turn, design improvements and efficiency increases should result. Although these relationships are yet to be thoroughly tested, their formulation is an important step in the quantifying of solar distiller design and performance.

The two investigations summarized briefly above represent an approach to the solar distiller design problem which should be fruitful. Considerably more work is needed along these lines. For example, thermal storage in the salt water pool and the distiller structure is believed an important factor in average distiller productivity. The results previously reported are based on an assumption of instantaneous response to atmospheric variables. But because the distiller is never at steady state conditions, particularly with solar radiation constantly changing, any thermal lag due to heat capacity will affect distiller performance. A computation program in which this factor is evaluated along with the other operating and design variables is clearly needed. In addition, a clearer insight into the heat and mass transfer processes and the several resistances which they encounter in the distiller enclosure would be of major benefit in improving the performance of these units.

Improvements in Solar Distiller Efficiency.—Along with recent studies of the fundamental processes in solar distiller operation, there have been numerous efforts to improve solar distiller efficiency through changes in materials and design. A review of some of the more significant developments illustrates the potential benefits from such work.

1. *Fundamental studies in materials:* Typical of studies in the improvement of materials for solar distillers are the investigations of surfaces, particularly of plastic films. Without modification, plastics are not suitable for the transparent covers of solar stills. But since these materials have attractive economic aspects, studies of their properties and their improvement for this application have recently been initiated. The primary consideration has been the improvement in outdoor exposure life, particularly as affected by ultraviolet radiation. The application of ultraviolet absorptive coatings to films, such as of the polyester type, has been beneficial; and the development of other polymers, such as polyvinyl fluoride, which are almost completely transparent to ultraviolet radiation, are good illustrations of the efforts along these lines.

Other studies and experimental programs have been directed toward alteration of the surface characteristics of plastic films in order to change their wettability or their optical characteristics. Droplet condensation causes increased reflection losses and the dripping of condensate back into the salt water pool. Surface coatings, such as titanium monoxide, and the mechanical alteration of the film surface

have improved the wettability of these inherently hydrophobic materials. The optical performance of plastic films can be improved if their reflectivity for solar radiation and their emissivity for long-wave thermal radiation can both be reduced. Work has therefore been directed toward the production of selective radiation surfaces on plastic films. Some success along these lines has already been achieved, and further research may lead to substantial improvements in these properties and result in higher distiller efficiencies.

2. *New distiller designs:* Although some of the modified solar distiller designs are not new, recent studies have augmented their potential for efficient use. By illustration, improvements in the tilted solar still utilizing a porous evaporating wick have contributed to improved performance. These benefits have been due, in part, to superior materials, including synthetic fibers and plastic films. There appears to be further need for developing more durable porous evaporating surfaces and other components.

Another design improvement, yet to be tested, has suggested itself as a result of the theoretical studies previously summarized. In the basin-type distiller, the correlation between high efficiency and high operating temperatures suggests the use of double transparent covers to increase distiller temperature and yield. Whether the increased reflection loss from the two surfaces would be greater than the gain in thermal efficiency remains to be seen. Theoretical determination of the expected results and experimental confirmation should be made. Any other measures which might increase operating temperature should be explored.

Another study in progress is the separation of the solar heat collector from the function of a condenser. The use of a forced circulation system with external condensation is being evaluated. There appears to be a theoretical advantage in this arrangement, in so far as productivity is concerned, but this gain needs to be weighed against the added costs of equipment.

Several methods for utilizing the multiple-effect evaporating principle in a solar distiller are being explored. One of these is associated with the system of forced circulation and external condensation, wherein reuse of some of the heat of condensation can be effected by using brine as the condenser coolant and heating it successively in the condenser and in a solar water heater. Water production per square foot of solar heat absorption area may be increased possibly three fold by use of such a system. Again, added costs must be balanced against the increased yield.

In another proposal for multiple-effect operation, several evaporating basins containing salt water in various depths would be employed. Because of varying thermal lag, the salt water temperatures would differ, basin to basin. Thus, air and vapor forced from the warmest basin could be brought to a heat-exchange surface in the salt water in a slightly cooler basin, and so on to the last and coolest basin. In this manner, the heat of condensation from one unit could be recovered in the next. At night, the temperature distribution in the various basins should reverse, and the air could therefore be moved in the opposite direction for continuous water production. Additional theoretical and experimental analysis of this system appears desirable.

Several designs have been suggested which involve multiple layers of evaporating and condensing surfaces, where the heat from vapor condensation on one surface

is conducted into evaporating salt water on the other side of the surface. Plastic films appear of potential value in most of these arrangements. Most of the proposals require theoretical evaluation and experimental confirmation.

Solar Distillation Research and Economics.—The costs of a solar still and the cost of the water produced are almost exclusively dependent on the cost of constructing the heat-absorbing surface and accompanying structures. As the cost of a unit of surface is minimized and as its productivity is increased, demineralized water becomes increasingly competitive with fresh water in suitable locations. Clearly, both effects are needed. Savings in materials and increases in efficiency all will lead toward the one-dollar-per-thousand-gallon cost that many feel is a threshold for substantial application and which is being approached in advanced work.

Research in the fundamental factors affecting the solar distillation process is now beginning to yield important information contributing to these improvements. There can be little doubt that some of these programs, and others which lack of space precludes mention, will yield substantial benefits in the solution of some of the most critical of the world's water supply problems.

* Consulting Chemical Engineer: also Research Associate, University of Wisconsin and Resources for the Future, Inc.

[1] Bloemer, J. W., R. A. Collins, and J. A. Eibling, *Summary Report on First Two-Years Progress on Study and Field Evaluation of Solar Sea-Water Stills*, Report to Office of Saline Water, U.S. Department of the Interior, from the Battelle Memorial Institute, June 16, 1960.

[2] Grune, W. N., T. L. Thompson, and R. A. Collins, "New Applications of Thermodynamic Principles to Solar Distillation," paper presented at meeting of the American Society of Mechanical Engineers, June 1961.

[3] Löf, G. O. G., J. A. Eibling, and J. W. Bloemer, "Energy Balances in Solar Distillers," paper presented at meeting of American Institute of Chemical Engineers, December 1960, to be published, *A.I.Ch.E. Journal*.

General references.—Löf, G. O. G., *Demineralization of Saline Water with Solar Energy*, Office of Saline Water, U.S. Department of the Interior, Progress Report No. 4 (1954). Mason, M. A. (editor), *Proceedings of the Symposium on Saline Water Conversion, 1957*, Publication 568, National Academy of Sciences—National Research Council (1958).

THE STORAGE OF HEAT AND ELECTRICITY

By Bertrand A. Landry

BATTELLE MEMORIAL INSTITUTE

The earth provides examples of numerous ways of storing or releasing heat energy: (1) the sensible heat in the atmosphere, in the oceans, and in the crust and mantle of the earth; (2) the cooling effect of the heat of vaporization leading to cloud formation and the warming due to rain; (3) the similar thermal stabilizing effects of the formation and fusion of ice and snow; (4) the long-range stabilization of the temperature of the earth's crust through the equilibrium between the solid and liquid phases of the inner core of the earth in conjunction with the generation of heat by radioactivity in the mantle and crust;[1] and (5) the thermal or free energy released by the oxidation of fuels.

In order to have an indefinite supply of solar energy for use in an earth satel-

lite, some energy must be stored for use during eclipses, and the type of storage must be reversible and not subject to wear or degradation. Energy storage may also be required if information is to be broadcast to earth periodically with an expenditure of energy greater than the rate of its capture from the sun.

On earth, man stores energy in a number of ways. Energy may be stored as potential mechanical energy as in the weight system, or wound springs of clocks; as compressed air in the braking systems of trains and trucks; as high pressure, high temperature, heat-generated steam; as stream water impounded behind a power dam.

Mention should be made here of the Taum Sauk Project to be completed in 1963, in Missouri, where water will be pumped from the tailrace to a high reservoir during periods of low demand at steam generating stations, and electricity will be generated and fed into the lines during periods of high demand. It is believed that the total costs of the energy storage in this pioneering plant will be less than those of the equivalent additional steam generating capacity.

Mechanical energy is also stored as kinetic energy in flywheels; and buses have been operated on this principle.

Electrical energy cannot be stored as such except in capacitors and superconductors, but ionizing media exist such that the free energy of chemical reactions can appear as an electrical current. Primary cells cannot do this reversibly but storage batteries can.

Fuel energy, after winning, is stored in the form of coal or coke piles, oil-tank farms, repressurized gas fields, or gas-filled underground cavities. Natural gas can even be transported and stored in liquid form.

Heat energy is stored as sensible heat in the recuperators of open-hearth furnaces, in the so-called pebble furnace, in the walls of buildings, or in a tank of water or mass of gravel in connection with solar heating of dwellings. Negative latent heat is stored in ice, dry ice, and liquefied gases.

The durations of time associated with the practical storage of energy are probably longest in the solid fuel reserves of central stations and least in high-pressure steam on its way to a turbine. Sensible heat in recuperators is stored for a matter of minutes only, but if sensible heat is well-insulated, it can be stored for days, weeks, months, and even for many years as in laccoliths, which are large masses of hot igneous rock that have intruded in sedimentary rocks.

Energy stored in primary batteries is also available for months and even years. The same holds true for rechargeable or secondary batteries particularly if the electrolyte is added at the time that current will be needed.

Any practical energy or heat-storage device, if long life is required, must be reversible through many cyclic charges and discharges. Secondary batteries exhibit under cycling definite structural changes which eventually make them useless. A large amount of research has been done and is being done to alleviate this situation by avoiding deep discharges within weight limitations.

Sensible heat storage in solid media is reversible indefinitely if thermal shock and erosion can be avoided; in liquid media, evaporation is a factor which is useful in solar distillation.

Inasmuch as a constant level of temperature is important if work is to be performed at a preassigned efficiency from stored thermal energy, the utilization of a

change of phase is a desirable process for this purpose. Latent heat storage is generally reversible but experience has shown that, in certain instances, heat of hydration is not indefinitely reversible probably because of molecular transformations. Latent heat of vaporization is usually an order of magnitude or more greater than heat of fusion but the volume of vapor or gas is so much larger than that of the liquid that containment may be a real difficulty.

Another important consideration is the potential or thermodynamic head of the stored energy. In principle, a ton of water falling one foot makes available kinetically as much energy as one pound of water falling 2,000 feet. But it would take enormous equipment, clearly beyond engineering practice, to use the low head, whereas use of the high head is extremely simple. This is the primary reason why electricity from the free energy of chemical reactions requires heavy equipment; voltage is so low that power is obtained mostly from current, and heavy conductors are needed.

Finally, in a practical sense, the energy source must be capable of releasing energy at an acceptably high rate. It would be of little value to have a source of water 2,000 feet above its surroundings if only one pound was available per hour. Solar energy, because of the high temperature of the source, is of high potential, but the amount of energy received per unit area, per hour, at earth's distance from the sun, is exceedingly small by comparison with rates of heat transfer in industrial energy generators. For capture of significant amounts, large areas must be employed as in solar distillation and in solar furnaces. The latter involves concentration of energy giving an increase in temperature, the temperatures of the sun's surface being the limit. By choosing suitable areas of capture and of focus, one can obtain temperatures as high as may be practical to employ together with a commensurate amount in the total energy captured.

This property of solar radiation makes it possible to convert solar thermal energy to electrical energy by thermoelectric devices, or to mechanical energy from a working fluid, provided that a suitable heat sink is available in both instances. On earth, this method of solar energy utilization does not at present compete with conventional sources of energy. In the distant future, however, it can be imagined that such devices, if firm power is to be provided, will be placed around and directly above the large artificial lakes behind power dams. The impounded water will serve as a heat sink, and energy storage will take place during hours of sunshine by a decrease in hydraulic generation with concomitant rise of the water level. Because of the limited hours of sunshine, the theoretical load factor of the solar plant would not exceed 33 per cent, and that of the hydraulic plant 67 per cent. This means that the total cost of the solar plant could not exceed one-half that of the hydraulic plant. This is unlikely, but in the future it may not be a weighty factor.

The sun plays an important role in the heating of our dwellings. On a bright winter day, the thermostat often remains high without the furnace's operation. Houses have been designed and built that absorb enough solar energy to store sensible heat not only for overnight use but for several cloudy days.

In principle, it should be possible to store sensible heat during the summer months in a large underground tank or gravel-filled cavity and to use this as a heat source for a heat pump during the winter months. Conversely, the installation could also

serve as a heat sink, during the summer season, by reversing the heat pump. However, it can be calculated that an annual heating load of 100 million Btu's required for a six-room well-insulated house in Ohio would cost over $600 in annual interest charges alone for heat storage. This is several times greater than the cost of heating and cooling by conventional methods. Seasonal solar thermal energy storage does not appear to be economically possible today.

Thermal energy may be stored as sensible heat at fairly high temperatures for a period of several days if off-peak electricity is used as the energy source. This would permit an air heat pump to continue to supply the heating load during unusually cold weather without supplementary direct electric heating, which is at present the only alternative but which requires extra peaking capacity at the utility with a corresponding lowering of the annual load factor. The total costs of such storage systems, if borne by the utility, must be compared with the cost of additional generating equipment. There apparently are not enough data at present to make a choice.

Returning to earth satellites, energy storage takes another complexion because costs are relatively unimportant whereas mass, volume, and reliability are tremendously important. Assuming a continuing mission, the most plausible energy source is the sun. The area required for capture, which must develop from the satellite while passing into orbit, will depend on the amount of energy to be expended by the satellite and on the process employed to transform solar energy to electrical, mechanical, or thermal energy. If a photoelectric process is used, concentration of solar energy is not indicated and there is no need for a heat sink; however, only a small part of the energy spectrum can be utilized and a larger area of capture may be required by comparison with an efficient thermal device utilizing the entire energy spectrum. All thermal devices, on the other hand, require a heat sink that has appreciable mass, and the capturing device must be so shaped as to concentrate the radiation to obtain a temperature as high as the process can accept. In thermoelectric processes, the temperature limit is that at which the solid state characteristics employed are lost. The challenge here is to find materials that will operate at temperature as high as conventional working fluids. The maximum temperature for purely thermal processes will depend on the thermodynamic properties of the fluid and on whether it can be confined with reasonable equipment weights. The choice of an optimum system will be sought in research for a long time.

If solar energy is converted directly to electricity, the means for storage can be chemical only as in secondary batteries where the reactions involve only solids and their ions, or in reversible fuel cells where the reactions may involve a gas and a solid or only gases. These devices must be as light as possible, must discharge at the proper rate, and must last through cycle after cycle.

If conversion takes place through a thermal cycle, with generation of mechanical and therefore electrical energy, the means for storage may be thermal or chemical. If thermal, it should accept heat at the temperature at which it is made available and release it at approximately the same temperature to maintain the proper efficiency. Obviously the heat storage material must be as light as possible and the surface area over which heat transfer takes place must bear such a relation to the volume of material that the required heat flow will be obtained.

A material has been found that seems to have the desired properties.[2] This is lithium hydride (LiH) which melts at 1250°F, has a latent heat of fusion of more than 1,000 Btu's per lb, and has a density about one-half that of water. Unfortunately, LiH reacts violently with water. This poses difficult engineering problems in manufacture and assembly as well as increased hazards if living conditions are to be maintained or re-entry envisaged. The next most advantageous material may well be lithium fluoride which melts at the rather high temperature of 1,600°F and has only half the latent heat of LiH but is stable to water. The only motive fluid indicated with these qualities is mercury. This is heavy and can be toxic, although extensive knowledge through experience exists on its use for power generation.

Other light materials, such as silicon, are also under investigation. These have even higher fusion temperature than the lithium compounds. This will require that the collector have a high accuracy of focussing, which may not be possible to achieve because of thermal distortion due to eclipse, unless the back of the collector is a heat sink radiator that will maintain a constant temperature as long as heat is available from storage. A metal lighter than mercury, such as sodium, could serve as the motive fluid if silicon were used for heat storage and if corrosion of the silicon container can be avoided.

It appears that a practical system of thermal energy generation and storage can be provided for an earth satellite or even for a space craft not straying too far from earth's orbit if the total mass involved can be shown to be similar to that employed for the direct generation of electrical energy and its chemical storage.

Some types of storage batteries have a nontrivial advantage over a regenerative thermal system in that they can be discharged at a much higher rate than their rate of charge, whereas a thermal generator cannot be overloaded. Thus, if information is to be broadcast to earth intermittently, then a much higher rate of energy output can be supplied for this purpose from a battery than by any other means.

Efficient batteries, however, generally use elements or compounds of high atomic or molecular weight such as zinc, silver, nickel, cadmium, or lead, and their oxides, and are therefore heavy, the weight increasing in the order listed. Inasmuch as an electrochemical equivalent is a simple multiple of the atomic weight, the question may well be asked: "Why not use light metals such as lithium, sodium, magnesium, or calcium?" The answer, of course, is that such metals cannot be reduced in an electrolyte containing water because of their reactivity with water. Could suitable organic electrolytes be discovered? This has been investigated, but may be worthy of far more research. Fused salts may also be indicated; the difficulty here, besides that of temperature, is to find an electrolyte which will ionize the active materials, but not dissolve them excessively.

Fuel cells may belong to this group if the electrolyte is a fused salt and one or more of the reactants is a gas that can be ionized but does not dissolve excessively. An alternative also exists in fuel cells using an aqueous electrolyte.

The efficiency of such systems is dependent, however, not only on the free energy of the reaction but must reflect also the efficiency of regeneration if this is thermal, or of repressurization if this is mechanical or due to surface action such as adsorption.

Important current research, illustrative of thermal regeneration, includes a regenerative fuel cell employing alkali or alkaline-earth metals for one electrode and hydrogen for the other.[3] The electrolyte is an alkali halide. By ionic reaction, with current generation, the metallic hydride is formed and dissolves in the electrolyte. This is circulated through a heated regenerator where the hydride dissociates to release hydrogen gas and liquid metal. The freed hydrogen is pumped back to the hydrogen electrode, which is metal that does not enter into the reaction but has a high surface area. The electrolyte is returned to the cell after cooling by heat interchange, and liquid metal is also returned to replenish the anode. This, of course, can be done continuously. The regenerator requires an independent heat source and the thermal efficiency of regeneration cannot exceed the Carnot relation between the regenerator and cell temperatures. The voltage of such a cell decreases with an increase in its temperature but the current generated increases so that a high rate of power output may be obtained, for a short time, within the thermal reserves of the system.

A regenerative fuel cell using hydrogen and oxygen, say, when generating electricity, must be able to store the water formed and, conversely, must generate hydrogen and oxygen from the water when electrical energy is applied. To find electrodes that will do this and utilize the fuel and oxidant at a rate high enough to maintain voltage under load is a real challenge that is under intensive exploration.

For space use, the gases may be stored in bags external to the satellite if meteorites and radiation permit this. Otherwise, pressurizing systems, whose weight will be an important factor, will be needed. The alternative of storing the gases within the electrodes is also under investigation. The problem here is to make available for adsorption large and effective surfaces that will not be damaged by repeated cyclings and yet will permit a rapid rate of discharge. An understanding of the actual surface details of solids and of their role in adsorption and catalysis is needed as a basis for the kinetics of these actions. Work now in progress indicates that this knowledge will eventually become available.

Summary.—The earth provides examples of many ways of storing thermal, chemical, and nuclear energy. Together, they have made life possible for a long time.

Man has added to these methods principally through the storage of potential mechanical energy and potential electrical energy from the free energy of chemical reactions.

Man uses solar energy mostly for growing food, for heating houses, for drying various crops, in salt flats, and in photography. In the future, solar distillation and eventually power generation will become important but will remain a fractional part of the rain fall and stream flow.

Man-made satellites operating in the vicinity of the earth's orbit will probably use solar energy to record and transmit information and to sustain life. This will be possible because of the large areas for capture that can be developed from the satellite after it leaves the atmosphere. Stored energy will be required when the satellite is eclipsed by the earth or if information is to be broadcast at a high energy rate. A great deal of research will be required before it can be decided, in terms of a given mission, whether generating and storage systems shall be electrical, thermal, or a combination of the two.

[1] Verhoogen, John, "Temperatures within the earth," *Am. Scientist*, **48**, 134–158 (1960).

[2] Walker, Curtiss L., and James D. Matchett, "A thermal energy storage system for solar powered earth satellite power plants," *Gen. Motors Eng. J.*, **7**, 10–12 (1960).

[3] Ciarlariello, T. A., and R. C. Werner, "Fuel cells based on nuclear reactors," *Chem. Eng. Progr.*, **57**, 42–45 (1960).

PHOTOCHEMICAL UTILIZATION OF LIGHT ENERGY

BY EUGENE RABINOWITCH

DEPARTMENT OF BOTANY, UNIVERSITY OF ILLINOIS, URBANA

1. *Introduction.*—Nature offers us an imposing example of photochemical storage and utilization of light energy in the photosynthesis of plants. All life energy of animals, as well as the overwhelming proportion of energy man uses to heat his dwellings, smelt metals, and keep the wheels of industry turning, is derived from recent or ancient photosynthesis.

Of course, plants are not only energy converters, producing fuel, but also photochemical factories, synthesizing carbohydrates from water and carbon dioxide. These, in turn, serve as substrates for the enzymatic synthesis of all other types of food and of a variety of components of living organisms.

For his food, man still is entirely dependent on plants; but he may be approaching plants in his capacity of converting light into other, usable forms of energy. As we have heard in this symposium, solar batteries, thermoelements, or barrier layer cells can now convert sunlight into electrical energy with a yield of between 5 and 10 per cent. However, no known photoelectric or thermoelectric conversion devices are cheap enough to consider covering large areas—open fields, deserts, rooftops—with such converters to produce commercial energy.

Out of an average of 1×10^{13} kcal of solar energy (visible and infrared) reaching the surface of the earth (including the oceans) each second, about 5×10^{10} kcal, or 0.5 per cent, are stored as chemical energy by plants growing on land or floating in the ocean. (A considerable uncertainty of this estimate is caused by the limited data available on the rate of photosynthesis by phytoplankton in different parts of the world ocean.)

The efficiency of utilization, by plant-covered land areas, of the incident visible light (excluding the infrared), averaged over the annual growth period, has been estimated as of the order of 2–3 per cent. In experiments with intensely stirred algal suspensions, this yield could be raised to 5–7 per cent, and in short-time laboratory experiments, to 20–30 per cent. The assertion by O. Warburg, that the conversion yield of photosynthesis can be pushed, in manometric experiments, up to 90–100 per cent is implausible and could not be confirmed by other investigators, employing the same or a variety of other methods.

The above figures suggest that the efficiency of photosynthetic energy storage under natural conditions is determined, not by intrinsic limitations of the efficiency of the photochemical process itself, but by some secondary causes. The most fundamental of these may be the limited supply of carbon dioxide in nature. With a normal atmospheric concentration of only 0.03 per cent CO_2, it is truly re-

markable that land plants can maintain a rate of about 20 mg CO_2 reduced per hour per 100 cm^2 of leaf surface, which is needed to produce an average conversion yield of 2 per cent. Other limitations of the over-all rate of photosynthesis are caused by enzymatic bottlenecks; these do not allow a much higher rate of photosynthesis to be reached even with an artificially increased supply of CO_2. However, these enzymatic limitations may be due to the adaptation of plants to the naturally available supply of CO_2: there would be no use for them to accumulate enzymes in amounts capable to handle much more substrate than is available under natural conditions. For the same reason, it is of no particular significance to plants (at least, to land plants) whether their pigments—in particular, chlorophyll—absorb all or only part of the available light, since the average supply of light exceeds that of carbon dioxide. (Plants living deep under water are in a different position—they often depend on the presence of additional pigments, such as fucoxanthol or phycoerythrin, to insure absorption of sufficient amounts of the dim, greenish light that reaches them.)

This suggests the possibility not only of imitating *in vitro* the photosynthetic performance of plants but even of improving on it by devising photochemical systems with wider spectral sensitivity and higher primary energy conversion yield, and (most importantly) without an early "light saturation," caused in photosynthesis by enzymatic "bottlenecks."

There is no reason to assume that man will never discover inexpensive photochemical systems permitting the conversion of, say, 10 or 20 per cent of incident solar energy either into potential chemical energy (such as that of an explosive gas mixture) or into electrical energy. Some such attempts have been made, using simple inorganic systems. An example is the system $2NOCl \overset{h\nu}{\rightleftharpoons} 2NO + Cl_2$, studied by Daniels and co-workers. However, I intend to discuss here not these simple reactions, but the more complex ones which could be considered as analogous to the primary process in photosynthesis.

2. *The Primary Photochemical Process in Photosynthesis.*—The exact nature of the reaction by which light energy is first converted into chemical energy in plants remains uncertain. From indirect biochemical evidence there is a widespread inclination to believe that this reaction is two-fold, involving the reduction of a pyridine nucleotide, such as TPN, by water, the latter being oxidized to free oxygen:

$$TPN + H_2O \overset{h\nu}{\rightarrow} TPNH_2 + {}^1/_2O_2, \qquad (1)$$

and the conversion of adenosine diphosphate into adenosine triphosphate (photophosphorylation):

$$ADP + \tilde{P} \overset{h\nu}{\rightarrow} ATP, \qquad (2)$$

where $\tilde{P}$ stands for "low energy," inorganic phosphate. Repeated suggestions—revived in a recent review by Stanier in the *Bacteriological Reviews*—that photophosphorylation is the *only* primary energy-storing reaction in photosynthesis, appear to me very implausible and unsupported by the totality of experimental evidence. It seems more plausible that photophosphorylation itself is a secondary process; it could result from partial reversal of a reaction of type (1). It is well known that in respiration, the oxidation of pyridine nucleotide produces several molecules of ATP.

It is known that $TPNH_2$ and ATP together can bring about (in the presence of proper enzymes) the reduction of carbon dioxide (incorporated in a carboxyl group) to the carbohydrate level.

Since the oxidation-reduction potential of the couple $TPN/TPNH_2$ is about -0.3 volt and that of the couple $H_2O/{}^1/_2O_2$ about $+0.8$ volt, reaction (1) leads, under standard conditions, to the storage of 2×1.1 ev, or about 50 kcal/mole, of free chemical energy (the factor 2 originating from the involvement of two electrons), whereas reaction (2) stores, under standard conditions, only about 10 kcal/mole.

Recently, evidence has been obtained (in our and in other laboratories) that photosynthesis involves (at least) *two* primary photochemical processes, sensitized by two different forms of chlorophyll *a*. These two processes could conceivably correspond to equations (1) and (2), respectively: an oxidation-reduction, and a photophosphorylation. However, even if this be the case, reaction (2) could still result from the reversal of a process of type (1): both forms of chlorophyll *a* could sensitize an oxidation-reduction against the gradient of chemical potential; but one of these reactions could be reversed, with the formation of high-energy phosphate, while the products of the other could be prevented from recombination and become available for the reduction of carboxyl groups.

According to a plausible hypothesis by James Franck, the two types of chlorophyll *a* differ by their association with either a hydrophilic or a hydrophobic medium.

3. *Prevention of Back Reactions.*—A chlorophyll molecule excited by visible light contains about 45 kcal/mole or about 2 ev of electronic excitation energy. This is enough to transfer an electron, even from a very weak reductant, to a very weak oxidant, since two volts span almost the whole series of oxidation-reduction potentials. The difficulty, which requires ingeneous solution, lies therefore not so much in the achievement, by means of visible light, of a sufficiently endergonic oxidation-reduction reaction, as in effective prevention of the reversal of this reaction, which would lead to the loss of stored energy. In principle, this could be done in two ways—by chemical stabilization, or by physical separation of the unstable products.

The structure of the photosynthetic apparatus makes tempting the second hypothesis—that of physical separation of the intermediates. This structure is characterized by thin parallel lamellae. These are not always as neatly arranged as shown in Figure 1 (a) or (c), but they are always there, even in the most primitively organized blue-green algae (d) and photosynthetic bacteria. Each lamella probably consists of alternating layers of hydrophilic (proteidic) and hydrophobic (lipoproteidic) materials. Chlorophyll probably is located on the interfaces between hydrophilic and hydrophobic layers, forming monomolecular (or bimolecular) layers. One can imagine an excited chlorophyll molecule transferring one electron to an "acceptor" molecule in the adjacent lipoidic layer and recovering it on the other side from a proteidic layer (or vice versa). The two reaction products thus find themselves in two different phases and can undergo enzymatic stabilization, ultimately leading to their conversion into carbohydrate and molecular oxygen, without danger of immediate recombination.

It has been suggested, e.g., by Calvin, that this separation of products may be based on an electron migration similar to that occurring in crystalline photoelectric conductors. However, with a monomolecular pigment layer, all that is needed is for the electron to migrate across a single chlorophyll molecule, and this is always

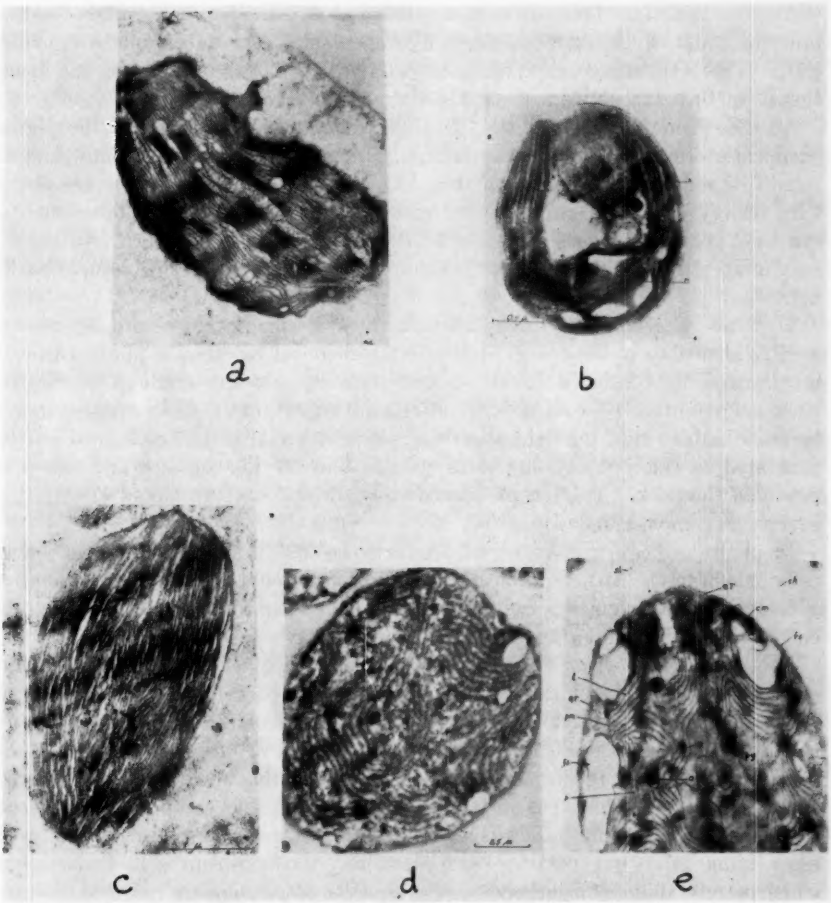

FIG. 1.—Cross-sections through (a) a chloroplast from a corn leaf, (b) a cell of *Chlorella* (green alga), (c) a chloroplast from a young shoot of *Aspidistra*, (d) a cell of *Synechococcus* (a blue green alga) and (e) a cell of *Porphyridium* (red alga). Illustrations (a) and (e) after Vatter; (b) and (c) after Leyon and Albertson; (d) after Elbers, Minnaert and Thomas.

possible in an aromatic ring system. No *intermolecular* photoconductivity is needed in this case; and such conductivity is made unlikely by the non-crystalline nature of chlorophyll monolayers *in vivo*, evidenced by the position of their absorption bands.

4. *Variations of the Photosynthetic Process.*—The photochemical apparatus can be used for different variations on the general theme of photosynthesis. In one class of them, carbon dioxide is replaced by another oxidant. For this purpose, cell-free chloroplasts are best used, because the membrane of the intact cell blocks the passage of many oxidizing compounds which can otherwise participate in the reaction. The only "substitute oxidant" so far found to be usable with whole cells is benzoquinone, but with chloroplast fragments, a large variety of oxidants, such as ferric salts, quinones, and dyes have been successfully employed.

Another variation of photosynthesis is based on substitution of a different reductant for water—molecular hydrogen, hydrogen sulfide, or an organic compound, RH_2. This is the normal form of photosynthesis in *bacteria;* but Gaffron has shown that it can be induced, by incubation in hydrogen, also in certain algae.

All these variations affect little, if at all, the quantum efficiency of the photochemical process, or its action spectrum; but, since all substitute oxidants and all substitute reductants are stronger than CO_2 and H_2O, respectively, the amount of light energy converted into chemical energy in these varieties of normal photosynthesis is quite low or even negative. In these reactions, it is the activation energy of an otherwise sluggish reaction that is primarily or exclusively supplied by light.

5. *Model Reactions in Vivo.*—Reactions *in vitro*, which could be broadly considered as analogous to the energy-storing photochemical reaction in photosynthesis, are various light-induced oxidation-reductions against the gradient of electrochemical potential. Two additional criteria are important: (1) The reaction should be sensitized, so that the light-absorbing pigment would be not consumed but regenerated, as chlorophyll is in photosynthesis, and (2) the oxidation and reduction products should not react back immediately, dissipating the stored energy, but survive long enough to be separated.

In photosynthesis, the two final products, O_2 and $\{CH_2O\}$, are stable practically indefinitely. An acceptable alternative *in vitro* would be *delayed* recombination —delayed long enough to permit the conversion of a considerable part of the stored energy into some useful form, such as electrical energy.

Photochemical electron transfers against the gradient of chemical potential are common; every electronically excited molecule can be considered as a powerful reductant, able to transfer its excited electron to a reluctant acceptor—and often also as a powerful oxidant, able to take an electron away from a reluctant donor. Electrochemical and spectroscopic evidence suggests that in every "stable" light-absorbing system which contains oxidizable or reducible components, there do occur, despite apparent stability, hidden photochemical oxidation-reduction processes, immediately reversed by back reactions. The problem is to find systems which permit rapid stabilization or spatial separation of the energy-rich oxidation and reduction products. Only a few such systems have been identified and studied in some detail.

Systems involving dissolved *chlorophyll* or its derivatives and analogues have received particular attention. The best known is the "Krasnovsky reaction" involving chlorophyll and ascorbate dissolved in pyridine. (Other reductants, such as phenylhydrazine, can be used instead of ascorbate but give a lower quantum yield.) This system reacts according to reaction:

$$\text{Chl. } a + \text{ascorbate} \xrightarrow{h\nu} \text{Chl.}a\ H_2\ (\text{"eosinophyll"}) + \text{dehydroascorbic acid}, \quad (3)$$

where "eosinophyll" denotes a pink compound, probably derived from chlorophyll by addition of two hydrogen atoms. (Contrary to early suggestions, it is *not* a free radical, since it exhibits no paramagnetic resonance.)

The normal redox potential of the couple ascorbate/dehydroascorbate is 0.0 volt; that of the system chlorophyll *a*/eosinophyll must be negative, because reaction (3) is reversed in the dark. How much more negative, is shown by the fact

that if riboflavin or certain other oxidants with normal potentials down to −0.3 volt are present, eosinophyll reduces them to the corresponding leucocompounds and is itself converted back into chlorophyll. The free-energy storage in the photoreduction of riboflavin by ascorbate is of the order of 2 × 0.2 ev, or about 9 kcal per mole. According to Bannister's work in our laboratory, this reaction occurs with a quantum yield of the order of 0.2, so that the energy conversion yield (in red light) is of the order of 4 per cent.

The Krasnovsky system thus satisfies, albeit with a relatively low yield, the first two above-suggested criteria—it stores chemical energy, and it can be used for sensitization. Its products—e.g., leucoriboflavin and dehydroascorbic acid—do react back, but only relatively slowly. So far, no experiments have been made on separating these products (e.g., by distribution between immiscible solvents) or on utilizing the back reaction for the production of electric current. (However, Evstigneev did demonstrate the occurrence of a photogalvanic potential between two platinum electrodes immersed into an illuminated and a darkened zone, respectively, in a chlorophyll-ascorbate solution.)

More extensive measurements of this "photogalvanic" effect and of the electric work which can be derived from it have been made on an analogous redox system, consisting of an aqueous solution of the purple thiazine dye, thionine, and a ferrous salt, reacting according to the equation

$$\text{Thionine} + 2\text{Fe}^{++} \xrightarrow{h\nu} \text{Leudothionine} + 2\ \text{Fe}^{3+} \qquad (4)$$

The reversible bleaching of this system was discovered by K. Weber, and its kinetics and its photogalvanic properties were studied by us first in 1938–1940; recently, the study of this reaction has been resumed in our and in several other laboratories. Photogalvanic potentials up to 400 mv can be easily obtained, and currents can be produced in an external circuit with a wattage equivalent to a few tenths of one per cent of the absorbed light energy. The yield of conversion to electric energy depends in this case on the ratio between the rates of the *homogeneous* and the *heterogeneous* back reaction. (The latter can be considered as a reaction catalyzed by the electrodes: electrons are conveyed, from leucothionine to ferric ions, via the electrodes and the external circuit.) To minimize this ratio, one must decrease electrolytic polarization, which depresses the concentration of the oxidation product at the anode and of the reduction product at the cathode. The electrode surface must be made large and the volume of the solution small; and effective stirring must be provided. Without stirring, the illuminated compartment is gradually enriched in Fe^{3+} and the non-illuminated compartment in Fe^{2+}, and the pH in the two compartments becomes different.

It is easily seen that a photogalvanic system is rather similar to a solar battery, or a barrier layer cell. These, too, can be considered as oxidation-reduction systems, in which the light-absorbing layer serves as a photoreductant, donating electrons to the dark (or transparent) layer. The direct return of the electron and its recombination with the positive hole it has left behind are delayed by a potential barrier at the interface of the two layers, so that a large fraction of the liberated electrons can be channeled back through an external circuit.

It is possible, indeed likely, that the stability and efficiency of crystalline systems in the conversion of light into electricity will never be matched by photogalvanic

systems; but one cannot be sure, and the costs per unit area are likely to be more favorable in the latter case.

We now turn to the problem of utilizing stored chemical energy by stabilization rather than by immediate conversion into electrical energy. Crystalline convertors cannot store energy, because the potential barrier against direct recombination is low, and the "condensor capacity" of the system is relatively small. One could, however, envisage photochemical systems able to store chemical energy for indefinite time, as plants do in accumulating organic matter and releasing oxygen into the air. Particularly tempting would be the production of an explosive but metastable gas mixture, such as knallgas, $H_2 + O_2$. Heidt has tried to produce knallgas photochemically from ferric/ferrous (or ceric/cerous) solutions. Light-excited ferric (or ceric) ions are able to oxidize water, e.g.,

$$Fe^{3+} + H_2O \xrightarrow{h\nu} Fe^{2+} + H^+ + OH\ (\rightarrow O_2), \tag{5}$$

while excited ferrous (or cerous) ions can reduce water

$$Fe^{2+} + H_2O \xrightarrow{h\nu} Fe^{3+} + OH^- + H\ (\rightarrow H_2) \tag{6}$$

While some evidence for the occurrence of these reactions could be adduced, the quantum yields were minimal. This may be due not to the low quantum yield of the primary photochemical processes in (5) and (6) but to the high probability of various back reactions, permitting only a very small proportion of the primary products to escape as oxygen or hydrogen gas. In this case, again, an ingenious invention is needed to separate the products and to prevent, or, at least, to limit, the back reactions between them.

The following experiment illustrates the problem. The thionine-ferrous iron reaction can be performed in a stirred water-ether emulsion (under exclusion of air). The two liquids are then permitted to separate. In the dark, the aqueous layer recovers only a little of its original coloration, while the ether layer remains colorless. If now enough methanol is added to permit mixing of the two phases, the full color returns. Obviously, much of the reduced thionine has been preserved in the ether layer, while ferric ions have stayed in the aqueous layer. Light energy, stored in this way, was released upon mixing. If two platinum electrodes are placed, one in the aqueous layer and one in the ether layer (with some methanol added to increase conductivity), a potential difference of the order of 0.3 volt is found—similar to that found between two electrodes immersed in the illuminated and the darkened zone in a homogeneous, aqueous solution of thionine and ferrous ions.

Another pertinent experiment has been recently described by Kallmann. He found that when two compartments, filled with an electrolyte such as NaCl, are separated by a thin ($\sim 10\mu$ thick) anthracene crystal and the latter illuminated from one side by near-ultraviolet light absorbed by anthracene, a "photovoltaic effect" results, with the illuminated side of the crystal becoming negative and the "back side" positive. If now two electrodes are placed in the two compartments and an external connection provided, a current flows across the illuminated crystal plate. It must be supported by electrons released into the electrolyte at the illuminated side (neutralizing some cations present in solution) and taken up by the crystal plate at the opposite side, neutralizing some anions in solution. (Ulti-

mately, H_2 gas should be evolved from one compartment and O_2, or Cl_2, gas from the other compartment; but no actual gas evolution has been as yet observed.) Kallmann suggested that this mechanism of water decomposition, with spatial separation of the two products, may be relevant to the photolysis of water in photosynthesis. An analogy between the thin anthracene crystal and the chlorophyll monolayers in the chloroplasts presents in fact a tempting hypothesis. Whether it is truly pertinent to photosynthesis or not, Kallmann's system illustrates the kind of "ingeneous arrangement" needed to solve the problem of separating the oxidation and the reduction products of an endergonic photochemical process and thus achieve a durable storage of light energy.

PHOTOELECTRICITY

By Paul Rappaport

RCA LABORATORIES, PRINCETON, N. J.

It has been seven years since groups at Bell Telephone Labs, Wright Air Development Division, and RCA Labs first worked on the solar cell. During that time the cell has changed from a scientific curiosity to the only reliable long-term power source available to our space program. Tiros, Courier, Advent, Pioneer and other satellites have used such devices satisfactorily and Vanguard has been transmitting solar-cell powered signals back to earth for three years now. In these satellites, the single crystal silicon solar cell operating as a photovoltaic device converts the sun's photon energy directly into electricity to provide the needed power.

Several papers; [1–3] have been written which review the basic principles and state of the art of solar cells so that this will not be discussed here. The silicon solar cell is fairly well developed, yielding a conversion efficiency in the 10–15% range; however, there are still a number of important research problems to be solved before the space scientists and mankind have the desired solar power source. These problems include among others reliability, lower cost, lighter weight and higher efficiency and are summarized here.

The Efficiency Problem.—For several years research has been directed to higher efficiency, especially at higher temperatures. Such materials as gallium arsenide, indium phosphide, cadmium sulfide and gallium phosphide, which theoretically should have an advantage over silicon, have not been developed to the extent necessary for this. Table 1 shows the results to date on all important photovoltaic materials.

TABLE 1

BEST EFFICIENCY RESULTS OF SOLAR CELL MATERIALS

Material	Efficiency	Reference
Silicon	14%	1
Gallium arsenide	>10%	4
Cadmium sulfide	8%	4
Cadmium telluride	4%	5
Indium phosphide	3%	3
Gallium phosphide	1%	6
Selenium	1%	7

The best developed material other than silicon has been gallium arsenide which has given efficiencies over 10%. The maximum theoretical efficiency of any single material is about 25%, so that one might eventually expect to see a practical device with efficiencies in the 18 to 20% range. This range is not sufficiently above the 15% value already achieved to warrant a large additional effort except for very special requirements. It is certain that such cells would be quite expensive. Where operation at temperatures above 100°C are required, such materials as gallium arsenide and gallium phosphide will definitely be superior to silicon. It should be possible to produce elevated temperatures by employing simple and inexpensive light concentrators. Such devices coupled with the high temperature materials should make economically attractive power sources.

Increasing the efficiency of solar cells is reaching a state of diminishing returns. This can be achieved by special techniques such as fabrication of a wide gap semiconductor layer onto a semiconductor with narrower gap as for example the growth of a gallium phosphide (2.3 ev gap) layer onto gallium arsenide (1.35 ev gap). Such a technique would increase the photon utility of the device, thus increasing the short circuit current of the generator. Other means of increasing efficiency by combining different semiconductors for better spectrum utilization and the use of metal semiconductors contacts are possible. A metal semiconductor contact on CdS, for example, utilizes the transmitted radiation through the crystal. An ordinary p-n junction yields conversion of the absorbed radiation.

Reliability.—One of the chief advantages of solar cells is their supposed basic reliability; they are simple devices with no moving parts. However, it has been found that particle radiation has a deleterious effect on semiconductor devices and solar cells are no exception. Therefore, in outer space use where the Van Allen radiation exists, consisting of energetic electrons and protons, the cell reliability has been questioned. Laboratory measurements have indicated that cells deteriorate 25% in power output when struck by 10^{10} to 10^{11} protons/cm^2. The maximum outer space proton flux is on the order of 4×10^4 p/cm^2/sec so that cell life (25% reduction) in this flux would be 2×10^5 to 2×10^6 seconds, or a maximum of 1,000 hr. Of course, it should be pointed out that few missions require constant operation in the most intense portion of the radiation belts; a duty cycle of about 13%, however, would mean a 25% power reduction in about one year.

Recent work on p-n junctions indicate some appreciable differences in damage rates depending on the construction and starting materials of the cells. For example, a cell made with an n-type top layer (the so-called n on p cell) shows a slower damage rate than the one with a p-type top layer. Work going on in understanding this effect may lead to a more radiation resistant cell. Figure 1 shows a comparison of the damage due to protons for GaAs and both types of silicon cells.

Because of the many connections required to make up a large area array from the present 1- × 2-cm cells, the reliability of a solar cell system would be increased if cell size were increased. For this reason a considerably larger area cell is desirable. Since such cells would be difficult to make up from single crystals, a different approach has to be taken in cell fabrication. Research is required in techniques for making semiconductor depositions in large areas.

This type of cell is of course possible with selenium using the well-developed technique used for exposure meter devices. However, such cells yield no more than

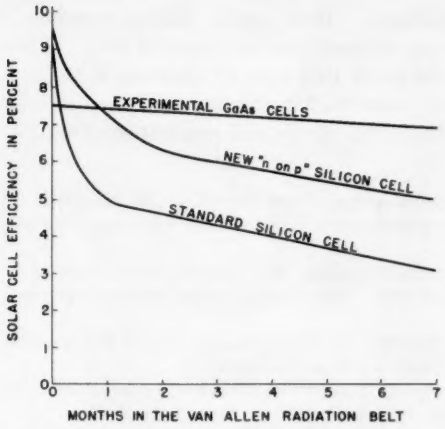
SOLAR CELL EFFICIENCY IN PERCENT
EXPERIMENTAL GaAs CELLS
NEW "n on p" SILICON CELL
STANDARD SILICON CELL
MONTHS IN THE VAN ALLEN RADIATION BELT

FIG. 1.—Degradation of various types of solar cells in the Van Allen Belt.

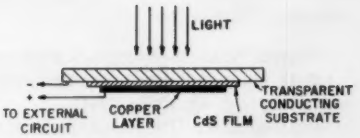

FIG. 2.—Geometry of CdS evaporated layer photovoltaic cell.

1% efficiency. The minimum efficiency acceptable should be about 5%. There is promise of achieving this using CdS evaporated layers or pyrolytically deposited layers of silicon or GaAs. There is even some hope that these films may be made into single crystal layers.

The Cost and Weight Problem.—The weight/kw of a power source is a most critical parameter in determining suitability for space application. The cost problem is more important to ground application, where use is contemplated in sun-rich but power-poor areas. Both of these problems, as well as the reliability problem, would be reduced by further research on films. Such work is going on and will probably be the source of the next real breakthrough in solar cells. Already, cadmium sulfide films with 4% efficiency have been made. Figure 2 shows the cross sectional structure of such a cell. These cells can be made in large areas and are competitive with 10% silicon cells from the weight viewpoint, and should be considerably less expensive.

If a large area deposited solar cell were made at the cost of $1–10 per square foot, we would have a practical source of electricity that could be placed on home roofs. At the rate of $.02/kw hr and assuming a continuous average daily sunshine of 33 watts/sq., ft. a 1000 sq. ft. unit would pay for itself in 2 years with a duty factor of 85%, and in ten years with a 15% duty factor. The duty factor involves the number of sunless days and the angle of incidence of the sun that vary according to location on the Earth. Certainly in areas where sunshine is plentiful such a device would be economically attractive. Other costs such as electrical power storage and installation are not included. Much work is going on in storage systems and it is assumed here that advances will produce a suitably economic device.[8]

Conclusions.—For solar cells the drive for higher efficiency seems over, although work towards higher temperature operation is still required. Gallium arsenide cells may satisfy both needs. Work towards better reliability should continue

especially in the area of radiation resistance. Here, again, gallium arsenide is promising. For light weight and low cost, we must look to deposited films. When film-type cells are perfected so as to yield about 10% over-all efficiency in the conversion of sunlight to electricity, we will have reached the next milestone in solar cell development, that of practical utility for terrestrial application from the economic viewpoint.

[1] Pearson, G. L., "Conversion of solar to electrical energy," *Amer. Jour. Phys.*, **25,** 591 (1957).

[2] Wolf, M., "Limitations and possibilities for improvements of photovoltaic solar energy converters," *Proc. IRE*, **48,** 1246 (1960).

[3] Rappaport, P., "The photovoltaic effect and its utilization," *RCA Review*, **20,** 373 (1959).

[4] Cherry, W. R., "Advanced photovoltaic devices," 14th Annual Power Sources Conference, Atlantic City, N. J., May 17–19, 1960.

[5] Vodakov, Yu. A., G. A. Lomakina, G. P. Naumov, and Yu. P. Maslakovets, "A P-N Junction photocell made of CdTe," *Soviet Physics, Solid State*, vol. 2, no. 1, 1 (1960).

[6] Wysocki, J. J., J. J. Loferski, and P. Rappaport, "Research on photovoltaic converters," 14th Annual Power Sources Conference Proceedings, Atlantic City, N. J., May 17–19, 1960.

[7] Zworykin, V. K., and E. G. Ramberg, *Photoelectricity* (New York: John Wiley, 1949).

[8] Evans, G. E., "Electrochemical energy storage for intermittent power sources," presented at U. N. Conference on New Energy Sources, August, 1961.

ERRATUM

In the article entitled "The Net Hydration of Deoxyribonucleic Acid," by John E. Hearst and Jerome Vinograd, which appeared on pages 825-830 of this volume, the numerals on the abscissa of Figure 1 (p. 827) should be 2, 4, 6, and 8.

INFORMATION TO CONTRIBUTORS

THE PROCEEDINGS is the official organ of the NATIONAL ACADEMY OF SCIENCES and of the NATIONAL RESEARCH COUNCIL for the publication of brief accounts of important current researches of members of the ACADEMY and of the COUNCIL and of other American investigators. The PROCEEDINGS will aim especially to secure prompt publication of original announcements of discoveries and wide circulation of the results of American research among investigators in other countries and in all branches of science.

ARTICLES should be brief. The viewpoint should be comprehensive in giving the relation of the paper to previous publications of the author or of others and in exhibiting, where practicable, the significance of the work for other branches of science. Elaborate technical details of the work and long tables of data should be avoided, but authors should be precise in making clear the new results and should give some record of the methods and data upon which they are based.

MANUSCRIPTS should be prepared with a current number of the PROCEEDINGS as a model in matters of form, and should be typewritten in duplicate with double spacing, the author retaining one copy. Illustrations should be confined to text figures of simple character, though more elaborate illustration may be allowed in special instances to authors willing to pay for their preparation and insertion. Particular attention should be given to arranging tabular matter in a simple and concise manner.

MANUSCRIPTS will be accepted only from members of the Academy who will assume responsibility for the propriety and scientific standards of the paper and for any printing costs in excess of those allowed them by the Academy. Manuscripts should be addressed to THE PROCEEDINGS OF THE NATIONAL ACADEMY OF SCIENCES, 2101 Constitution Ave., Washington 25, D. C.

GALLEY PROOF will be sent, with the understanding that charges for author's corrections shall be billed to him. Authors should therefore make final revisions on the typewritten manuscripts. Original artwork or figures will be returned if requested when the manuscript is submitted. Because of time limitations, page proofs will not be sent.

REPRINTS should be ordered when proof is returned, on the reprint order form which will be enclosed with the proof. They will be furnished at cost, approximately as follows:

SCHEDULE OF REPRINT RATES (POSTAGE NOT INCLUDED)

Quantity	*up to 4 pp.*	*up to 8 pp.*	*up to 12 pp.*	*Standard Covers*
50	$ 7.85	$15.10	$22.30	$6.90
100	8.95	17.30	25.60	8.40
150	10.10	19.50	28.95	9.95
add'l 100's	2.20	4.40	6.60	3.05

CONTENTS

	Page
BIOCHEMISTRY.—SYMPOSIUM ON ENERGY-LINKED BIOLOGICAL REACTIONS. *By David R. Goddard, Chairman*	1089
LOCAL AND π-π INTERACTIONS IN CHARGE TRANSFER. *Albert Szent-Györgyi, Irvin Isenberg, and Jane McLaughlin*	1089
COMMENTARY ON PAPER BY SZENT GYÖRGYI. *J. S. Griffith*	1093
HYDROGEN ION EFFECTS IN HIGH-ENERGY PHOSPHATE REACTIONS. *Robert J. Rutman and Philip George*	1094
THE REQUIREMENT OF ENERGY FOR RESPIRATION IN MITOCHONDRIA (A COMMENTARY). *E. C. Slater and W. C. Hülsmann*	1109
BIOCHEMISTRY.—THE MOLECULAR WEIGHTS OF T2 BACTERIOPHAGE DNA AND ITS FIRST AND SECOND BREAKAGE PRODUCTS. *By I. Rubenstein, C. A. Thomas, Jr., and A. D. Hershey*	1113
BIOCHEMISTRY.—THE STRUCTURAL UNITY OF THE DNA OF T2 BACTERIOPHAGE. *By P. F. Davison, D. Freifelder, R. Hede, and C. Levinthal*	1123
BIOCHEMISTRY.—STEREOSPECIFICITY AND FIREFLY BIOLUMINESCENCE. A COMPARISON OF NATURAL AND SYNTHETIC LUCIFERINS. *By H. H. Seliger, W. D. McElroy, E. H. White, and G. F. Field*	1129
BIOCHEMISTRY.—THE OCCURRENCE OF NATURAL DNA-RNA COMPLEXES IN *E. coli* INFECTED WITH T2. *By S. Spiegelman, Benjamin D. Hall, and R. Storck*	1135
BIOCHEMISTRY.—CORRELATION BETWEEN BASE COMPOSITION OF DEOXYRIBONUCLEIC ACID AND AMINO ACID COMPOSITION OF PROTEIN. *By Noboru Sueoka*	1141
BIOCHEMISTRY.—ON THE SPECIES SPECIFICITY OF ACCEPTOR RNA AND ATTACHMENT ENZYMES. *By Seymour Benzer and Bernard Weisblum*	1149
BIOCHEMISTRY.—ANOMALOUS ROTATORY DISPERSION OF ENZYME COMPLEXES, II. THE ASYMMETRIC BINDING OF COENZYMES AND INHIBITORS TO LIVER ALCOHOL DEHYDROGENASE. *By David D. Ulmer, Ting-Kai Li, and Bert L. Vallee*	1155
BOTANY.—INDUCTION OF PLANT TUMORS BY ULTRAVIOLET RADIATION. *By Carl R. Partanen and Jane Nelson*	1165
CHEMISTRY.—ON THERMODYNAMIC COUPLING OF CHEMICAL REACTIONS. *By G. J. Hooyman*	1169
ENGINEERING.—THEORETICAL STRUCTURE OF PLASMA EQUATIONS AND APPLICATION TO A SIMPLE PROBLEM. *By Joseph Slepian*	1173
GENETICS.—GENETIC CONTROL OF THYMUS LYMPHOID DIFFERENTIATION. *By Robert Auerbach*	1175
GENETICS.—ACTION OF RADIATION ON MAMMALIAN CELLS, IV. REVERSIBLE MITOTIC LAG IN THE S3 HELA CELL PRODUCED BY LOW DOSES OF X-RAYS. *By Masa-atsu Yamada and Theodore T. Puck*	1181
MATHEMATICS.—RENORMALIZATION TECHNIQUES AND MEAN SQUARE AVERAGING, I. DETERMINISTIC EQUATIONS. *By Richard Bellman and John M. Richardson*	1191
MATHEMATICS.—ON GROUP REPRESENTATIONS OVER A VALUATION RING. *By Alex Heller*	1194
MATHEMATICS.—SOLUTION OF THE ∂-NEUMANN PROBLEM ON STRONGLY PSEUDO-CONVEX MANIFOLDS. *By J. J. Kohn*	1198
MATHEMATICS.—EXAMPLES FOR DIFFERENTIABLE GROUP ACTIONS ON SPHERES. *By D. Montgomery and H. Samelson*	1202
MATHEMATICS.—DEFORMATION OF PSEUDOGROUP STRUCTURES. *By D. C. Spencer*	1205
MATHEMATICS.—GRAPHICAL ANALYSIS OF MULTI-RESPONSE EXPERIMENTAL DATA USING ORDERED DISTANCES. *By M. B. Wilk and R. Gnanadesikan*	1209
MICROBIOLOGY.—EFFECT OF MITOMYCIN C ON THE GROWTH OF SOME ANIMAL VIRUSES. *By E. Reich and R. M. Franklin*	1212
PHYSICS.—MANY-ELECTRON THEORY OF ATOMS AND MOLECULES. *By Oktay Sinanoğlu*	1217
PHYSIOLOGY.—RATE-INCREASING ACTION OF CORTICOTROPIN AND OF α-INTERMEDIN IN THE ISOLATED MAMMALIAN HEART. *By O. Krayer, E. B. Astwood, D. R. Waud, and M. H. Alper*	1227
PHYSIOLOGY.—RESPIRATORY ENZYME CHANGES DURING FROG EMBRYOGENESIS. *By Calvin A. Lang and Philip Grant*	1236
N.A.S. SYMPOSIUM.—RESEARCH FRONTIERS IN SOLAR ENERGY UTILIZATION	1245
INTRODUCTION—SURVEY OF RESEARCH FIELDS AND NEEDS. *Farrington Daniels, Chairman*	1245
SOLAR ENERGY IN THE EXPLORATION OF SPACE. *Hugh L. Dryden and A. E. von Doenhoff*	1253
RESEARCH ON THE USE OF SOLAR ENERGY MADE IN THE SOVIET UNION. *V. A. Baum*	1262
SOLAR COLLECTORS, SELECTIVE SURFACES, AND HEAT ENGINES. *H. Tabor*	1271
FUNDAMENTAL PROBLEMS IN SOLAR DISTILLATION. *George O. G. Löf*	1279
THE STORAGE OF HEAT AND ELECTRICITY. *Bertrand A. Landry*	1290
PHOTOCHEMICAL UTILIZATION OF LIGHT ENERGY. *Eugene Rabinowitch*	1296
PHOTOELECTRICITY. *Paul Rappaport*	1303
ERRATUM	1306